Mineralogy, Lithostratigraphy and Geochemistry of North Ingebright Lake, Saskatchewan, Canada

By

Yuqiang Shang

A Thesis
Submitted to the Faculty of Graduate Studies
in Partial Fulfillment of the Requirements
for the Degree of

Doctor of Philosophy

Department of Geological Sciences
University of Manitoba
Winnipeg, Manitoba

0-612-57516-0

THE UNIVERSITY OF MANITOBA

FACULTY OF GRADUATE STUDIES

****

COPYRIGHT PERMISSION PAGE

Mineralogy, Lithostratigraphy and Geochemistry of

North Ingebright Lake, Saskatchewan, Canada

BY

Yuqiang Shang

A Thesis/Practicum submitted to the Faculty of Graduate Studies of The University of Manitoba in partial fulfillment of the requirements of the degree

of

Doctor of Philosophy

ABSTRACT

North Ingebright Lake, containing Canada's thickest known Holocene terrestrial salt sequence, is a small (1.25 km^2), hypersaline playa basin located in the Great Sand Hills area of southwestern Saskatchewan. Because of its remarkably thick lacustrine sedimentary fill, the basin offers considerable potential for providing a high resolution record of past environmental changes in a region that has few other sources of Holocene paleoenvironmental information. Until recently, efforts to acquire cores of this thick sequence of well-indurated but very soluble salt have been unsuccessful using conventional coring techniques. However, exceptional sediment recovery was achieved using a compressed-air diamond drilling technique that permitted collection of continuous, large-diameter, undisturbed and chemically unaltered cores.

The 10,000 year long lacustrine sequence recovered from the basin consists of well-indurated salt, with only minor dispersed mud and organic debris. Indeed, the section is remarkable in its lack of obvious bedding, colour variation or other visible sedimentary structures. The mineral suite of these Holocene salts consists mainly of hydrated Na, Mg, Ca, and Mg+Na sulfates, carbonates, and chlorides. Minor amounts of nitrate evaporitic minerals also occur. This long uninterrupted sequence of soluble salts implies that the lake was characterized by high salinity throughout its Holocene history. However, variations in the mineralogy of the salts suggest that the basin experienced significant changes in brine composition. These evaporites, which allow a detailed reconstruction of specific ion activities and ratios in the brine through time, provide our evidence of the complexity of brine evolution in a closed-basin lacustrine environment in western Canada.

TABLE OF CONTENTS

LIST OF FIGURES

LIST OF TABLES

Chapter 1 Introduction

1.1 Overview

Limnology is a well established science, but paleolimnology is relatively new. Paleolimnology is generally considered to be a multidisciplinary science dealing with the reconstruction of past lacustrine environments through the interpretation of fossil records and the study of sediments. Most of the older (pre-1970's) published work addresses the biological aspects of paleolimnology, whereas comparatively few papers attempt to integrate studies of the lacustrine deposits from which various parameters have been extracted.

Saline and hypersaline lakes have been largely ignored by paleolimnologists because they are generally deficient in paleobiological parameters such as ostracodes, chrysophytes, diatoms, chironomids, and plant macrofossils which are conventionally employed to reconstruct past environments. However, non-biological sediment parameters, such as endogenic mineral composition, geochemistry, and isotopes provide important information about paleolimnological, paleochemical, and paleohydrological changes (Last, 1990; 1999; Sullivan and Charles, 1994; Fernandez, 1994; Zuniga et al., 1991). The Canadian Prairies contain thousands of saline and hypersaline lakes and playas. The modern biological and hydrochemical characteristics of many of these lakes have been well studied (Hammer, 1978a; 1978b; Hammer and Haynes, 1978) but, until recently, little work has been done in the sedimentary realm of these lakes (Last and Schweyen, 1983).

1.2 General Characteristics of Saline Lakes

Salt lakes are usually located in arid to semi-arid regions of the world. The volume of the world's saline lake water (about 100,000 km^3) is nearly equal to the volume of its fresh water (125,000 km^3) (Hammer, 1986). Saline water bodies range from a few m^2 to thousands of km^2 in area. For example, both the Caspian Sea (436,400 km^2) and the Aral Sea (62,00 km^2) in eastern Europe/Asia are large salt lakes.

Saline lakes have a wide range of salinities, from 3 to over 400 g/l. Williams (1964) defined saline waters as those which have a salinity greater than 3 g/l, whereas water with a salinity less than 3 g/l is considered to be fresh. This definition has been well accepted as an arbitrary division point. Figure 1.1 shows classifications of saline lakes by several different workers (SIL, 1959; Hammer, 1978; Hammer et al., 1988; Williams, 1964; 1991; Last, 1992; 1993). The salinity of hyposaline lakes ranges from 3 to 20 g/l; mesosaline lakes range from 20 to 50 g/l; and hypersaline lakes have salinities above 50 g/l.

Saline waters display a remarkable diversity in their chemical composition: some are carbonate-rich, many are chloride-rich, or sulphate-rich. Regardless of whether calcium, magnesium, or potassium are the dominant cations in the water, sodium is usually the most abundant cation. Anion constituents are much more diverse (Hardie et al., 1978; Eugster, 1970; 1982; Eugster et al., 1975; 1978). Solutes in saline lake brines may be derived from the soils and bedrock of the watershed, through precipitation and fallout of salts in the atmosphere, or from wind-blown material. Normally, bedrock lithology is a key factor which controls the

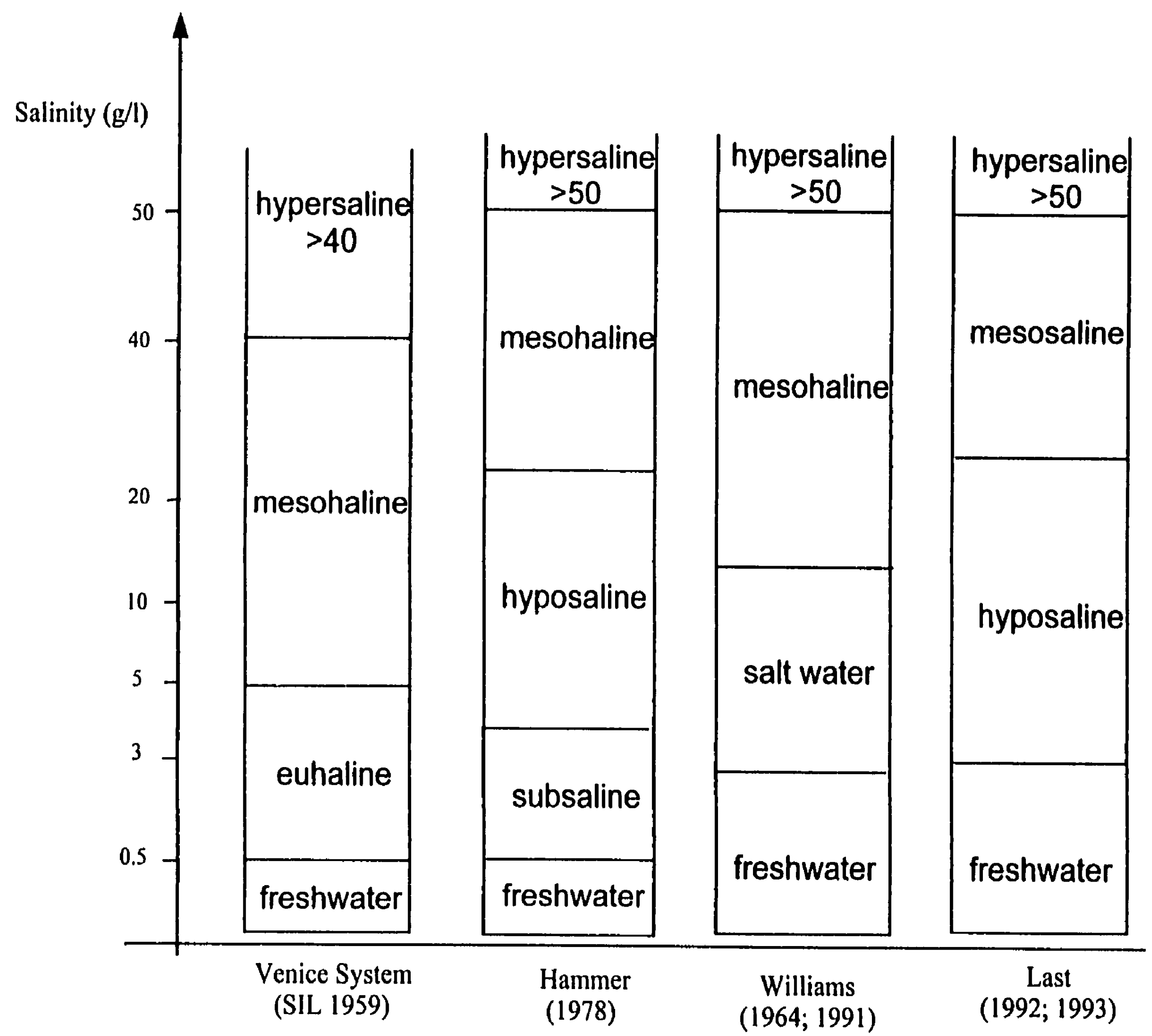

Figure 1.1 Classification of Saline Lakes

final composition of brines (Hardie et al., 1978).

1.3 Conditions of Lake Formation in the Canadian Prairies

Saline lakes can form wherever evaporation exceeds precipitation and the lake basin is hydrologically closed (Hammer, 1986; Mungoma, 1990; Williams, 1991; Seaman et al., 1991). In Canada, after the last episode of glaciation and deglaciation, millions of closed-basins were left in the Prairie region. These lakes show a tremendous diversity in size, basin morphology, hydrochemistry, and sedimentary characteristics (Last, 1988; 1994; 1999). Most of these lake basins are the result of either depositional or erosional processes associated with the glaciation and deglaciation of the region. The most common ways in which such lake basins originated include: (a) ice erosion of bedrock; (b) drainage barriers composed of moraine or outwash dams; (c) depressions formed in glacial deposits; and (d) ice dams (Smith and Ashley, 1985).

As the Lauretide ice sheet began to retreat from the Canadian Prairies, extensive proglacial lakes developed at or near the front of the ice. Proglacial lakes ranged in size from a few km^2 to hundreds of thousands of km^2. Most of these were formed when ice blocked preglacial valleys (drainage routes). For example, North Ingebright Lake is part of the drift-filled channel of a preglacial valley (Cole, 1926; Rueffel, 1968). Other lakes developed when the weight of the ice depressed the earth's crust sufficiently so that closure between the solid rock margin and ice margin formed. Most proglacial lakes have vanished either because the ice has retreated and the ice barrier has disappeared, or because the land has rebounded to its preglacial position. During deglaciation, meltwater from the retreating glacier carved numerous ice-marginal channels and spillways. Although now abandoned or buried under more recent sediment, these depressions are often sites of saline lakes. For example, Ceylon Lake in southern Saskatchewan is presently a shallow, hypersaline playa. The basin originated as a glacial meltwater spillway (Last, 1989; Cole, 1926).

As the margin of the Laurentide Ice Sheet retreated to the northeast during deglaciation, altering drainage patterns, and changes in the extent of these proglacial lakes produced major changes in the Prairies. During its retreat, the Laurentide Ice Sheet blocked the preglacial drainage that flowed to Hudson Bay. The older lakes in Alberta tended to be long and narrow, while those in Saskatchewan and Manitoba were far more extensive because the relief of the Prairies is generally greater in the west than in the east. In Alberta there were lakes centred around the major valleys; these included Lake Edmonton, Lake Red Deer, Lake Bycroft, and Lake Peace. In general, the Saskatchewan proglacial lakes were larger and fewer than the southern Alberta lakes. These include Lake Swift Current, Lake Saskatoon, and Lake Rosetown which all drained either southeast or east. In Manitoba, Lake Agassiz was formed by the damming of glacial melt waters between the ice margin of the continental ice sheet and the Manitoba Escarpment (Meneley et al., 1957; Christiansen, 1967; 1979; Bird, 1972). Lake Agassiz initially drained southwards and eastwards and finally drained to Hudson Bay as the ice barrier to the north disappeared about 7700 B.P.(Andrews, 1987; Klassen, 1972; 1989; Teller, 1985; 1987; 1990; Teller and Thorleifson, 1983).

Although most of the proglacial lakes related to ice dams have disappeared, widely-distributed glacio-lacustrine deposits were left in the Canadian Prairies (Teller, 1987; Stalker, 1976). Sometimes beaches also were left. In the deeper parts of the lake, laminated clay and silts were deposited and formed extremely level clay plains, such as Lake Regina.

In shallow, nearshore lake waters, sands were deposited as deltas or fans; the large sand underflow fan (delta) of the Assiniboine River along the western shores of former glacial Lake Agassiz is a large-scale example of this. The coarse-grained Little Manitou fan, which was deposited in the western shores of glacial Last Mountain Lake during an outburst event near Watrous, Saskatchewan is an example a small fan (Kehew and Teller, 1993). During the last deglaciation, Lake Saskatchewan, Lake Elstow, and Last Mountain Lake were impounded in lowlands between ice margin to the north and upland tracts including the Hawarden Hills and the Allen Hills. These proglacial lakes often released outburst floods as ice dams failed in the edges of the upland areas. The drainage bursts deeply eroded the spillway channels and commonly emptied the lakes. During an outburst flood event from Lake Elstow, Watrous spillway was incised more than 30 m into the drift. The coarse sediment eroded at this time was deposited as the Little Manitou fan at the mouth of the spillway in the Last Mountain Lake basin (Kehew and Teller, 1993).

1.4 Economic Significance of Salt Lakes

In continental environments, sediments of closed-basin lakes often contain the best records of past hydrochemical, hydrological, and climatic variations. Closed-basin lakes potentially yield the most sensitive and explicit record of changes in past environmental conditions and thus are valuable indicators of past climates. In addition, the sediments themselves are an important industrial mineral resource. For example, sodium sulphate is the second largest non-metallic mineral resource in western Canada (Last and Slezak, 1986; Douglas, 1970). Therefore, a knowledge of sedimentary processes and the mineralogy of these lacustrine sodium sulphate deposits has science and economic importance.

Commercial extraction of salts has occurred from numerous saline wetlands and playas in the Northern Great Plains region for over 80 years (Tomkins, 1953, 1954; Last and Slezak, 1987). One of North America's largest sodium sulfate mines and processing plants is located a few kilometres to the south of Ingebright Lake. Salts have also been extracted from nearby Chain, Snakehole, Corral, Boot, Verlo, and Vincent Lakes, all within 30 km of the North Ingebright basin. Although North Ingebright Lake has, to date, not been mined, the lake is presently under mineral lease. Cole (1926) calculated a total anhydrous Na_2SO_4 reserve of about 3 million tonnes.

Early geological work by Cole (1926) on the salt lakes of the Canadian Prairies was mainly based on their potential as a reserve for sodium and magnesium sulphates. Subsequently the biological and hydrochemical characteristics of many of these lakes were documented by the works of Rawson and Moore (1944), Tomkins (1953; 1954), and Hammer (1978). By comparison, relatively little work has been done on the sedimentary realm of the salt lakes. Up to the early 1990s, the stratigraphic records of only eighteen of the basins had been examined (Last, 1992). Extensive research on the stratigraphic records of lakes in this region was part of a large multidisciplinary Palliser Triangle project by the Geological Survey of Canada (Last, 1996; Last et al., 1997; Lemmen, 1996; Vance et al., 1992, 1993, 1995; Vance; Last, 1994; Last, 1999; and Shang and Last, 1999).

1.5 Previous Work on North Ingebright Lake

North Ingebright Lake, also known locally as Ingebright North or Ingebright No.2, was named after the Norwegian immigrant Ingebright Selseth who homesteaded in 1912 near the lake (Rueffel, 1968). This sodium sulphate deposit was first reported in the Annual Report of the Topographical Survey, 1913-1914 (Tomkins, 1954; Rueffel, 1968); however, the deposit has not been exploited/mined to date (Last and Slezak, 1986).

Cole (1926) undertook an extensive investigation on the chemical composition of the brine and sediment of North Ingebright Lake. His study provides valuable scientific data for our understanding of chemical sedimentation history in the lake. In addition, North Ingebright Lake was also discussed by Tomkins (1954) and Rueffel (1968).

The glacial history, surficial geology, and stratigraphy of the North Ingebright Lake region have been discussed by a number of authors. Comprehensive reports and maps of the surficial geology of the Prelate area (72K), including North Ingebright Lake were done by David (1964). Christiansen (1968, 1979) described the Quaternary history and stratigraphy of southern Saskatchewan including the Great Sand Hills area. Klassen (1991, 1994) discussed, in detail, the deglaciation history and proglacial lake development of southwestern Saskatchewan. Epp and Townley-Smith (1980) addressed modern morphology and terrestrial ecology of the Great Sand Hills area, including North Ingebright Lake area.

1.6 Objective of Research

The Ingebright Lake chain in southwestern Saskatchewan, comprising North Ingebright Lake and Ingebright Lake, contains the thickest known sequence of Holocene salts in Canada and provides a relatively complete record of Holocene environmental change. A detailed examination of the stratigraphic record of North Ingebright Lake may yield important information that will enhance our understanding of the paleoclimate and paleohydrology of the northern Great Plains.

In order to conduct this Ph.D research within the monetary and temporal constraints imposed by available funding, this project focuses on selected aspects of the North Ingebright Lake record, namely the lithostratigraphy, sedimentology, mineralogy, and geochemistry of the sediments. The general objective of this research project is to contribute the understanding of the geolimnology and history of North Ingebright Lake. The specific objectives of this research project are to: (1) acquire cores and samples from North Ingebright Lake; (2) describe and document the characteristics of the Holocene sediments in the lake basin; (3) identify the major spatial and temporal variations within this sediment record; and (4) relate these changes to hydrological fluctuations, climatic variation as well as other changes.

1.7 Acknowledgements

I would like to thank my supervisor, Dr. W. M. Last, for his guidance, support, encouragement and patience courteously extended throughout this thesis research. I am also grateful to Dr. J. T. Teller for his many helpful insights into the study of Quaternary geology, as well as his help with specific details and problems. Sincere thanks are due to Drs. B. J. Hann and R. E. Vance for their critical reading and assistance in preparing this dissertation.

Thanks are due to Drs. L. N. Plummer and W. E. Sanford, United States Geological Survey, for making available the geochemical simulation computer program, PHRQPITZ. Grateful acknowledgements are made to S. Mejia for assistance in carrying out the scanning electron microscopy work and to N. Ball for assistance in the X-ray diffraction analyses. Special thanks are also due to M. Malainey for the many hours she devoted to correct my English.

My studies were made possible financially by NSERC research grants awarded to Professor Last, support from the Palliser's Triangle Project of the Geological Survey of Canada, and a teaching assistantship from the Department of Geological Sciences, for which I am grateful.

The final acknowledgement is reserved for my family and friends. Throughout my entire time at University of Manitoba, my parents and family provided unwavering encouragement. Last, but not least, I would like to thank my wife, Susan S. Xu, a co-sufferer and constant supporter throughout this entire process.

Chapter 2 Regional Setting

2.1 Physiography

The northern Great Plains of western Canada is bounded by the Precambrian Shield on the north and east, and by the Rocky Mountain foothills and Cordillera on the west. This is a vast region of flat to gently rolling terrain interrupted by occasional steeply sided river valleys and punctuated by scattered groups of low hills or uplands (DMR, 1969; Richards and Fung, 1969 Prest, 1970; 1984; Bird, 1972). The major geomorphological features are the result of differential fluvial erosion of the weak bedrock and of Pleistocene glaciation. Prior to glaciation, the Prairies had undergone a prolonged interval of erosion. This produced broad northeast-trending valleys separated by low uplands. Stream deposits in the valleys were derived from the Cordillera or reworked from older Tertiary and Cretaceous deposits (DMR, 1969; Richards and Fung, 1969; Bird, 1972).

The gradual up slope east to west trend exhibited by the Canadian Prairies is interrupted by a number of sharp rises or steps. In general, these northwestward trending rises are most prominent in the south and become lower towards the north. The Manitoba Escarpment separates the Manitoba Plain on the east from the Saskatchewan Plain. The Missouri Coteau rises about 100 m above the Saskatchewan Plain on the east to the Alberta Plain on the west (Prest, 1984).

Glaciation is responsible for most superimposed features on the broader bedrock physiography. When ice advanced, the northeast drainage was dammed so that lakes developed in the valleys and depressions, and water was diverted to the south. When ice retreated, ice marginal lakes developed and steep-walled valleys were cut because meltwater flowed from one lake basin to the next or the flow was channelled southward along the ice margin. Repeated glacial and nonglacial intervals produced a complex of valley fills of different ages (Fenton, 1984; Fulton et al, 1984; Teller, 1985; 1987; Gravenor et al., 1959). Normally these glacial valleys trend east or southeast, in contrast with the large nonglacial valleys that typically trend northeastward.

2.2 Summary of Late Deglaciation History of the Canadian Prairies

The Laurentide Ice Sheet advanced to its last maximum position across South Dakota and Iowa about 14 ka ago. After this maximum advance, the ice began to retreat northward, interrupted by both stoppages and minor readvances of major ice lobes between 14 and 8 ka (Klassen, 1979; Teller, 1985; 1987; Teller and Thorleifson, 1983; Teller and Fenton, 1980). In the Canadian Prairies, a series of proglacial lakes formed mainly by ice dams. Widely distributed glaciolacustrine deposits were left on the Prairies (Wolfe and Teller, 1993). Although Late Wisconsinan deposits make up much of the surface of the Canadian Prairies and outcrops are abundant, both the location and timing of the Late Wisconsinan deglaciation limits remain controversial. In the past decade a number of regional scale histories of the deglaciation in the Prairies have been reported (Christiansen, 1979; Clayton and Moran, 1982; Klassen, 1989; Teller and Fenton, 1980). The differences among these reports are significant.

There are two general approaches to chronology and the use of radiocarbon dates among these reports. One approach advocates using all of the available stratigraphically significant dates. For example, nine ice-marginal positions have been recognized across the Prairies based on all available dates (Christiansen, 1979). The other approach suggests using only dates from wood (Teller and Fenton, 1980a; Teller et al, 1980b; Clayton and Moran, 1982). Teller and Fenton (1980) stated that dates on very fine organic matter are unreliable in areas where pre-Quaternary organic matter could contaminate the sediments. Therefore, dates based on finely-disseminated organic matter may be too old. They identified five lithostratigraphic units of Late Wisconsinan till and established the history of Late Wisconsinan glaciation and deglaciation in southwestern Manitoba.

The retreat of Late Wisconsinan ice from the Prairies appears to have proceeded by the melting of stagnant ice along broad marginal belts. Christiansen (1979) proposed an average of 60 m/a for the early stages and 275 m/a for final stages of retreat; Klassen (1983) derived retreat rates of 250 m/a and 300 m/a in northern Manitoba from varve counts and radiocarbon dates, respectively. Figure 2.1 shows the change in area of the ice sheet, area of ice-marginal lakes in southern Saskatchewan through late glacial time between 14 and 8 ka. Kehew and Teller (1994) show the history of proglacial lakes in southern Saskatchewan as related to the ice margin during deglaciation.

In southwestern Saskatchewan, by 11-10 ka, virtually all of the area was ice free. Residuals of drift-mantled stagnant ice may have remained within parts of the

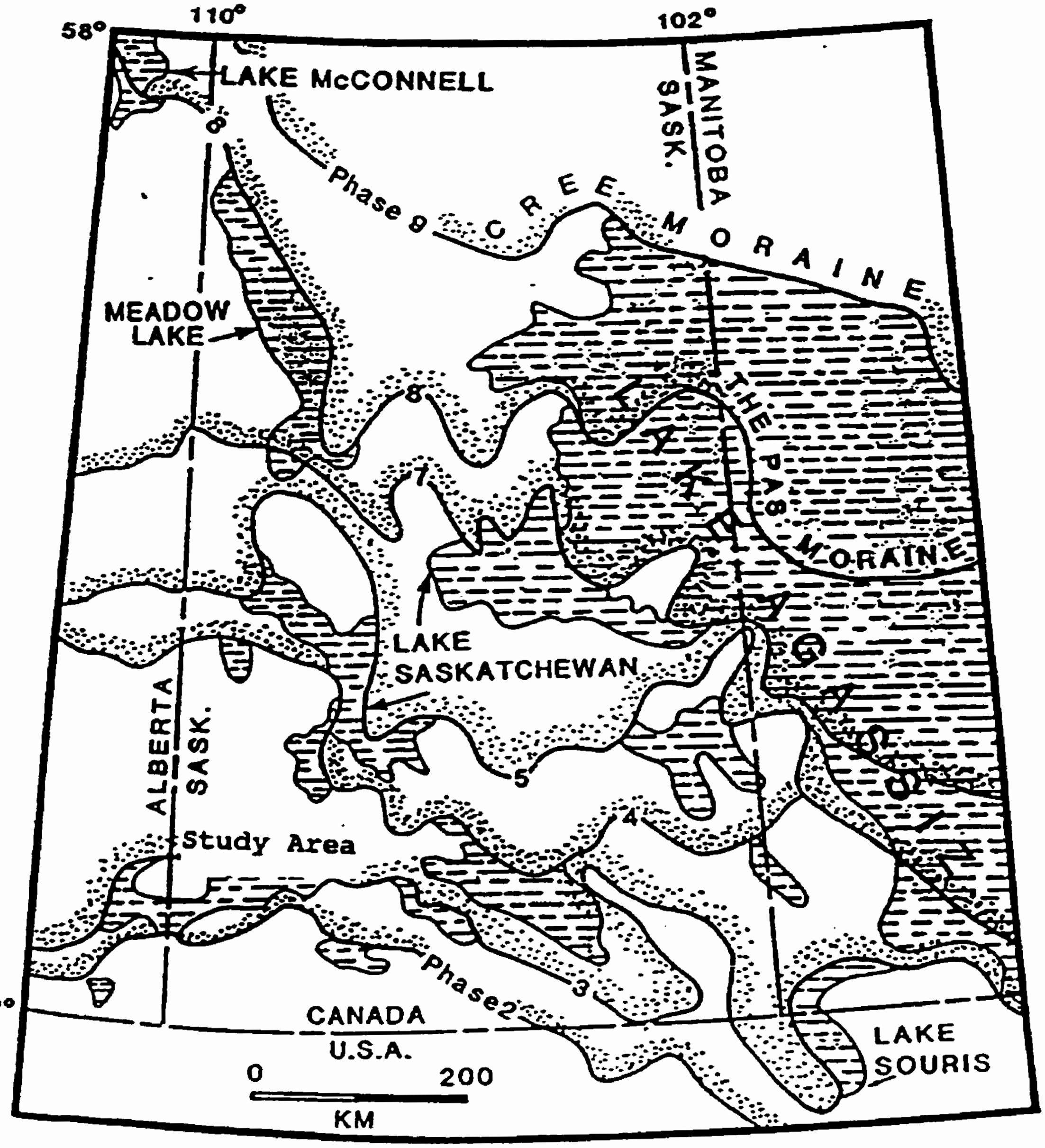

Figure 2.1 Sequence of proglacial lakes in Saskatchewan and adjacent areas (from Teller, 1987, after Quigley, 1980). The phase 2 glacial boundary represents the late Wisconsin position about 13 ka. By about 11 ka the ice had retreated to the phase 8 position

hummocky moraine belts in the area.

2.3 Study Area

2.3.1 Location

North Ingebright Lake occupies a narrow riverine basin located within the Great Sand Hills region of southwestern Saskatchewan, about 100 km west of Swift Current (lat 50°24'N, long 110°22' W) (Figure 2.2). The closed, riverine-shaped basin of North Ingebright Lake is about 3 km long and relatively narrow (<500 m), with a surface area (at normal high water level) of 1.25 km^2 (Table 2.1).

The basin probably originated about 11,000 years ago as a glacial meltwater spillway that was superposed on a buried, preglacial valley (David, 1964; Christiansen, 1979). In the 1960's 65 test holes were drilled in the Ingebright Lake area in an attempt to locate an adequate water supply for the sodium sulfate plant operation (Rueffel, 1968). The results of this comprehensive drilling program revealed that the lowest-lying areas in which the two Ingebright Lakes and a number of potholes are located is a "V"-shaped valley, incised into the bedrock, approximately 60 to 90 m deep and 240 m wide at the top. This valley may have originated as a preglacial valley or by the melting of ice during the last glacial retreat. Besides Ingebright Lakes, many other salt lakes in south Saskatchewan are also located in the preglacial valleys (Christiansen, 1967). Basal radiocarbon dates of nonglacial sediments in southwestern Saskatchewan show an average of 10,000 B.P. (Table 2.2). Therefore, it is likely that sedimentation in North Ingebright Lake

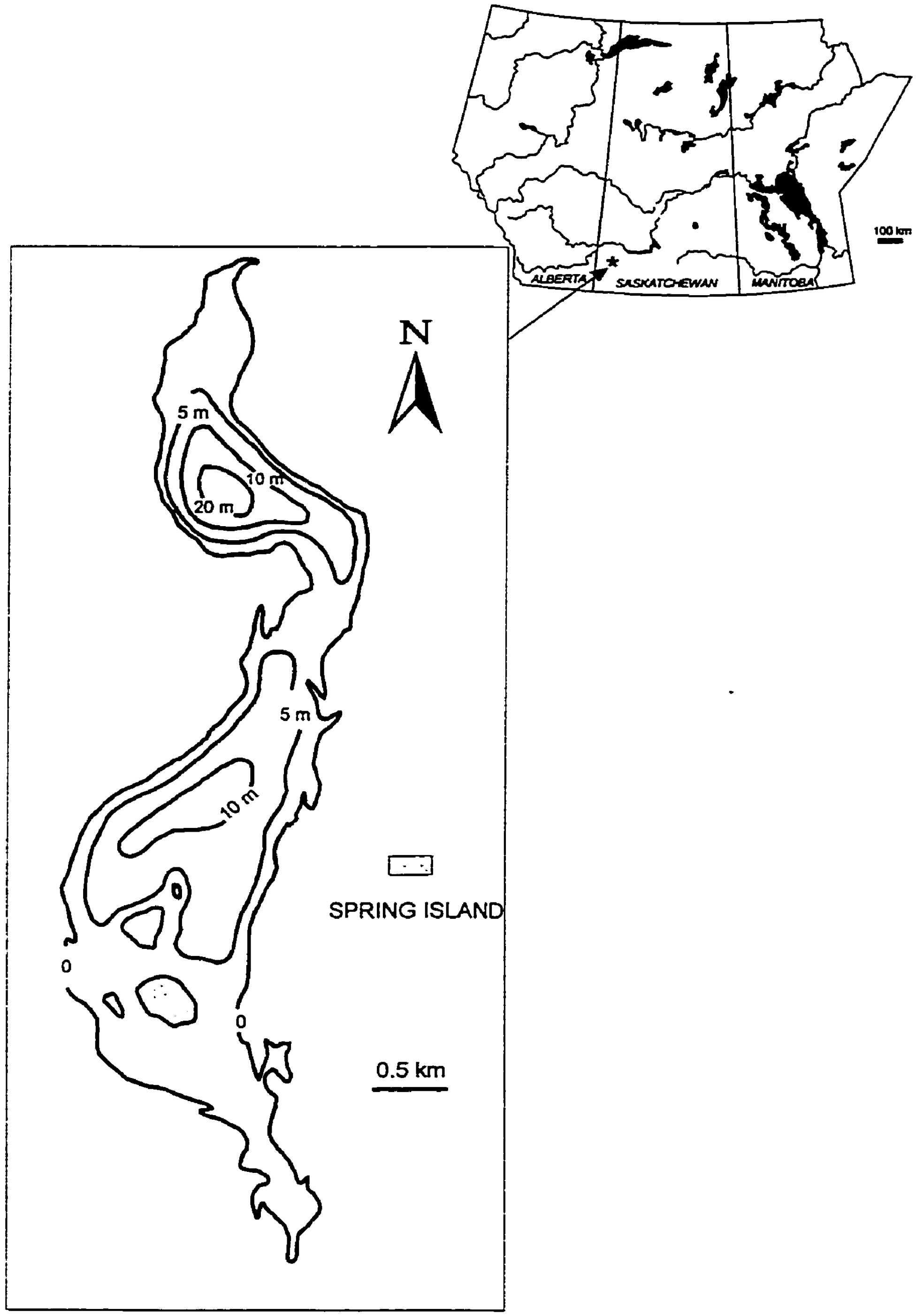

Figure 2.2 Map showing the sediment thickness of North Ingebright Lake
Inset shows the location of North Ingebright Lake in the northern Great Plains of western Canada

Table 2.1 Selected Morphometrical, Climatic, and Sediment Parameters of North Ingebright Lake

Maximum length	3 km
Maximum width	0.5 km
Area	1.25 km^2
Maximum thickness of salt sediments	>23 m
Mean daily temperature	-15°C (January)
	20°C (July)
Mean annual temperature	3.3°C
Extreme temperatures	-46°C to 45°C
Average annual precipitation	<30 cm
Average annual evaporation	>125 cm

Table 2.2 Basal Radiocarbon Dates of Nonglacial Sediments in Southwestern Saskatchewan and Adjacent Area

9,120 ± 250 B.P.	**Harris Lake** (Sauchyn, 1990; Sauchyn & Sauchyn 1991)
9,240 ± 260 B.P.	**Harris Lake** (Last & Sauchyn, 1993)
9,500 B.P. **10,000 B.P.**	**Horseman Site** (Klassen, 1994)
12,600 B.P.	**Ham Site** (Vreeken, 1994)
10,250 B.P.	**Metiskow Lake** (Wallick, 1981)
11,460 B.P.	**Val Marie Site** (Christiansen & Sauer, 1988)
9,000 B.P. **9,989 ±70B.P.**	**Clearwater Lake** (Vance, 1994; Last et al., 1997)

was initiated at about 10 ka and possibly contains a complete record of Holocene environment change.

The drainage basin of the lake is characterized by hummock to gently rolling topography. The landforms surrounding North Ingebright Lake consists of sand flats, stabilized dunes, and active dunes (Figure 2.3). Most of the sand flats and dunes have developed no drainage system, and precipitation usually percolates through the sand directly into the water table instead of accumulating on the surface (Epp and Townley-Smith, 1980). Therefore, surface runoff is weak in the North Ingebright Lake area, and sedimentation is dominated by endogenic processes.

2.3.2 Climate

The region has a cold continental climate. In winter, in response to the equatorward displacement of the Equatorial Trough and the zonal westerlies, a cold, dry Arctic air mass dominates the area. Penetration of Pacific air into the continental interior is blocked by this cold, stable air. The influence of moist tropical air is also reduced. The lowest temperature during January can reach -46°C (Connor, 1920; Currie, 1953). In summer, as the Equatorial Trough and westerlies move northwards, the influence of the Arctic air mass is limited. Both Pacific and maritime tropical air masses penetrate further into the continental interior. The climate is typically dry and windy, characterized by great temperature variation, both daily and seasonally (Currie, 1953). The average annual temperature for the Great Sand Hills region for the period 1941 to 1970 was 3.3° C (CNC/IHD, 1978), and mean annual precipitation for this same period was less than 300

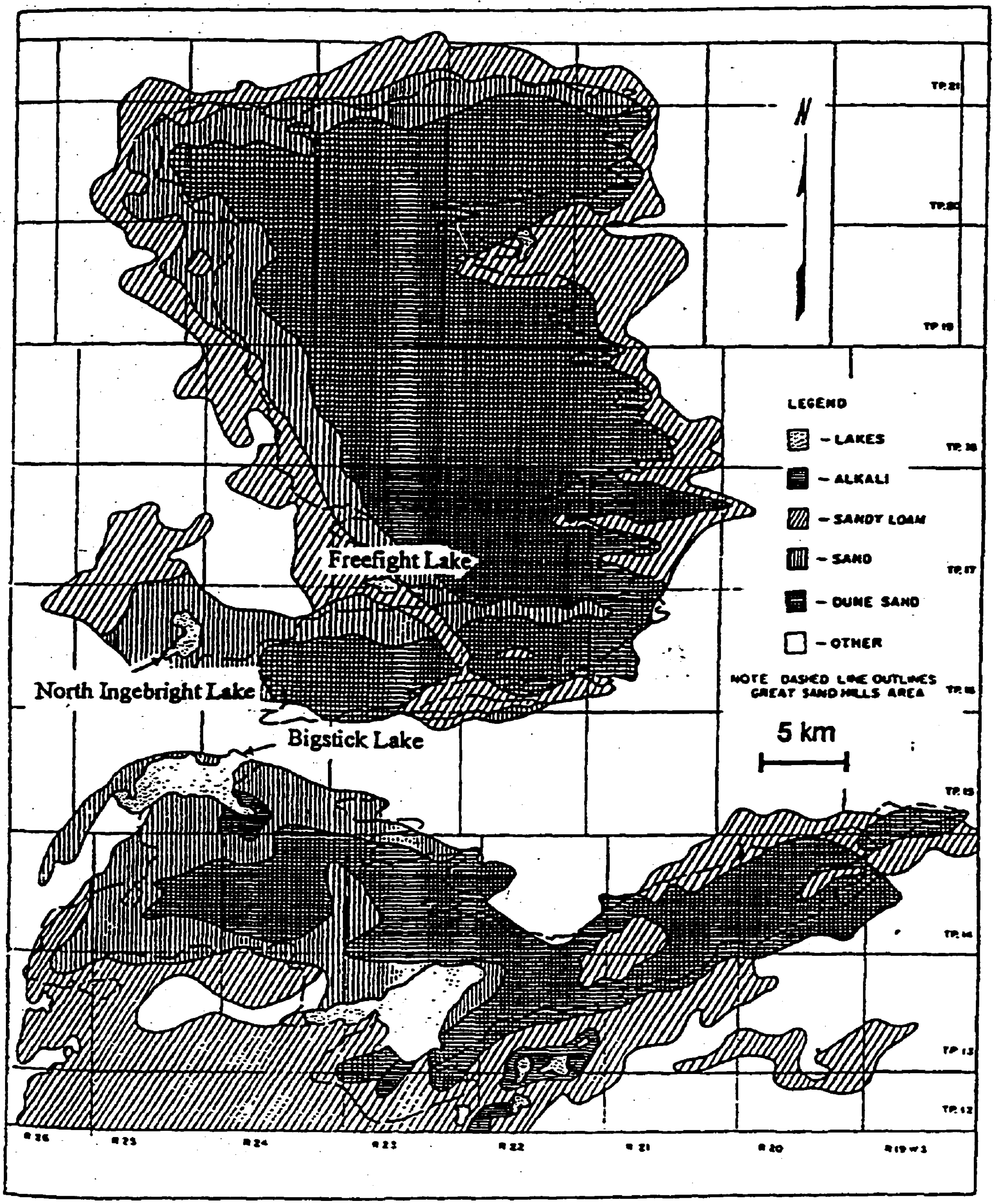

Figure 2.3 Surface deposits of the Great Sand Hills region
(From Epp and Townley-Smith, 1980)

Table 2.3 Temperature and Precipitation Data for the North Ingebright Lake Region (1941-70)

	Jan.	Feb.	Mar.	Apr.	May	June	July	Aug.	Sep.	Oct.	Nov.	Dec.	Annual
Mean daily temperature (C°)	-14	-11	-6	3.7	10.3	15	19	18	12	6.1	-4	-10	3.3
Mean rainfall (mm)	1	0.5	0.8	12.7	32.8	78	52	46	33	10	2.3	0	268.9
Mean snowfall (cm)	22	17.3	18	13.5	3.3	0.3	0	0	2.3	10	17	20	123.8
Mean total precipitation(mm)	22	17.3	18	26.2	36.1	78	52	46	35	21	19	19	299

Data from ***Environment Canada*** (1980) mm (Table 2.3). The town of Fox Valley, 20 km north of the basin, receives approximately 300 mm of precipitation annually, and has a mean daily temperature of -14°C in January and +21°C in July. Precipitation occurs as sporadic rain during the summer and as snow in the winter. Most of the precipitation occurs between May and September at the time of the most intensive evaporation. More than 125 centimetres of water evaporate annually from open bodies of water (CNC/IHD, 1978). Average annual moisture deficits are in the range of 20 to 30 centimetres as evaporation greatly exceedsprecipitation (Fremlin, 1974; Hammer, 1978).

2.3.3 Regional Geology

Southwestern Saskatchewan is underlain by nearly horizontal Phanerozoic sedimentary rocks. The Paleozoic section mainly consists of carbonate-evaporite cycles. The overlying Mesozoic and Cenozoic bedrock is dominantly a sand-shale sequence. The bedrock of the region is mantled by unconsolidated Quaternary sediment over 300 m thick in places. These deposits consist of till, fluvial sands and gravels, and lacustrine silts and clay (DMR, 1969; Richards and Fung, 1969).

Bedrock outcrops in the Great Sand Hills area are mainly concentrated on the north side along the South Saskatchewan Valley. Bedrock topography is reflected by the present day topography. The bedrock highs, which could have obstructed glacier flow and caused the development of hummocky moraines and ice-thrust ridges, have the highest elevation today. Preglacial valleys were usually filled with thick drift, with a series of sinkholes comparable in size to that of the valley. Most of these sinkholes are filled with

Table 2.4 Bedrock Stratigraphy of Great Sand Hills Area
(from David, 1964)

Time	Formations
Pleistocene or Late Pliocene	Saskatchewan gravels
Miocene-Oligocene	Cypress Hills
Eocene	Swift Current Creek
Paleocene	Ravenscrag
Late Cretaceous	Eastend Bearpaw Belly River Lea Park

shallow lakes, marking the former positions of preglacial valleys. For example, Bigstick Lake, South Ingebright Lake, North Ingebright Lake, and the sags around Johnsborough outline the buried Johnsborough valley.

The major bedrock formations are listed in Table 2.4. The Lea Park Formation consists of dark grey to black, non-calcareous shale, sandy shale, and fine-grained sand. The Belly River beds lie between the underlying Lea Park and overlying Bearpaw shales. They are comprised of fine-grained sandstone, shale, and sandy shale and uncemented sands. Along the preglacial valley, the Belly River beds directly underlie the drift.

The Bearpaw Formation consists mainly of dark grey marine shales, with layers of fine-grained sands and shaly sands. It overlies the Belly River beds and underlies the drift in most of the area. Eastend and Ravenscrag Formations appear to overlie the Bearpaw Formation and underlie the Swift Current Creek and Cypress Hills Formations. They consist chiefly of yellowish green fine-grained sand, coarse-grained silts, and grey shales (David, 1964).

Swift Current Creek and Cypress Hills Formations consist mainly of light coloured fine-grained sandstones and conglomeratic sandstones. These sandstones contain large amounts of quartzite pebbles and cobbles (David, 1964).

The Saskatchewan gravels are late Pliocene to early Pleistocene in age and are clearly preglacial. They consist of pebbles that are hard, well-rounded, and similar in appearance to the Cypress Hills Formation, from which they were derived (David, 1964).

The best preserved and most complete Pleistocene stratigraphic sections are in the buried preglacial valleys, such as Johnsborough Valleys in the Ingebright Lake area. Fine-grained preglacial sand and silt were commonly found at the base of valley fill. These sediments may have been deposited when the first ice in the area blocked the northward drainage and a preglacial lake formed in the valley (David, 1964).

2.3.4 Hydrogeology and Hydrologic Setting

North Ingebright Lake is one of a series of distinct, separate, riverine salt playas occupying a 50 km long, north-south oriented meltwater channel. Closure of the North Ingebright basin is small and a water level of more than approximately 1.5 m above today's surface will spill over to Ingebright Lake less than a kilometre to the south. The W-E spill point for the entire Ingebright-North Ingebright chain of basins is approximately 20 m above the present-day surface of the valley.

David (1964), Ruffel (1968), and Rutherford (1967, 1970) provide important regional and local groundwater and hydrochemical data of lakes in the region. Typical of most of the shallow, salt-dominated playas in western Canada, the hydrologic budget of North Ingebright Lake is dominated by groundwater inflow and evaporation. There is no perennial streamflow into this topographically closed basin and evaporation exceeds mean annual precipitation by a factor of 3 (CNC/IHD, 1978). Groundwater enters the lake via both diffuse inflow and through several discrete springs. The lake exhibits typical playa characteristics, filling with water during the spring and early summer and usually drying completely by late summer or fall. Maximum water depths are generally less than 50 cm.

David (1964) investigated the shallow groundwater and deep groundwater chemistry in North Ingebright Lake region; his data are summarised in Figures 2.4, 2.5 and 2.6. Cole (1926) analysed the chemical compositions of lake brines and spring water surrounding North Ingebright Lake basin (Figures 2.4, 2.5, and 2.6). The shallow

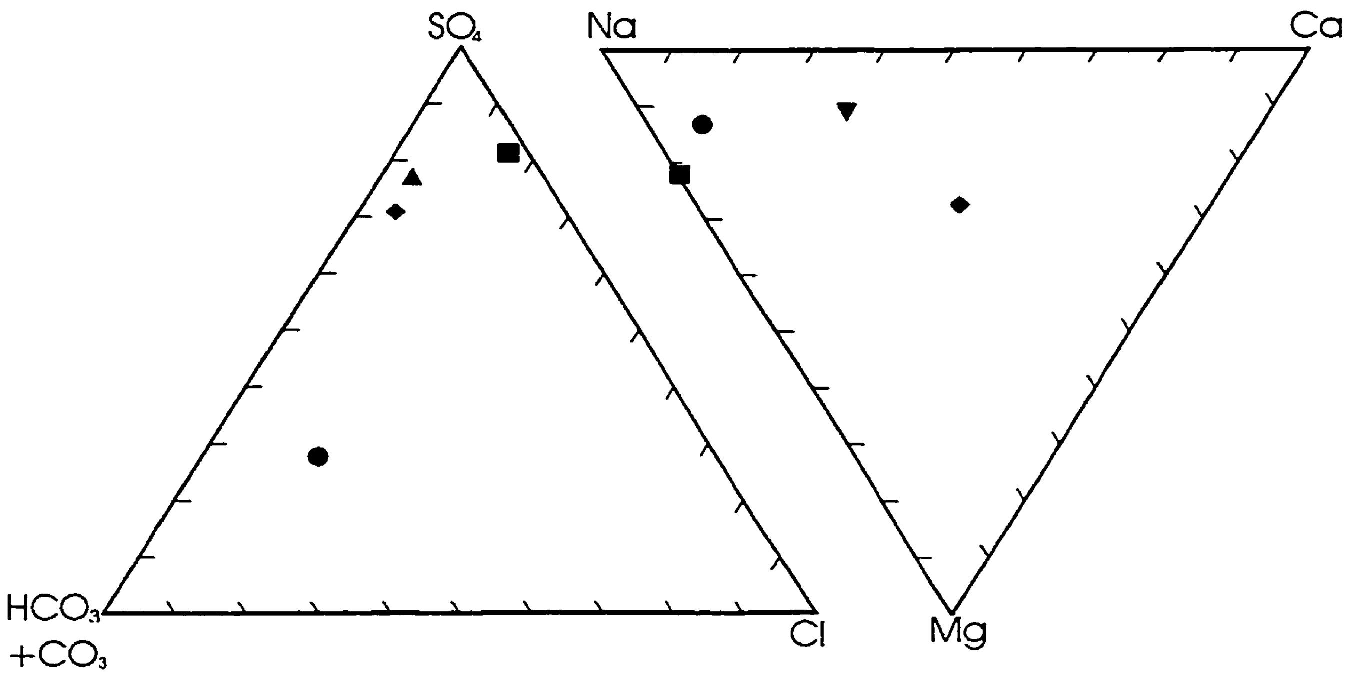

Figure 2.4 Mean water composition (milli-equivalent %) of North Ingebright Lake (■), inflowing springs(●), deep groundwater (▼)and shallow groundwater (♦)

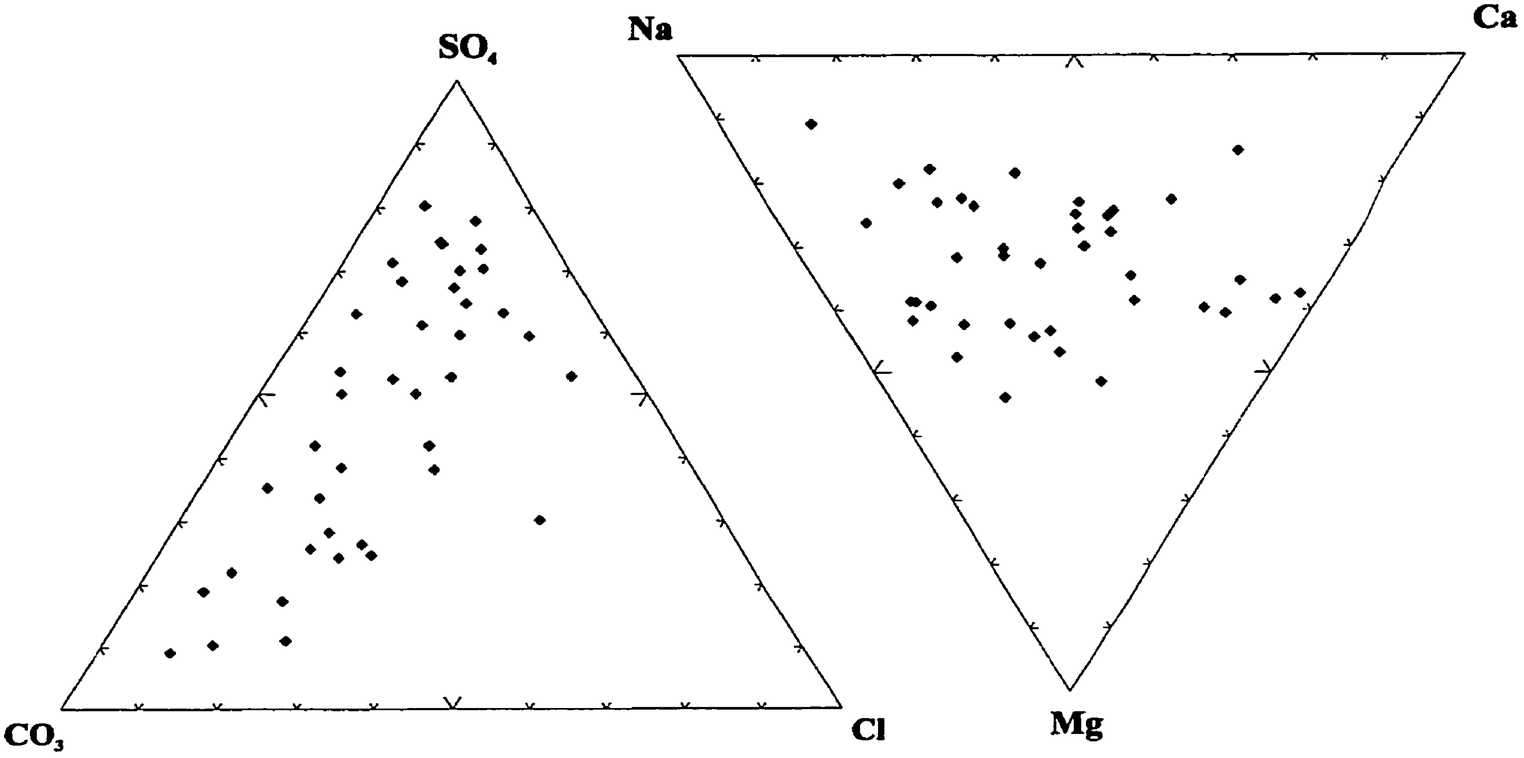

Figure 2.5 Trilinear diagrams of ionic composition (milli-equivalent %) of shallow groundwater in North Ingebright Lake region

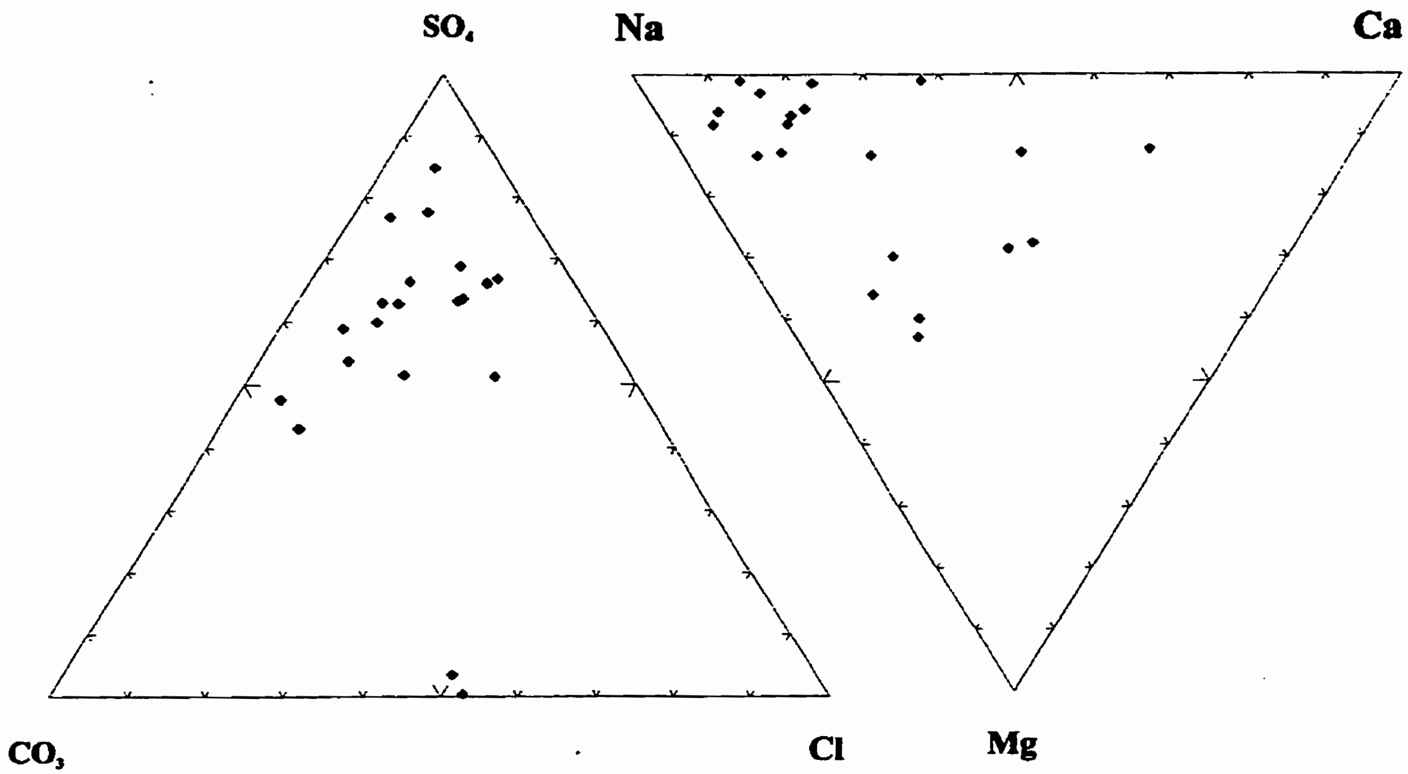

Figure 2.6 Trilinear diagrams of ionic composition (millii-equivalent %) of deep groundwater in North Ingebright Lake region

groundwater in North Ingebright Lake region has relatively low salinity, ~1.7 gl^{-1} total dissolved solids. These waters vary in composition; dominant anions tend to be SO_4^{2-} and CO_3^{2-}+HCO_3^- and the dominant cations, Na^+ and Mg^{2+} (Figure 2.5). These shallow groundwaters are slightly alkaline, with a pH of 7.8. Deep groundwaters contain 2.2 gl^{-1} total dissolved solids with a pH of 7.5. The dominant anions are $SO_4^{2-}$and the dominant cation is Na^+, sometimes with appreciable Ca^{2+} and Mg^{2+} (Figure 2.6).

North Ingebright Lake water is usually hypersaline, with salinities normally in the range of 100 to 300 g l^{-1} total dissolved solids (TDS). Although strong seasonal variation occurs in brine chemistry, the water is alkaline (pH > 8), and strongly dominated by Na^+, SO_4^{2-}, and Cl^- and nearly completely depleted of Ca^{2+} and HCO_3^-.

2.4 Modern Sedimentology of North Ingebright Lake

North Ingebright Lake is a salt-dominated playa. Except for a narrow, near shore fringe of organic-rich, fine grained and poorly sorted clastics, the modern sediments are almost entirely very soluble evaporitic salts (Figure 2.7). These endogenic precipitates of the modern salt pan sedimentary facies are comprised mainly of hydrated sodium and magnesium sulfates, including mirabilite (Na_2SO_4 $10H_2O$), bloedite [$Na_2Mg(SO_4)_2$ $4H_2O$], epsomite ($MgSO_4$ $7H_2O$), and leonhardtite ($MgSO_4$ $4H_2O$). Gypsum ($CaSO_4$ $2H_2O$), halite (NaCl), despujolsite [$Ca_3Mn(SO_4)_2$ $(OH)_6$ $3H_2O$], and protodolomite [disordered, nonstoichiometric $MgCa(CO_3)_2$] are also commonly present in small to trace amounts in the upper few centimeters. The inorganic fraction of the detrital sediments of the mudflat, sand flat and surrounding colluvium facies are composed of clay minerals (mostly illite and

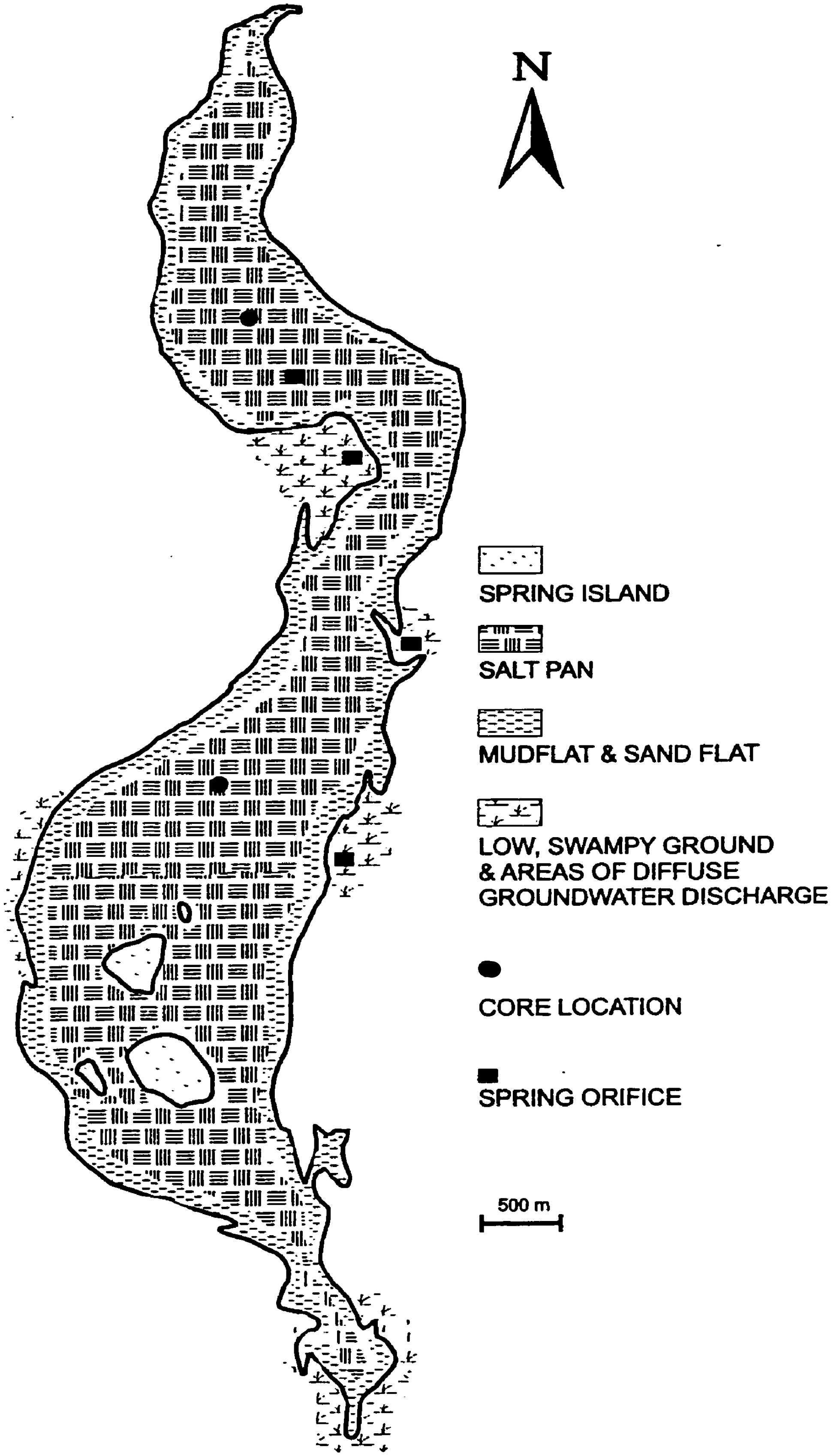

Figure 2.7 Map showing the generalized spatial distribution of modern sedimentary facies in North Ingebright Lake

expandable lattice clays), feldspars, carbonate minerals (mainly dolomite), quartz, and ferromagnesian minerals.

Modern sedimentation in North Ingebright Lake is controlled to a major degree by the seasonal (or periodic) sequence of flooding, evaporative concentration, and desiccation of the playa surface. The process sedimentology of the basin, like many other saline playas in the region, is dominated by: (a) formation of salt crusts, efflorescent crusts, spring deposits, and intrasedimentary salts, (b) subaqueous cumulate and bottom salt precipitation, (c) physical reworking and redistribution of clastic salt and accretionary salt grains, (d) formation of salt cements, (e) irregular dissolution of surface salt crusts and formation of solution pits on the playa surface and within the near-surface sediment, (f) formation of karst chimneys, and (g) mud diapirism and subsequent reworking of fine-grained siliciclastic material. These processes are discussed in detail in Last (1984, 1989, 1993).

Chapter 3 Methodology

3.1 Core Acquisition

3.1.1 Drilling Site Selection

Coring locations were determined by the following factors: expected sediment thickness, site distribution, and the need to avoid salt karst. Two drilling sites were initially chosen on the basis of a preliminary isopach map of the total salt thickness in North Ingebright Lake constructed by Cole (1926). In order to maximize the possibility of obtaining a continuous record, both sites are located on the thickest part of lake sediments where it was anticipated that the most complete and continuous stratigraphic record would likely exist (Figure 3.1).

3.1.2 Drilling Techniques

Several different drilling and coring methods were available for obtaining core samples. The decision of which to use was dependent on a number of criteria. The most important of these were: (a) the types of sediment to be recovered; (b) the types of data required; and (c) the depth of interval required for data collection. The major techniques commonly used in core acquisition for paleolimnological research are listed in Table 3.1.

Hand-operated Livingstone coring and hand augering are usually used to retrieve cores of relatively short length (4 m or less). Bombardier-mounted and power driven Shelby tube coring is designed to retrieve cores in long sequences; however, both are limited to coring relatively soft, unconsolidated muds (Last,

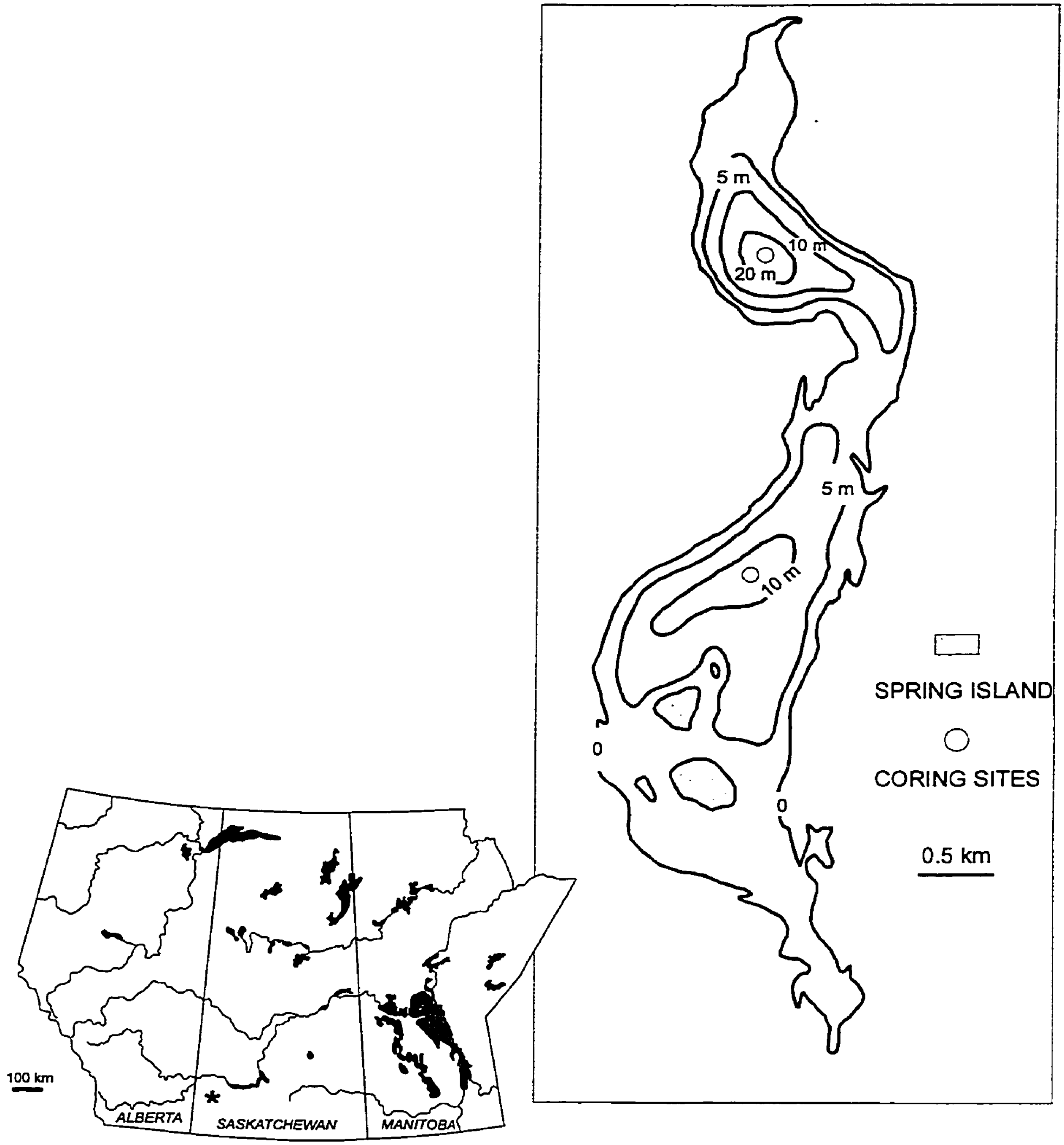

Figure 3.1 Map showing the sediment thickness distribution and the location of coring sites in North Ingebright Lake. North is toward the top of the map. Inset shows the location of the lake within the northern Great Plains of western Canada.

Table 3.1 Core Acquisition Techniques

1. Hand Operation Technique

Livingstone Coring

Hand Auger

2. Shelby Tube Coring

3. Rotasonic Drilling

4. Vibra-Coring Technique

5. Diamond Drilling Technique

Diamond Drilling Water Cooled

Diamond Drilling Air Cooled

1980). Because the sediments of North Ingebright Lake consist of very well consolidated salt, hand-operated Livingstone coring and Shelby tube coring techniques would not be able to penetrate the consolidated sediments.

Rotasonic drilling is a widely-used overburden drilling method for stratigraphic investigations and mineral exploration. With this drilling technique, a tungsten carbide-tipped core barrel string is drilled into the sediment, and then a tungsten carbide-tipped casing string is drilled outside of the core barrel string (Thorleifson and Kristjansson, 1993). The drill utilizes a combination of downhole pressure, rotary motion and ultrasonic vibration to penetrate both unconsolidated sediment and rock. However, rig time and tool rental costs make rotasonic drilling an expensive operation (Thorleifson and Kristjansson, 1993).

Vibra-coring technique, as the name implies, involves the use of intensive vibration to penetrate the sediment. This system consists of a powered concrete vibrator, drill pipe and liner or thin-walled aluminum irrigation tubing (Lanesky et al., 1979). The vibrator produces a low amplitude (0.1-1.0 mm) standing wave in the core tube. This standing wave fluidizes and displaces sediment adjacent to the core tube and allows it to pass through the sediment without resistance. Vibra-coring can only be used for acquisition of continuous cores up to 13 m in length in unconsolidated sediments (Lanesky et al., 1979).

After an extensive investigation of various drilling and coring techniques employed over the past ten years (Lanesky et al., 1979; Last, 1980; Thorleifson and Kristjansson, 1993), the wireline diamond drilling technique was chosen on the basis of equipment capability and cost.

3.1.3 Diamond Drilling

The drilling assembly for conventional coring consists of two parts: the core head or bit and the core barrel. Unlike drill bits, core bits do not cut a complete cylinder of formation. Instead, they are designed to cut an annular ring of formation, leaving a solid cylinder of uncut formation to pass through the centre of the bit into the core barrel.

Conventional diamond drilling uses a water-based circulation fluid to carry the cuttings away from the bit and to cool it. This water-based fluid would have dissolved the salt, resulting in poor core recovery. Therefore, I used a drilling system that circulates air, rather than water, to carry the cuttings and cool the bit. This method uses standard diamond drilling drill rods and wire-line core barrel. The bit has large surface set diamonds, modified water ways, and cuts a slightly larger borehole diameter than standard bits. These modifications of the bit are made to allow the use of air, rather than water, as the circulation medium. Because of the high cost and comparatively infrequent use of diamond core bits, a drilling operation is rarely equipped with a supply in all types and sizes. Commonly the core size is 63.5 mm.

A core barrel has a reaming shell following the bit near the bottom of the core barrel, and a stabilizer at the top of the core barrel (Figure 3.2). The purpose of these is to contact the borehole walls, and provide stability to the core barrel while it is rotated. The drilling apparatus uses a sequence of casing bits and core barrels in one or more 5 ft.(1.5 m) lengths. The drill utilizes varying intensities of rotation and downhole pressure to obtain a continuous core of material ranging from soft

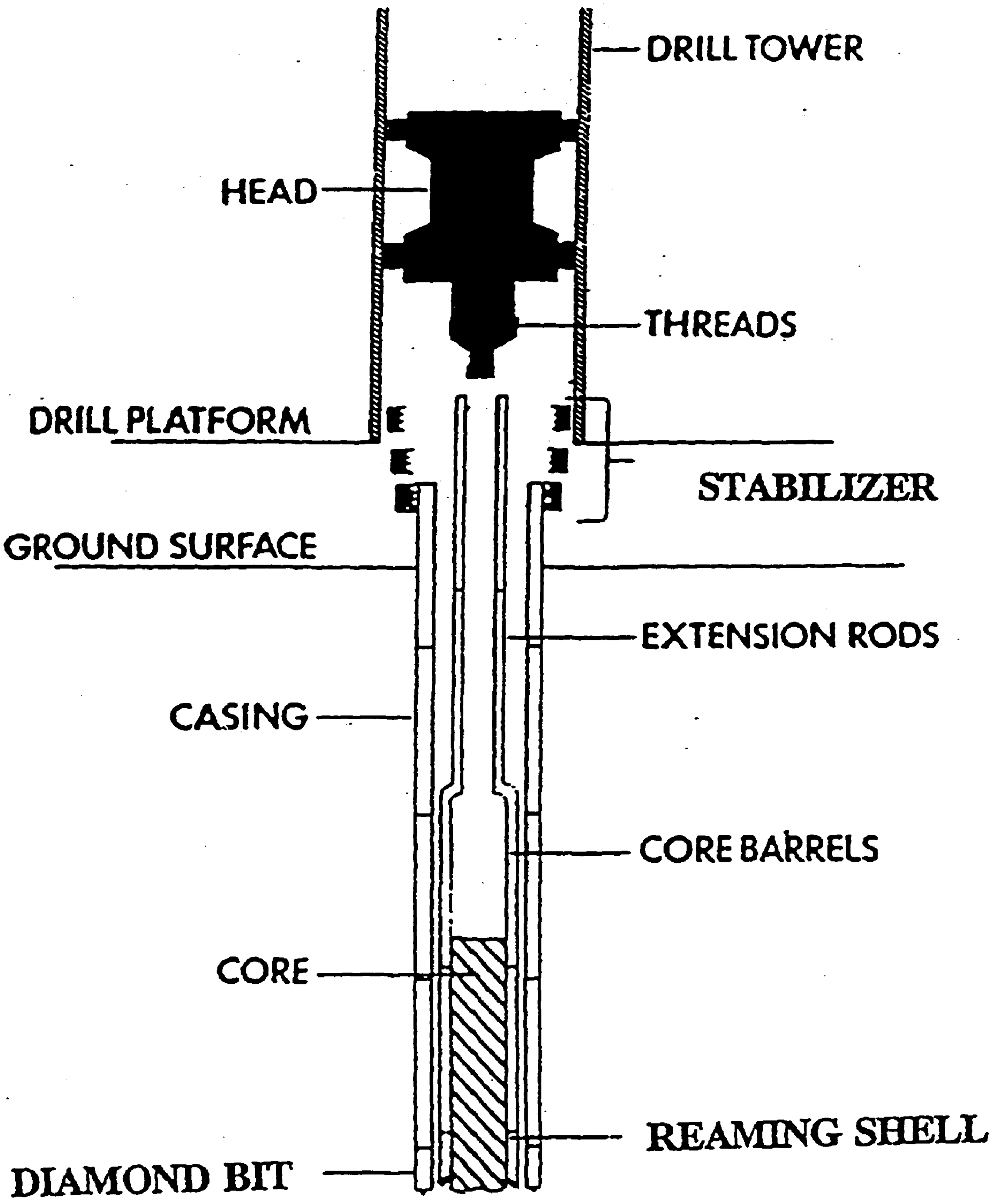

Figure 3.2 Schematic diagram of a diamond drill with air circulation system.

mud to hard salts. Any changes are made slowly and carefully. Sudden changes in drilling parameters (rotary speed and pump pressure) may damage the core bit or cause the core to break. The top unconsolidated sediment was cored without pumping air, but hard salt required the core to be recovered and drilling to be resumed with air pumped down the rods and core barrels to cool the bit. In tough, compact sediments, resistance against both the outer and inner walls of the core barrel dictated that the bit must occasionally be raised so that air reaches the bottom of the hole and "lubricated" drilling. Coring was completed in 5 ft.(1.5 m) increments as the casing and rods were added. Before the core was recovered, the casing was advanced to, or nearly to, the depth of the bit. The rods and then the core barrels were recovered and the core was extruded from each successive 5 ft.(1.5 m) core barrel into 5 ft.(1.5 m) long core boxes. The core barrels were raised and the core was extruded in most cases at 5 ft. intervals. These abnormally short drilling runs were dictated by the resistance exerted by the highly compact salt against the inner wall of the core barrel. The recovered core was usually found to be shorter than drilled depth due to missing or dissolving. Depths were assigned by interpolating between the top and bottom of each run.

3.1.4 Coring

In February, 1994, two boreholes were drilled at North Ingebright Lake. The sediment cores were retrieved using Mobile S-61 Drill, mounted on a Nodwell (all terrain) carrier (Figure 3.3). A core, approximately 23 m in length, was retrieved from the first borehole, and one 9 m in length was taken from the second borehole. Core

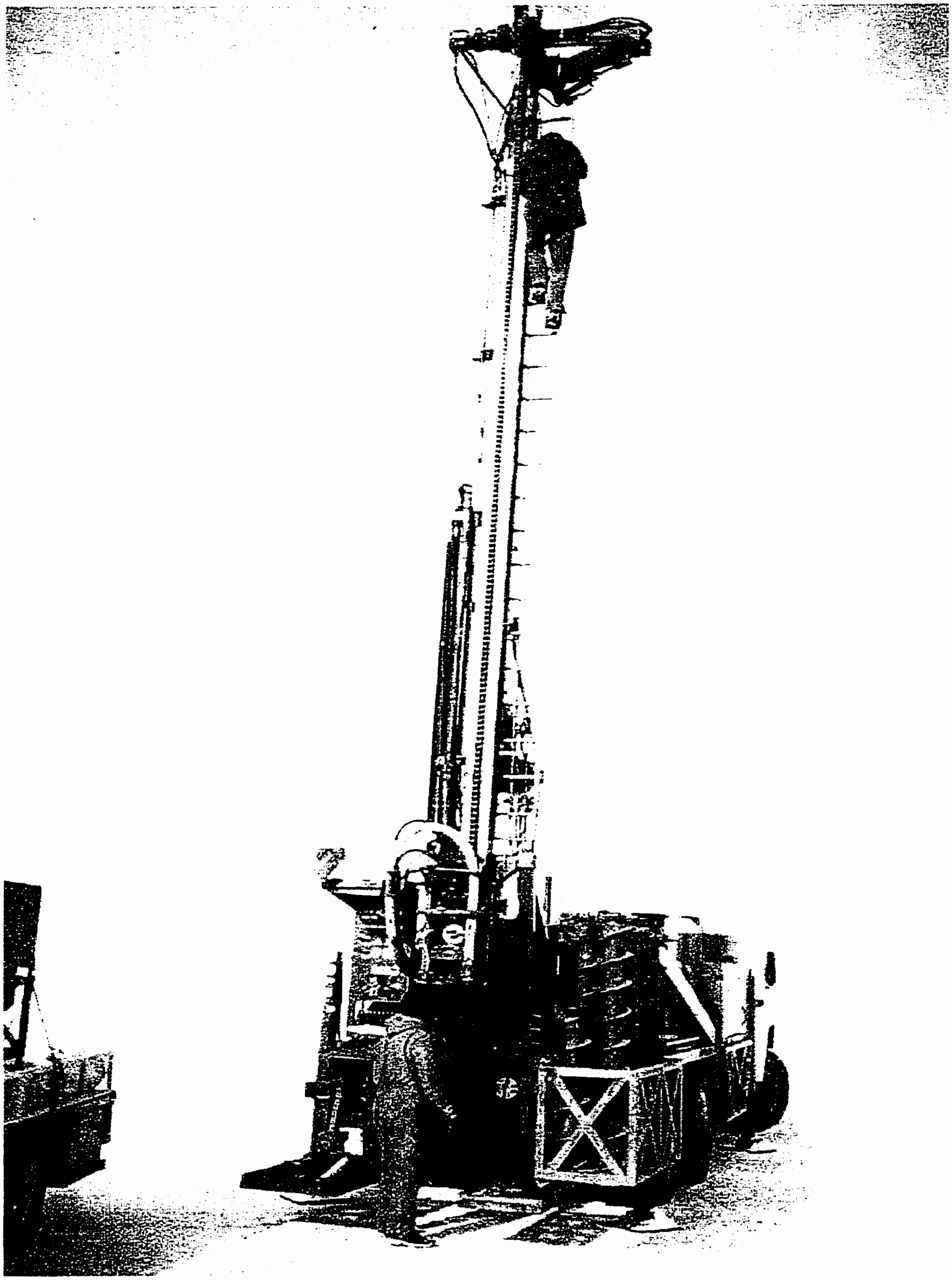

Figure 3.3 Compressed-air diamond drill at North Ingebright Lake (February 17, 1994)

recovery averaged about 85%. This wireline diamond coring work was done by Paddock Drilling Ltd of Brandon.

Immediately upon retrieval of the core from the lake, the cores were stored in the sample box (5 feet long) and labelled with respect to site number and depth below the surface (sediment/water interface). Sealed cores were transported to the University of Manitoba for physical, chemical, and mineralogical analyses. Prior to detailed subsampling, the cores were placed in cold storage in the Department of Geological Sciences, University of Manitoba.

3.2 Laboratory Analyses

The cores were photographed, described, and subsampled in the Sedimentology lab. Figure 3.4 shows a generalized procedure of sediment description, subsampling, and lab analysis. A 2 cm subsampling interval was used for the two cores in this study. About one-half of the core was retained to provide raw, unprocessed sediment for ^{14}C dating and additional analyses. This section of the core is also to be used for future paleolimnological research such as fluid inclusion research or biological research. No doubt the sediment record contains a wide variety of additional climatic information of which we are not yet aware, or which cannot be interpreted at present.

The other half of the core was subsampled for physical, chemical, and mineralogical analyses. Total of 1338 subsamples were prepared. These subsamples were analysed for bulk mineralogy, detailed carbonate mineralogy, detailed evaporite mineralogy, organic matter content, and total carbonate content.

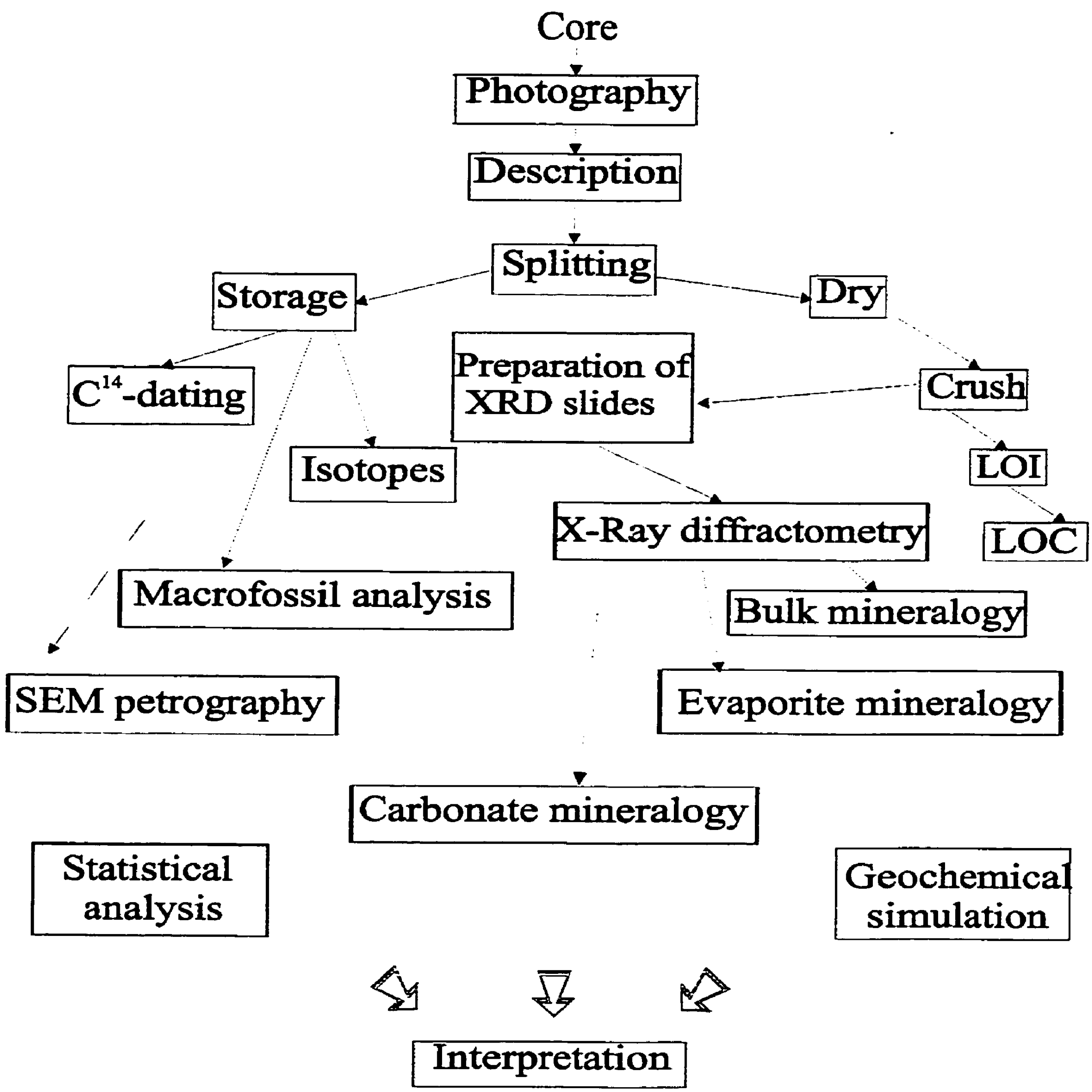

Figure 3.4 Generalized procedure of sediment description, subsampling lab analysis, and data treatment.

microstructure and morphology.

The number and types of sediment parameters selected for investigation were mainly based on: (a) potential importance of decoding and characterizing the paleohydrological fluctuation and paleoclimatic change; (b) availability of equipment and technical expertise within the departmental laboratories; and (c) budgetary restraints. Table 3.2 summarizes major sediment parameters which were analysed in this research.

3.2.1 Organic Matter Content

Organic matter content was determined by measuring weight loss upon heating, known as weight loss-on-ignition (LOI). Air dried sediment subsamples were heated for one hour at 400°C-500°C. Organic matter content is calculated using the following equation: [(weight of sample before heating)-(weight of sample after heating to 500°C)/(weight of sample before heating)] x 100 (Last, 1980).

3.2.2 Total Carbonate Content

After measurement of organic matter content, the subsample was heated further to 1000°C for another hour. The total amount of carbonate minerals in the sediments was measured by the weight loss-on-combustion (LOC) of a portion of the oven-dried sediment: [(weight of sample LOI)-(weight of sample after heating to 1000°C)/(weight of dry sample before heating)] x 100. The weight loss is expressed as a percentage of the oven-dry-weight (Last, 1980).

Table 3.2 Summary of Evaluated Sediment Parameters

Thermal Analyses	Mineralogy	SEM	Geochemistry	Isotope	Statistics
Organic matter content	Allogenic mineralogy Carbonate mineralogy	Microstructure	Major ion ratio	C^{14} dating	Factor analysis Correlative analysis
Total carbonate content	Evaporite mineralogy	Morphology	Numerical simulation		

Selected samples were examined using scanning electron microscopy to determine

3.2.3 Chronology

The chronostratigraphy of the recovered sequence of salts from North Ingebright Lake is only poorly constrained owing to the paucity of datable material. Large quantities of core were processed and examined in an unsuccessful attempt to find datable, well-preserved upland and shoreline macrofossils. The absence of macroscopic organic remains in the core necessitated the use of finely disseminated organic matter from two samples in order to establish a preliminary chronostratigraphy for the recovered sedimentary sequence. There are 3 ^{14}C dates from the lake sequence. A ^{14}C age of 5544 ±66 years was determined on disseminated organics from the base of the Muddy Mg-Calcite--Na-Sulfate Unit at 3.2-3.4 m depth and a sample of disseminated organics from the base of the Na-Sulfate Unit at 22.1-22.9 m depth yielded a ^{14}C age of 10,250 ±150 years. In addition to the two radiocarbon dates from this core, a sample of endogenic carbonate material from the Ca-Sulfate--Na-Sulfate Unit at the base of a 9 m long core in the southern portion of the basin yielded a ^{14}C date of 8240 ±120 years. Further temporal control is provided by the presence of a borate mineral zone (inderborite) at 5.6 m depth which may be an indication of a diagenetically-altered volcanic ash interval corresponding to the 6800 year B.P. Mazama eruption.

The organic matter samples from the cores were prepared for C^{14} dating by separating the finely disseminated organic material and clay-size material from the soluble evaporite minerals. The procedure is as follows: first, the sediment sample is heated at 32°C until completely dehydrated and remove liquid brine. Distilled water is added and the sediment is allowed to sock for one hour. The water is then removed and the sediment sample dehydrated again. This procedure is repeated until all the soluble salt is removed.

3.2.4 Mineralogy

The mineralogy of the sediment of North Ingebright Lake was quantitatively measured by X-ray diffractometry (Philips PW1710). An unoriented sample was prepared by packing the finely powdered subsample onto a glass slide. Traces were run by using nickel-filtered copper radiation generated at 40 kilovolts and 40 milliampere, 1° beam slit and a 0.006 inch detector slit. Each slide was irradiated in one direction from 3° two theta to 65° two theta.

A diffracted beam is produced when the Bragg law or the Laue equations are satisfied. The resulting diffraction pattern of a crystal, comprising both the positions and intensities of the diffraction effects, is a fundamental physical property of substances. Each substance in the mixture produces its pattern independently of the others. The diffraction pattern indicates the state of chemical combination of the elements in the sample. It serves not only for the speedy identification but also for the complete elucidation of mineral structure (Last, 1980; Klug and Alexander, 1974; Rosyse et al., 1971; Schultz, 1964).

After the X-ray diffraction pattern was obtained, the three strongest refection peaks were converted from 2θ angles to d-spacing values. A search to match the d-spacing values of the unknown pattern to those in given index book (PDF) is undertaken. The proper mineral identification can be made on the basis of the best match.

The abundance of minerals is determined from the strength of the strongest X-ray diffraction peak for each mineral on the X-ray trace of the unoriented powder. Mineral determination is aided by the use of an automated peak-match computer program-μPDSM (micro Powder Diffraction Search/Match). This computer program can carry out the entire searching-and-matching process using the reference data collected by the JCPDS-International Centre for Diffraction Data. It contains a complete package of functions designed to assist researchers in the analysis of diffraction patterns. The input information consists of the d (d-spacing) and I (intensities) values for the lines in the pattern and elemental information about the sample. The output of program lists the experimental diffraction data juxtaposed with 10-20 of the most intense lines for each standard matched (uPDSM User's Manual, 1992; Chen, 1977).

3.2.5 Geochemical Simulation

In the past decades, the thermodynamic modelling of equilibrium-reaction has experienced two generations of development. Early computer programs of chemical models include WATEQF (Truesdell and Jones, 1974; Plummer et al., 1976), WATEQ2 (Ball et al., 1979), and SOLMNEQ (Kharaka and Barnes, 1973). These models use extended Debye - Huckel activity coefficients and can match experimental data up to ionic strengths of about 10; however, for highly concentrated solutions, these extended Debye-Huckel models are in poor agreement with experimental data (Harvie and Weare, 1980; Weare, 1987).

Recently, Harvie et al. (1980; 1984) developed a new interaction model based on Pitzer's phenomenological equations which can be used to describe complex aqueous systems to high concentration and for a range of temperatures up to 250°C (Weare, 1987). This model places a larger emphasis on solubility data than other models. It is intended for the prediction of mineral solubility in natural water systems. The agreement of model phase diagram with measurements is within experimental error. With extensive validation with laboratory data, the model can be applied with confidence to field settings.

At present, there are two computer programs available for this model: ACTIVITY and PHRQPITZ. ACTIVITY was written by J. S. Hanor, Louisiana State University; PHRQPITZ was developed by L.N. Plummer and others (1988). They can be run so that a solution can be kept in equilibrium with a designated set of minerals. The model monitors how much of each mineral precipitates or dissolve. Different options, such as solute input and leakage ratio, can be chosen to fit the specific study. When the regional hydrological system surrounding a lake is well known, ACTIVITY/PHRQPITZ can generate various mineral sequences with different thickness by changing the ratio of the different source inputs. By comparing the results of the chemical model with that in the field sequence, a more lealistic scenario of the hydrological history of lake basin can be developed. In this study, the computer code PHRQPITZ was used to establish the sequence of evaporite mineral precipitation and hydrological history of North Ingebright Lake.

3.2.6 Statistical Methods

Various statistical analyses were used to evaluate the interrelationships among the sediment parameters of North Ingebright Lake in this study. First, the linear correlation coefficient matrix (Table F-1) was calculated from a data set consisting of twenty-one mineralogical and geochemical variables from the cores of North Ingebright Lake. Second, the same data set underwent cluster analysis to test the homogeneity of the data population in each lithostratigraphic unit. Using the results of this analysis, a factor analysis of seventeen mineralogical variables was carried out. The results are discussed in Appendix F. All these multivariate statistical analyses of the sediment data set were undertaken using the various subroutines of SAS package (University of Manitoba Unix system).

Chapter 4 Lithostratigraphy of North Ingebright Lake

4.1 General Description

Playa lakes in southwestern Saskatchewan show a tremendous diversity in size, basin morphology, hydrochemistry, and sedimentary characteristics. No two playa basins have an identical stratigraphy (Last and Slezak, 1987; Last, 1983; Egan, 1984). Despite this broad variation, some generalized stratigraphic associations still can be made due to their approximately synchronous glaciation-related origins. The stratigraphy of a typical Saskatchewan hypersaline playa lake exhibits a three-layer structure: black mud at the bottom, indurated crystalline salts in the middle, and muddy salt at the top (Last and Slezak, 1987; Egan, 1984). The stratigraphic sequence retrieved from North Ingebright Lake also shows a similar three-layer structure. One core, the 23 m core, is mainly composed of indurated sulfates in the bottom and organic-rich muddy salts in the top. This core does not extend down to the bottom black mud association; however, the second core (9 m) constitutes a complete three-layer stratigraphic structure. The black mud unit directly underlies the salt unit and consists of highly reducing, fine-grained sand, silt and clay.

In general, the two sediment cores recovered from North Ingebright Lake are composed of structureless, colourless, and well indurated salt, with small amounts of mud and organic debris (Figure 4.1). The section is remarkable in its lack of obvious bedding, colour variation or other visible sedimentary features (Figure 4.1,

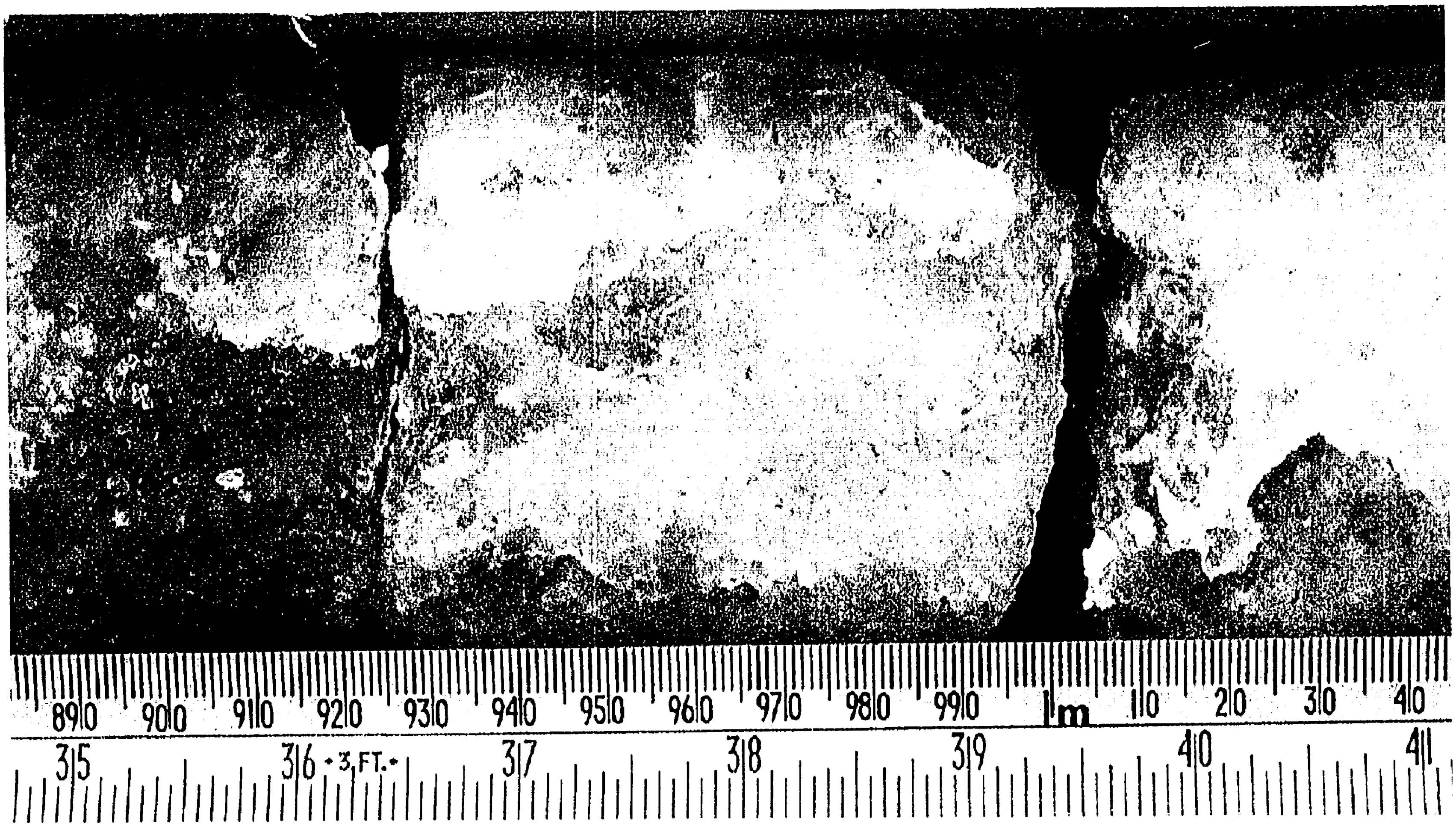

Figure 4.1 Structureless, colourless, and indurated salt (north core: 20.5-20.66 m) in North Ingebright Lake

Appendix E). The degree of compaction and crystal size generally increase downward. The upper part of the core is dominated by friable and fine crystalline salts, whereas at depth the sediment is very well consolidated and coarsely crystalline salts.

Based on the sediment texture, bulk mineralogy, detailed carbonate and evaporite mineralogy, and organic matter content of the cores, eight lithostratigraphic units were recognized and named on the basis of their dominant composition. Usually, the contacts between units are not visually distinctive and are gradational. Unit boundaries were defined on the basis of variation in the mineralogy/mineralogical composition. Table 4.1 and Figures 4.2-4.11 summarize the variation of major and minor mineralogical composition in eight salt-dominated stratigraphic units. When examined and analysed in detail, the salt sequence (units 1-8) can be further subdivided into 31 individual zones based on the composition of the later stage evaporate minerals (Table 4.2, Appendix C). Each zone is distinguished by a specific suite of chemical precipitates that indicate significant differences in the chemical nature of the lake at the time of their deposition.

In the following sections, characteristics of different lithostratigraphic units are summarized from two cores. However, determination and description of each mineral zone in the salt sequence is largely based on the 23 m long north core because of its continuity and central location in the lake basin.

Table 4.1. Summary of average characteristics of mineral composition in North Ingebright Lake Cores (includes north and south cores; nc: not calculated; nd: not detected)

	Stratigraphic Unit								
	1	2	3	4	5	6	7	8	Average
% Total Clay Minerals	40.9	0.3	6.7	12.2	6.2	0.6	6.9	3.4	5.2
% Quartz	25.2	<0.1	0.6	1.2	1.5	1.2	3.6	9.9	2.6
%Total Feldspar Minerals	14.6	0.2	1.8	0.5	11.8	3.4	1.1	2.7	3.1
% Potassic Feldspars	1.6	<0.1	0.1	0.1	0.4	<0.1	0.5	1.8	0.4
%Plagioclase	13	0.2	1.7	0.5	11.4	3.4	0.6	0.9	2.7
% Total Calcite	nd	<0.1	0.1	0.1	0.1	<0.1	0.7	0.3	0.2
% Low-Mg Calcite	nd	<0.1	<0.1	<0.1	0.1	<0.1	0.1	<0.1	<0.1
% Magnesian Calcite	nd	<0.1	0.07	0.1	0.1	<0.1	0.7	0.3	0.2
mol% $MgCO_3$ in Mg-calcite	nc	nc	8.7	6.3	9.4	12.2	13.4	11.4	10.4
% Total Dolomite	4.5	0.1	1.6	2.0	1.3	0.4	3.4	11.9	3.1
% Stoichiometric Dolomite	4.1	0.1	0.3	0.6	0.6	0.2	1.8	2.0	0.8
% Protodolomite	0.4	0.1	1.2	1.4	1.7	0.3	1.6	9.9	2.3
mol% $CaCO_3$ in Protodol.	nc	nc	62.6	63.8	62.5	60.3	54.3	60.1	60.9
% Magnesite	nd	0.1	1.0	1.0	0.4	<0.1	0.1	nd	0.4
% Aragonite	nd	<0.1	0.3	0.2	0.1	<0.1	0.1	<0.1	0.1
%Ca-Sulfates	3.2	1.3	3.5	17.2	5.6	0.6	6.8	1.8	5.1

% Na-Sulfates	12.8	98.9	83.9	65.5	72.1	93.7	76.3	65.8	79.5
% Mg-Sulfates	nd	0.2	0.4	0.1	<0.1	<0.1	0.3	4.2	0.7
% Chlorides	nd	<0.1	0.1	<0.1	<0.1	<0.1	<0.1	<0.1	<0.1
% Pyrite	nd	nd	<0.1	nd	nd	nd	nd	nd	<0.1
% Allogenic Fraction	83.2	0.53	9.4	14.5	20.1	5.4	13.3	18.2	11.6
% Endogenic + Authigenic	16.8	99.5	90.6	85.5	79.9	94.6	85.8	81.8	88.2
% Total Organic Matter	22.7	0.34	1.4	2.5	1.9	0.6	2.5	5.3	2.1

Table 4.2 Stratigraphic units and mineral zones in North Ingebright Lake cores.

UNIT	MINERAL ZONE	DEPTH (m)	SALT MINERAL ASSEMBLAGES Major	Ancillary	Minor & Trace
8 Dolomitic Na-Sulfate	3	0.1-0.4	Bloedite Protodolomite Thenardite	Gypsum Mg-calcite	Ankerite Benstonite Leightonite Minrecordite
	2	0.4-0.8	Protodolomite Thenardite	Gypsum Mg-calcite	Bichofite
	1	0.8-1.2	Thenardite	Bloedite Mg-calcite Protodolomite	Hanksite Niter
7 Muddy Mg-calcite--Na-Sulfate	3	1.2-1.6	ProtodolomiteThenardite	Gypsum Mg-calcite	Arcanite Artinite Hanksite
	2	1.6-2.4	Gypsum Thenardite	Aragonite Bloedite Gypsum Magnesite Protodolomite	Arcanite Hanksite Mercallite Rapidcreekite
	1	2.4-3.4	Gypsum Thenardite	Mg-calcite Protodolomite	Benstonite Epsomite Görgeyite Hanksite Mercallite Polyhalite
6 Na-Sulfate	3	3.4-3.9	Thenardite	Aragonite Gypsum Protodolomite	Hanksite Tychite
	2	3.9-4.1	Thenardite	Gypsum Protodolomite	Niter
	1	4.1-4.5		Protodolomite	Hanksite Niter
5 Muddy Na-Sulfate	5	4.5-4.9	Thenardite	Mg-calcite Magnesite Protodolomite	Hanksite
	4	4.9-5.6	Gypsum Thenardite	Aragonite Mg-calcite Protodolomite	Arcanite Hanksite Inderborite
	3	5.6-6.2	Thenardite	Gypsum Magnesite Protodolomite	Arcanite Gaylussite Hanksite Sepiolite Wattevilleite
	2	6.2-7.2	Gypsum Thenardite	Aragonite Protodolomite	Arcanite Hanksite Polyhalite Sepiolite
	1	7.2-8.2	Gypsum Protodolomite Thenardite	Aragonite Magnesite Mg-calcite	Burkeite Epsomite Hanksite Mercallite Görgeyite Sepiolite

	5	8,2-9,4	Gypsum Thenardite	Aragonite Gypsum Magnesite Protodolomite	Carnallite Hanksite Polyhalite
	4	9,4-10,2	Gypsum Magnesite Thenardite	Aragonite Halite Mg-calcite Protodolomite	Hanksite Mercallite Polyhalite Görgeyite Rapidcreekite Sepiolite
4 Ca-Sulfate-- Na-Sulfate	3	10,2-10,5	Gypsum Thenardite	Aragonite Magnesite Protodolomite	Hanksite Mercallite Polyhalite
	2	10,5-10,9	Gypsum Thenardite	Aragonite Magnesite Protodolomite	Hanksite Polyhalite
	1	10,9-11,7	Gypsum Thenardite	Aragonite Halite Magnesite Mg-calcite Protodolomite	Hanksite Rapidcreeksite Sepiolite
	7	11,7-13,4	Gypsum Magnesite Thenardite	Aragonite Protodolomite	Hanksite
	6	13,4-14,1	Gypsum Magnesite Thenardite	Aragonite Bloedite Halite Mg-calcite Protodolomite	Arcanite Eugsterite Hanksite Rapidcreekite
3 Mg-Carbonate-- Na-Sulfate	5	14,1-15,1	Gypsum Protodolomite Thenardite	Aragonite Magnesite	Hanksite Görgeyite
	4	15,1-15,8	Gypsum Thenardite	Aragonite Magnesite Protodolomite	Gaylussite
	3	15,8-16,4	Magnesite Thenardite	Aragonite Protodolomite	Bradleyite Hanksite Pyrite
	2	16,4-17,4	Gypsum Magnesite Protodolomite Thenardite	Mg-calcite	Hanksite Rapidcreekite
	1	17,4-17,6	Thenardite		Görgeyite
	5	17,6-19,5	Thenardite/gypsum	Magnesite Protodolomite	Hanksite
	4	19,5-20,6	Thenardite	Halite	Hanksite Nitratine Nitrobarite
2 Na-Sulfate	3	20,6-21,1	Thenardite		Nitratine Protodolomite

	2	21.1-22.2	Thenardite	Gypsum	Hanksite Nitratine
	1	22.2-23.0	Thenardite		
1					
Basal Black Mud		8.96-9.16 m (south core)	Gypsum	Thenardite	

4.2 General Stratigraphic Variation of Mineralogical Constituents

The mineralogy of detrital (allogenic) components in sequence shows a varying trend; it is high in Units 1, 5 and 8, low in Units 2 and 6 (Figures 4.2 and 4.3). The content of quartz and K-feldspar in the sediment core displays an upward increasing trend (Figures 4.4 and 4.5). The percentage of plagioclase and total clay minerals do not show any systematic change with depth. Overall, the content of plagioclase and total clay minerals is high in Units 1, 3, 5 and 8, low in Units 2 and 6 (Figures 4.4 and 4.5).

The endogenic+authigenic fraction, crystallized in-situ in the basin, dominates the sedimentary sequence (average: 88%; Figures 4.2 and 4.3; Table 4.1), and consists of a complex assemblage of mainly hydrated Na, Mg, Na+Mg, and Ca sulfates, with smaller amounts of Mg, Ca+Mg, Na, and Ca carbonates and chlorides (Figures 4.6, 4.10 and 4.11). The concentrations of endogenic+authigenic components display systematic changes with depth; they are relatively low in Units 1, 5, and 8, high in Units 2 and 6 (Figures 4.2 and 4.3). As can be seen in Figures 4.6 and 4.7, the amount of thenardite is high in Units 2 and 6, low in Units 1, 5, and 8, and average in Units 3, 5 and 7 (Figures 4.6 and 4.7). The amount of gypsum fluctuates significantly but there is no obvious trend with depth (Figure 4.6). On average, it is low in Units 2 and 8 and high in Units 1 and 4. Anhydrite occurs only in the upper 3.4 m of sediment and at 8.75 m (Figure 4.6) and its concentration increases upward.

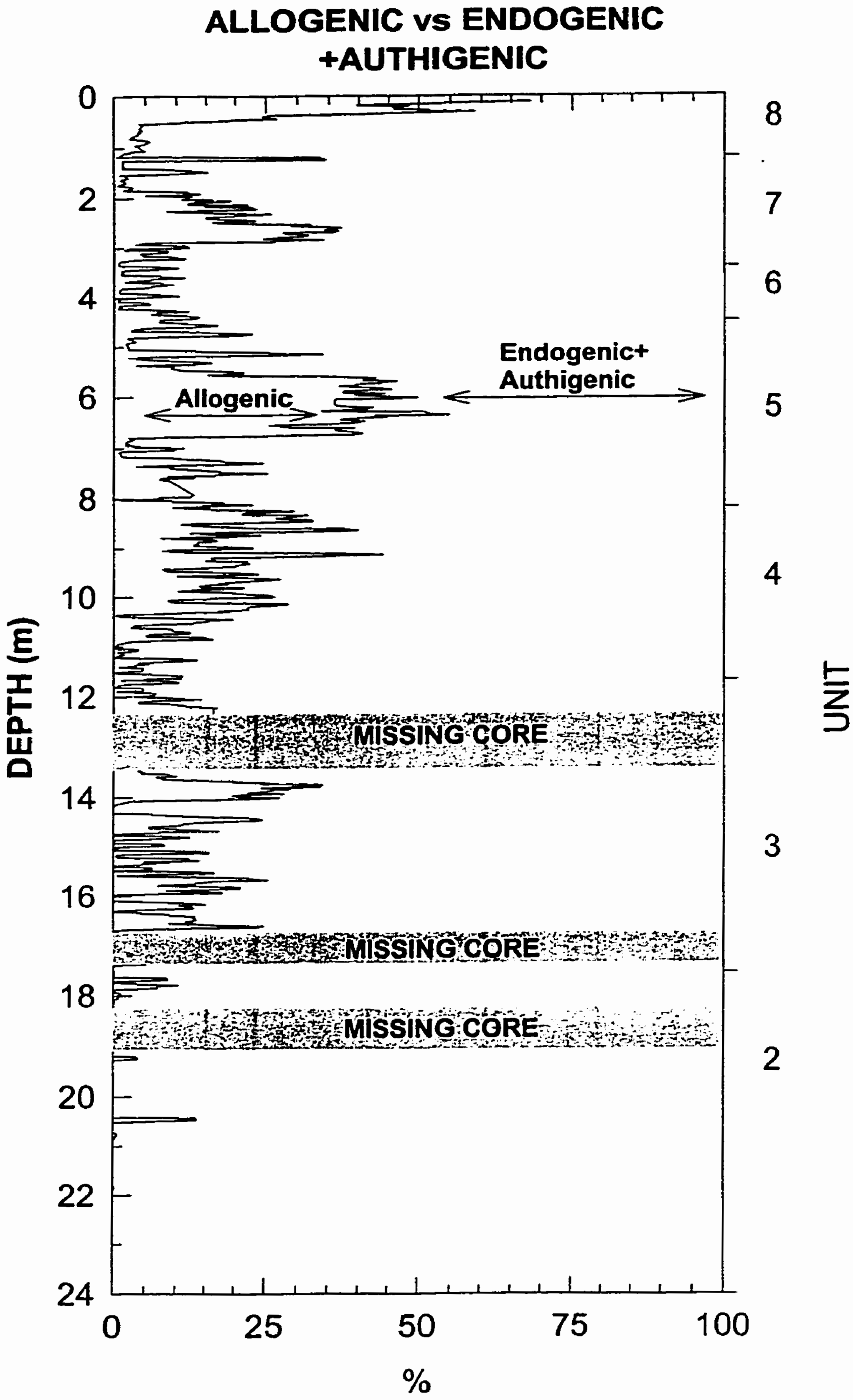

Figure 4.2 Stratigraphic variation in proportion of allogenic material versus endogenic plus authigenic components in the north core of North Ingebright lake

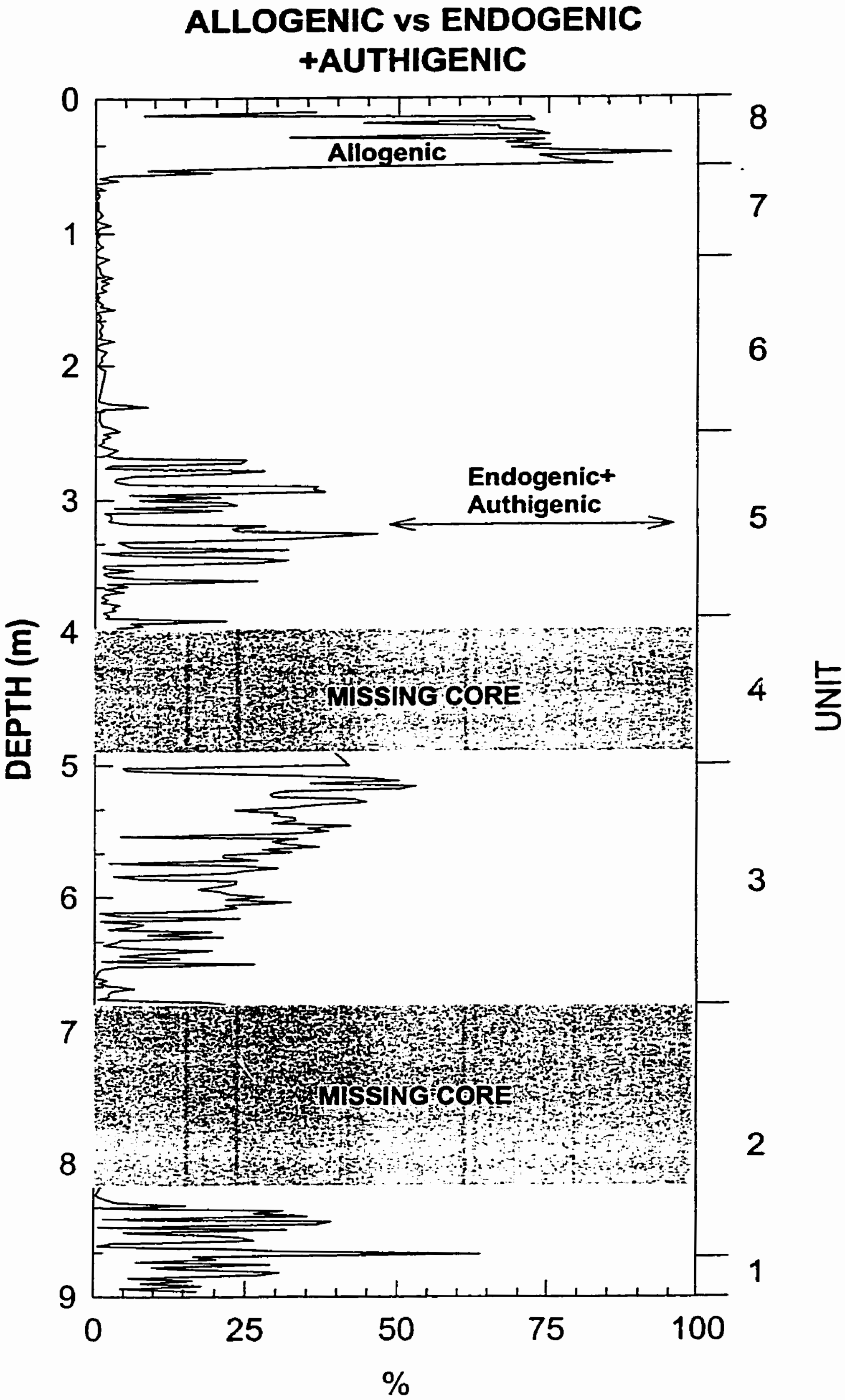

Figure 4.3 Stratigraphic variation in proportion of allogenic material versus endogenic plus authigenic components in the south core of North Ingebright lake core

Bloedite is common in sediment above 3.4 m and below 8.2 m in the north core, but is only sporadically present below that and shows no consistent trends with depth (Figures 4.6 and 4.7).

The carbonate mineral suite of North Ingebright Lake consists of protodolomite, magnesite, dolomite, high-Mg calcite, aragonite, and low-Mg calcite. The total amount of carbonates increases slightly upward and is well correlated with the organic matter content (Figures 4.8 and 4.9). Most of the carbonate minerals show no stratigraphic variation trend. Mg-carbonates are most abundant in Units 3, 4, and 5, whereas the carbonates in the upper meter of section are dominated by disordered, nonstoichiometric dolomite (Figures 4.10 and 4.11). The trace amounts of low-Mg calcite and aragonite are only present in Units 3, 4, 5, and 6 (Figures 4.10 and 4.11). The percentages of high-Mg calcite and magnesite show little systematic fluctuation with depth. Magnesite occurs only in the sediment of Units 1, 3, 4, and 5, whereas high-Mg calcite is present in each of eight units and increases slightly upward (Figures 4.10 and 4.11). The contents of both dolomite and protodolomite increase upward in the cores and are significantly correlated with quartz and K-feldspar (Figures 4.4, 4.5, 4.10, and 4.11).

4.3 Lithostratigraphy

4.3.1 Unit 1 Basal Black Mud (south core: 8.96-9.16 m)

Unit 1 was penetrated only in the 9 m core. Approximately 20 cm of black mud of Unit 1 was retrieved and consists mainly of black, highly reducing, fine-grained sand, silt and clay. It is easily recognized by a high ratio of detrital to

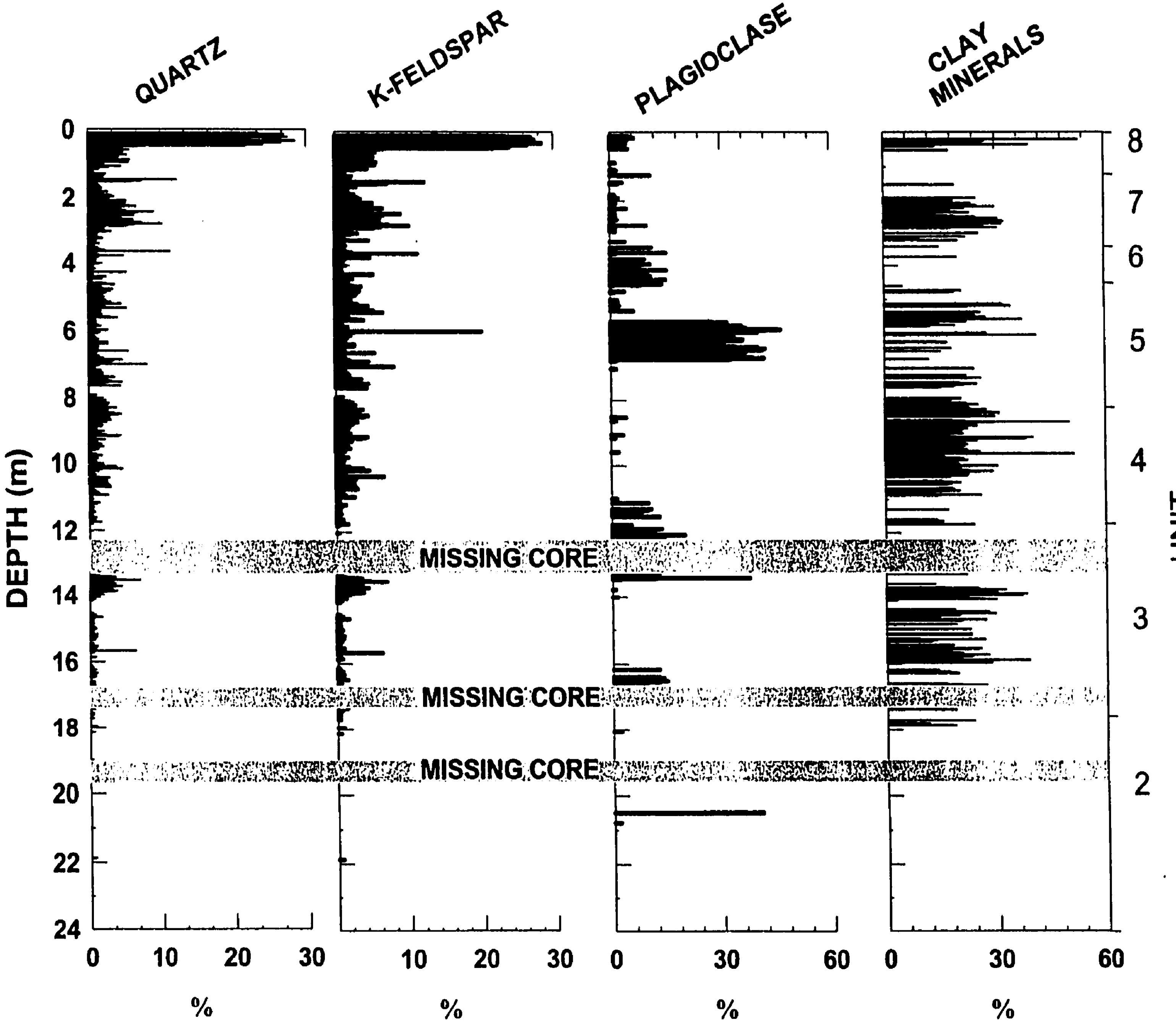

Figure 4.4 Stratigraphic variation in percentages of quartz, K-feldspar, plagioclase, and clay minerals in the north core of North Ingebright Lake

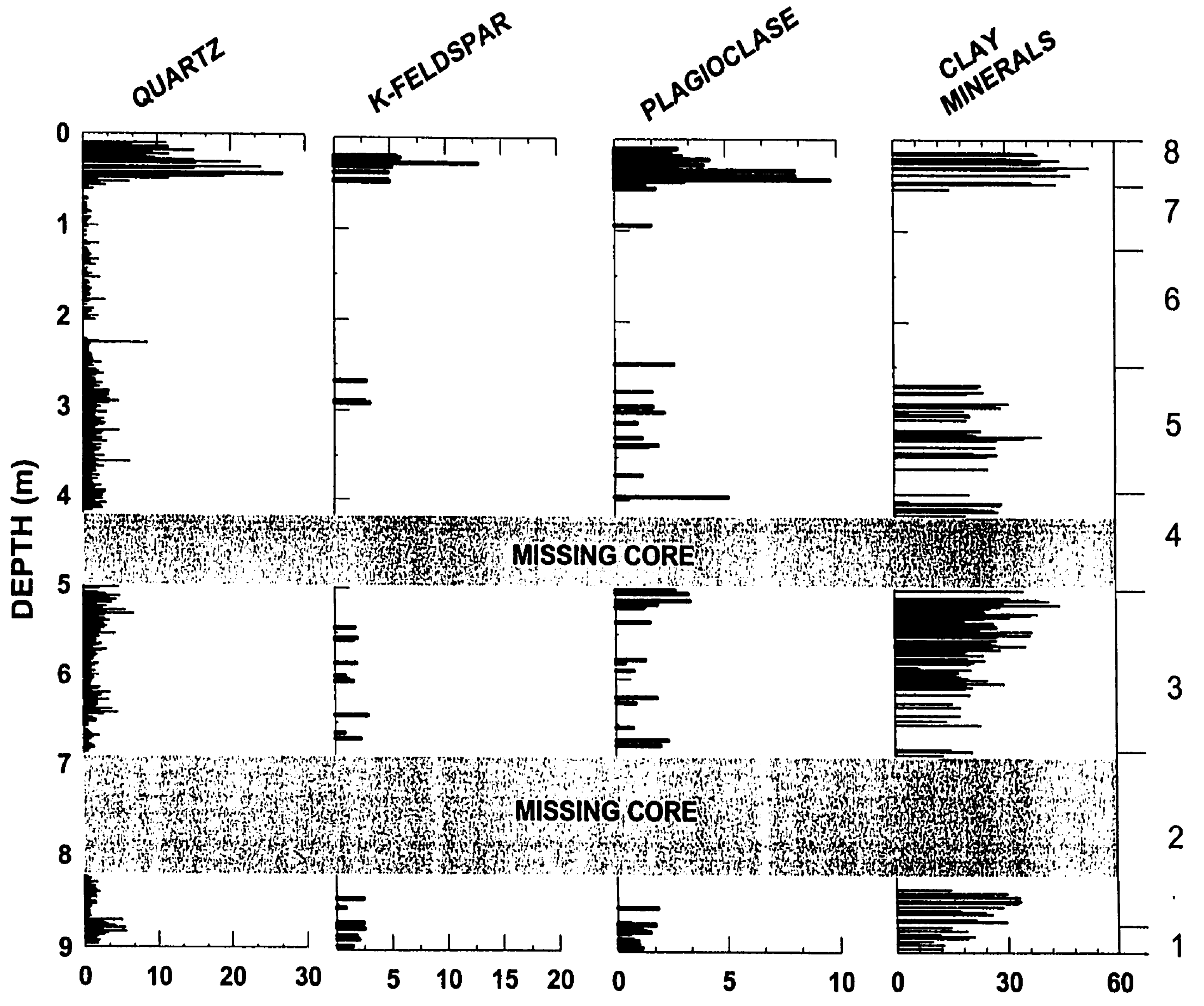

Figure 4.5 Stratigraphic variation in percentages of quartz, K-feldspar, plagioclase, and clay minerals in the south core of North Ingebright Lake

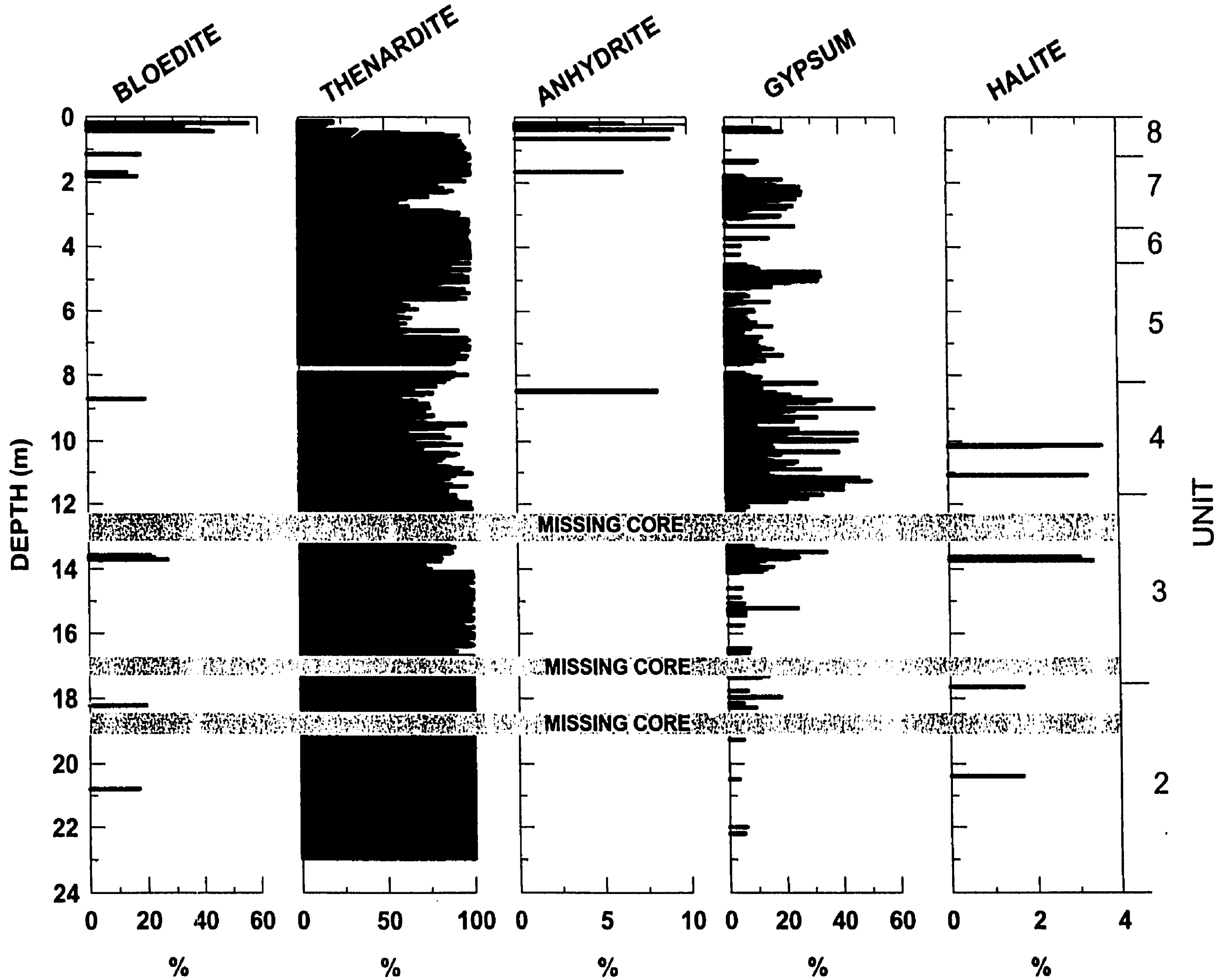

Figure 4.6 Stratigraphic variation in percentages of bloedite, thenardite, anhydrite, gypsum, and halite in the north core of North Ingebright Lake

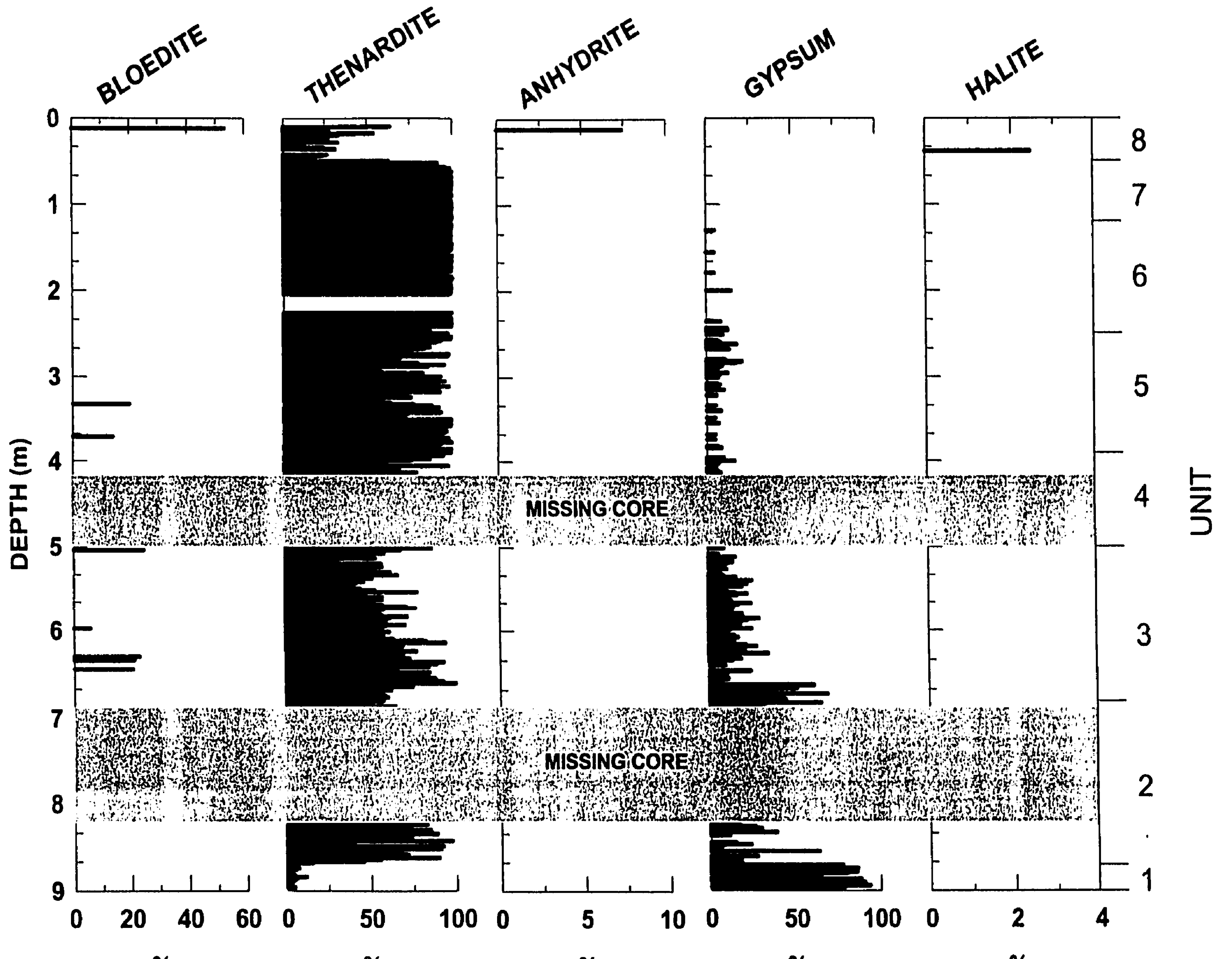

Figure 4.7 Stratigraphic variation in percentages of bloedite, thenardite, anhydrite, gypsum, and halite in the south core of North Ingebright lake

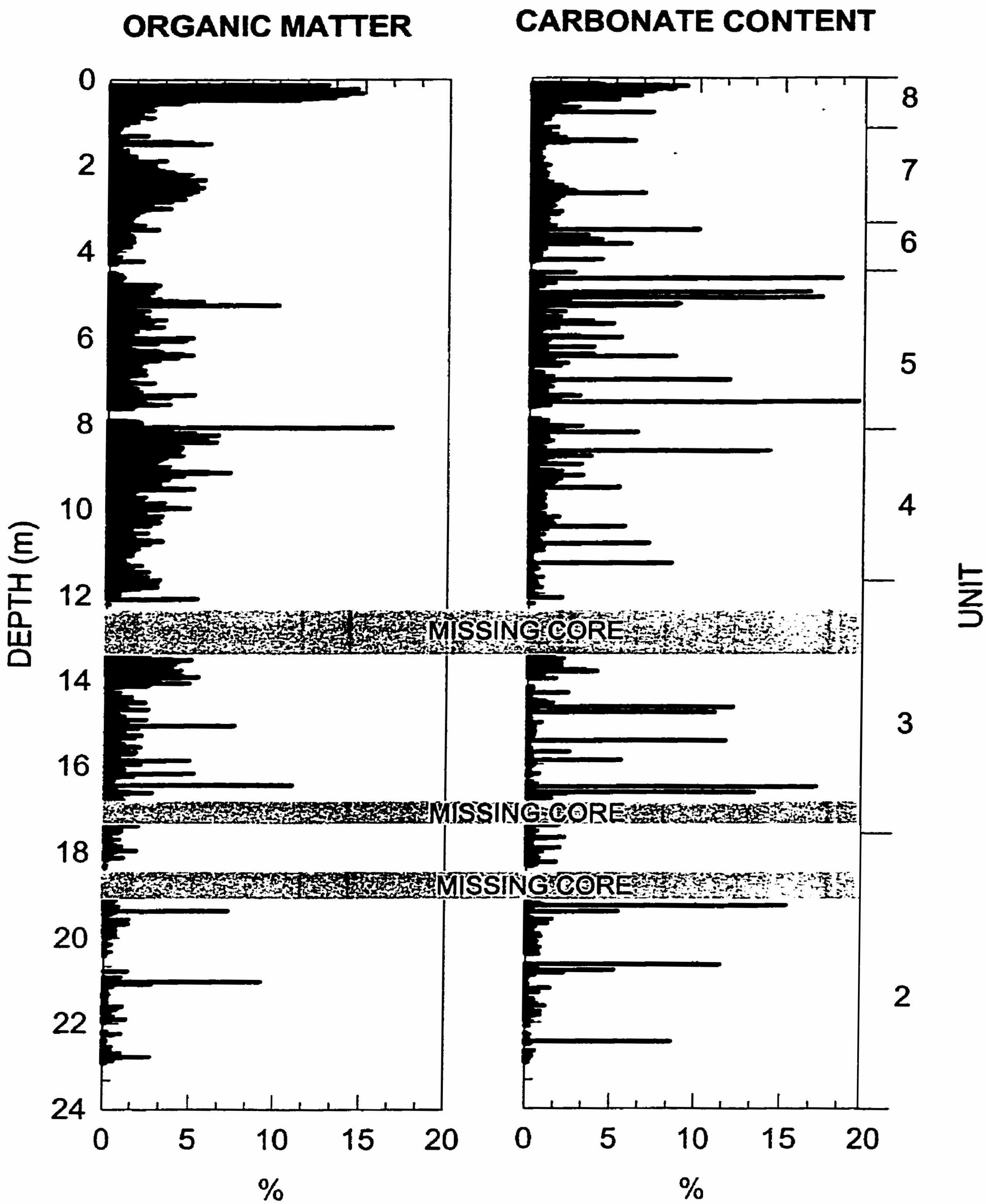

Figure 4.8 Variation of organic matter and carbonate content with depth in the north core of North Ingebright Lake

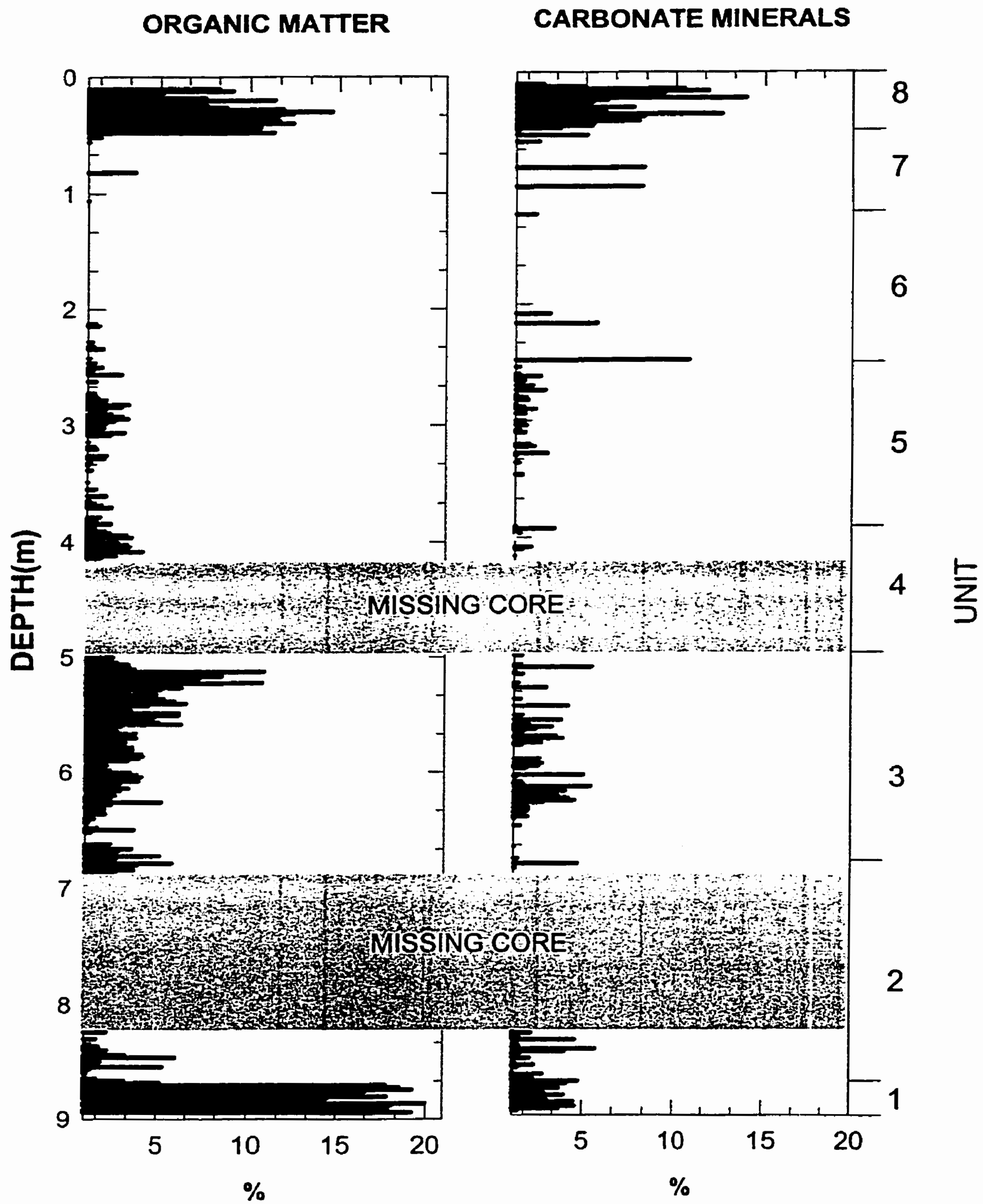

Figure 4.9 Stratigraphic variation in percentages of organic matter and carbonate content in the south core of North Ingebright Lake

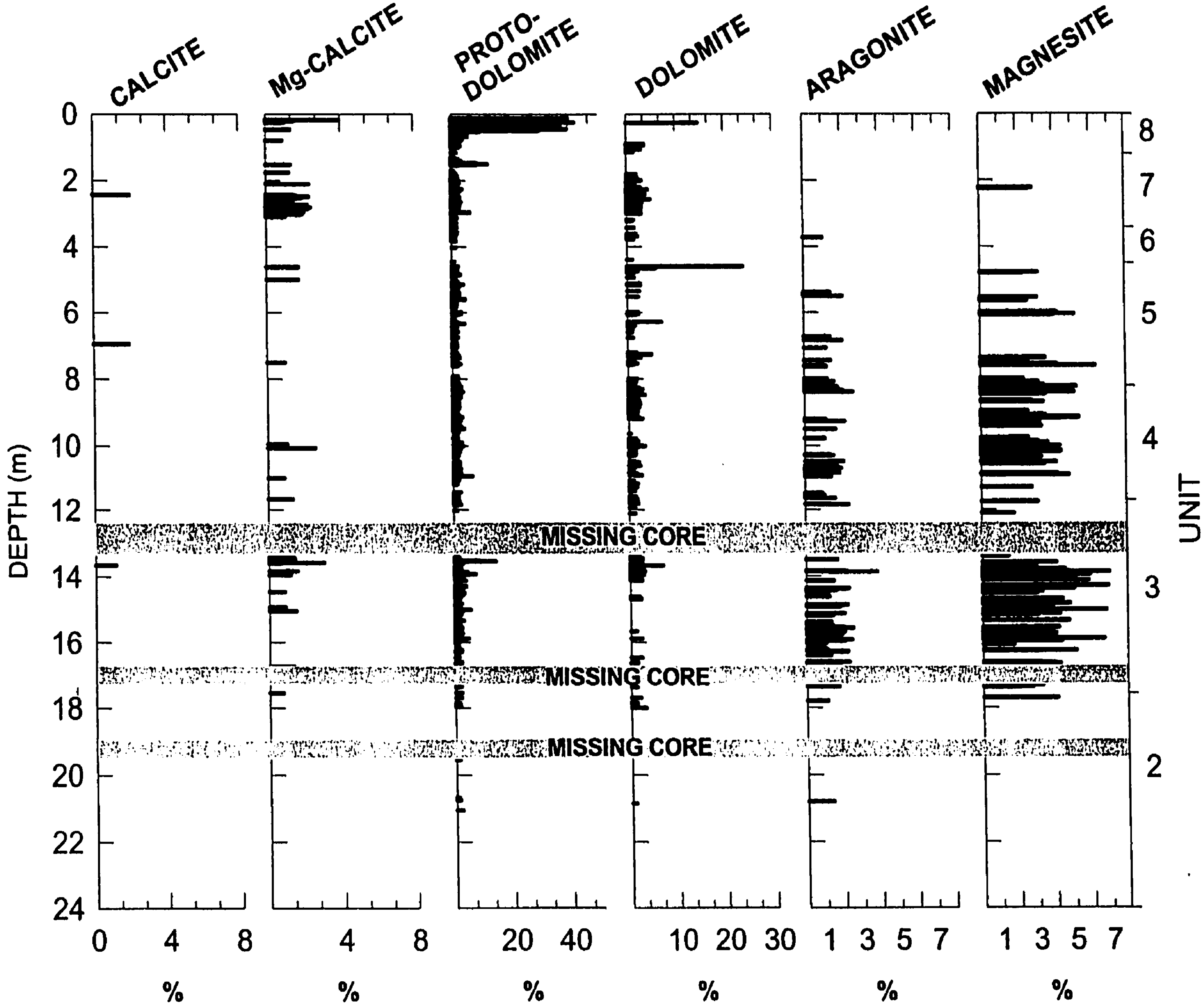

Figure 4.10 Stratigraphic variation in percentages of calcite, Mg-calcite, protodolomite dolomite, aragonite, and magnesite in the north core of North Ingebright Lake

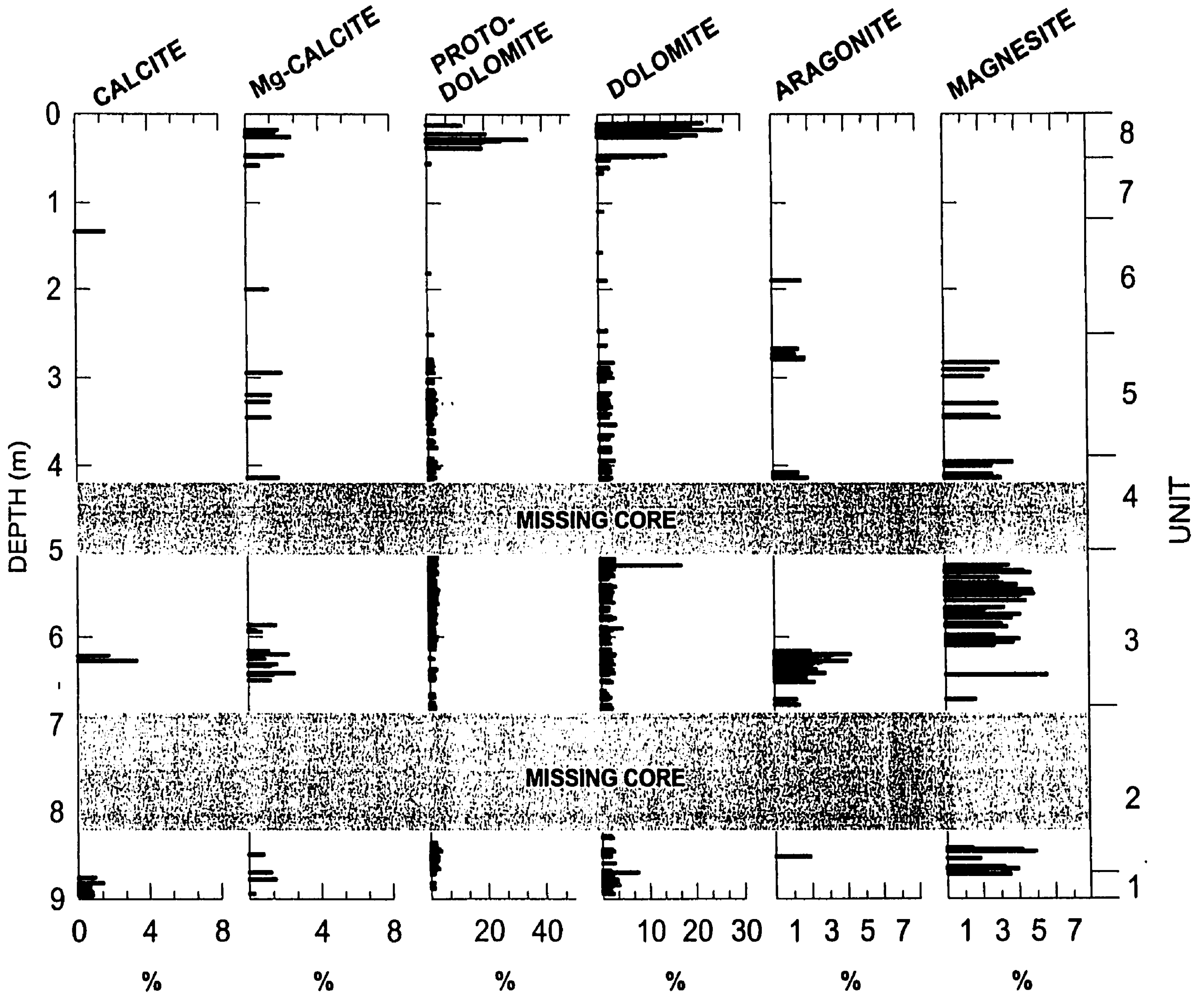

Figure 4.11 **Stratigraphic variation in percentages of calcite, Mg-calcite, protodolomite dolomite, aragonite, and magnesite in the south core of North Ingebright Lake**

endogenic components and the high content of organic matter (up to 25%) relative to the overlying sediments. Minerals in the unit are dominantly clays (40.9%), quartz (25.2%), and feldspar (27.6%), but also present are gypsum, thenardite/mirabilite, quartz, feldspar, and dolomite (Table 4.1).

4.3.2 Unit 2 Na-Sulfate Salt (north core: 17.60-23.00 m; south core: 7.00-8.96 m)

Unit 2 is characterized by a simple mineral composition. It consists almost entirely (98.9%) of Na sulfate, with 1.3% Ca sulfate, 0.2% Mg sulfate, and <0.3% of all other components (Table 4.1). The major minerals are thenardite/mirabilite and gypsum with minor amounts of halite, protodolomite, and dolomite (Figures 4.2-4.11). The endogenic/allogenic ratio of Unit 2 is the highest one among the eight stratigraphic units (Figure 4.2 and 4.3). Relative to the overlying units of North Ingebright Lake evaporites, this Na-sulfate salt unit is much thicker (1.9-5.4 m). The Na-sulfate salt unit is divided into five stratigraphic zones whose boundaries separate deposits characterized by specific assemblages of evaporite minerals, as can be seen in Table 4.2).

Zone 1 Mirabilite zone (22.20-23.00 m)

Zone 1 consists mostly of pure thenardite/mirabilite. Traces of nitratine and hanksite occur in a few samples. The preponderance of thenardite/mirabilite over other saline minerals and lack of variation distinguish this zone from zones above it.

Zone 2 Gypsum zone (21.10-22.20 m)

Gypsum appears in the lower part of zone 2, and this characteristic distinguishes zone 2 from zone 1. Locally there are trace quantities of nitratine and hanksite.

Zone 3 Mirabilite zone (21.00-21.10 m)

Salts in zone 3 are dominated by thenardite/mirabilite and contain traces of protodolomite and nitratine.

Zone 4 Halite zone (19.50-21.00 m)

In zone 4, organic matter content is relatively low and carbonate minerals are absent. Most samples contain minor amounts of halite, and this distinguishes the deposits from those of zone 3. Traces of hanksite, nitratine and nitrobarite also occur in several samples.

Zone 5 Magnesite zone (17.60-19.50 m)

Zone 5 consists chiefly of thenardite/mirabilite and gypsum. Protodolomite, magnesite, and fairchildite are commonly found. Trace amounts of hanksite are also detected in several samples.

4.3.3 Unit 3 Mg-Carbonate--Na-Sulfate Salt (north core: 11.70-17.60 m; south core: 5.00-7.00 m)

Unit 3 is dominantly Na sulfate (83.9%) and clay (12.2%); there is <5% other silicate minerals and 3.5% Ca sulfate (Table 4.1). It is recognized by a relatively high content of magnesite, gypsum, bloedite, and feldspar (Figures 4.4-4.11). The endogenic/allogenic ratio (Figures 4.2 and 4.3) is relatively low, and the organic matter content is considerably higher than that of Unit 2 (Figures 4.8 and 4.9). The total carbonate content is also higher than that of the underlying sediments. Carbonates are dominated by magnesite and protodolomite, with small amounts of high-Mg calcite and dolomite (Figures 4.10 and 4.11). Trace amounts of starkeyite, eugsterite, hanksite, and niter occur in few samples (Appendix C). Small quantities of quartz and clay minerals also appear in the mud.

Unit 3 in the north core is divided into seven mineral zones on the basis of detailed evaporite mineralogy. The most significant changes in mineral composition of Unit 3 are as follows: the lower four zones consist mainly of thenardite/mirabilite; zones 5, 6, and 7 consist of thenardite/mirabilite and gypsum with some detrital materials.

Zone 1 Mirabilite zone (17.40-17.60 m)

Zone 1 is almost entirely composed of mirabilite/thenardite with traces of görgeyite. Fine grained detrital materials commonly appear but form less than 10%.

Zone 2 Starkeyite-gypsum zone (16.40-17.40 m)

The main saline minerals in zone 2 are thenardite/mirabilite, gypsum, protodolomite, aragonite, and magnesite. Gypsum and magnesite are concentrated in the middle part, whereas thenardite/mirabilite, protodolomite, and aragonite appear in the lower and upper parts. Calcite and dolomite are found in several samples. Trace amounts of starkeyite, nitratine, hanksite, and rapidcreekite are also determined in few samples.

Zone 3 Magnesite zone (15.80-16.40 m)

Gypsum is absent in zone 3, and this feature distinguishes it from both zone 2 and zone 4. Thenardite/mirabilite and magnesite are predominant minerals; the average percentage of protodolomite is much higher than that of the underlying zones. Small amounts of aragonite occur in a number of samples. Trace minerals include nitratine, hanksite, and bradleyite.

Zone 4 Gaylussite zone (15.10-15.80 m)

Zone 4 is mainly composed of thenardite/mirabilite, gypsum, protodolomite, aragonite, and magnesite. Mud impurities are common in this zone. Trace amounts of gaylussite and fairchildite are found respectively at 15.5 m, 15.1 m, and 15.2 m depths.

Zone 5 Starkeyite zone (14.10-15.10 m)

Zone 5 is similar to zone 2 in terms of mineral composition. Like zone 2, it consists largely of thenardite/mirabilite, gypsum, protodolomite, aragonite, and magnesite, with traces of hanksite, görgeyite, starkeyite, fairchildite, and nitratine.

Zone 6 Bloedite-eugsterite (13.40-14.10 m)

Zone 6 is characterized by relatively high organic matter, carbonates, and bloedite contents. Sulfate minerals consist mainly of thenardite/mirabilite, gypsum, and bloedite; carbonate minerals include high Mg calcite, aragonite, protodolomite, and magnesite. Magnesite reaches its highest concentration in this zone; much of the magnesite is concentrated near the base of the zone. Trace amounts of halite, eugsterite, görgeyite, hanksite, rapidcreekite, arcanite, inderborite, nitrobarite, and phosphate minerals are also detected.

Zone 7 Gypsum zone (11.70-13.40 cm)

Like zone 6, zone 7 consists chiefly of thenardite, gypsum, protodolomite and magnesite, with small amounts of aragonite and dolomite. Bloedite is absent. Trace minerals include hanksite and nitratine.

4.3.4 Unit 4 Ca-Sulfate--Na-Sulfate Salt (north core: 8.20-11.70 m; south core: 3.90-5.00 m)

Unit 4 is characterized by high gypsum (3.%) and total clay mineral (12.2%), relatively low thenardite/mirabilite (65.5%) and plagioclase contents (0.5%), and high magnesite content (Figures 4.2-4.11 and Table 4.1). Trace amounts of hanksite, polyhalite, gaylussite, carnallite, and burkeite are found mixed with the other saline minerals. Unit 4 also displays relatively high organic matter and total carbonate contents (Figures 4.8 and 4.9). Generally, organic matter content, quartz, and total clay minerals increase upward, whereas gypsum and thenardite/mirabilite decrease upward. Unit 4 has been subdivided into five zones on the basis of compositional changes in the saline mineral assemblage.

Zone 1 Halite zone (10.90-11.70 m)

Thenardite/mirabilite and gypsum are the major mineral components of zone 1, together forming more than 85% of the total mineral composition. Small amounts of quartz, clay minerals, high-Mg calcite, aragonite, protodolomite, and magnesite occur. Sepiolite, fairchildite, halite, hanksite, rapidcreekite, nitratine, and inderborite constitute the trace mineral assemblage.

Zone 2 Polyhalite zone (10.50-10.90 m)

Similar to zone 1, zone 2 is composed mainly of Na and Ca sulfate salts (mirabilite/thenardite, gypsum) with lesser amounts of Ca, Mg and K carbonates (aragonite, protodolomite, dolomite, magnesite, and fairchildite). A wide variety of other soluble minerals have been identified in trace amounts including polyhalite, starkeyite, and hanksite.

Zone 3 Gaylussite zone (10.20-10.50 m)

Zone 3 is distinguished from the underlying zones by the presence of trace amounts of gaylussite at the base. This zone is composed of thenardite/mirabilite, clay minerals, gypsum, and protodolomite. Minor minerals include aragonite, dolomite, and magnesite. Mercallite, polyhalite, hanksite, and phosphate minerals constitute rare mineral components.

Zone 4 Polyhalite zone (9.40-10.20 m)

Zone 4 is characterized by the common occurrences of trace polyhalite, hanksite, and halite. Quantities of quartz, protodolomite, and thenardite/mirabilite are relatively low, but gypsum and magnesite are very high. Other minor minerals include high Mg calcite, aragonite, dolomite, sepiolite, mercallite, görgeyite, and rapidereekite.

Zone 5 Carnallite zone (8.20-9.40 m)

Main minerals include carnallite, burkeite, and bloedite. Thenardite/mirabilite, gypsum, and clay minerals constitute major minerals. Minor minerals include aragonite, protodolomite, dolomite, magnesite, and anhydrite. Hanksite, polyhalite, inderborite, arcanite, and phosphate minerals are present in trace amounts. Organic matter and detrital components are higher than any of the other zones within this unit.

4.3.5 Unit 5 Muddy Na-Sulfate Salt (north core: 4.50-8.20 m; south core: 2.50-3.90 m)

The sediment of Unit 5 is dominated by mirabilite/thenardite and plagioclase, with higher protodolomite and dolomite contents relative to the underlying unit (Figures 4.6-4.11). The organic matter content of Unit 5 is also relatively high (Figures 4.8 and 4.9). Muddy material, approximately 10%, is scattered among the structureless and colourless salts. Five stratigraphic zones are identified on the basis of the appearance of specific late-stage evaporite minerals.

Zone 1 Epsomite zone (7.20-8.20 m)

Zone 1 is characterized by the presence of epsomite, starkeyite, and burkeite. Thenardite/mirabilite, gypsum, protodolomite, and clay minerals constitute major minerals. Minor minerals include high Mg calcite, aragonite, dolomite, and magnesite. Sepiolite, görgeyite, mercallite, hanksite, and phosphate minerals are present in trace amounts.

Zone 2 Polyhalite zone (6.20-7.20 m)

Zone 2 is distinguished from zone 1 by the occurrence of polyhalite and hanksite. This zone is mainly composed of thenardite/mirabilite and gypsum, with minor amounts of aragonite, protodolomite, and dolomite. Trace minerals include sepiolite, arcanite, and phosphate minerals.

Zone 3 Gaylussite zone (5.60-6.20 m)

Zone 3 is identified by the appearance of gaylussite. Thenardite/mirabilite and clay minerals are major components. Minor minerals include protodolomite, dolomite, magnesite, and gypsum. Hanksite, wattevilleite, arcanite, and sepiolite are present in trace amounts.

Zone 4 Inderborite zone (4.90-5.60 m)

Zone 4 is characterized by the occurrence of inderborite. Major minerals include thenardite/mirabilite, gypsum, plagioclase, and clay minerals. High Mg calcite, aragonite, protodolomite, and dolomite constitute minor minerals. Trace minerals include arcanite and hanksite.

Zone 5 Mirabilite zone (4.50-4.90 m)

Zone 5 is distinguished from zone 4 by the presence of görgeyite and hanksite. This zone consists mainly of thenardite/mirabilite, with minor amounts of high Mg calcite, protodolomite, dolomite, and magnesite.

4.3.6 Unit 6 Na-Sulfate Salt (north core: 3.40-4.50 m; south core: 1.20-2.50 m)

Similar to Unit 2, Unit 6 is composed almost entirely of thenardite/mirabilite

(93%), with lesser amounts of plagioclase (3.4%). The sediment of Unit 6 is also recognized by its relatively low protodolomite and gypsum contents, the absence of high-Mg calcite and magnesite, and a low organic matter content (Figures 4.2-4.11). The endogenic/allogenic ratio is 17 (Figures 4.2 and 4.3). Three sedimentation zones have been delimited on the basis of the trace mineral assemblage.

Zone 1 Kainite zone (4.10-4.50 m)

Zone 1 is mainly composed of thenardite/mirabilite, plagioclase and other minerals, including protodolomite and dolomite. Trace minerals consist of kainite, hanksite, and niter.

Zone 2 Niter zone (3.90-4.10 m)

Zone 2 is distinguished from zone 1 by the common occurrence of trace niter. Major mineral is thenardite/mirabilite, with minor amounts of gypsum and protodolomite.

Zone 3 Tychite zone (3.40-3.90 m)

This zone is characterized by thenardite/mirabilite with disseminated minerals of protodolomite, aragonite and gypsum. Tychite and hanksite are present in trace amounts.

4.3.7 Unit 7 Muddy Mg-calcite–Na-Sulfate Salt (north core: 1.20-3.40 m; south core: 0.50-1.20 m)

Unit 7 is black, relatively poorly consolidated, and muddy salts. Non-evaporite material content is approximately 30-40%. Sediment of Unit 7 is characterized by higher protodolomite, high-Mg calcite, and gypsum contents (Figures 4.5, 4.6, 4.10, and 4.11). The organic matter and carbonate contents are also high compared to the underlying stratigraphic units (Figures 4.8 and 4.9). Three stratigraphic zones are recognized within Unit 7.

Zone 1 Polyhalite zone (2.40-3.40 m)

Zone 1 consists chiefly of thenardite, gypsum, protodolomite, and clay minerals, with minor amounts of dolomite and high Mg calcite. Traces of fairchildite, benstonite, kutnohorite, epsomite, mercallite, görgeyite, polyhalite, and hanksite also occur. The organic matter and carbonate contents are relatively high.

Zone 2 Anhydrite zone (1.60-2.40 m)

Zone 2 consists thenardite/mirabilite, gypsum, protodolomite, with small amounts of aragonite, magnesite, anhydrite, detrital, and organic matter, and traces of niter, mercallite, arcanite, leightonite, rapidereekite, and hanksite. The amount of the dominant mineral, thenardite/mirabilite, is low relative to the underlying and overlying zones. Bloedite occurs at 1.7 and 1.8 m depths.

Zone 3 Gypsum zone (1.20-1.60 m)

Thenardite and protodolomite are major components. High-Mg calcite, dolomite, and gypsum constitute minor components. Trace minerals include artinite, hanksite, leightonite, and arcanite.

4.3.8 Unit 8 Dolomitic Na-Sulfate Salt (0.12-1.20 m)

This is the uppermost unit in the sequence, and is black, nonbedded, and loosely consolidated muddy salt. The mineral composition of Unit 8 is distinctively different from the other units in this sequence. The top 25 cm of Unit 8 consists mainly of non-evaporite materials. Mud and organic matter not only fill the spaces between crystalline salt grains but sediment and organic debris inclusions are also common within individual crystals.

Unit 8 is characterized by several general trends. Quartz, feldspar, clay minerals, organic matter, protodolomite, and bloedite contents all increase markedly upward. Conversely, thenardite and gypsum contents decrease upward. The endogenic/allogenic ratio is relatively low (4.5)(Figures 4.2 and 4.3). The organic matter and carbonate contents are much higher than that of underlying units (Figures 4.8 and 4.9). On the basis of mineralogical composition, three stratigraphic zones are recognized in Unit 8.

Zone 1 Thenardite zone (0.80-1.20 m)

Zone 1 is distinguished by high percentages of thenardite/mirabilite. Extremely high bloedite content occurs at 1.1 m depth. High-Mg calcite, protodolomite, and detrital components are generally low, but variable.

Zone 2 Bichofite zone (0.40-0.80 m)

Zone 2 is identified by the appearance of trace amounts of bichofite. The main minerals are thenardite and protodolomite, with minor amounts of high Mg calcite and anhydrite.

Zone 3 Anhydrite zone (0.10-0.40 m)

Zone 3 is distinguished from the underlying zones by its wide variety of mineral constituents: major components include thenardite/mirabilite, bloedite, and protodolomite; minor components consist of high-Mg calcite, dolomite, gypsum, and anhydrite; and trace components are niter, starkeyite, minrecordite, benstonite, and leightonite. The thenardite/mirabilite reaches its lowest in the entire section at zone 3. Conversely, organic matter, quartz, and carbonate contents reach their highest percentage.

4.4 Stratigraphic Correlation Within North Ingebright Lake Basin

As is well known, evaporites form in a continuum of depositional environments, ranging from nonmarine to marine. Three main environmental groups of evaporite precipitation are identified (Shreiber et al., 1976; Kendall, 1984; Warren, 1986; Hsü et al., 1969; Hsü, 1972): continental, coastal sabkha, and subaqueous. However, very few examples of ancient continental facies evaporites have been identified in the geological record (Hardie et al., 1978, Rosen, 1991). Most ancient evaporites have been interpreted as marine in origin (Kinsman, 1969). The establishment of a facies model for many bittern salt deposits in continental environments is extremely difficult because of the lack of original fabrics and structures. No single facies model can be applied to diversified evaporites. Accordingly, stratigraphic correlations of evaporite sequences are very difficult to determine.

Stratigraphic correlations within evaporite sequences, and between evaporites and other facies are affected by the lack of biostratigraphic control, rapidity of evaporite deposition, complexity of stratigraphic relationships, and removal of soluble evaporites by groundwaters and surface solution (Kendall, 1988; Last, 1990; Handford, 1982). The complex products resulting from the effect of these factors make stratigraphic correlations of an evaporite sequences one of most challenging and controversial subjects in sedimentology.

The difficulty is best illustrated by the attempt to make stratigraphic correlations in the evaporite sequences of Bristol Dry Lake Basin (Rosen, 1991). Bristol Dry Lake is a large playa (155 km^2) in the Mojave Desert, USA, filled with over 500 m of sediment. Two continuous cores over 400 m in length were retrieved from lake basin less than 3 km apart. Unfortunately, no beds in the salt sequences of the two cores can be correlated. Correlation with other short cores taken virtually in the same site is also nearly impossible.

Two cores were retrieved from the North Ingebright Lake Basin. The sediments consist of well-indurated salt, with only minor mud and organic debris. The general lack of organic matter, obvious bedding, colour variation or other visible sedimentary structures in the sediments indicates that oxygenated, well-mixed, and shallow water conditions dominated in lake basin. Further, the poorly developed marginal facies and steeply-walled morphology of the North Ingebright Lake Basin suggest that the vertical sequences in the evaporites most likely reflect basin-wide changes in evaporite depositional environments, rather than lateral facies relationships. Therefore, stratigraphic correlations can be established by comparing variation in mineralogical composition reflected in the cores. Figure 4.12 shows the stratigraphic correlation of two cores based on the mineral composition. The good correlation of the salt beds between the two cores suggests that the sequence found in the two cores depicts a series of changes that probably affected the entire basin simultaneously.

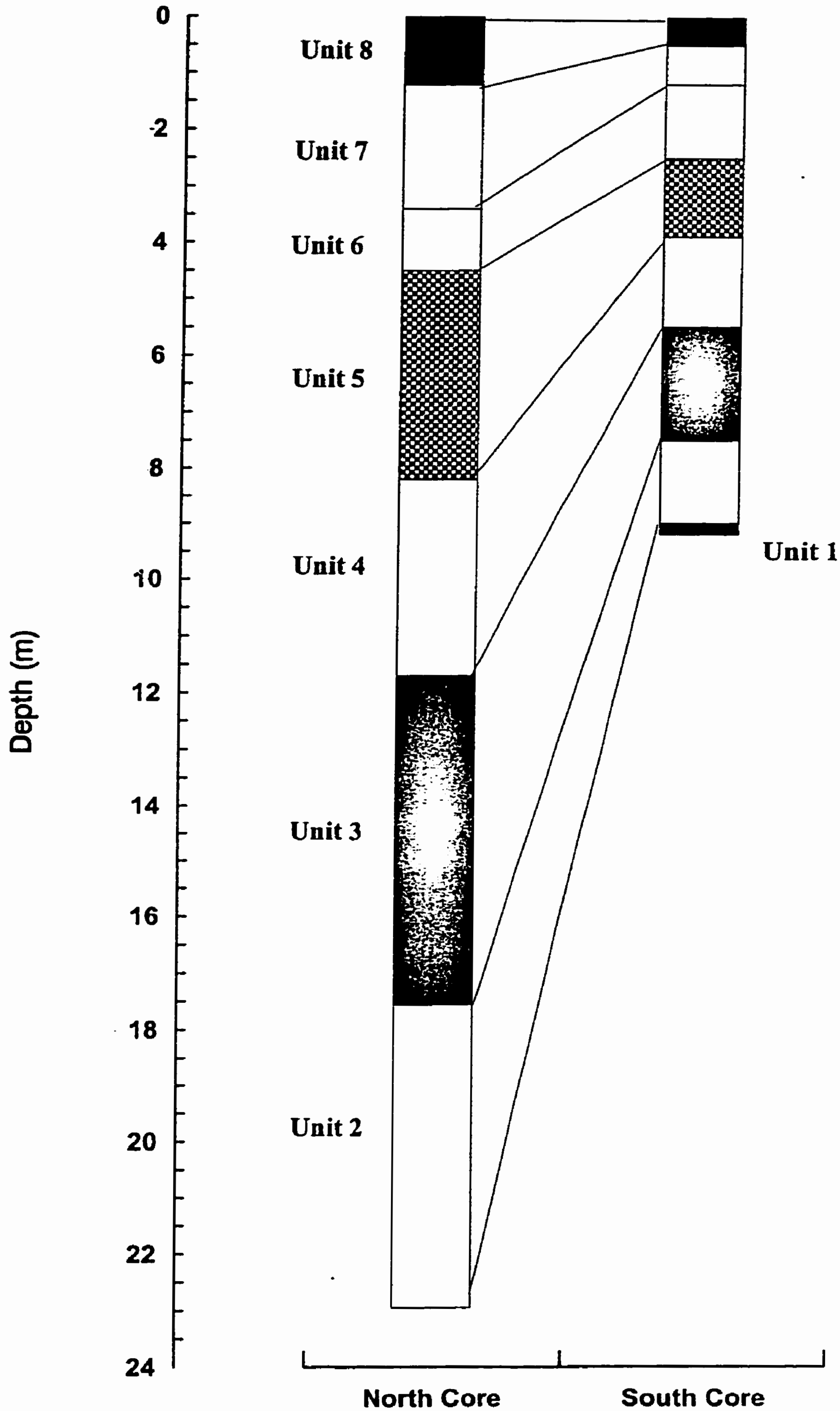

Figure 4.12 Subsurface Section Showing Relationship between Stratigraphic Units of North Ingebright Lake

Chapter 5 Mineralogy of North Ingebright Lake Core

5.1 General Description

The mineral suite of the sediment retrieved from the basin of North Ingebright Lake consists mainly of thenardite/mirabilite, gypsum, carbonates, clay minerals, feldspar minerals, and quartz (Tables 4.1 and 4.2). Thenardite and gypsum are two dominant minerals in most samples throughout the entire stratigraphic section. Carbonate minerals present in the sediment core include protodolomite, dolomite, magnesite, aragonite, high-Mg calcite, and calcite. The feldspars comprise an average of 3% of the mineral suite, primarily plagioclase, with minor amounts of potassic feldspar. Small quantities of halite and pyrite are present in many samples. Anhydrite and bloedite were also identified in a small number of samples. Most of these samples are from the upper part of the sediment core. Trace quantities of nitrate, borate, carbonate-sulfate, carbonate-sulfate-chloride minerals, Na+Ca (or K+Ca, Ca+Fe, Ca+Mn) carbonates, and Na+Mg (or Mg, K, Fe, Na+Ca, K+Ca+Mg) sulfates occur locally (Table 5.1, Appendix C).

5.2 Origin of Mineralogical Constituents

The mineral components of the North Ingebright Lake sediment cores can be divided into three genetic types: allogenic, endogenic, and authigenic. Minerals derived from outside the lake are referred to as allogenic (Jones and Bowser, 1978). Allogenic components in the North Ingebright lake sediments consist of clay minerals, quartz, feldspar and some of the carbonate minerals. These minerals are derived from the surrounding watershed sediments by means of fluvial, sheetwash, and aeolian transport and closely reflect the composition of the surrounding glacial materials (David, 1964). The proportions of all of these detrital minerals are significantly correlated (linear correlation coefficients, γ, are more than 0.5).

The endogenic fraction is that portion of the sediment that originated from within the water column of the lake, whereas authigenic components are derived from syndepositional reactions of early formed minerals with the evolving brine or pore water (Jones and Bowser, 1978; Last, 1993, 1997). The paragenesis of the endogenic and authigenic mineral suite in North Ingebright Lake is exceedingly complex. In a groundwater-dominated, hypersaline salt pan/playa environment such as is present in the modern basin, the distinction between endogenic and authigenic mineral components becomes obscure (see also discussions in Smoot and Lowenstein, 1991; and Sonnenfeld, 1984; Talbot and Kelts, 1986). Salts that may have formed as true endogenic precipitates are very likely dissolved and re-precipitated numerous times at the sediment-water interface as the composition of the overlying brine changes during the year, or at the surface of the playa upon subaerial exposure and desiccation (Last, 1997). Likewise, both fresh and saline pore waters within the upper few centimetres of the playa surface can readily modify the precipitated salts. Although seasonal and longer-term mineralogic changes and accompanying diagenesis of the non-detrital suite in North Ingebright sediment is a complex process, observations from numerous other saline playas in western Canada and other areas of North America (e.g., Last, 1989; Smith and Friedman,

1986) indicate that the evaporite mineral suite is largely stabilized within a few tens of centimetres below the playa surface.

The carbonate mineral suite of North Ingebright Lake consists mainly of magnesite, protodolomite, dolomite, high-Mg calcite, aragonite, and low-Mg calcite. Non-stoichiometric dolomite (protodolomite), high-Mg calcite, aragonite, and magnesite are absent from the bedrock, till, and surface soils of Western Canada (Last, 1982). For this reason, it is reasonable to conclude that these metastable minerals in the sediment of North Ingebright Lake were derived from inorganic precipitation within the water column in response to supersaturated conditions or by diagenetic reactions. In this study, stoichiometric dolomite and low-Mg calcite are considered detrital in origin, being derived from erosion of the surrounding glacial deposits or bedrock. Most of the carbonate minerals and the soluble late stage evaporitic minerals in the North Ingebright Lake sediment are considered as either endogenic or early authigenic in origin.

5.3 Significance of Carbonate Mineralogy in North Ingebright Lake

Origins of the carbonates in lacustrine sediments can be detrital, endogenic, and/or authigenic. Carbonate minerals can be produced by inorganic precipitation, by biologically-induced inorganic precipitation, and/or by purely organic precipitation (Last, 1982; Last et al., 1994; Last and Deckker, 1992). For hypersaline lakes, carbonate minerals are dominantly derived by inorganic precipitation because these waters are generally deficient in microorganisms. With evaporative concentration and calcite precipitation, the Mg content of the lake water and the Mg/Ca ratio will increase. Müller et al. (1972) have outlined the relationship between the Mg/Ca ratio in waters and associated carbonate formation. With an increase in the Mg/Ca ratio, calcite, low-Mg calcite, high-Mg calcite, aragonite and dolomite may precipitate in turn (Müller, 1970). Thus, it is commonplace to use the stratigraphic variation of these species in a lacustrine basin to deduce past ionic ratios and the salinity of the lake water (Last, 1982; Last and Schweyen, 1985).

The presence of endogenic carbonates throughout the entire sediment core of North Ingebright Lake indicates the past presence of a pH of at least 7.0. There are several high peaks of high-Mg calcite, protodolomite, and magnesite contents in the sediment core, which imply that North Ingebright Lake experienced periodic or extended episodes where the Mg/Ca ratio was high. During the deposition of the north core at 8.2-17.6 m depths, the Mg/Ca ratio was around 100 because carbonate minerals in these sections of the core mainly consist of magnesite. During the deposition of the north core at 0.1-3.4 m depths, the Mg/Ca ratio was also very high (>10) as indicated by the presence of high-Mg calcite and protodolomite. Generally, the Mg/Ca ratio displays a slightly systematic upward increase, as shown by the variation of $MgCO_3$ in protodolomite and high-Mg calcite with depth (Figure 5.1). Therefore, the water chemistry experienced an overall gradual shift from a sodium dominated brine to one of mixed sodium and magnesium.

White/dark laminae may form in perennial closed-basin lakes. The white laminae are usually calcareous sediment (calcite or aragonite), whereas the darker laminae are organic-rich with admixtures of clay, quartz and calcite (Eugster and

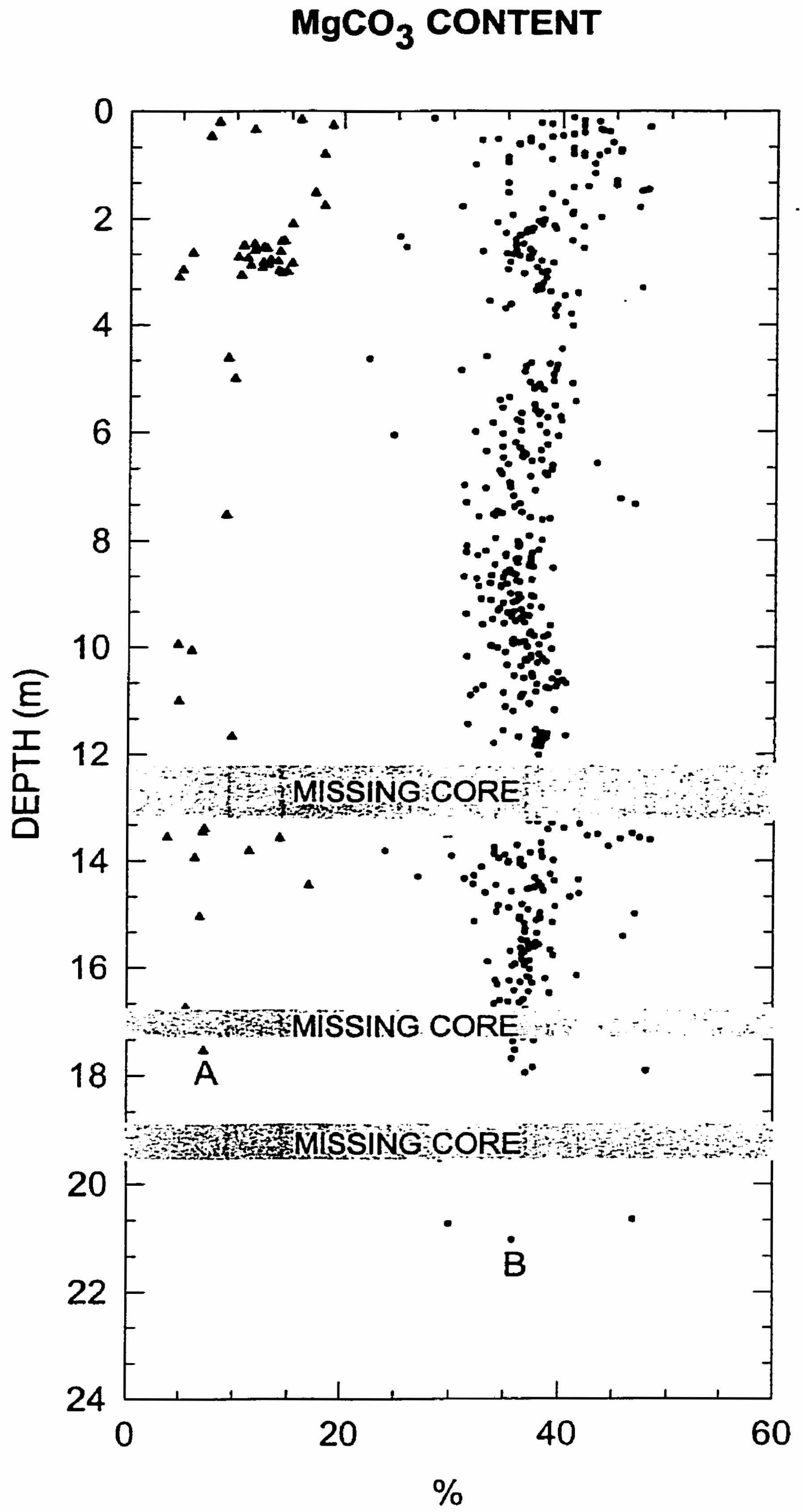

Figure 5.1 Variation of $MgCO_3$ content in high Mg-calcite (A) and protodolomite (B) with depth at North Ingebright Lake

Kelts, 1983; Kelts and Hsü, 1978; Lambert and Hsü, 1979). In ephemeral North Ingebright Lake basin, however, seasonal lowering of the lake waters might lead to subaerial exposure, mudcracking and intrasedimentary growth of saline minerals. These processes can completely destroy laminations (Eugster and Kelts, 1983). Therefore, the subaerial exposure, mudcracking and saline minerals intrasedimentary growth probably best explains the lack of carbonate laminae in North Ingebright Lake, which are commonly found in other closed-basin lakes in southern Saskatchewan (e.g. Ceylon Lake, Little Manitou Lake)(Last, 1990; Sack and Last, 1994). Overall, the carbonate content in the sediments of North Ingebright Lake is very low (3%). The periodic appearance of the small percentage of aragonite, protodolomite, and magnesite probably resulted from brief changes in the chemical composition of lake waters caused by an influx of freshwater.

5.4 Soluble Evaporitic Mineralogy in North Ingebright Lake

Over 40 species of endogenic+authigenic minerals have been identified in North Ingebright Lake deposits (Table 5.1). Most of the late stage evaporitic minerals in North Ingebright Lake were formed by syndepositional reaction of early formed minerals with the evolving brine. These reaction minerals should be regarded as a proper part of a primary depositional sequence (Braitsch, 1971; Dean, 1978). However, exact origins (primary or syndepositional) of these minerals are not essential for the deduction of hydrological and chemical conditions. The important thing is their existence because each mineral represents particular hydrological-chemical conditions (Braitsch, 1971; Bradley et al., 1969; Dean, 1978;

Table 5.1. Endogenic and Authigenic Mineralology of North Ingebright Lake Sediments Identified by XRD

Mineral Name	Composition	Occurrence[1]
	Carbonate Minerals	
Aragonite	$CaCO_3$	common
Artinite	$Mg_2CO_3(OH)_23H_2O$	very rare
Ankerite	$Ca(Fe,Mg)(CO_3)_2$	rare
Benstonite	$Ca_7Ba_6(CO_3)_{13}$	very rare
Calcite	$CaCO_3$	rare
Fairchildite	$K_2Ca(CO_3)_2$	very rare
Gaylussite	$Na_2Ca(CO_3)_2\ 5H_2O$	very rare
Kutnohorite	$Ca(Mn,Mg)(CO_3)_2$	very rare
Magnesite[2]	$MgCO_3$	common
Magnesian Calcite	$(Mg_xCa_{1-x})CO_3$	common
Minrecordite	$CaZn(CO_3)_2$	very rare
Protodolomite	$CaMg(CO_3)_2$	very common
Zemkorite	$Na_2Ca(CO_3)_2$	very rare
	Sulfate Minerals	
Arcanite	$(K,NH_4)_2SO_4$	rare
Bloedite	$Na_2Mg(SO_4)_2\ 4H_2O$	very common
Epsomite	$MgSO_4\ 7H_2O$	common
Eugsterite	$Na_4Ca(SO_4)_3\ 2H_2O$	very rare
Görgeyite	$K_2Ca_5(SO_4)_64H_2O$	very rare
Gypsum	$CaSO_4\ 2H_2O$	very common
Krausite	$Fe_2(SO_4)_3\ 2H_2O$	very rare
Leightonite	$K_2Ca_2Cu(SO_4)_42H_2O$	very rare

Mercallite	$KHSO_4$	very rare
Mirabilite[3]	$Na_2SO_4\ 10H_2O$	very common(?)
Polyhalite	$K_2Ca_2Mg(SO_4)_4 2H_2O$	rare
Starkeyite	$MgSO_4\ 4H_2O$	very rare
Thenardite	Na_2SO_4	very common
Wattevilleite	$Na_2Ca(SO_4)_2\ 4H_2O$	very rare

Carbonate-Sulfate, Carbonate-Sulfate-Chloride, and Carbonate-Phosphate Minerals

Bradleyite	$Na_3Mg(PO_4)(CO_3)$	very rare
Burkeite	$2(Na_2SO_4)Na_2CO_3$	very rare
Hanksite	$KNa_{22}(CO_3)_2(SO_4)_9Cl$	common
Kainite	$KMg(SO_4)Cl3H_2O$	rare
Rapidcreekite	$Ca_2(CO_3)SO_4\ 4H_2O$	very rare
Tychite	$Na_6Mg_2SO_4(CO_3)_6$	very rare

Chloride Minerals

Bischofite	$MgCl_2\ 6H_2O$	very rare
Carnallite	$KMgCl_3\ 6H_2O$	very rare
Halite	$NaCl$	rare
Korshunovskite	$Mg_2Cl(OH)_3\ 4H_2O$	very rare

Nitrate and Borate Minerals

Inderborite	$CaMgB_6O_{11}H_2O$	rare
Niter	KNO_3	very rare
Nitratine	$NaNO_3$	very rare

	Other	
Pyrite	FeS_2	very rare
Sepiolite	$Mg_4Si_6O_{15}(OH)_2 6H_2O$	very rare

[1]Very common: mineral occurs in greater than 75% of the samples analyzed; common: mineral occurs in 25-75% of the samples analyzed; rare: mineral occurs in 10-25% of the samples analyzed; very rare: mineral occurs in less than 10% of the samples analayzed. These qualifications apply only to occurrence within the core and are not meant to imply any information about the relative abundance of the particular mineral. For example, some of the phases that are listed as having rare or very rare occurrence can, nonetheless, be relatively abundant in a particular sample, and minerals that may be listed as common occurrence can have very low abundances.
[2]Includes hydromagnesite and psuedohydromagnesite.
[3]Because of its extreme instability and very rapid dehydration, mirabilite was rarely identified by X-ray diffraction.

Hosler, 1979; Kendall, 1988; Last, 1990). In the following section, the formative physical-chemical conditions of evaporitic minerals in Table 5.1 are noted.

Arcanite ($(K,NH_4)_2SO_4$)

Arcanite is a rare salt mineral. It was first found in the Santa Ana mine, Orange County, California (Palache et al., 1951; Frondel, 1950). It occurs as thin, pseudo-hexagonal tablets. Origin and paragenesis of the arcanite are unclear. However, the arcanite crystals can be artificially made in lab and its crystal morphology and cell parameters have be well studied by McGinnety (1972).

Bloedite ($Na_2Mg(SO_4)_2 4H_2O$)

Bloedite is commonly found together with gypsum, thenardite, and magnesite in North Ingebright Lake sediments. As discussed by Madsen (1966), dehydration of bloedite only occurs at above 120°C. It is a stable mineral (its metastable phase is konyaite ($Na_2Mg(SO_4)_2H_2O$)) under room temperature and primarily precipitated from the concentrated brine containing Na_2SO_4 and $MgSO_4$ in a molar ratio of 1:1 (Van Doesburg, 1982).

Epsomite ($MgSO_4 7H_2O$)/hexahydrite ($MgSO_4 6H_2O$)/kieserite ($MgSO_4 H_2O$)

Kieserite is the most common Mg sulfate in evaporites, while both epsomite and hexahydrite are rarely found in salt deposits (Holser, 1979; Braitsch, 1971). Usually, kieserite, epsomite and hexahydrite coprecipitate from Na-Mg-Cl-SO_4 type brine with carnallite and polyhalite (Eugster et al., 1980).

Eugsterite ($Na_4Ca(SO_4)_32H_2O$)

Eugsterite was first reported to occur in Kenya and Turkey and named after Hans P. Eugster (Vergouwen, 1981). The mineral is commonly found in the salt efflorescence in most playa lakes, where it originates from Na-SO_4-Cl type waters. Experimental results indicate that eugsterite can form together with thenardite and gypsum in considerable amounts in solutions with a molar ratio Na/Ca more than 4 (Vergouwen, 1981).

Görgeyite ($K_2Ca_5(SO_4)_64H_2O$) and starkeyite ($MgSO_44H_2O$)

Görgeyite and starkeyite are rare secondary minerals. Görgeyite could formed by the reaction of brines with previously deposited gypsum: [$CaSO_42H_2O + K^+ \leftrightharpoons K_2Ca_5(SO_4)_64H_2O$]. Starkeyite might be a result of dehydration of epsomite ($MgSO_47H_2O$) under the extremely concentrated conditions (Eugster and Smith, 1965).

Gypsum($CaSO_42H_2O$) and anhydrite($CaSO_4$)

Anhydrite can be produced by either direct precipitation or by gypsum dehydration. Gypsum is, however, reported to exist down to a depth of 1200 m in other area (Sonnenfeld, 1984), which indicates that neither the geothermal gradient nor the overburden pressure is the primary agent of anhydritization in the North Ingebright Lake basin. Anhydrite precipitation and gypsum-dehydration in modern lake environments are primarily controlled by the brine concentration. Contact between the previously precipitated gypsum and brines is necessary to alter gypsum to anhydrite (Braitsch, 1971). Primary anhydrite precipitation usually occurs when the brine becomes sufficiently concentrated and the water activity has been greatly reduced (0.2-0.7)(Sonnenfeld, 1984). Neutron diffraction studies (Atoji, 1958) have shown that the water molecules around gypsum are so weakly bound that the hygroscopic bitterns can readily dehydrate gypsum. Gypsum dehydration usually starts when a brine is concentrated beyond the stage of the saturation with respect to sodium chloride (Eugster et al., 1980).

Krausite ($Fe_2(SO_4)_3 2H_2O$)

Krausite was found in borate deposits in San Bernardino County, California (Foshag, 1931). It occurs in the alunite as large crystals or in the nests and irregular cavities in the fine clay-like alunite and coquimbite. Krausite is commonly associated with jarosite, fibroferrite, gypsum and anhydrite (Foshag, 1931). The mineral probably originated from the oxidation of pyrite (Foshag, 1931).

Leightonite ($K_2Ca_2Cu(SO_4)_4 2H_2O$)

Leightonite was first identified in the Chuquicamata mine in Atacama province, Chile (Palache, 1938; Van Loan, 1962; Cook, 1978). It is named in honor of Dr. Tomas Leighton, University of Santiago, Chile (Palache, 1938). Leightonite is commonly associated with gypsum, bloedite, atacamite and natrochalcite (Van Loan, 1962).

Mercallite ($KHSO_4$)

Mercallite is named after Giuseppe Mercalli (1850-1914), a former director of Vesuvius Observatory (Palache, 1951). It was identified in a saline efforescence from Vesuvius as minute orthorhombic crystals (Embrey and Fuller, 1979). It can primarily precipitate from the concentrated solutions (Palache et al., 1951).

Mirabilite($Na_2SO_4 10H_2O$) and thenardite (Na_2SO_4)

Mirabilite and thenardite constitute one mineral pair which depends on the brine composition, temperature, and activity of water. At one atmosphere, in the presence of a pure sodium sulfate solution, the transition temperature of mirabilite to thenardite is 32°C (Cole, 1926)(Figure 5.2); mirabilite can crystallize at temperatures near 0°C from brines having total salinities between 30 and 70 ppt (Smith, 1979). However, the presence of NaCl and Na_2CO_3 dissolved in the brine can lower the mirabilite/thenardite transition temperature. For example, the transition temperature decreases from 32°C for a pure sodium-sulfate solution to 17.9°C for a solution saturated with respect to both sodium sulfate and sodium chloride (Figure 5.3). In brines containing 16.3% Na_2CO_3, the transition occurs at about 27°C (Eugster and Smith, 1965). In a simple ternary system of calcium sulfate, sodium sulfate, and water, mirabilite and thenardite usually are precipitated when $CaSO_4$ concentration reaches 22% and 34% at 25°C (Hill and Wills, 1938). The pronounced effect of common-ion compounds in solution on the transition

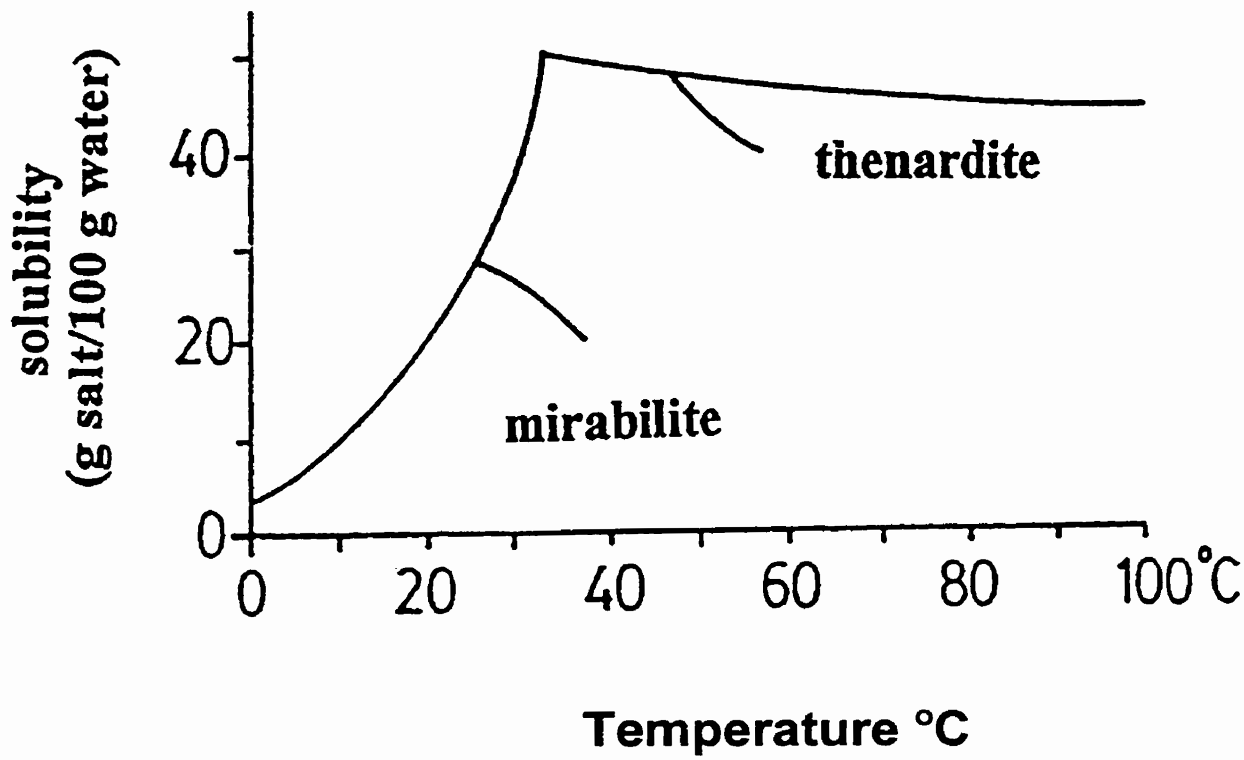

Figure 5.2 Solubility of sodium sulfate in water (from Cole,1926)

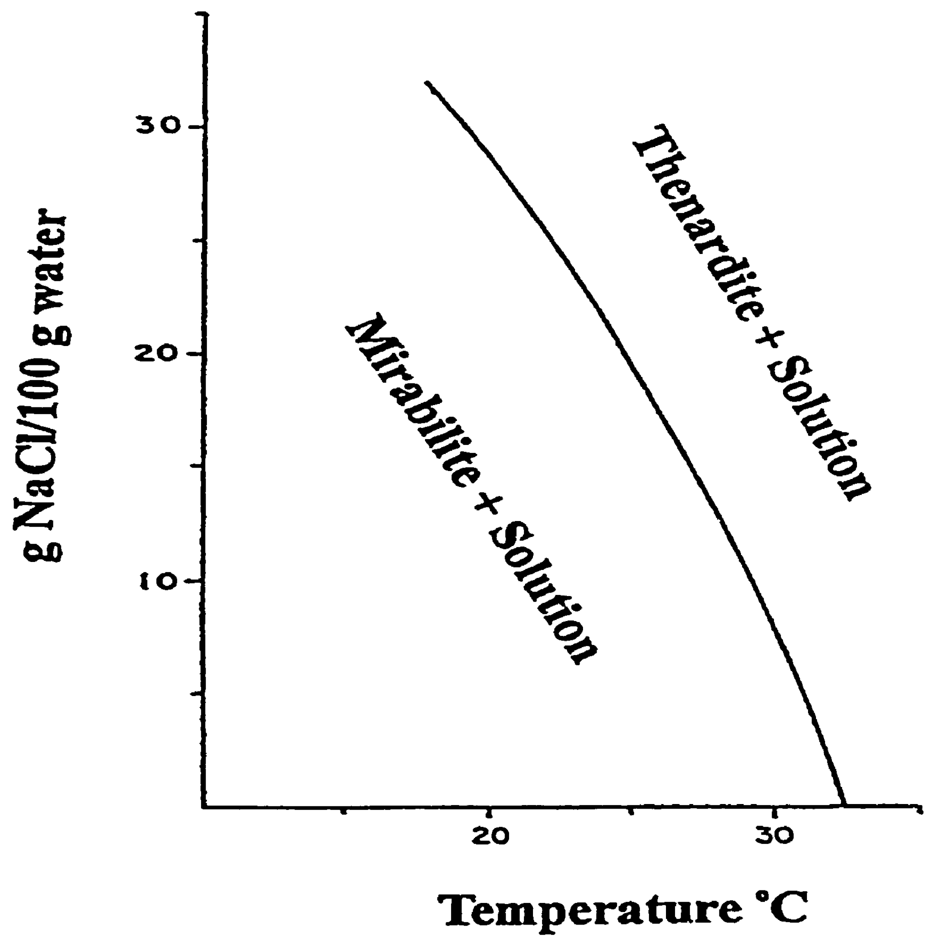

Figure 5.3 Diagram showing the effect of dissolved NaCl on the mirabilite-thenardite transition temperature (from Eugster and Smith, 1965)

temperature of mirabilite and thenardite shows that the phase of sodium sulfate precipitated from brines is strongly controlled not only by the temperature and water activity, but also by the chemical composition of brines.

Polyhalite ($Ca_2K_2Mg(SO_4)_4 2H_2O$)

Origin of polyhalite can be both secondary and primary. In lacustrine environments, most of the polyhalite is secondarily formed by the conversion of gypsum or anhydrite, such as [$CaSO_4 2H_2O + K^+ + Mg^{2+} \leftrightharpoons Ca_2K_2Mg(SO_4)_4 2H_2O + 2Ca^{2+}$](Hite, 1983; Sonnenfeld, 1984). Polyhalite may also be formed at the expense of glauberite by reaction: [$Na_2Ca(SO_4)_2H_2O + CaSO_4 + 2K^+ + Mg^{2+} + SO_4 + 2H_2O \leftrightharpoons Ca_2K_2Mg(SO_4)_4 2H_2O + 2Na^+$]. The occurrence of polyhalite implies that brines are relatively enriched in K and Mg and new brine-solid phase equilibrium is reached by the back-reaction with previously deposited sulfates.

Wattevilleite ($Na_2Ca(SO_4)_2\ 4H_2O$)

Wattevilleite was found in pyritic lignite in the Einigkeit mine, near Bischofsheim, Germany (Palache et al., 1951; Roberts et al., 1990). However, origin and paragenetic data of this mineral are not available in the published literature.

Artinite ($Mg_2CO_3(OH)_2 3H_2O$)

Artinite was found in Val Malenco, Italy and in San Benito County, California (Cisneros et al., 1977). It occurs as crusts of acicular crystals, cross-fiber veinlets, and as spherical aggregates of radiating fibers coating fracture surfaces in serpentinized volcanic rocks. The mineral is commonly associated with hydromagnesite, magnesite, calcite, pyroaurite and dypingite (Cisneros et al., 1977).

Ankerite ($Ca(Fe,Mg)(CO_3)_2$)

Ankerite (also called ferroan dolomite) is one member of $CaCO_3$-$MgCO_3$-$FeCO_3$ mineral system (Goldsmith et al., 1962). The effect of the substitution of the magnesium ions by the larger ferrous iron ion in the ankerite is an increase in both the *a* and *c* dimensions of the cell parameters (Howie et al., 1958). This mineral commonly occurs in sedimentary rocks and ore deposits, such as at the Antwerp iron mine, New York and at Oldham, Lancashire, England (Roberts et al., 1990; Broadhurst et al., 1958). Ankerite is most likely resulted from the alteration of previously precipitated calcite or dolomite (Broadhurst et al., 1958).

Benstonite ($Ca_7Ba_6(CO_3)_{13}$)

Benstonite was found at the large barite deposit in Hot Spring County, Kansas (Lippmann, 1962). The beds of deposit lie between the Devonian-Mississippian novaculite and the Pennsylvanian shale. The barite rock is fine-grained with varying amounts of interspersed shaly materials. Benstonite occurs as irregular white veins in the barite rock and is commonly associated with calcite and barite (Lippmann, 1962). It is likely that the barium of benstonite came from the barite, whereas calcium was introduced by percolating water. Benstonite is primarily precipitated from the concentrated solution as a carbonate mineral (Lippmann, 1962).

Fairchildite ($K_2Ca(CO_3)_2$)

Fairchildite is named in honor of John G. Fairchild, chemist of Geological Survey, United States Department of the Interior (Milton and Axelrod, 1947). It has been found in wood ash of partly burned forest trees in the western United States (Milton and Axelrod, 1947). Fairchildite has also been identified in ash from the biomass combustion (Navrotsky et al., 1997). Experiental works indicate that fairchildite can primarily precipitate from the concentrated K^+-Ca^{+2}-CO_3^{-2} solutions or form by the reaction of previously precipitated gaylussite with the K^+-CO_3^{-2} aqueous solutions (Milton and Axelrod, 1947).

Gaylussite ($Na_2Ca(CO_3)_25H_2O$)

In the lacustrine environment, gaylussite is usually result of back-reaction of evaporating alkaline brine with early-formed calcite (or aragonite), controlled by the magnitudes of the activity of water (Eugster and Smith, 1965): [$CaCO_3 + 2Na^+ + CO_3^{2-} + 5H_2O \rightleftharpoons Na_2Ca(CO_3)_25H_2O$]. The presence of gaylussite rather than pirssonite ($Na_2Ca(CO_3)_23H_2O$) indicates a relatively low temperature and high ^aH_2O conditions.

Kutnohorite ($Ca(Mn,Mg)(CO_3)_2$)

Differential thermal and X-ray analysis indicate that kutnohorite is a maganese member of the dolomite group (Frondel et al., 1954). Kutnohorite occurs as anhedral masses with curved cleavage surfaces up to three centimeters in Franklin and Sterling Hill, New Jersy. It is associated with calcite and rhodochrosite (Frondel et al., 1954). Recently, kutnohorite was commonly identified in modern lake deposits (Radovanovic, 2000; Radovanovic and Last, 2000; and Stevens et al., 2000). In the Big Watab Lake, MN, USA, the kutnohorite occurs as a true authigenic mineral associated with calcite in a reducing environemnt (Stevens et al., 2000). In the West Basin Lake, Victoria, Australia, the kutnohorite occurs as cement in beach rocks and lithified microbialites (Radovanovic and Last, 2000).

Minrecordite ($CaZn(CO_3)_2$)

Minrecordite is the Ca and Zn member of the dolomite series, found in the dioptase deposit of Tsumeb, Namibia (Garavelli et al., 1982). It normally occurs as two distinct variants: nearly pure $CaZn(CO_3)_2$ with only minor substitution of Mg, Fe, and Mn for Zn and a magnesian variety. However, these two minrecordite variants differ only slightly in chemical composition, unit-cell parameters and physical properties (Garavelli et al., 1982). The paragenetic mineral assemblage includes calcite, zincian dolomite, dolomite, magnesian minrecordite and minrecordite.

Zemkorite ($Na_2Ca(CO_3)_2$)

Zemkorite was first identified in cores, Yakutiya, Russia (Yegorov et al., 1990). It is a secondary mineral, resulted from the alteration of alkaline volcanic rock by highly concentrated brine solutions. Associated minerals include shortite and halite (Yegorov et al., 1990).

Bradleyite ($Na_3MgPO_4CO_3$)

Bradleyite, sodium phosphate-magnesium carbonate, was first found in the oil shale of Green River formation, Sweetwater County, Wyoming (Fahey and Tunell, 1941). It is commonly associated with trona, shortite, pirssonite, gaylussite, bromlite, and northupite. It was determined that bradleyite in the oil shale of Green River formation is a secondary mineral, originated from the alteration of sodium-calcium carbonate mineral, shortite [$Na_2Ca_2(CO_3)_3$] (Fahey and Tunell, 1941).

Burkeite ($2(Na_2SO_4)Na_2CO_3$)

Burkeite is a common mineral in lacustrine sediments; it is formed by the reaction of previously precipitated thenardite with CO_3^{-2} bearing brine: [$2NaHCO_3 + 2Na_2SO_4 \leftrightharpoons 2(Na_2SO_4)(Na_2CO_3) + H_2O + CO_2$]. Usually the occurrence of burkeite implies existence of the following conditions: solid carbonates are present in excess over solid sulfates (Eugster and Smith, 1965).

Hanksite ($9Na_2SO_42Na_2CO_3KCl$)

Hanksite is a secondary mineral formed by the reaction of previously precipitated thenardite, halite, or burkeite with K or CO_3 bearing brine: [$12NaHCO_3 + K_3Na(SO_4)_2 + 3NaCl + 25Na_2SO_4 \leftrightharpoons 3(2Na_2CO_3\ 9Na_2SO_4\ KCl) + 6H_2O + 6CO_2$] (Smith, 1979). The occurrence of hanksite usually means that brine composition is characterized by high pH (Smith, 1979). The ratios of Na_2CO_3 to Na_2SO_4 that allow hanksite to form, when the solution is saturated in halite and contains the correct percentage of K, are 0.3-4 (Smith, 1979).

Kainite ($KClMgSO_4 3H_2O$)

Kainite is formed only if the ratio between magnesium sulfate and potassium chloride in the brine exceeds 0.1 by the following reaction: [$MgSO_4 7H_2O + K^+ + Cl^- \rightleftharpoons KClMgSO_4 3H_2O + H_2O$]. At a ratio between 0.1-0.3, kainite coprecipitates with carnallite; at a ratio < 0.1, kainite occurs mixed with epsomite (Sonnenfeld, 1984). The Harvie-Weare model (1982) predicts kainite saturation at water activity of 0.42-0.62. Therefore, the presence of kainite in sediments usually shows the existence of the arid condition during deposition of sediments.

Rapidcreekite ($Ca_2SO_4CO_3 4H_2O$)

Rapidcreekite was first identified by Roberts et al. (1986) from a sequence of Lower Cretaceous (Albian) ironstones and shales in the Rapid Creek area, northern Yukon Territory. It is originated from recent surface weathering and occurs as a secondary phase on dilated joint-surfaces and bedding planes in a blocky quartz-rich bed in sideritic iron-formation. The mineral is commonly associated with aragonite, gypsum, hexahydrite, epsomite and diadochite (Roberts et al., 1986).

Tychite ($Na_6Mg_2SO_4(CO_3)_6$)

Tychite is a secondary mineral. It precipitates at the expense of thenardite, nahcolite and dolomite by the following reaction: [Na_2SO_4 + 4NaHCO3 + 2CaMg(CO_3)2 $\rightleftharpoons$ 2$CaCO_3$ + $Na_6Mg_2SO_4(CO_3)_6$ + 2H_2O + 2CO_3]. Occurence of tychite usually implies the existence of the following conditions: solid carbonates are present in excess over solid sulfates and consistently contact with brines (Eugster and Smith, 1965).

Bischofite ($MgCl_26H_2O$)

Bischofite is a late stage evaporite mineral. It can primarily precipitate from a concentrating brine after the potassium supply has been exhausted. Bischofite can also form by diagenetic alteration of previously precipitated carnallite minerals (Sonnefeld, 1984).

Carnallite ($KMgCl_3\,6H_2O$)

Carnallite occurs mainly as a component of sedimentary saline deposits, often associated with kieserite, halite, sylvite, and polyhalite. Carnallite can precipitate primarily from the concentrated brine when the the solution reach the the point of carnallite saturation. It can also form by secondary alternation after kainite as a result of the following reaction (Braitsch, 1971; Sonnefeld, 1984): [$KMg(SO_4)Cl3H_2O$ + 4$MgCl_2$ + 32H_2O $\rightleftharpoons$ 4$MgSO_4H_2O$ + 4 $KMgCl_3\,6H_2O$ + 15H_2O].

Korshunovskite ($Mg_2Cl(OH)_34H_2O$)

Korshunovskite was first identified from the Korshunov iron-ore deposit, Irkutsk region, Russia (Dunn and Fleischer, 1983). Paragenetic minerals include magnesite, dolomite and antigorite. However, the origin data of Korshunovskite is incomplete at present.

Inderborite ($CaMgB_6O_{11}H_2O$)

Borate minerals are usually present in potassium-magnesium salt sequences. This suggests that borate minerals precipitate only during the late evaporation stage. For example, in Germany borate minerals only appear in the carnallite or polyhalite-kieserite region of the evaporite sequence (Sonnefeld, 1984). In most cases, borate deposits are also closely associated with volcanic rocks. The thick Miocene borate deposits at Kramer, California are underlain by the Saddleback Basalt and overlain by beds of volcanic ash. Borate minerals have been shown to have originated from diagenetically altered volcanic rocks (Barnard and Kistler, 1966). In Mississippian evaporites of southern New Brunswick, Canada, a number of borate minerals are found in sylvite, halite, anhydrite and red mudstone. The addition of boron from volcanic exhalation is postulated to account for these borate mineral deposits (Rouslston and Waugh, 1981). Therefore, the presence of borate minerals can be explained by the occurrence of syndepositional volcanic activity, which is a source of boron for the evaporite basin.

Nitrate (KNO_3) and nitratine ($NaNO_3$)

Niter and nitratine are commonly found in some lacustrine deposits. The largest known deposits of lacustrine nitrates are located in the deserts of Atacama and Tarapaca, in the northern part of Chile. Niter and nitratine are also reported to occur in large quantities in Searles Lake, California (Smith, 1979). The nitrates are usually associated with anhydrite, gypsum, thenardite, mirabilite, bloedite, and epsomite. The nitrates possibly are precipitated from the concentrated brine or formed by the oxidation of organic matter (Clarke, 1924).

Chapter 6 Geochemistry of Sedimentation

6.1 Introduction

Evaporite formation and related physical-chemical conditions in the sedimentary realm are subjects of long-standing interest and study over the last two centuries (Eugster, 1971; Multhauf, 1978; Warren, 1989; Rosen, 1991). Numerous chemical models have been established to predict the sequence of salts precipitated during evaporative concentration of a brine. In general, two approaches have been used to determine the stable mineral-solution assemblages for the various component systems in evaporating brines: (i) direct evaporation experiments, and (ii) thermodynamic and solubility calculations. Since the early experimental work of Van't Hoff (Eugster, 1971) and his successors, a large number of solubility measurements of salts in different aqueous systems has accumulated (see Assarsson, 1950a; 1950b; 1950c; Braitsch, 1971; Eugster, 1971; Stewart, 1963). These solubility data have been used to predict successfully the sequence of major minerals precipitated from evaporating brines by means of concentration-temperature diagrams and phase (or Jänecke) diagrams. Clearly, this graphical approach is best applied to simple binary and common-ion aqueous systems and cannot readily manage the more complex ionic systems that commonly occur in natural brines (Hardie, 1984). To solve this problem, several generations of computer models based on equilibrium thermodynamics have emerged over the past two decades, such as WATEQF (Truesdell and Jones, 1974; Plummer et al., 1976), WATEQ2 (Ball, Jenne, and Nordstrom, 1979), SOLMNEQ (Kharaka and Barnes, 1973), and ACTIVITY and PHRQPITZ (Plummer et al., 1988). Although many of these models are limited to dilute aqueous solutions with ionic strengths less than 0.7, some are valid to high ionic strengths (Harvie et al., 1984; Weare, 1987).

These experimental and theoretical geochemical models provide powerful tools that can assist in deciphering past chemical and hydrologic conditions and depositional processes during evaporite formation in a sedimentary basin. In this chapter, these mineral solubility models are used as the theoretical basis to interpret the observed mineral assemblages and chemical compositions of brines in North Ingebright Lake, Saskatchewan, and the hydrologic conditions under which these evaporites were deposited. Although commonly applied to brine reconstruction in marine and lacustrine settings elsewhere, this is the first such effort to apply these models to lake deposits of the Great Plains of North America.

6.2 Basis of Chemical Composition Reconstruction

Two approaches have been used to determine the chemical sedimentation history of North Ingebright Lake: mass balance calculations and physical-chemistry reasoning. For the bulk chemical composition determination of lake water, a basic tenet is that in a hydrologically closed system undergoing evaporative concentration, a complete assemblage of nondetrital minerals must have the same bulk ionic composition as the original water (Hardie, 1984). As discussed elsewhere (Nesbitt, 1974; Wasson et al., 1984; Torgersen et al., 1986; Teller and Last, 1990; Spencer et al., 1985a; 1985b; Last, 1994; 1999), there are many assumptions and limitations that must be accepted in the application of this straightforward principle to paleolimnology.

For North Ingebright Lake, no perennial streams enter or exit the lake, and the catchment area is very small, which limits clastic input. Sediments are dominantly endogenic/authigenic rather than detrital, and chemical sedimentation is the main process. High density of subsampling (2 cm interval) in the North Ingebright Lake cores provides a good basis for the proper identification of the composition of the parent brine. For each sample, the complete assemblage of saline minerals (qualitative) and the abundance of the major saline minerals (semi-quantitative) have been determined. From simple mass balance considerations, the major ion ratios of the parent brine for North Ingebright Lake evaporite sequence can be related to the mineral contents as follows (in molar proportion) (Hardie, 1984):

Ca/Na ≈ (protodolomite+gypsum+anhydrite+calcite+aragonite)/(thenardite+2bloedite+halite)

Mg/Na ≈ (magnesite+protodolomite+bloedite)/(thenardite+2bloedite+halite)

SO_4/Na ≈ (gypsum+anhydrite+bloedite+thenardite)/(thenardite+2bloedite+halite)

CO_3/Na ≈ (aragonite+magnesite+2protodolomite+calcite+Mg calcite)/(thenardite+2bloedite+halite)

CO_3/SO_4 ≈ (aragonite+magnesite+2protodolomite+calcite+Mg calcite)/(gypsum+anhydrite+bloedite+thenardite)

Table 6.1 and Figure 6.1 show changes in the major dissolved components in the precipitating brine in North Ingebright Lake through the Holocene. Further refinement of the brine composition is accomplished by the occurrence of minor and trace minerals. Over 40 species of primary and authigenic minerals have been

Table 6.1 Variations of average ion ratios in different stratigraphic units of north core at North Ingebright Lake

	Stratigraphic Unit							
	2 Na-Sulfate	3 Mg-Carbonate-- Na-Sulfate	4 Ca-Sulfate-- Na-Sulfate	5 Muddy Na- Sulfate	6 Na- Sulfate	7 Muddy Mg-calcite- Na-Sulfate	8 Dolomitic Na- Sulfate	Average
Ca/Na	0.1	0.1	0.3	0.1	0.1	0.1	0.2	0.2
Mg/Na	<0.1	0.1	0.1	<0.1	<0.1	<0.1	0.2	0.1
SO_4/Na	1	1.1	1.3	1.1	1	1.1	0.9	1.1
CO_3/Na	0.1	0.1	0.1	<0.1	<0.1	0.1	0.6	0.2
CO_3/SO_4	<0.1	0.1	0.1	<0.1	<0.1	0.1	0.5	0.1

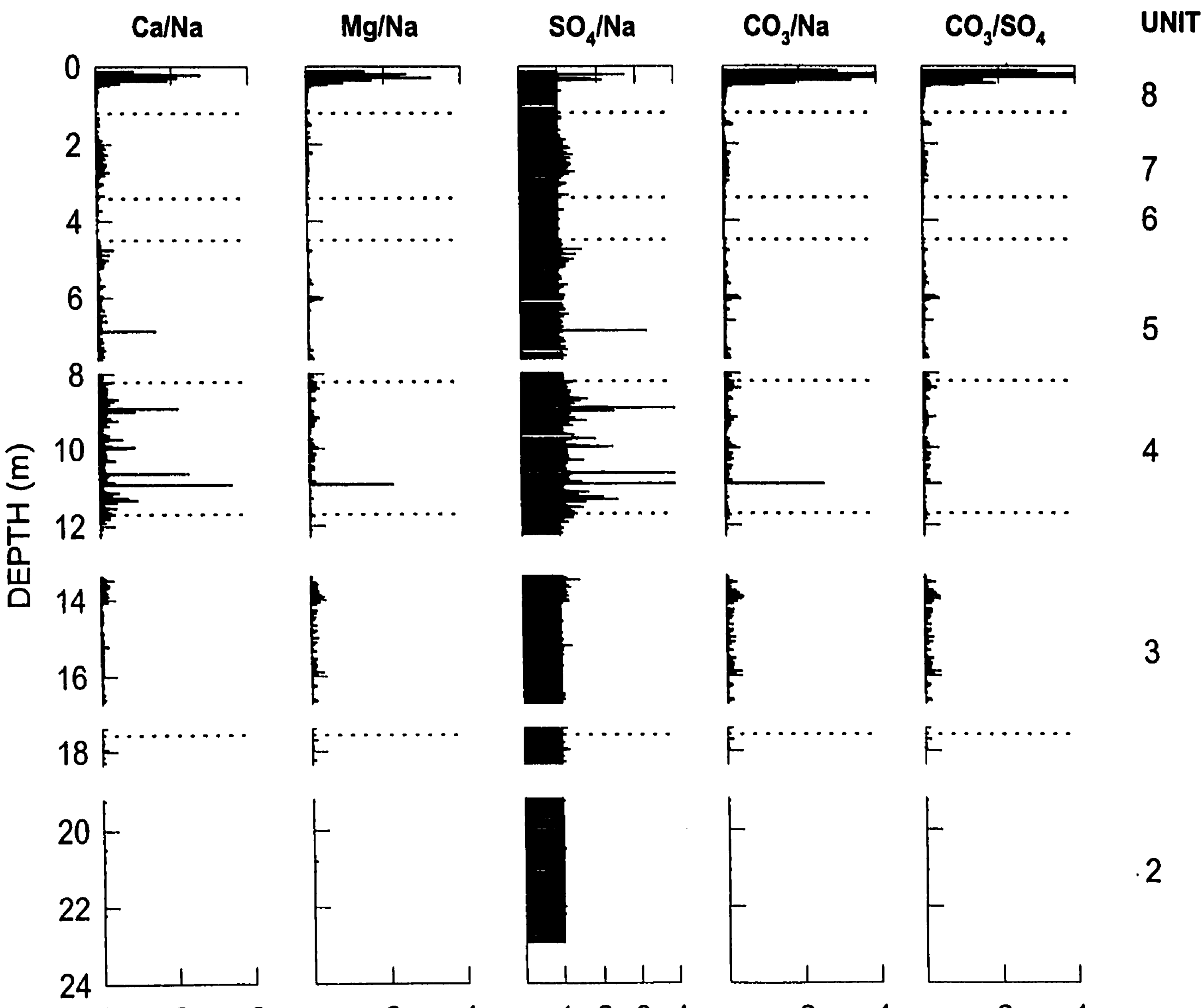

Figure 6.1 Variation in major ion ratios of lake brines versus depth in North Ingebright Lake

identified in North Ingebright Lake deposits (Table 5.1; Appendix C). Many of these minerals may provide important information on the hydrochemical and climatic conditions at the time of precipitation (Hosler, 1979; Last, 1990). The physical-chemical conditions for the formation of trace minerals, such as gaylussite, epsomite, eugsterite, polyhalite, bischofite, carnallite, and burkeite, follow Bradley and Eugster (1969); Braitsch (1971); Eugster and Smith (1965); Eugster et al. (1984); Hardie and Eugster (1970); and Smith (1979). However, modeling data on some trace minerals detected in North Ingebright Lake, such as fairchildite, starkeyite, and rapidcreekite are less complete or unavailable. By combining results from bulk composition determination and physical-chemistry reasoning, the generalized evolutionary paths of brine types at North Ingebright Lake are reconstructed.

6.3 Geochemical History of North Ingebright Lake

The mineral assemblage of North Ingebright lake salts can be represented by phase relationships in the reciprocal quinary system Na-Mg-Ca-Cl-SO_4-H_2O and its subsystems (4-, 3-, or 2-component systems) (Figure 6.2). In that system, at 25°C, gypsum, anhydrite, and mirabilite occupy the bulk of the prism, with thin slices for thenardite, bloedite, and halite (Harvie and Weare, 1980; Harvie et al., 1980; Eugster et al., 1980). The general composition change and evaporative stage of the brine during deposition of the salts are deduced with the aid of these phase diagrams. However, this reconstruction only represents an extremely simplified version of the chemical events that occurred in the lake. In certain cases theoretical

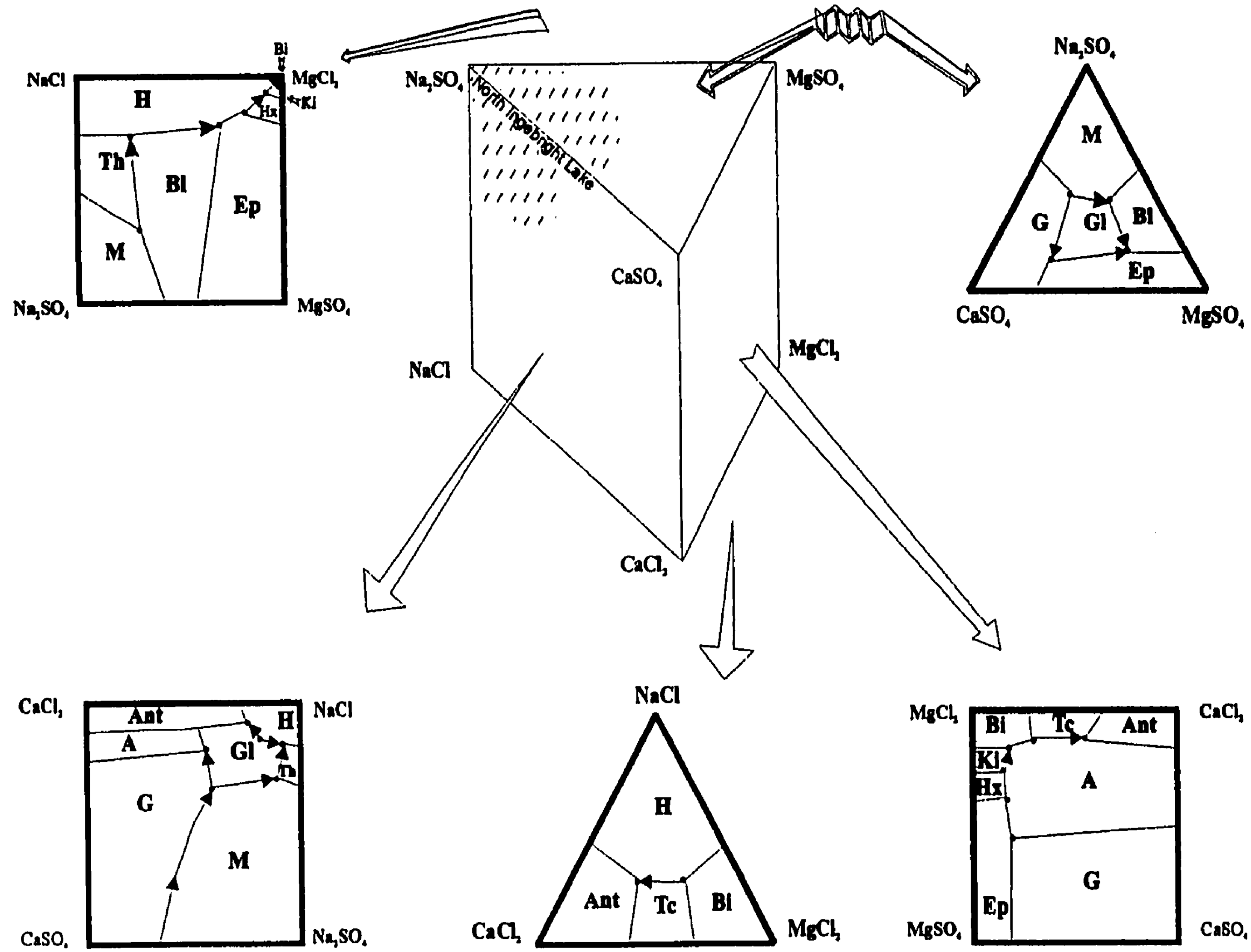

Figure 6.2 The reciprocal quinary system Na-Mg-Ca-Cl-SO$_4$-H$_2$O and its subsystems at 25°C. Modified from Harvie and Weare (1980), Harvie, Eugster, and Weare (1982), and Eugster, Harvie and Weare (1980) For abbreviations see Table 6.2.

Table 6.2 Mineral abbreviations

A	anhydrite	$CaSO_4$
Ap	aphthitalite	$NaK_3(SO_4)_2$
Ant	antarcticite	$CaCl_26H_2O$
Bi	bischofite	$MgCl_26H_2O$
Bl	bloedite	$Na_2Mg(SO_4)_24H_2O$
Car	carnallite	$KMgCl_36H_2O$
Ep	epsomite	$MgSO_47H_2O$
G	gypsum	$CaSO_42H_2O$
Gl	glauberite	$Na_2Ca(SO_4)_2$
H	halite	$NaCl$
Hx	hexahydrite	$MgSO_46H_2O$
Ka	kainite	$KMgClSO_43H_2O$
Ki	kieserite	$MgSO_4H_2O$
Le	leonite	$K_2Mg(SO_4)_24H_2O$
M	mirabilite	$Na_2SO_410H_2O$
Pic	picromerite	$K_2Mg(SO_4)_26H_2O$
Po	polyhalite	$K_2MgCa_2(SO_4)_22H_2O$
Syl	sylvite	KCl
Syn	syngenite	$K_2Ca(SO_4)_26H_2O$
Tc	tachyhydrite	$Mg_2CaCl_612H_2O$
Th	thenardite	Na_2SO_4

equilibrium models cannot predict the observed mineral sequence so more complicated geological processes have to be proposed to explain the mineral formations.

Unit 1 was only penetrated in the south core. It consists mainly of gypsum, fine-grained sand, silt, clay and organic materials. Unlike Units 2-8, Unit 1 was dominated by physical sedimentation process. Therefore, only chemical sedimentation processes of Units 2-8 are discussed in the following section.

6.3.1 Unit 2 Na-Sulfate Salt

The saline minerals in Unit 2 are mostly mirabilite or thenardite with minor amounts of gypsum, bloedite, and halite. This simple mineral assemblage indicates that the saline lake waters were chemically simple and dominated by Na and SO_4 (SO_4/Na molar ratio = 1) (Table 6.1, Figure 6.1). The small percentage of Ca, Mg, and HCO_3+CO_3 ions may indicate brief changes in the chemical compositions of the lake waters perhaps caused by episodes of freshwater.

The evaporites in Unit 2 are composed chiefly of minerals that represent phases in the quaternary system $CaSO_4$-Na_2SO_4-NaCl-H_2O. The stability fields of the solid phase assemblages in terms of the anhydrous composition of the co-existing solutions at 25°C and 1 atm total pressure are shown in Figure 6.3 (Hardie, 1968). The data in Unit 2 show that of the related minerals in Figure 6.3, only mirabilite-gypsum, mirabilite-thenardite, and thenardite-halite coexist in appreciable quantities; glauberite and anhydrite are not present.

Zones 1 and 3 are similar in that they consist solely of monomineralic beds

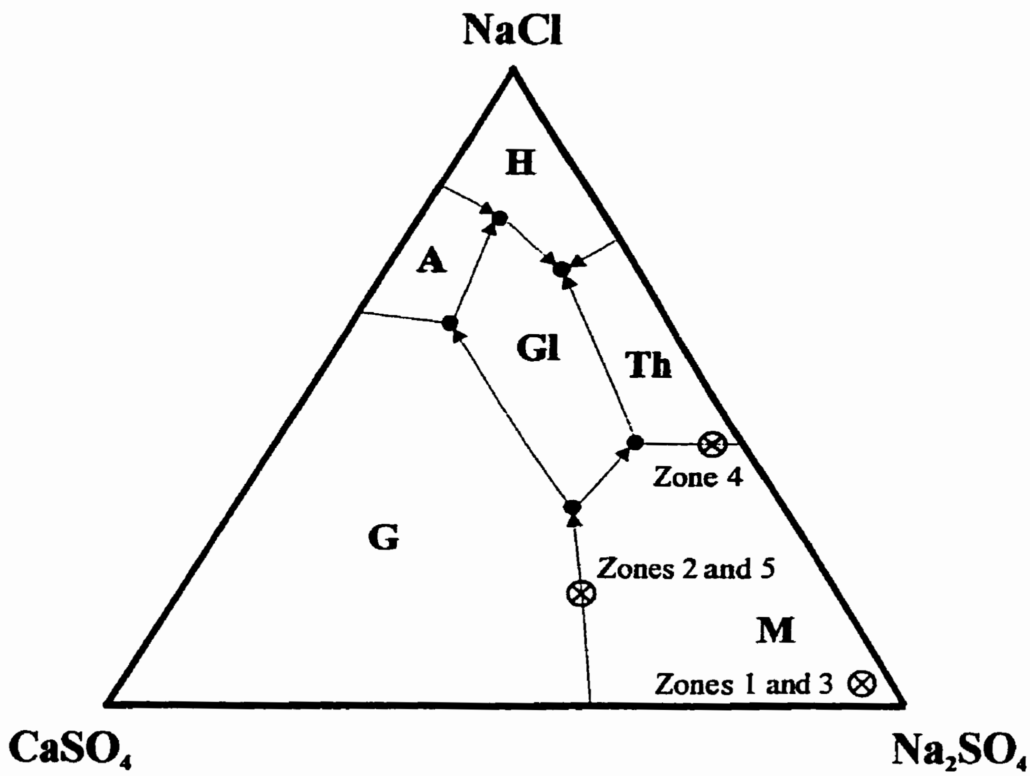

Figure 6.3 Schematic phase relations in $CaSO_4$-Na_2SO_4-$NaCl$-H_2O system of Unit 2. Modified from Hardie (1968). For abbreviations see Table 6.2.

of mirabilite, while zones 2 and 5 are also similar because both of them contain gypsum (see Section 4.3.2). Halite is only found in zone 4, which may indicate that the brines of zone 4 were desiccated more extensively than those that produced zones 1, 2, 3, and 5. In the $CaSO_4$-Na_2SO_4-NaCl-H_2O system, the mirabilite and thenardite stability fields are small and close to the NaCl-Na_2SO_4 boundary (Figure 6.3). This implies that the brines of zones 1 and 3 were very close to the Na_2SO_4 corner at the time crystallization began. The crystallization of mirabilite forced the composition of the remaining brine toward the $CaSO_4$-NaCl edge of the phase diagram. However, it never reached the boundary of the mirabilite and gypsum adjoining field. Zones 2 and 5 both contain mirabilite and gypsum, which indicates that the initial brines were represented by points in the mirabilite or gypsum field but close to the phase boundary.

Zone 4 is composed mainly of mirabilite and thenardite with traces of halite. This mineral composition shows that the brines that produced salts in zone 4 experienced a short-term shift toward the NaCl corner along the Na_2SO_4-NaCl edge of the diagram shown in Figure 6.3.

It is evident, therefore, that the brines that produced salts in zones 1 and 3 had an initial composition of Na-SO_4, the brines that desiccated to produce salts in zone 4 were dominated by Na-SO_4-Cl, and the initial composition of zones 2 and 5 brines were Na-Ca-SO_4. Thus, the whole salt sequence of Unit 2 is obviously not a result of one evaporating event. However, the mineral assemblage points toward three evaporating cycles from zone 1 to zone 5: Na-SO_4→Na-Ca-SO_4 (zone 1-zone 2), Na-SO_4-Cl (zone 3), and Na-SO_4→Na-Ca-SO_4 (zone 4-zone 5).

The existence of nitrates in zone 4 (also little in 1, 2, and 3) provides further insight into the depositional environments. Niter and nitratine are commonly believed to be either (i) precipitated from a highly concentrated brine or (ii) formed by the oxidation of organic matter. The trace amounts of nitrates of zone 4 were most likely produced by the oxidation of organic matter, which is supported by a general low organic matter content (average: 0.4%) in Unit 2 (Figures 4.8 and 4.9). Therefore, the presence of nitrates might indicate that oxygenated shallow water conditions existed during the deposition of Unit 2.

6.3.2 Unit 3 Mg-Carbonate--Na-Sulfate Salt

The evaporite minerals in the sediments of Unit 3 consist of high-Mg calcite, aragonite, protodolomite, magnesite, gypsum, mirabilite, thenardite, eugsterite, bloedite, starkeyite, and halite. The number of components involved in the mineral assemblages of most zones in Unit 3 is large and makes complete graphic representation of the phase relations impossible. However, the post-carbonate mineral assemblage can be represented by phases in the quinary system: Na-Mg-Ca-Cl-SO_4-H_2O. A complete analysis of the phases in this six-component system is rather complex. According to Gibbs phase rule, a maximum of four solids and one liquid phase can coexist at an arbitrary pressure (P) and temperature (T) (Harvie et al., 1982). Based on the semi-empirical equations for the excess solution free energy, Harvie and Weare (1980) and Harvie et al. (1982) determined the invariant points and associated solution composition in this quinary component system and subsystems at 25°C. The stability fields of the solid phase assemblages have been plotted in a trigonal prism diagram representing the reciprocal system. Ten single solid phase fields have been delimited. Gypsum dominates the phase volume; mirabilite, thenardite, bloedite, and epsomite occupy very small percentage of the phase volume. Halite, anhydrite, hexahydrite, and kieserite occur in smaller volume near the base (Figure 6.2).

The evolution of brine composition during deposition of salts in Unit 3 can be qualitatively described through the phase relations in the Na_2SO_4-$CaSO_4$-$MgSO_4$ system (Figure 6.4). The salts in zones 1 and 3 are mostly pure mirabilite and the mud content is relatively high (Figures 4.4-4.6). Therefore, the initial composition must have been close to the Na_2SO_4 corner in Figure 6.4. These zones were probably the result of winter cooling of the lake during periods when its concentration reached 30-70 ppt. In solutions dominated by sodium-sulfate, mirabilite solubility is very sensitive to temperature, and when cooled, mirabilite could be "frozen out" exclusive of the other minerals. During the following warmer seasons, freshwater influxes carry a new group of dissolved solutes (Mg, Ca, and HCO_3+CO_3) and suspended materials to the lake. The deposition of carbonates and clastic mud cover the floor of the lake and protect the mirabilite salts from being dissolved by warmer, summer season waters (Last, 1989).

Zones 2, 5, and 7 consist mainly of mirabilite and gypsum. The brines that produced these salts must have shifted in composition toward the boundary of the mirabilite and gypsum fields, therefore, the initial brines were represented by points in either the mirabilite or gypsum field but close to the phase boundary as noted in Figure 6.4. Zones 2 and 5 contain trace amounts of görgeyite [$K_2Ca_5(SO_4)_6 4H_2O$]

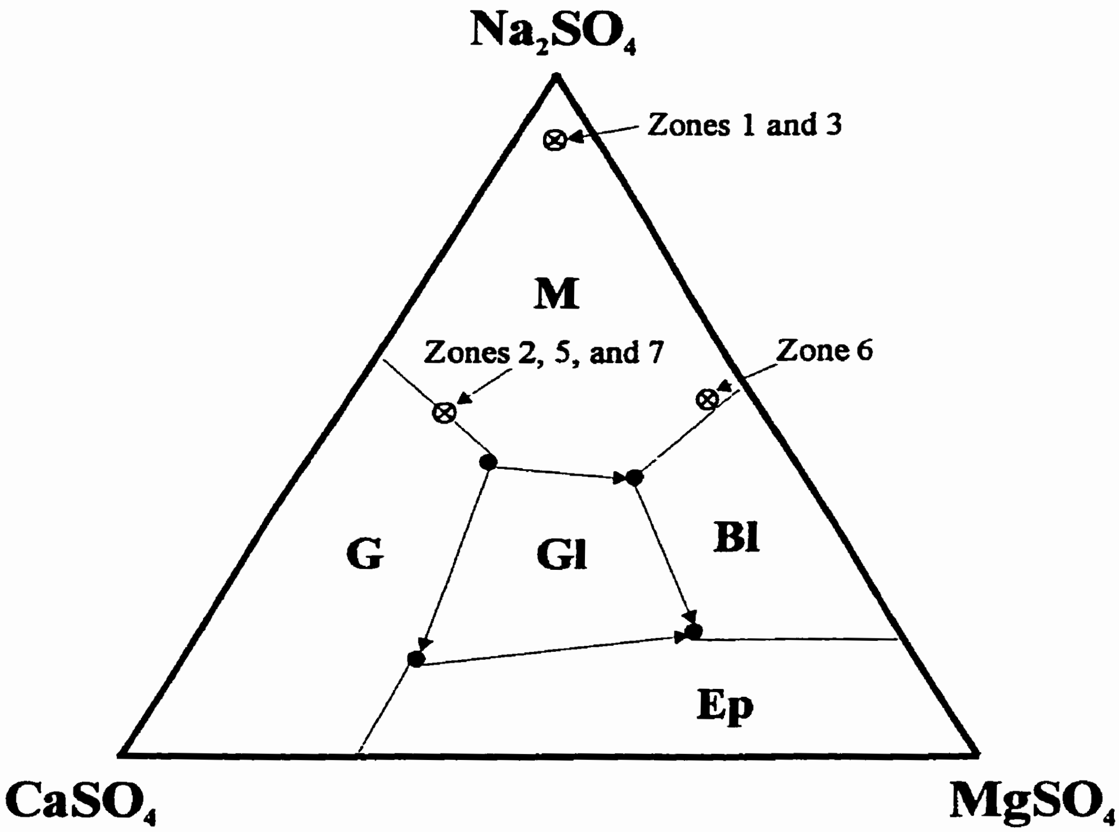

Figure 6.4 Phase relations in $NaSO_4$-$CaSO_4$-$MgSO_4$ system, projected from the H_2O apex (Harvie et al., 1982). For abbreviations see Table 6.2.

and starkeyite ($MgSO_44H_2O$), which are rare secondary minerals. The presence of starkeyite and görgeyite indicates the lake might have been completely dry for a short period of time. Although as discussed by Harvie et al. (1982), stable phase diagrams cannot be readily applied to the minerals that result from complete desiccation of the solution phase to track changing compositions, the existence of starkeyite and görgeyite does show that the brines during deposition of zones 2 and 5 contain K^+ and Mg^{+2}.

Small amounts of gaylussite [$Na_2Ca(CO_3)_25H_2O$] have been detected in zone 4 of Unit 3. The presence of gaylussite, rather than pirssonite, indicates relative low temperature and high ^aH_2O conditions (Eugster and Smith, 1965). The occurrence of sodium-carbonate minerals also implies that the brine composition was a high pH, alkaline brine, poor in Ca and Mg (i.e., Na-K-CO_3-SO_4-Cl) during the deposition of zone 4.

The initial composition of brines during deposition of zone 6 is much more complicated than that of zones 1, 2, 3, 4, 5, and 7, as shown by its saline assemblage of mirabilite, gypsum, bloedite, eugsterite, arcanite, and halite. The appearance of eugsterite and bloedite provides significant information for understanding the chemical composition of brines that produced the salts of zone 6. Eugsterite [$Na_4Ca(SO_4)_32H_2O$] is commonly found in salt efflorescence in playa lakes, where it originates from Na-SO_4-Cl type waters with Na/Ca molar ratios more than 4 (Vergouwen, 1981). Bloedite [$Na_2Mg(SO_4)_24H_2O$] is primarily precipitated from concentrated brines containing Na, Mg and SO_4 in a molar ratio of 1:1 (Van Doesburg, 1982). These show that saline lake waters were dominated by Na, Ca, Mg, and SO_4, with trace K and Cl indicated by the existence of arcanite and halite.

6.3.3 Unit 4 Ca-Sulfate--Na-Sulfate Salt

Unit 4 is largely composed of Ca-Mg carbonate and Na-Ca sulfate minerals, which indicate that the starting compositions of the solution that produced these salts in North Ingebright Lake consisted mainly of Na, Ca, Mg, SO_4, and CO_3 However, a wide variety of minor mineral assemblages in the different zones show that the lake waters experienced diverse variations in the chemical composition, but no general pattern is discernable. These minor minerals include: halite, hanksite, polyhalite, burkeite, carnallite, and gaylussite; most of these are formed by the syndepositional reaction of early formed minerals with the evolving brine. These reaction minerals may be regarded as part of a primary depositional sequence.

Polyhalite [$Ca_2K_2Mg(SO_4)_4H_2O$] occurs in all salt zones of Unit 4, except zone 1, but mainly as a trace mineral. The occurrence of polyhalite implies that brines were relatively enriched in K and Mg and the new brine-solid phase equilibrium was reached by the back-reaction with previously deposited sulfates. Another trace mineral commonly found in Unit 4 is hanksite ($9Na_2S0_42Na_2CO_3KCl$). The occurrence of hanksite indicates that brine composition was characterized by a high pH (alkaline) brine, which is also evidenced by the presence of fairchildite in zones 1 and 2, gaylusite in zone 3, and burkeite in zone 5. The ratios of Na_2CO_3 to Na_2SO_4 that allow hanksite to form are 0.3-4, when the solution is saturated with halite and contains the proper percentage of K (Smith, 1979). Minor amounts of anhydrite occur in zone 5, indicating that ^aH_2O has been decreased to below 0.7

(Braitsch, 1971).

Physical-chemical conditions deduced from the above mineral composition suggest that the minerals making up Unit 4 precipitated over an extreme range of brine concentrations from nearly fresh water to concetrated brines. Each zone approximately represents one continuous evaporating event. In general, brine compositions were dominated by Na-Ca-Mg-CO_3-SO_4 in early stages, and shifted to Na-K-SO_4-Cl in late stages.

6.3.4 Unit 5 Muddy Na-Sulfate Salt

Compared to previous stages, the saline components in Unit 5 suggest that unusual lake conditions existed at this time. The lake was relatively stable and contained more suspended sediment than previous lakes. The high organic matter content and dark colouration of Unit 5 indicate that deposition occurred subaqueously under reducing conditions. However, the lack of lamination suggests that lake water body was not stratified.

Unit 5 is composed mainly of mirabilite/thenardite and gypsum, with lesser amounts of Ca-Mg carbonates. The post-carbonate composition of the brines that formed the salts can be represented by points around the boundaries between the mirabilite and gypsum phase fields and the thenardite and mirabilite phase fields in the $CaSO_4$-Na_2SO_4-NaCl-H_2O system (shaded area in Figure 6.5). Although the lake was consistently occupied by brines saturated in respect with gypsum and mirabilite/thenardite at the time of zones 1-5 deposition, there were probably several short episodes of nearly complete desiccation.

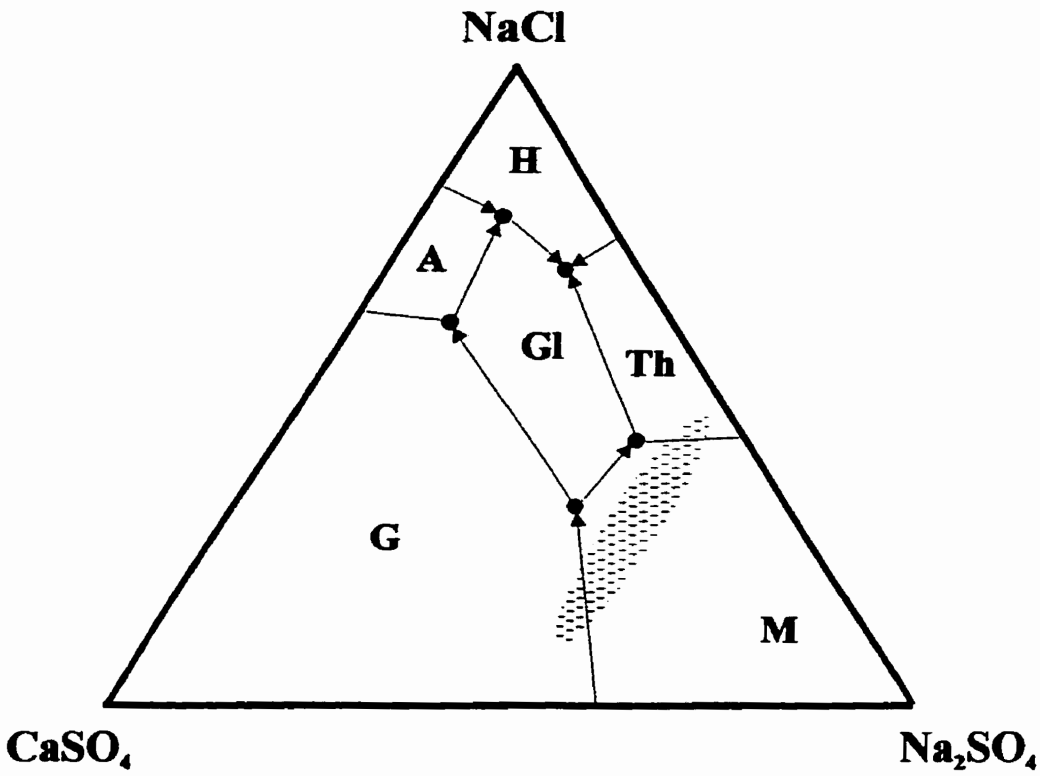

Figure 6.5 Schematic phase relations in $CaSO_4$-Na_2SO_4-NaCl-H_2O system. Modified from Hardie (1968). For abbreviations see Table 6.2.

conditions. In addition, polyhalite is found in zone 2. As discussed in Chapter 5, polyhalite likely resulted from the back-reaction of evaporating K-Mg-SO_4 brine with early-formed gypsum, anhydrite, or glauberite. It is evident, therefore, that the brine composition was dominated by Na, Ca, Mg, and SO_4 (Appendix D) and climate was dry during the deposition of zones 1 and 2.

In contrast with zones 1 and 2, salts in zones 3, 4, and 5 were deposited under relatively dilute waters and cool conditions, as indicated by the presence of gaylussite in zone 3, inderborite in zone 4, and pure mirabilite in zone 5. Gaylusite usually forms under a relative low temperature and high $^{a}H_2O$ environments by back-reaction of evaporating alkaline brine with early-formed carbonates (Eugster and Smith, 1965). Inderborite ($CaMgB_6O_{11}H_2O$) crystallization is also favored by cool temperatures (Smith, 1979), while mirabilite can precipitate from pure sodium-sulfate solution at low temperatures . It is clear that relatively wet and cool conditions are well documented in zones 3, 4, and 5.

6.3.5 Unit 6 Na-Sulfate Salt

Changes in bulk brine composition during the crystallization of zones 1, 2, and 3 are rather gradual. The starting composition of the brine that produced the salts in zone 1 must have been close to the Na_2SO_4 corner along the boundary between NaCl and Na_2SO_4 of Figure 6.6, which is shown by its nearly pure mirabilite component. The saline minerals in zones 2 and 3 are mostly mirabilite and gypsum, implying that the composition of the brine responsible for zones 2 and 3 gradually shifted from the Na_2SO_4 corner to the boundary between the gypsum and mirabilite

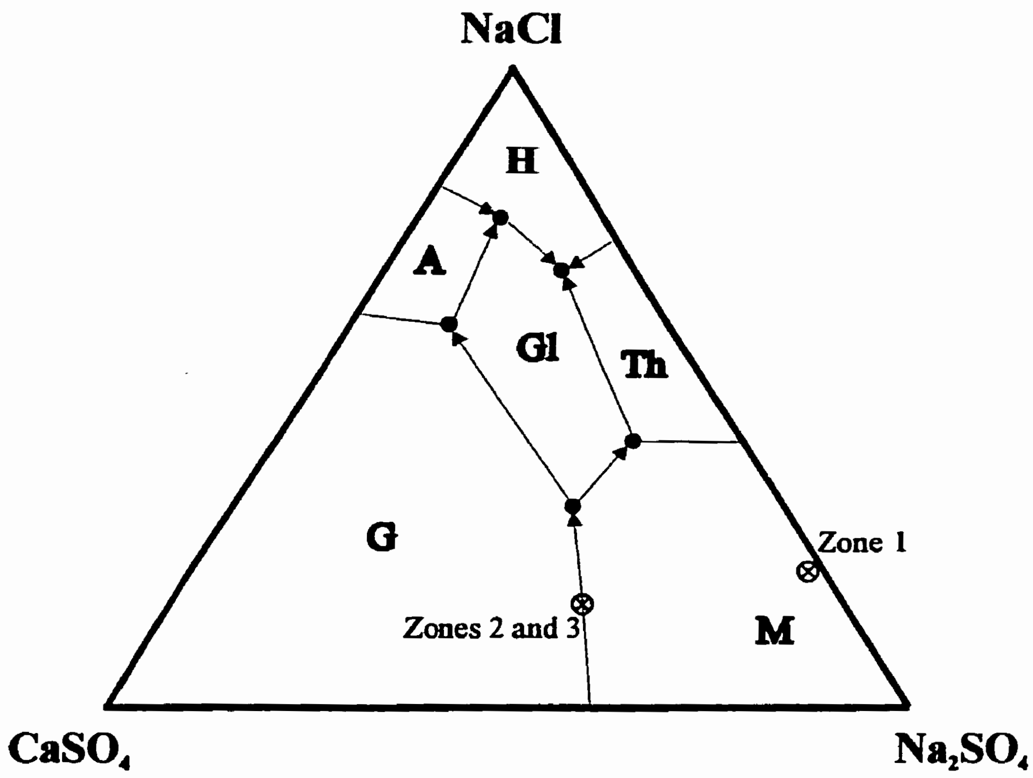

Figure 6.6 Schematic phase relations in $CaSO_4$-Na_2SO_4-$NaCl$-H_2O system. Modified from Hardie (1968). For abbreviations see Table 6.2

Trace amounts of epsomite ($MgSO_47H_2O$) were detected in zone 1 as an admixture to mirabilite and gypsum, suggesting the existence of the concentrated phase fields. In addition, trace amounts of kainite ($4KCl4MgSO_411H_2O$) are in zone 1. As discussed by Sonnenfeld (1984), kainite is formed only if the ratio between magnesium sulfate and potassium chloride in the brine exceeds 1:9; therefore, the brine of zone 1 also contained a small amount of K and Cl ions. In comparison with other units, Ca, Mg, and CO_3 ions are generally low; Na ion is mostly high. However, variations in the Ca, Mg, and CO_3 profiles shown in Figure 6.1 and Appendix D are rather erratic and do not show any overall trends with depth.

The salts in Unit 6 were likely deposited under oxygenated and shallow water conditions. This resulted in a general low content of organic matter and absence of sulfide minerals, which are commonly found in other units (see Appendix C). Niter (KNO_3) is detected in Unit 6; it is most likely a product of organic matter decomposition under this oxygenated shallow water condition.

6.3.6 Unit 7 Muddy Mg-calcite--Na-Sulfate Salt

The evaporite minerals making up this unit consist primarily of mirabilite, thenardite, and gypsum. Carbonate, polyhalite, epsomite, bloedite, and anhydrite occur in lesser amounts. Similar to Unit 6, the composition of the brines that formed the salts of Unit 7 are dominated by Na, Ca, and SO_4 ions, with small amounts of Mg and HCO_3+CO_3 ions. Figure 6.1 and Appendix D show that Na and SO_4 concentrations remain constantly high from zones 1 to 3. Ca, Mg, and CO_3 concentrations vary broadly. In general, Ca and CO_3 decrease and Mg increases upward.

Although the depth of the brine is difficult to assess, the lake was likely quite deep during deposition of salts in Unit 7. The salt was deposited subaqueously under reducing conditions, which is indicated by its relatively high organic matter content and black coloration.

6.3.7 Unit 8 Dolomitic Na-Sulfate Salt

The saline components in Unit 8 consist mainly of high-Mg calcite, protodolomite, mirabilite, thenardite, bloedite, and gypsum. The most abundant mineral assemblage is mirabilite, thenardite, and bloedite, which suggests that the initial composition during the crystallization of Unit 8 can be represented by points in $NaCl$-Na_2SO_4-bl triangle region (Figure 6.7, shaded area). In general, as shown in Figure 6.1, Mg, Ca, SO_4, and CO_3 ion concentrations increase upward. Magnesium calcite with 4-9 mol% $MgCO_3$ is dominant in zone 1, whereas zones 2 and 3 contain high Mg calcite with 11-15 mol% $MgCO_3$ as a major phase. Concurrently with this change, the molar Mg/Na ratio in the waters increases from 0.01 at zone 1 to 1% at zone 3.

Most evaporite beds in Unit 8 show only the earlier and very late parts of the expected succession with some repetition of sequence, such as protodolomite-bloedite, mirabilite-starkeyite, and thenardite-bichofite assemblages. Many transitional mineral phases in these sequences are not present. One possible reason is that dramatic changes of climate caused the rapid drying of the lake. If the brines were concentrated in a short period, there may simply not have been enough

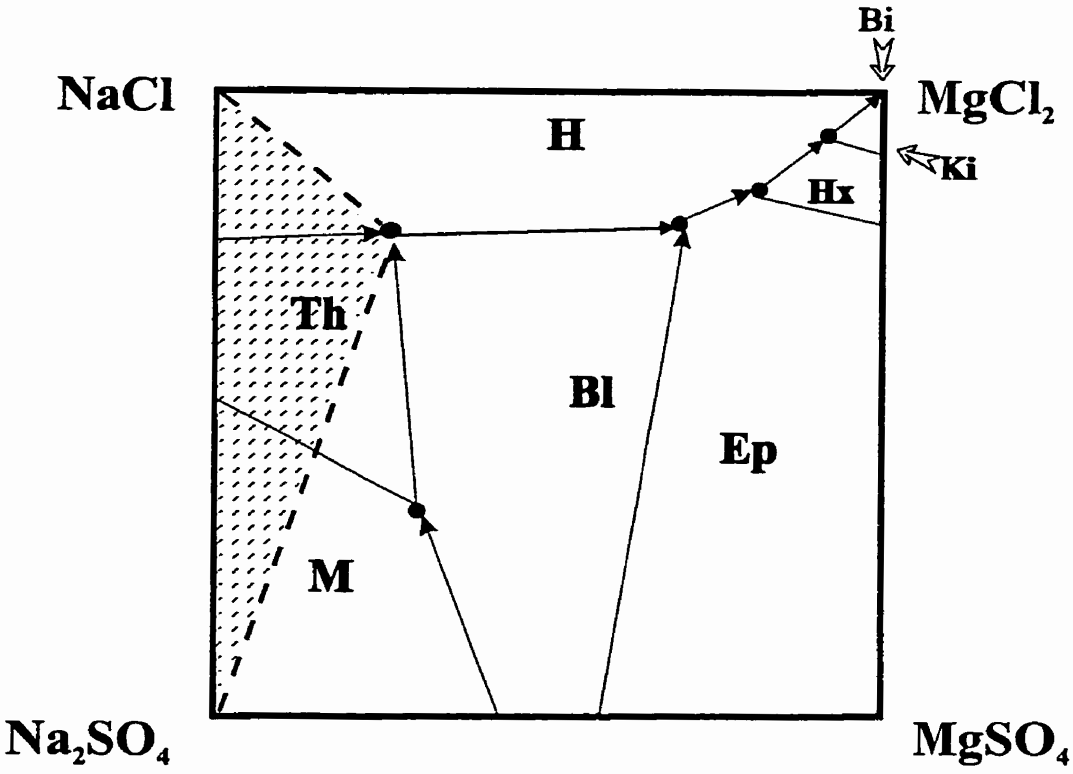

Figure 6.7 Phase relations in the reciprocal system Na-Mg-SO_4-Cl (after Harvie, Eugster, and Weare, 1982). For abbreviations see Table 6.2.

time for equilibrium precipitation (Smoot and Lowenstein, 1991).

6.4 Summary of Chemical Sedimentation

Understanding the intricate processes controlling relationships between hydrological condition and lake chemical sedimentation is a difficult task. In general, variations in mineralogical composition in sediments are often viewed as indices of hydrological fluctuation (see overviews in Vance, 1997; Xia et al., 1997; Last, 1999; Van Stempvoort at al., 1993). Because there is no permanent inflow, North Ingebright Lake was fed by groundwater, direct precipitation, and diffuse overland runoff throughout its history. These input sources contributed at differing proportions over time, and these variations are recorded by the mineral assemblage. Among these different sources, groundwater plays a key role in maintaining the existence of North Ingebright Lake. Analyses of the lake waters and sediment mineralogy suggest that North Ingebright Lake may be fed by two distinct groundwater sources. The first is a deep groundwater aquifer with a very high content of SO_4 and Na; the second is a shallow groundwater aquifer which is less evolved, less saline, and has relatively lower content of SO_4 and Na. The shallow groundwater has very high Mg, Ca, and CO_3 contents, resulting from contact with Mg-rich bedrock (till) and early precipitation of calcite cements in soils.

The initial sediments of Unit 1 (Basal Black Mud) were deposited as the lake developed in the remnant of preglacial valley. This stage of North Ingebright Lake is represented by clastic deposits under freshwater lacustrine conditions. After this early clastic sedimentation in Unit 1, the basin evolved under an endoreic regime, where seasonal recharge and the recycling of previously-formed soluble minerals led to the deposition of thick salt sequence.

During the deposition of Units 2 and 6, the lake level dropped dramatically and is interpreted to have been fed by deep groundwater. Lake water was saturated with Na and Na+Mg sulfates. This represents the most concentrated period of lake water history.

During the deposition of Units 3, 5, and 7, lake-levels were relatively high. The spring and deep groundwater inputs were negligible during this period. The increase in surface runoff and shallow groundwater inputs resulted in dilution of SO_4 and Na, while Ca, Mg, and CO_3 increased slightly and remained nearly constant due to carbonate precipitation. Protodolomite and magnesite are the two main carbonate minerals found in Units 3, 5, and 7, but magnesite is the more abundant of the two minerals. These proportions suggest that the lake in which the Units 3, 5, and 7 were deposited was characterized by a high Mg/Ca ratio. The presence of trace gaylussite in these three units suggests a positive moisture condition. In addition, the coexistence of gaylussite, aragonite, and magnesite with soluble evaporitic minerals in Units 3, 5, and 7 means there were rapid fluctuations in lake levels.

During the deposition of Units 4 and 8, the lake is interpreted to be fed by both shallow and deep groundwater sources. The continued high input of SO_4 and Na from the deep groundwater resulted in a stable high concentration of SO_4 and Na in the lake. The concentration of Ca and Mg in solution also increased as a result of the relatively high input from surface inflow. The uppermost section of Unit 8 is a mottled coloration mud layer. These mottled mud materials are inferred to represent times when the lake was dry and the sediments were exposed to oxidation by the atmosphere. However, mottled mud layers are rarely found in Unit 4. This indirectly indicates that the lake never experienced long-term desiccation in the central area during much of the time Unit 4 was deposited, rather a fluctuating lake that desiccated only for relatively brief periods is indicated by the very soluble evaporate minerals in Unit 4.

In its entire history, North Ingebright Lake appears to have been saturated with Na-SO_4. It was diluted during occasional wet periods and concentrated during dry periods. It is evident that the thick accumulations of evaporites in North Ingebright Lake did not result from one evaporative event but are the result of continuous input and evaporation.

Chapter 7 North Ingebright Lake: A Dynamic Closed-Basin Lake System

7.1 Introduction

Salt minerals in North Ingebright Lake basin result from the complex interaction of water, solute, and energy fluxes. The number of factors that control the precipitation of salt minerals is large but mainly include: temperature, relative humidity, salinity, water activity, bedrock lithology, hydrological balance, and energy budget. The relationships among these factors are rather complex and are not readily resolvable with presently available data. In this chapter, the relationships of several major factors that control the deposition of North Ingebright Lake sequence are discussed.

7.2 Thermodynamic Activity of H_2O and Salinity

The thermodynamic activity of water (${}^{a}H_2O$) changes insignificantly in most dilute solutions. It can be regarded as a constant with a value of one in many near surface geochemical processes. However, in concentrated brines, the effects of changing the activity of water on evaporation rate and reaction coefficients must be considered (Helgeson et al., 1970). The thermodynamic activity of water in a simple electrolyte solution at a given temperature and pressure can be represented by

$$\ln {}^{a}H_2O = -0.018\vartheta_{\pm,e} m_e \Psi_e$$

where m_e is the total molality of the solute, $\vartheta_{\pm,e}$ refers to the stoichiometric number of moles of ions in one mole of the eth electrolyte, and Ψ_e is the molal osmotic coefficient of the electrolyte, which can be determined from an extended Debye-Hückel power function of the ionic strength (I) of the solution (Helgeson et al., 1970). When the total molality of the solute, m_e, is zero (pure water) the activity of water equals 1.

The addition of ions (such as sodium and sulphate) to water has a substantial electrostrictive effect on water structure, and they introduce disorder into the normal tetrahedral coordination of water molecules. Because of the electronic polarity of water molecules, some water molecules become structurally bound in hydration sheaths around ions and the thermodynamic activity of the water molecules will be significantly reduced (Dingman, 1994; Kinsman, 1976; Harbeck, 1955). Salts commonly found in natural waters, such as sodium sulfate, sodium carbonate, and sodium chloride, have a similar effect on the water activity in varying concentrations, as shown in Figure 7.1 (Harbeck, 1955; Eugster and Jones, 1979; Langbein, 1961). The dissolved solids in North Ingebright Lake largely consist of sodium sulfate; thus, the curve in Figure 7.1 best represents the relationship between salinity and water activity in North Ingebright Lake brine at high concentration. Overall, the water activity of brine decreases about 1 percent for a change in salinity of 10 ppt.

7.3 Water Activity, Relative Humidity, and Mineral Facies

As discussed by Kinsman (1976), the water activity in a solution can also be represented by the saturated vapour pressure of the solution. Essentially, the

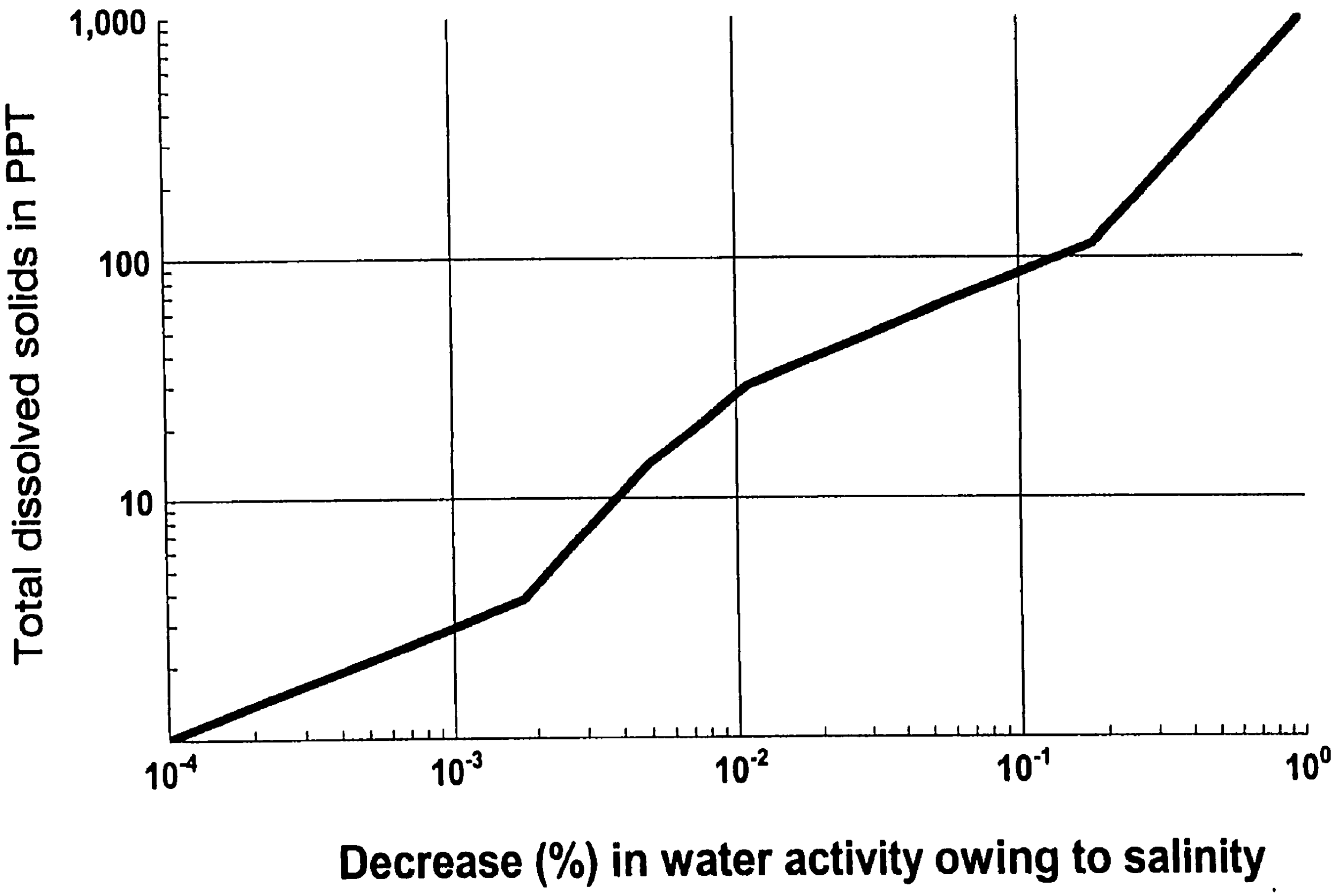

Figure 7.1 Schematic relation between salinity and reduction in water activity at 15°C (modified from Harbeck, 1955)

saturated vapour pressure of the solution is another way to reflect the same property of the solution: thermodynamic activity of water. It is generally held that the amount of evaporation is directly proportional to the vapour pressure difference between the saturated vapour pressure of the solution and the vapour pressure of the air. Dissolved solids affect evaporation by reducing the saturated vapour pressure of solution/thermodynamic activity of water (Harbeck, 1955; Kinsman, 1976).

Relative humidity is the ratio of the actual water vapour pressure of the air to the saturation or equilibrium water vapour pressure of the air. The ratio is normally expressed as a percentage (Dingman, 1994). As is well known, the moisture content of the atmosphere (better known as relative humidity) exerts a significant influence on weather. Relative humidity determines cloud formation and precipitation, but also, through changes of vapour pressure, is intimately involved in the precipitation of salt minerals in a lake (Dingman, 1994; Kinsman, 1976). It is the vapour pressure that determines the movement of moisture across the interface between the lake water surface and air above it. If the saturated water vapour pressure (thermodynamic activity of water) of the lake water is greater than the vapour pressure of the atmosphere, then there will be a net transfer of water molecules from lake water to the atmosphere across interface. The evaporation rate from the lake surface depends upon the vapour pressure difference between the evaporating surface and the air into which the moisture is moving. As a result of the transfer, the atmospheric water vapour pressure will increase until equilibrium is achieved. Thus, the most important prerequisite for net evaporation across the water-air interface is that the atmospheric relative humidity must be less than the saturated water vapour pressures exerted by the lake water. In other words, in order to maintain continuous evaporation from saline water, saturation vapour pressure (thermodynamic activity of water) of the solution must be close to vapour pressure of the air. At each establishment of the equilibrium between the saturated vapour pressure (thermodynamic activity of water) of the solution and vapour pressure of the air, particular evaporitic minerals may precipitate from the solution. Therefore, water activities deduced from evaporitic minerals are approximately equal to the atmospheric vapour pressure of the air/humidity.

In the past, the occurrence of evaporite sequences has simply been explained as resulting from evaporation exceeding precipitation and a closed basin. The constraining control of atmospheric relative humidity has been largely ignored. For the formation of late stage evaporation facies minerals, very low mean relative humidities in a locality are required. In general, the average relative humidity is high both in the equatorial region and in the polar regions. It is lowest in the subtropical regions since moisture moves outward in both directions from these zones by trade winds and westerlies (Lydolph, 1985). Mean annual relative humidity in the equatorial zone, as well as parts of higher latitudes, mainly over the oceans, is higher than 86%. The interiors of middle-latitude continents, particularly in North America, are occupied by air with low relative humidity values (below 60-50%) (Lydolph, 1985). Therefore, late stage evaporitic minerals can be precipitated only in evaporite basins in areas of high continentality.

Although the relationships among relative humidity, salinity, evaporation rate, temperature, and other physical processes are extremely complex, and it is impossible to define a simple relationship between any two variables, a general relationship between the average relative humidity of a location and the ultimate evaporite mineral suite should exist. Figure 7.2 shows a generalized sequence of mineral precipitation with the decrease of relative humidity. The relative humidity values are mainly compiled from Kinsman (1976), Eugster et al. (1980), and Harvie et al. (1982).

7.4 Hydrological Balance and Mineral Precipitation

7.4.1 Hydrological balance

The interaction between precipitation, evaporation, groundwater and surface water in a lake determines not only its hydrological balance but also affects its hydrochemistry, which in turn affects the mineral precipitation. Relatively small changes in the balance between groundwater or surface water and precipitation inputs may induce shifts in the mineral sequences. The hydrogeology in North Ingebright Lake region is controlled by a three-layer system: glacial till overlies fluvial sand, which in turn rests on the erosional surface of Cretaceous bedrock (David, 1964). A buried preglacial valley along the course of the present-day potholes was identified by David (1964) and Ruffel (1968). The buried valley was infilled with alluvial sands and silts containing lenses of gravel. The groundwater contribution to the water balance of North Ingebright Lake basin arises from this unique local geological situation that allows the vertical movement of groundwater to the surface under an upward head gradient (David, 1964; Ruffel, 1968).

Despite the importance of groundwater inputs to playa lakes, very few studies

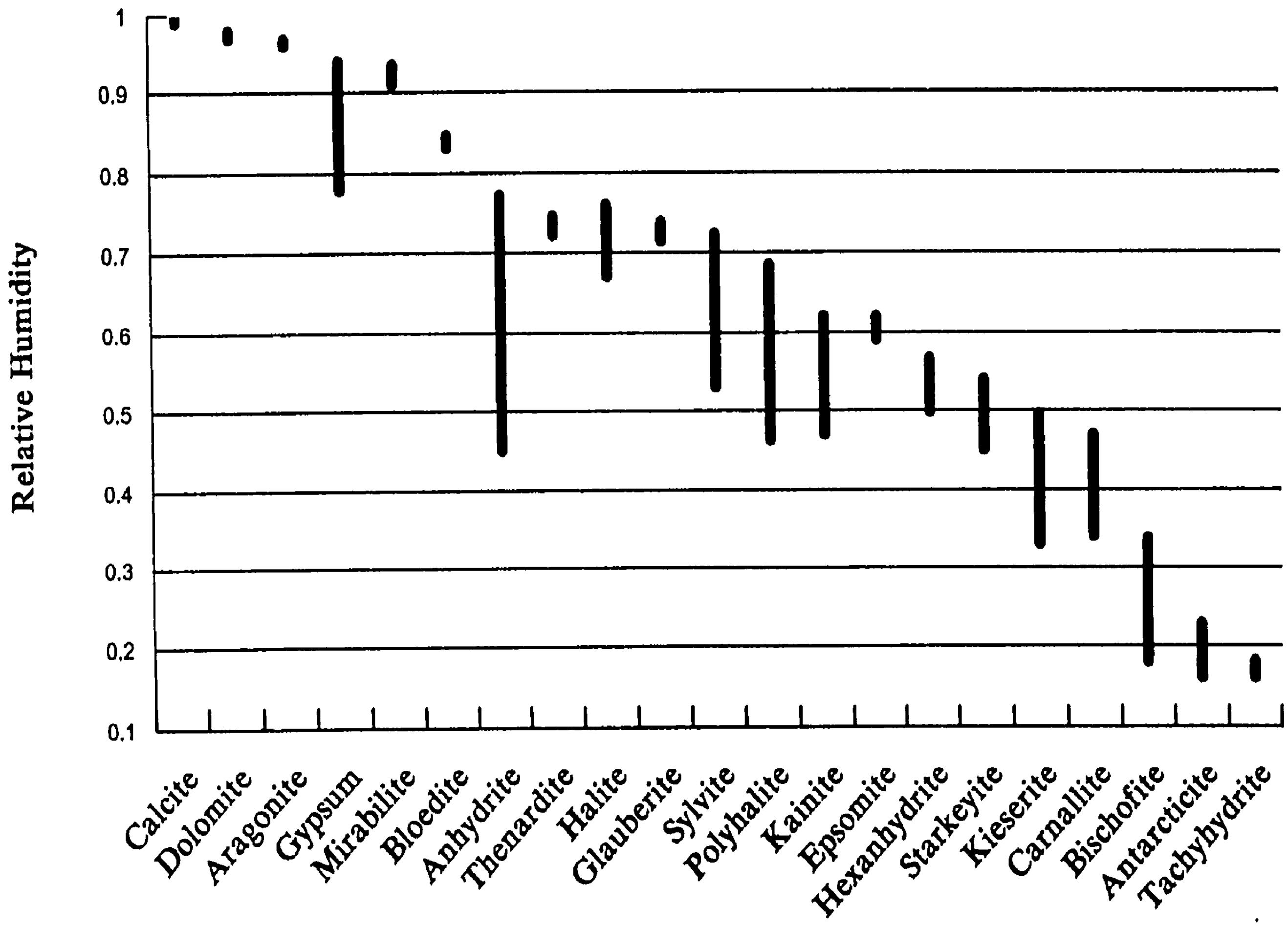

Figure 7.2 Relative humidity and evaporite mineralogy (compiled from various sources; see text)

have been undertaken in the Canadian Prairies (Price, 1993; van der Kamp and Maathuis, 1991; Woo, 1992; Birks and Remenda, 1999). In most cases, groundwater inflow has been omitted because of the difficulty of its measurements, or calculated as a residual term. In this study, the groundwater contribution is considered to be an important component of the water balance and the hydrogeological mechanisms operating within North Ingebright Lake.

Playa lakes in hummocky moraine are either expressions of groundwater discharge from miniature flow systems or infiltration ponds from which groundwater is being replenished. Meyboom (1966) presented the annual fluctuation patterns of groundwater flows underneath a typical playa lake in hummocky moraine of south-central Saskatchewan. One annual sequence of groundwater flow conditions approximately consists of three flow patterns. From January to April, groundwater flow in the playa lake area is downward and the lake basin acts as a major recharge area for deeper aquifers. As soon as the melt water accumulated in the lake basin starts to infiltrate, a complete flow pattern of lateral and vertical dissipation forms around the playa basin. During the summer and fall a reversal of groundwater flow occurs. This condition of inverted water flow is characterized by radial flow toward the lake basin and groundwater discharges to the lake basin. This annual recharge-discharge cycle actually also operates on the long term scale in playa lakes. During the dry period, the lake basin is maintained by groundwater discharge. The lack of lunette dunes around the playa basin further indicates that the lake basin has never experienced long-term desiccation. During the wet period, lake water recharges to the groundwater aquifers.

The thermodynamic properties of the ionic components of the groundwaters and brine have been calculated using a computer program PHRQPITZ (Plummer et al, 1988). The ionic strengths, activity coefficients of major ions and water, and saturation indices with respect to major salt minerals are listed in Table 7.1. The results reveal that shallow groundwater, deep groundwater, and spring waters are all strongly supersaturated with respect to calcite, dolomite, and aragonite. Magnesite is at or near saturation in all water sources, suggesting precipitation of magnesite is thermodynamically favoured in the lake basin. Gypsum, anhydrite, mirabilite and halite are undersaturated everywhere, and therefore should not be precipitating at present conditions.

7.4.2 Numerical simulation-mineral precipitation

Although the general water activity and evaporite mineral facies relationship shown in Figure 7.2 are well established by experiments and theoretical calculations (see Assarsson, 1950a; 1950b; 1950c; Braitsch, 1971; Eugster, 1971; Stewart, 1963; Harvie et al., 1984; Weare, 1987), it is still necessary to examine the actual order of mineral precipitation in an individual lake basin before evaporite mineral facies can be used as indicators of relative humidity. As discussed previously, North Ingebright Lake is maintained by either shallow groundwater influx, deep groundwater discharge or mixtures of both. Significant mineral composition variation in the evaporite mineral suite is a result of complex alternating inflow processes of shallow groundwater influx and deep groundwater discharge. In this research, the computer program, PHRQPITZ has been used to simulate evaporation paths

Table 7.1 Chemical parameters of deep groundwater, shallow groundwater, spring water, and lake water from North Ingebright lake (from Cole; 1926 and David, 1968)

	Deep groundwater	Shallow groundwater	Spring water	Lake water
Ca (mol)	4.69e-03	4.37e-03	3.39e-03	n.d.
Mg (mol)	2.98e-03	5.38e-03	9.42e-03	1.35e-01
Na (mol)	1.71e-02	7.36e-03	6.01e-02	5.07e-01
Cl (mol)	1.84e-03	1.71e-03	8.62e-03	1.59e-01
CO_3+HCO_3(mol)	4.70e-03	4.91e-03	1.81e-02	1.79e-02
SO_4(mol)	1.23e-02	8.98e-03	5.52e-03	3.00e-01
pH	7.5	7.8	7.4	7.9
^aH_2O	0.9993	0.9995	0.9983	0.9853
I (Ionic strength)	0.0515	0.0443	0.0793	1.2117

Saturation Index: log (IAP/KT)

Calcite	0.2	0.6	0.5	n.c.
Aragonite	0.0	0.4	0.3	n.c.
Dolomite	0.4	1.4	1.6	n.c.
Magnesite	-0.6	0.0	0.3	1.3
Gaylussite	-7.8	-7.9	-6.0	n.c.
Pirssonite	-17.2	-8.0	-6.2	n.c.
Natron	-8.3	-8.6	-6.8	n.c.
Gypsum	-0.5	-0.6	-1.1	n.c.
Anhydrite	-0.8	-0.9	-1.3	n.c.
Mirablite	-4.3	-5.2	-3.7	-1.0
Bloedite	-8.9	-9.6	-8.3	-3.7
Epsomite	-3.3	-3.1	-3.2	-1.4
Hexanhydrite	-3.5	-3.4	-3.5	-1.7

Kieserite	-5.1	-5.0	-5.1	-3.3
Halite	-6.2	-6.6	-5.0	-3.1
Bischofite	-13.1	-12.8	-11.3	-8.3
Glauberite	-5.9	-6.8	-5.8	n.c.
Burkeite	-20.4	-22.5	-17.6	-10.2

n.d. - not detected; n.c - not calculated.

(Plummer et al., 1988). PHRQPITZ uses thermodynamic equilibrium and mass balance principles and contains the Pitzer virial-coefficient approach for calculating the thermodynamics of minerals in solutions with high ionic strength developed by Harvie et al. (1980 and 1984).

Throughout most of its history, the basin is assumed to have been hydrologically closed and evolved with a constant volume of water. Hence, the evaporated volume of water was replaced by shallow groundwater or deep groundwater, and complete mixing was assumed. Using PHRQPITZ to simulate this closed system is accomplished by a two-step procedure. In the first step, shallow and deep groundwaters are speciated in order to calculate ionic strengths, thermodynamic activity, and saturation indices with respect to various minerals. Program options within PHRQPITZ were used to mix shallow groundwater and deep groundwater at ratios of 1:9, 3:7, 5:5, 7:3, and 9:1. Results of the speciation calculation for these mixing solution are presented in Table 7.2. They constitute a spectrum of inflow waters to North Ingebright Lake basin in different stages of the basin's history.

In the second step, evaporation to complete dryness of each of inflow waters in Table 7.2 is simulated using the computer code PHRQPITZ. Mineral precipitation during evaporation is governed by the thermodynamic equilibrium between the minerals and the brine at a constant temperature of 15°C. Due to the complex relationships between multiple solute components and mineral precipitation, numerical methods must be used to solve the mass balance problems. Thus, the simulation process is undertaken in a series of evaporation steps. At each step, the

Table 7.2 Chemistry composition of various mixing solutions

	Deep groundwater (solution 2)	Shallow groundwater (solution 1)	Mixing solutions 1 and 2 in different proportions (ratio=solution 1/solution 2)				
			9:1	7:3	5:5	3:7	1:9
Ca (mol)	4.69e-03	4.37e-03	4.66e-03	4.59e-03	4.53e-03	4.47e-03	4.40e-03
Mg (mol)	2.98e-03	5.38e-03	3.22e-03	3.70e-03	4.18e-03	4.66e-03	5.14e-03
Na (mol)	1.71e-02	7.36e-03	1.61e-02	1.42e-02	1.22e-02	1.03e-02	8.33e-03
Cl (mol)	1.84e-03	1.71e-03	1.82e-03	1.80e-03	1.77e-03	1.75e-03	1.72e-03
CO_3 +HCO_3(mol)	4.70e-03	4.91e-03	4.72e-03	4.76e-03	4.28e-03	4.85e-03	4.89e-03
SO_4(mol)	1.23e-02	8.98e-03	1.19e-02	1.13e-02	1.06e-02	9.96e-03	9.30e-03
pH	7.5000	7.8000	7.4885	7.4667	7.4462	7.4269	7.4087
^aH_2O	0.9993	0.9995	0.9994	0.9994	0.9994	0.9995	0.9995
I (Ionic strength)	0.0515	0.0443	0.0508	0.0493	0.0479	0.0464	0.0450

Saturation Index: log (IAP/KT)

Calcite	0.2	0.6	0.2	0.2	0.2	0.2	0.1
Aragonite	0.0	0.4	0.0	0.0	0.0	0.0	-0.1
Dolomite	0.4	1.4	0.4	0.4	0.4	0.5	0.5

Magnesite	-0.6	0.0	-0.6	-0.6	-0.5	-0.5	-0.5
Gaylussite	-7.8	-7.9	-7.9	-8.0	-8.2	-8.4	-8.6
Pirssonite	-17.2	-8.0	-8.1	-8.2	-8.4	-8.6	-8.8
Natron	-8.3	-8.6	-8.3	-8.5	-8.6	-8.8	-9.0
Gypsum	-0.5	-0.6	-0.5	-0.5	-0.6	-0.6	-0.6
Anhydrite	-0.8	-0.9	-0.8	-0.8	-0.8	-0.8	-0.9
Mirablite	-4.3	-5.2	-4.4	-4.5	-4.7	-4.9	-5.1
Bloedite	-8.9	-9.6	-9.0	-9.1	-9.2	-9.3	-9.5
Epsomite	-3.3	-3.1	-3.2	-3.2	-3.1	-3.1	-3.1
Hexanhydrite	-3.5	-3.4	-3.5	-3.4	-3.4	-3.4	-3.4
Kieserite	-5.1	-5.0	-5.1	-5.1	-5.0	-5.0	-5.0
Halite	-6.2	-6.6	-6.3	-6.3	-6.4	-6.5	-6.6
Bischofite	-13.1	-12.8	-13.0	-13.0	-12.9	-12.9	-12.8
Glauberite	-5.9	-6.8	-5.9	-6.1	-6.3	-6.5	-6.7
Burkeite	-20.4	-22.5	-20.5	-20.9	-21.4	-21.9	-22.5

evaporation of a certain volume of water is achieved by simply adding the solute mass that is representative of solutes in the input water to the evaporating brine rather than by the removal of water from the solution (Ayora et al., 1994; Wood and Sanford, 1990; Sanford and Wood, 1991). The inflow water may be either shallow groundwater, deep groundwater or mixtures of both. During each series of evaporation steps, the number of basin volumes evaporated at that step depends on the concentration of the starting solution and the stage of evaporation. For relatively dilute shallow groundwater, a time-step size of 1-50 evaporated basin volumes was chosen. A time-step size of 0.1-20 evaporated basin volumes was used for the deep groundwater evaporation simulation because of its relatively high concentration. The result indicates that the choice of time-step size in this study is adequate for the evaporation simulation to illustrate the effects of hydrological balance on the sequence of mineral precipitation.

Output from PHRQPITZ is comprehensive. Following a printout of the input data set, the starting solution is speciated for each evaporation step. The ionic strengths, activity coefficients of major ions and water, and the saturation state of minerals are also included. By visually inspecting the saturation indices of the minerals at the different evaporation steps, the point in time when any new mineral would begin to precipitate can be identified. Correspondingly, the sequence of mineral precipitation for each inflow waters in Table 7.2 can be established.

The sequence of mineral precipitation, with respect to different inflow waters, are listed as a function of number of evaporated lake volume in Tables 7.3a-g. For most of the inflow waters, the temporal succession of minerals remains basically the

Table 7.3a Mineral facies as a function of evaporated lake volumes for shallow groundwater at 15°C

Mineral Facies	Cal	Dol	Mag	G	A	Ga	Pi	Ga	M	Bl	H	Ep	Hx	Ki	Bi
Evaporated Lake Volume	0	0	1	3	6	30	35	125	350	550	780		880		
Water Activity	0.9995	0.9995	0.9991	0.9983	0.9971	0.9884	0.9866	0.9528	0.8289	0.702	0.574		0.5291		
Ionic Strength	0.0443	0.0443	0.0866	0.17	0.2955	1.327	1.5466	5.5854	15.2153	22.73	30.96		35.5979		

Table 7.3b Mineral facies as a function of evaporated lake volumes for mixing solution of shallow and deep groundwaters (Ratio = 9:1) at 15°C

Mineral Facies	Cal	Dol	Mag	G	A	Ga	Pi	Gl	M	Bl	H	Ep	Hx	Ki	Bi
Evaporated Lake Volume	0	0	1	3	5	30	35	115	350	530	750		880		
Water Activity	0.9995	0.9995	0.999	0.9982	0.9974	0.9879	0.986	0.9552	0.8244	0.709	0.587		0.5293		
Ionic Strength	0.045	0.045	0.0882	0.1733	0.2587	1.3522	1.5754	5.2117	15.4145	22.36	30.51		35.4011		

Table 7.3c Mineral facies as a function of evaporated lake volumes for mixing solution of shallow and deep groundwaters (Ratio = 7:3) at 15°C

Mineral Facies	Cal	Dol	Mag	G	A	Ga	Pi	Gl	M	Bl	H	Ep	Hx	Ki	Bi
Evaporated Lake Volume	0	0	1	3	5	25	30	100	340	510	700	880	880	>880	
Water Activity	0.9995	0.9995	0.999	0.9981	0.9972	0.9889	0.9869	0.9585	0.8223	0.712	0.605	0.5303	0.5303	>0.5303	
Ionic Strength	0.0464	0.0464	0.0913	0.18	0.2689	1.1736	1.4033	4.6734	15.4407	22.33	29.79	36.9592	36.9592	>36.959	

Table 7.3d Mineral facies as a function of evaporated lake volumes for mixing solution of shallow and deep groundwaters (Ratio = 5:5) at 15°C

Mineral Facies	Cal	Dol	Mag	G	A	Ga	Pi	Gl	M	Bl	H	Ep	Hx	Ki	Bi
Evaporated Lake Volume	0	0	1	3	5	25	30	90	320	490	670	830	830	>830	
Water Activity	0.9994	0.9994	0.9989	0.9979	0.997	0.9881	0.986	0.9603	0.8275	0.715	0.613	0.3848	0.3848	>0.3848	
Ionic Strength	0.0479	0.0479	0.0945	0.1867	0.2791	1.2165	1.4538	4.3377	15.023	22.26	29.72	27.3787	27.3787	>27.378	

Table 7.3e Mineral facies as a function of evaporated lake volumes for mixing solution of shallow and deep groundwaters (Ratio = 3:7) at 15°C

Mineral Facies	Cal	Dol	Mag	G	A	Ga	Pi	Gl	M	Bl	H	Ep	Hx	Ki	Bi
Evaporated Lake Volume	0	0	7	2	4			70	170	175	770	175	175	175	175
Water Activity	0.9994	0.9994	0.9956	0.9982	0.9972			0.9639	0.9032	0.901	0.411	0.9016	0.9016	0.9016	0.9016
Ionic Strength	0.0493	0.0493	0.4113	0.1528	0.2562			3.6687	6.0787	4.690	24.95	4.6902	4.6902	4.6902	4.6902

Table 7.3f Mineral facies as a function of evaporated lake volumes for mixing solution of shallow and deep groundwaters (Ratio = 1:9) at 15°C

Mineral Facies	Cal	Dol	Mag	G	A	Ga	Pi	Gl	M	Bl	H	Ep	Hx	Ki	Bi
Evaporated Lake Volume	0	0	1	2	4	12	13	75	180	450	590	720	720	>720	
Water Activity	0.9994	0.9994	0.9988	0.9982	0.9971	0.989	0.9866	0.9629	0.9055	0.722	0.637	0.4442	0.4442	>0.4442	
Ionic Strength	0.0508	0.0508	0.1008	0.1503	0.2494	1.0491	1.3011	3.8426	9.1458	22.00	28.39	24.9171	24.9171	>24.917	

Table 7.3g Mineral facies as a function of evaporated lake volumes for deep groundwater at 15°C

Mineral Facies	Cal	Dol	Mag	G	A	Ga	Pi	Gl	M	Bl	H	Ep	Hx	Ki	Bi
Evaporated Lake Volume	0	0	0.2	2	4	25	30	80	180	450	600	>730	>730	>730	
Water Activity	0.9993	0.9993	0.9992	0.9982	0.9970	0.9862	0.9837	0.9619	0.9015	0.711	0.614	>0.43	>0.4341	>0.4341	
Ionic Strength	0.0515	0.0515	0.0618	0.1527	0.2536	1.3219	1.5782	3.5587	9.1451	23.00	27.36	>24.1	>24.159	>24.159	

Note: Cal-calcite, Dol-dolomite, Mag-magnesite, G-gypsum, A-anhydrite, Ga-gaylussite, Pi-pirssonite, Gl-glauberite, M-mirabilite, Bl-bloedite, H-halite, Ep-epsomite, Hx-hexahydrite, Ki-kieserite, Bi-bischofite same. This result confirms the validity of using evaporite mineral facies and relative humidity relationship, shown in Figure 7.2, for determining the relative humidity from North Ingebright Lake evaporites.

7.5 Hydrological Conditions of North Ingebright Lake

The sediment cores recovered from the basin of North Ingebright Lake indicate that the basin has experienced water level and water chemistry fluctuations, as indicated by variations in the mineral composition and organic matter content of sediment record. Overall, the entire sediment sequence was deposited in shallow water and hypersaline conditions.

There is no evidence that North Ingebright Lake was ever a deep-water lake. Shallow water and oxygenated bottom conditions were present throughout much of the Holocene, as indicated by general low organic content and absence of bedding (Teller and Last, 1981; 1990). Common occurrences of halite and K-Mg sulfates in the evaporite deposits of North Ingebright Lake imply that the salinity of lake water has frequently reached a value of approximately 400 g/l, as compared to present day values between 100 to 300 g/l.

The general lack of bedding in the sedimentary fill could have been caused by many factors. The bedding was probably disrupted and destroyed by later groundwater discharges (creating porous surfaces) or by the growth and dissolution of ephemeral evaporite crystals and crusts (Kendall, 1984). It also may have been destroyed by wind generated waves which resuspend and physically mix the offshore bottom sediments (Last and Sauchyn, 1993). In addition, the absence of bedding suggests that this lake's water column has remained mainly nonstratified through much of its history.

The lake sediment is almost completely dominated by colourless salt. The lack of original fabric and textures in the salt make it very difficulty to interpret the depth of the brine in this hypersaline lake because both deep and shallow water salt deposition has been found in modern Saskatchewan lakes (Last, 1984). However, the final purpose of lake level determination is to reconstruct climatic conditions, so the evaporite mineral assemblage is used to establish mean surface humidity condition rather than lake level.

Figure 7.3 depicts the pattern of changes in relative regional humidity reconstructed for the past 10,000 years. During the episodes of 8700-10,350 yr B.P., 5500-6500 yr B.P., and 1000-2500 yr B.P., the mean relative humidity of the North Ingebright Lake basin was considerably lower than it is today. In contrast, comparatively humid conditions (but not wet enough to cause a basic change in the hydrologic setting of the playa) are suggested by higher relative humidities during the periods of 6500-7200 yr B.P. and 5500-3000 yr B.P. The 8000 to 7000 yr B.P. period was characterized by considerable variability with rapid, short-term fluctuations from high to low relative humidity conditions.

7.6 North Ingebright Lake Relative to Other Holocene Lacustrine Records

Although the purpose of this project was not to reconstruct the regional climatic history, nonetheless, it is tempting to compare the changes in relative humidity interpreted for North Ingebright Lake with paleolimnological fluctuations at

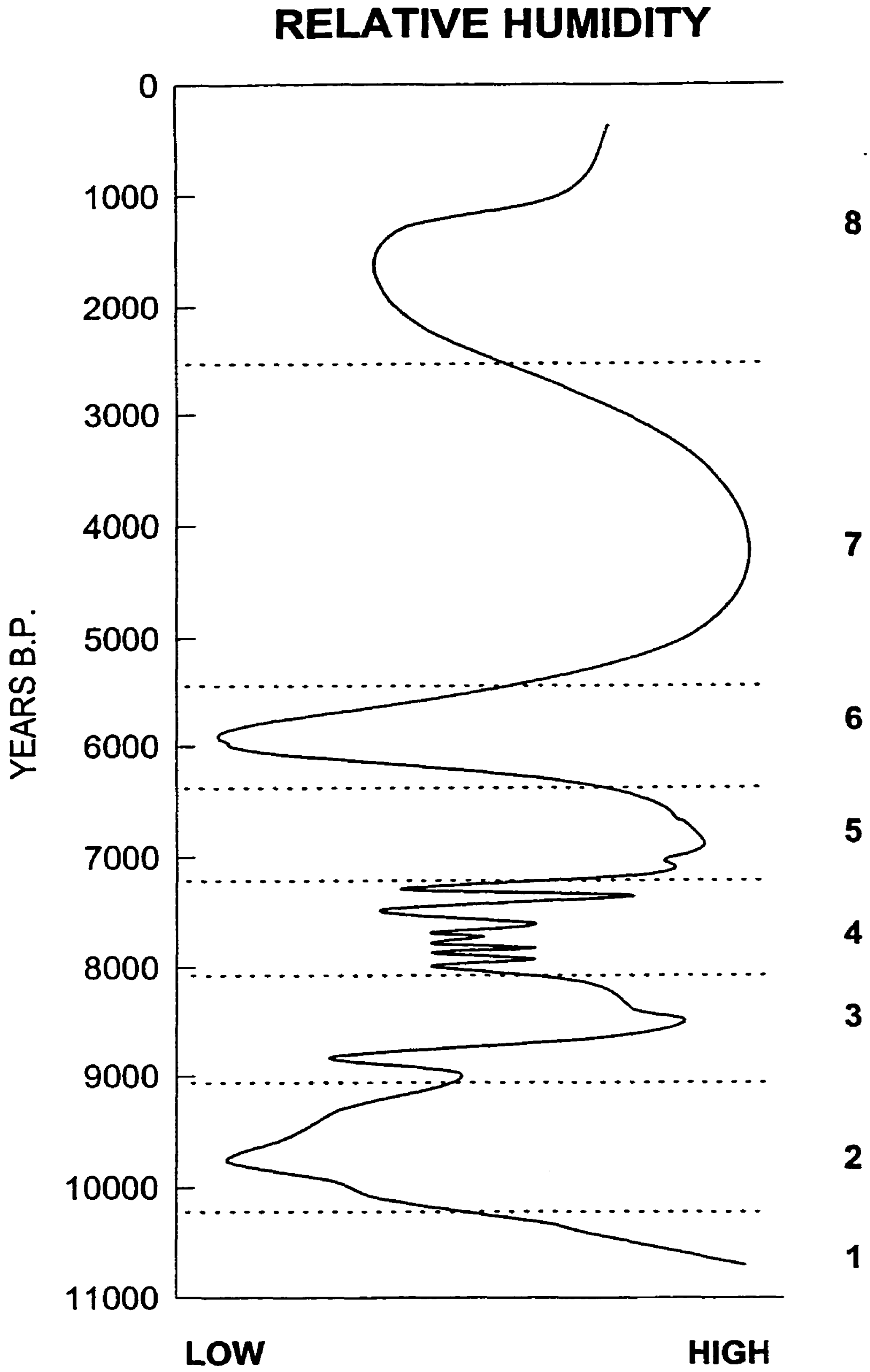

Figure 7.3 Variation in mean atmospheric relative humidity at North Ingebright Lake as estimated by the evaporitic mineral suite. Numbers on the right refer to the lithostratigraphic unit . Temporal scale is in ^{14}C years B.P.

other sites in the region having long Holocene records (Tables 7.4a and 7.4b).

The 7500 year long sediment record from Chappice Lake, Alberta, a hypersaline playa located about 80 km west of North Ingebright, is one of the longest and best documented lacustrine paleohydrological records in the entire northern Great Plains region (Vance et al., 1992, 1993, 1995). Even though the temporal aspect of the North Ingebright record is much less tightly constrained than that of Chappice Lake, broad similarities do exist. For example, both basins show an early Holocene episode (prior to 6000 yr BP in Chappice and 7000-8500 yr BP in North Ingebright) of significant fluctuation in humidity and water level/salinity conditions. Similar early Holocene periods of rapidly changing conditions, from high to low water levels and from hypersaline to fresh water, are noted in the stratigraphic records from Ceylon Lake, a salt playa located on the Missouri Coteau about 400 km southeast of Ingebright (Last, 1990) and from Clearwater Lake, a perennial freshwater lake 100 km to the northeast (Last et al., 1997). Similarly, a mid-Holocene interval of low water, saline to hypersaline conditions correlative to the very low mean atmospheric relative humidity at 5000-6000 yr in North Ingebright is also documented at Chappice and Ceylon, as well as several other lacustrine sites in the Prairie region (Vance et al., 1995).

The 10,000 year long, uninterprupted sediment sequence from Oro Lake in southern Saskatchewan, a perennial saline lake located about 160 km southeast of North Ingebright, also contains the well-preserved paleolimnological fluctuation records (Last and Vance, 2000). Early Holocene transitions from fresh to saline and/or hydrologically open to closed, evaporitic conditions have been well

Table 7.4a Comparison of mean relative humidity at North Ingebright Lake to interpreted water levels and salinities at Chappice Lake, Alberta, and Oro lake, Clearwater and Ceylon Lakes, Saskatchewan

^{14}C YR BP	North Ingebright Mean Relative Humidity	Chappice Water Level & Salinity	Oro Water Level & Salinity	Clearwater Water Level & Salinity	Ceylon Water Level & Salinity
Present		FLUCTUATION FROM LOW TO HIGH & FRESH TO SALINE			LOW & HYPERSALINE
	HIGH		DEEP & SALINE TO HYPERSALINE		HIGH & FRESH WATER
1000		LOW WATER			
	LOW			DEEP & FRESH WATER STABLE CONDITIONS	STABLE CONDITIONS LOW WATER & HYPERSALINE
2000					
		DEEP & RELATIVELY FRESH WATER	STABLE CONDITIONS DEEP & SALINE		HIGH & FRESH WATER
3000					STABLE CONDITIONS LOW WATER & HYPERSALINE
	HIGH				
4000					
		STABLE CONDITIONS LOW WATER & HYPERSALINE		[redacted]	
5000					VERY LOW TO DRY & HYPERSALINE
	VERY LOW		DEEP & RELATIVELY FRESH WATER		
6000					
	HIGH	REPEATED FLUCTUATION FROM DRY TO DEEP & FRESH TO HYPERSALINE			
7000					
	REPEATED FLUCTUATION FROM LOW TO HIGH			DEEP & FRESH WATER	REPEATED FLUCTUATION FROM SHALLOW TO DEEP & FRESH TO HYPERSALINE
8000		Base of Record	STABLE CONDITIONS DEEP & SALINE TO HYPERSALINE		
				DEEP TO SHALLOW (DRY AT 8200 BP) & SALINE TO HYPERSALINE	
9000	HIGH				
10000	VERY LOW TO LOW		DEEP & FRESH WATER	SHALLOW & HYPERSALINE	DEEP & FRESH WATER
11000	HIGH			SHALLOW & FRESH WATER	

Table 7.4b Comparison of mean relative humidity at North Ingebright Lake to interpreted water levels and salinities at Pickerel Lake, Medicine Lake and Williams Lake in United States

^{14}C YR BP	North Ingebright Mean Relative Humidity	Pickerel Water Level & Salinity	Medicine Water Level & Salinity	Williams Water Level & Salinity
Present				
	HIGH			
1000		REPEATED FLUCTUATION FROM LOW TO DEEP & FRESH TO SALINE	LOW TO DEEP SALINE TO HYPERSALINE	LOW WATER SALINE TO HYPERSALINE
	LOW			
2000				
3000		LOW WATER & SALINE	REPEATED FLUCTUATION FROM LOW TO DEEP & FRESH TO SALINE	STABLE CONDITIONS LOW WATER & FRESH TO SALINE
	HIGH			
4000				
5000			LOW WATER SALINE TO HYPERSALINE	
	VERY LOW			REPEATED FLUCTUATION FROM LOW TO DEEP & SALINE TO HYPERSALINE
6000		LOW & SALINE TO HYPERSALINE		
	HIGH			
7000	REPEATED FLUCTUATION FROM LOW TO HIGH		STABLE DEEP WATER MEROMITIC & SALINE TO HYPERSALINE	
8000				LOW WATER HYPERSALINE
9000	HIGH			
10000	VERY LOW TO LOW	STABLE CONDITIONS DEEP & FRESHWATER	STABLE CONDITIONS DEEP & FRESHWATER	STABLE CONDITIONS DEEP & FRESHWATER
11000	HIGH			

documented at Oro Lake. Sediments (prior to 9300 yr BP) in Oro Lake were deposited in a relatively deep, freshwater lake. However, this early Holocene freshwater lake changed rapidly to a saline lake with very high Mg/Ca ratio by about 9300 yr BP. During the two thousand year period between 9300 and 7400 yr BP, deep and saline conditions dominated the lake, with occasional excursions to hypersaline conditions. Similarly, low humid conditions are also recorded in North Ingebright Lake during 10350-8700 yr BP.

The mid-Holocene (4000-7400 yr BP) aragonite-laminated mud deposition in the Oro Lake basin reflects a positive hydrological budget. This mid-Holocene freshening of the brines in Oro Lake corresponds well with the occurrence of relatively humid conditions (6500-7200 yr BP) at North Ingebright lake.

In addition, the transitions from relatively deep and freshwater to shallow and higher salinity conditions in lakes of the northern Great Plains during the early and mid-Holocene period have also been documented at several lakes in United States. For example, dramatic increases in values of both $\delta^{18}O$ and $\delta^{13}C$ of carbonate at Pickerel Lake, South Dakota between 6000 and 10,000 yr BP indicate the shifts from hydrologically open conditions to more or less hydrological closed conditions (Dean and Schwalb, 2000). In Coldwater Lake, North Dakota, values of $\delta^{18}O$ and Sr/Ca ratios in ostracode shells in sediments suggest a transition from relatively deep and freshwater to shallow and higher salinity conditions between 6500 and 10800 yr BP (Xia et al., 1997). Shallow and higher salinity conditions during the early to middle Holocene have also been noted in Medicine Lake, South Dakota (Valero-Garces and Kelts, 1995) and Williams Lake in west-central Minnesota

(Schwalb et al., 1995).

In general, relatively humid conditions were dominant at North Ingebright Lake basin during the late Holocene period. This lengthy period of stable and relatively moist conditions between about 5000 and 2000 years ago is also recorded in numerous other basins in the northern Great Plains (see overviews in Vance, 1997; Xia et al., 1997; Lemmen, 1996; Lemmen and Vance, 1999).

Chapter 8 Summary

North Ingebright Lake originated in a remnant of a preglacial valley at about 11 ka. The continued collapse of buried ice blocks along the preglacial valley enhanced the elongate shape of the basin, and a series of smaller bodies of water coalesced to form a relatively large, freshwater lake. This stage of North Ingebright Lake is represented by clastic deposits; sediments of fine-grained sand, silt, and clay deposited under freshwater lacustrine conditions. At the close of the deposition of the Basal Black Mud Unit, climatic changes in the basin area resulted in a decrease in the size of North Ingebright Lake and a corresponding increase in chemical deposition. Playa conditions dominated the rest of its history.

Generally, the mineral suite of the sediment retrieved from the basin of North Ingebright Lake consists mainly of thenardite/mirabilite (80%), gypsum (5%), carbonates (4%), clay minerals (5%), and feldspar (3%). The most distinctive feature in North Ingebright Lake sediment is that large amounts of thenardite/mirabilite are present in most subsamples. The content of thenardite/mirabilite in samples ranges from 6 to 100%. Other very soluble evaporitic minerals, niter, polyhalite, epsomite, bloedite, anhydrite, tychite, and halite were identified in a small number of samples. Trace quantities of gaylussite, fairchildite, zemborite, and hanksite occur in some samples. The carbonate minerals present in the sediment core include protodolomite, dolomite, aragonite, high-Mg calcite, and magnesite. Minor quantities of calcite were identified in a small number of samples. Clastic silt and clay, and organic materials are always present but subordinate. The feldspars comprise an average of 3% of the mineral suite. Most of this amount is plagioclase (2.7%), with minor amounts of potassic feldspar (0.4%).

The mineral assemblage of North Ingebright Lake salts can be represented by phase relationships in the reciprocal quinary system Na-Mg-Ca-Cl-SO_4-H_2O and its subsystems - quaternary systems: three reciprocal systems (Na-Mg-Cl-SO_4, Mg-Ca-Cl-SO_4, and Na-Ca-Cl-SO_4) and two tetrahedra systems (Na-Ca-Mg-Cl and Na-Ca-Mg-SO_4). The bulk chemical composition calculation and physical-chemistry reasoning indicate that, through its history, North Ingebright Lake appears to have been dominated by Na-SO_4. During wet periods the brine was diluted and dominated by Na-Ca-Mg-SO_4; during dry periods it concentrated and shifted to Na-SO_4-Cl or Na-K-SO_4 type brines.

Overall, the entire sediment sequence was deposited in shallow water and saline to hypersaline conditions. There is no evidence that the lake basin ever contained a deep water lake. Shallow water and oxygenated bottom conditions were present throughout much of the Holocene as indicated by general low organic content, lack of colour, and absence of bedding. Common occurrences of halite and K-Mg sulfates in the evaporite deposits of North Ingebright Lake imply that the salinity of lake water has frequently approached 400 g/l. However, the lack of pedogenic horizons, erosional contacts, and coarse grained indicates that the lake has never undergone complete drying and desiccation.

The evaporite minerals were used as indicators of relative humidity throughout the stratigraphic column. The wide range of relative humidity (34-98%) deduced from the saline mineral assemblage indicates that dramatic changes of climatic and hydrological conditions occurred during the deposition of North Ingebright Lake evaporates. During the episodes of 8700-10,350 yr B.P., 5500-6500 yr B.P., and 1000-2500 yr B.P., the North Ingebright Lake basin experienced climatic conditions in which the mean relative humidity was considerably lower than that of today. In contrast, comparatively humid conditions (but not wet enough to cause a basic change in the hydrologic setting of the playa) are suggested by higher relative humidities during the periods of 6500-7200 yr B.P. and 5500-3000 yr B.P. Finally, the millennium between 8000 and 7000 yr B.P. was characterized by considerable variability with rapid, short-term fluctuations from high to low relative humidity conditions.

REFERENCES CITED

Andrews, J.T., 1987. The late Wisconsin glaciation and deglaciation of the Laurentide Ice Sheet. In "North America and Adjacent Oceans during the Last Deglaciation" (W.F. Ruddiman and H.E. Wright, Eds.), p. 13-37, Geological Society of America, The Geology of North America, k-3.

Assarsson, G.O., 1950a. Equilibria in aqueous systems containing K, Na, Ca, Mg and Cl. I. The ternary system $CaCl_2$-KCl-H_2O. J. Am. Chem. Soc. 72: 1433-1436.

Assarsson, G.O., 1950b. Equilibria in aqueous systems containing K, Na, Ca, Mg and Cl. I. The Quaternary system $CaCl_2$-KCl-$NaCl$-H_2O. J. Am. Chem. Soc. 72: 1437-1441.

Assarsson, G.O., 1950c. Equilibria in aqueous systems containing K, Na, Ca, Mg and Cl. II. The Ternary system $CaCl_2$-$MgCl_2$-H_2O. J. Am. Chem. Soc. 72: 1442-1444.

Atoji, M., 1958. Anhydrite obtained by the dehydration of gypsum. J. Chem. Phys. 30: 341-342.

Ayora, C., Garcia-Veigas, J., & J.J. Pueyo, 1994. The chemical and hydrological evolution of an ancient potash-forming evaporite basin as constrained by mineral sequence, fluid inclusion composition and numerical simulation. Geochim. Cosmochim. Acta 58: 3379-3394.

Ball, J. W., Jenne E. A. & D. K. Nordstrom, 1979. WATEQ2-a computerized model for trace and major element speciation and mineral equilibria of natural waters. In Chemical Modeling in Aqueous Systems: Speciation, Sorption, Solubility, and Kinetics (ed. E. A. Jenne). Amer. Chem. Soc. Symp. Series 93: 815-835.

Barnard, R.M. & R.B. Kistler, 1966. Stratigraphic and structural evolution of the Kramer sodium borate ore body, Boron, California. In: Second symposium on salt (J.L. Rau, ed.). North. Ohio Geol. Soc. 1: 133-150

Bird, J.B., 1972. The natural landscapes of Canada: a study in regional earth science, Wiley Publishers of Canada Limited, 191 pp.

Birks, S.J. & V.N. Remenda, 1999. Hydrological investigation of Chappice Lake, southeastern Alberta. Journal of Paleolimnlogy 21: 235-255.

Bradley, W.H. & H.P. Eugster, 1969. Geochemistry and paleolimnology of the trona deposits and associated authigenic minerals of the Green River Formation of Wyoming. U.S. Geol. Survey Prof. Paper 496-B, 71 p.

Braitsch O, 1971. Salt Deposits, their Origin and Composition. Springer-Verlag. 297 pp.

Broadhurst F.M. & R.A. Howie, 1958. On the occurrence of ankerite in a band of non-marine lamellibranchs from the Lancashire Coal Measures. Geol. Mag. 95: 397-404.

Chen, P.Y., 1977. Table of key lines in X-ray powder diffraction patterns of minerals in clays and associated rocks, Indiana Geological Survey Occasional Paper 21, 67 pp.

Christiansen, E.A., 1967. Preglacial valleys in southern Saskatchewan. Sask. Res. Coun. 87 pp.

Christiansen, E.A., 1968. A thin till in west-central Saskatchewan, Canada. Canadian Journal of Earth Sciences 5: 329-336.

Christiansen, E.A., 1979. The Wisconsinan deglaciation of southern Saskatchewan and adjacent areas. Canadian Journal of Earth Sciences 16: 913-938.

Cisneros, S.L., Witkowski R.E., & D.L. Oswald, 1977. Artinite from San Benito County, California. The Mineralogical Record 8: 457-460.

Clarke, F.W., 1924. The data of geochemistry. U.S. Geol. Survey Bull. 770: 871 pp.

Clayton, L., & S.R. Moran, 1982. Chronology of Late Wisconsinan glaciation in Middle North America. Quaternary Science Reviews 1: 55-82.

CNC/IHD (Canadian National Committee for the International Hydrologic Decade), 1978. Hydrologic Atalas of Canada. Fisheries and Environment Canada, Ottawa., 270 pp.

Cole, L.H, 1926. Sodium sulphate of western Canada. Occurrence uses and technology. Can. Dept. Mines Publ. 646, 155 pp.

Connor, A.J., 1920. The temperature and precipitation of Alberta, Saskatchewan, and Manitoba. Department of Marine and Fisheries, Meteorological Service of Canada, 57 pp.

Cook, R.B., 1978. Famous mineral localities: Chuquicamata, Chile. The Mineralogical Record 9: 321-333.

Currie, B.W., 1953. Temperature Prairie Provinces and Northwest Territories, Physics Department, University of Saskatchewan, 37 pp.

David, P.P., 1964. Surficial geology and ground water resources of the Prelate area (72k). PhD. thesis, Department of Geological Sciences, McGill University, Montreal, 329 pp.

Dean, W.E., 1978. Theoretical versus observed successions from evaporation of sea water. In Marine Evaporites (eds Dean, W.E. & B.C. Schreiber). Soc. Econ. Pal. Min. Short Course Notes, Tulsa, Okla. pp. 74-85.

Dean, W.E. & A. Schwalb, 2000. Holocene environmental and climatic changes in the Northern Great Plains as recorded in the geochemistry of sediments in Pickerel Lake, South Dakota. Quaternary International 67 (in press).

Dingman, S.L., 1994. Physical hydrology, Macmillan Publishing Company, New York. 550 pp.

DMR, 1969. Department of Mineral Resources, Government of Saskatchewan, Inventory and Outlook of Saskatchewan's Mineral Resources, Report No. 83, 123 pp.

Douglas, R.J.W., 1970. Geology and economic minerals of Canada. Maps and

Charts. Dept. Ener. Min. Resour.

Dunn, P.J. & M. Fleischer, 1983. New mineral names. American Mineralogist 68: 642-645.

Egan, D.M., 1984. Mineralogical and geochemical aspects of saline lake sediments of the northern Great Plains. M.S. thesis, University of Manitoba, Winnipeg, Manitoba, 129 pp.

Environment Canada, 1980. Canadian Normals: 2-SI. Atmospheric Environment Service.

Embrey, P.G., & J.P. Fuller, 1979. A manual of new mineral names: 1892-1978. Oxford University Press, 467 pp.

Epp, H.T. & L. Townley-Smith, 1980. The Great Sand Hills of Saskatchewan. Report prepared for Saskatchewan department of the Environment, Regina, 156 p.

Eugster, H.P., 1969. Inorganic bedded cherts from the Magadi area, Kenya. Contrib. Mineral. and Petrol. 22: 1-31.

Eugster, H.P., 1970. Chemistry and origin of the brine of Lake Magadi, Kenya. Mineralog. Soc. America Spec. Paper 3: 215-235.

Eugster, H.P., 1971. The beginning of experimental petrology. Science 173: 481-489.

Eugster, H.P., 1982. Climatic significance of lake and evaporite deposits. In: Climate in earth history. National Academy Press, Washington, D.C., p. 105-111.

Eugster, H.P. & L.A., Hardie, 1975. Sedimentation in an ancient playa-lake complex: the Wilkins Peak Member of the Green River Formation of Wyoming. Geol. Soc. Am. Bull. 86: 319-334.

Eugster, H.P. & L.A., Hardie, 1978. Saline lakes. In: Lakes (ed: Lerman, A.), p. 237-

294.

Eugster, H.P., Harvie, C.E. and J.H. Weare, 1980. Mineral equilibria in the six-component seawater system, Na-K-Mg-Ca-SO_4-Cl-H_2O, at 25°C. Geochim. et Cosmochim. Acta 44: 1335-1347.

Eugster, H.P & B.F. Jones, 1979. Behaviour of major solutes during closed-basin brine evolution. American Journal of Science 279: 609-631.

Eugster, H.P. & K. Kelts, 1983. Lacustrine chemical sediments. In: A.S. Goudie and K. Pye (Editors), Chemical sediments and geomorphology: Precipitates and residua in the near-surface environment. Academic Press, London, p. 321-360.

Eugster, H.P. & G.I. Smith, 1965. Mineral equilibria in the Searles lake evaporites, California. Journal of Petrology 6: 473-522.

Fahey, J. & G. Tunnel, 1941. Bradleyite, a new mineral, sodium phosphate magnesium carbonate. American Mineralogist 26: 646-650.

Fenton, M.M., 1984. Quaternary stratigraphy of the Canadian Prairies. Geological Survey of Canada Paper 84-10, p. 57- 68.

Fulton, R.J., Fenton, M.M., and Rutter, N.W., 1984. Summary of Quaternary stratigraphy and history, western Canada, in Fulton, R.J., ed., Quaternary stratigraphy of Canada Paper 84-10, p. 69-86.

Fernandez, C.A., 1994. An outline of paleolimnology in Argentina. J. Paleolimnology 10: 3-16.

Faire, G., 1991. Principles & applications of inorganic geochemistry. Macmillian Publ. Company, p. 349-352.

Foshag, W.F., 1931. Krausite, a new sulfate from California. American Mineralogist 16: 352-360.

Fremlin, G. (Editor), 1974. The national atlas of Canada, 4th edition. MacMillan Co., Department of Energy, Mines and Resources, Ottawa, 254 pp.

Frondel, C., 1950. Notes on arcanite, ammonian aphthitalite and oxammite. American mineralogist 35: 596.

Frondel, C. & L.H. Bauer, 1954. Kutnahorite: a mangnese dolomite, $CaMn(CO_3)_2$. American Mineralogist 38: 748-760.

Garavelli, C.G., Vurro, F. & G.C. Fioravanti, 1982. Minrecordite, a new mineral from Tsumeb. The Mineralogical Record 13: 131-136.

Garrels, R.M. & M.E. Thompson, 1962. A chemical model for seawater at 25°C and one atmosphere total. Amer. J. Sci. 260: 57-66.

Goldsmith, J.R., Graf, D.L., & J. Witters, 1962. Studies in the system $CaCO_3$-$MgCO_3$-$FeCO_3$: 1. Phase relations; 2. A method for major-element spectrochemical analysis; 3. Compositions of some ferroan dolomites. Journal of Geology. 62: 659-688.

Gravenor, C.P. and Kupsch, W.O., 1959. Ice-disintegration features in western Canada. Journal of Geology 67: 48 - 64.

Hammer, U.T., 1978. The saline lakes of Saskatchewan: 1. Background and rationale for saline lakes research. Int. Revue ges. Hydrobiol 63: 173-177.

Hammer, U.T., 1978. The saline lakes of Saskatchewan: 3. Chemical characterization. Int. Revue ges. Hydrobiol 63: 311-335.

Hammer, U.T., 1986. Saline lakes: their distribution and characteristics. In: D.T. Waite (ed.), Evaluating saline waters in a plains environment. Canadian Plains Proceedings 17: 1-12.

Hammer, U.T. & Haynes, R.C., 1978. The saline lakes of Saskatchewan: 2. Locale, hydrography and other physical aspects. Int. Revue ges. Hydrobiol 63: 179-203.

Hammer, U.T. & J.M., Heseltine, 1988. Aquatic macrophytes in saline lakes of the

Canadian Prairies. Hydrobiologia 158: 101-106.

Handford, C.R., 1982. Sedimentology and evaporite genesis in a Holocene continental-sabkha playa basin, Bristol Dry Lake, California. Sedimentology 29: 239-253.

Harbeck, G.E., 1955. The effect of salinity on evaporation. U.S. Geol. Survey Prof. Paper 272-A: 470-477.

Hardie, L.A., 1968. The origin of the Recent non-marine evaporite deposit of Saline Valley, Inyo County, California. Geochim. et Cosmochim. Acta 41: 833-834.

Hardie, L.A., 1984. Evaporites: Marine or non-marine? American Journal of Science 284: 193-240.

Hardie, L.A. & H.P. Eugster, 1970. The evolution of closed-basin brines. Mineral. Soc. Amer. Spec. Pap. 3: 273-290.

Hardie, L.A., J.P. Smoot & H.P. Eugster, 1978. Saline lakes and their deposits: a sedimentological approach. Spec. Publs Int. Ass. Sediment 2: 7-41.

Hare, F.K., 1976. Late Pleistocene and Holocene climates: some persistent problems. Quat. Res. 6: 507-516.

Harrison, S.P., 1993. Late Quaternary lake-level changes and climates of Australia. Quaternary Science Reviews 12: 211-231.

Harrison, S.P. & G. Digerfeldt, 1993. European lakes as palaeohydrological and palaeoclimatic indicators. Quaternary Science Reviews 12: 233-248.

Harrison, S.P. & S.E. Metcalfe, 1985. Variation in lake levels during the Holonce in north America: an indicator of changes in atmospheric circulation patterns. Geographie Physique et Quaternaire 39: 141-150.

Harvie, C.E., Eugster, H.P. & J.H. Weare, 1982. Mineral equilibria in the six-component seawater system, Na-K-Mg-Ca-Cl-SO_4-H_2O at 25°C. II: Compositions of the saturated solutions. Geochim. et Cosmochim. Acta 46:

1603-1618.

Harvie, C.E., Moller, N. & J.H. Weare, 1984. The prediction of mineral solubilities in natural waters: the Na-K-Mg-Ca-H-Cl-SO_4-OH-HCO_3-CO_3-CO_2-H_2O system to high ionic strengths at 25°C. Geochim. et Cosmochim. Acta 48: 723-751.

Harvie, C.E. & J.H. Weare, 1980. The prediction of mineral solubilities in natural waters: the Na-K-Mg-Ca-Cl-SO_4-H_2O system from zero to high concentrations at 25°C. Geochim. et Cosmochim. Acta 44: 981-997.

Harvie, C.E., J.H. Weare, L.A., Hardie, and H.P. Eugster, 1980. Evaporation of sea-water: calculated mineral sequences. Science 208: 498-500.

Helgeson, H.C., Brown, T.H., Nigrini, A. & T.A. Jones, 1970. Calculation of mass transfer in geochemical processes involving aqueous solutions. Geochim. et Cosmochim. Acta 34: 569-592.

Hill, A.E. & J.H. Wills, 1938. Ternary Systems XXIV: calcium sulfate, sodium sulfate and water. J. Amer. Chem. Soc. 60: 1647-1655.

Hitchon, B., Billings, G.K. and Klovan, J.E., 1971. Geochemistry and origin of formation waters in the western Canada sedimentary basin-III. Factors controlling chemical composition. Geochemica et Cosmochimica Acta 35: 567-598.

Hite, R.J., 1983. The sulfate problem in marine evaporites. Sixth International Symposium on Salt 1: 217-230.

Holser, W.T., 1979. Mineralogy of evaporites, in Burns, R.G., ed., Marine Minerals. Mineralog. Soc. America Short Course Notes. 6: 211-294.

Howie R.A. & F.M. Broadhurst, 1958. X-ray data for dolomite and ankerite. American mineralogist 43: 1210-1213.

Hsü, K.J., 1972. Origin of saline giants-a critical review after discovery of the Mediterranean evaporite. Earth Sci. Rev.. 8: 371-396.

Hsü,, K.J. & C. Siegenthaler, 1969. Preliminary experiments on hydrodynamic movement induced by evaporation and their bearing on the dolomite problem. Sedimentology 12: 11-15.

Hudec, P.P. & P. Sonnenfeld, 1974. Hot brines on Los Roques, Venezuela. Science 185: 440-442.

Imbrie, J. & E.G. Purdy, 1962. Classification of modern Bahamian carbonate sediment, in Classification of carbonate rocks. Am. Assoc. Petroleum Geologists Mem. 1: 253-272.

Imbrie, J. & Tj. H. van Andel, 1964. Vector analysis of heavy-mineral data. Geol. Soc. America Bull. 75: 1131-1155.

Jöreskog, K.G., Klovan, J.E. and Reyment, R.A., 1976. Geological Factor Analysis. Elsevier, Amsterdam.

Jones, B.F. & C.J., Bowser, 1978. The mineralogy and related chemistry of lake sediments. In: Lakes (ed: Lerman, A), p. 179-236.

Kehew, A.E. & J.T. Teller, 1993. History of late glacial runoff along the southwestern margin of the Laurentide ice sheet. Quaternary Science Reviews 13: 859-877.

Kehew, A.E. & J.T. Teller, 1994. Glacial-lake spillway incision and deposition of a coarse-grained fan near Watrous, Saskatchewan. Can. J. Earth Sci. 31: 544-553.

Kelts, K. & K.J. Hsü, 1978. Freshwater carbonate sedimentation. In: Lakes (ed: Lerman, A.), p. 295-323.

Kendall, A.C., 1984. Evaporites. In: R.G. Walker (editor), Facies models (2nd edition), Geoscience Canada Reprint Series 1: 259-296.

Kendall, A.C., 1988. Aspects of evaporite basin stratigraphy. In: Schreiber, B.C. (ed.), Evaporites and Hydrocarbons. Columbia Univ. Press, NY, p. 11-65.

Kharaka, Y.K. & I. Barnes, 1973. SOLMNEQ: Solution-mineral equilibrium computations. U.S. Geol. Surv. Comp. Contr., Nat. Tech. Inf. Rep. PB-215-899, 82 pp.

Kinsman, D.J.J., 1976. Evaporites: Relative humidity control of primary facies. Journal of Sedimentary Petrology 46: 273-279.

Kinsman, D.J.J., 1969. Modes of formation, sedimentary associations and diagnostic features of shallow-water and supratidal evaporites. Am. Assoc. Petroleum Geologists Bull. 53: 830-840.

Klassen, R.W., 1972. Wisconsin events and the Assiniboine and Qu'Appelle valleys of Manitoba and Saskatchewan. Canadian Journal of Earth Sciences 9: 544-560.

Klassen, R.W., 1989. Quaternary geology of the southern Canadian Interior Plains, in Chapter 2 of Quaternary Geology of Canada and Greenland, R.J. Fulton (ed.), Geological Survey of Canada, Geology of Canada, no. 1.

Klassen, R.W., 1991. Surficial geology and drift thickness, Cypress Lake, Saskatchewan. Geological Survey of Canada, Map 1766A, scale 1:250000.

Klassen, R.W., 1994. Late Wisconsinan and Holocene history of southwestern Saskatchewan. Can. J. Earth Sci. 31: 1822-1837.

Klovan, J.E., 1966. The use of factor analysis in determining depositional environments from grain-size distributions. Journal of Sedimentary Petrology 36: 115-125.

Klovan, J.E., 1975. R- and Q-mode factor analysis, in Chapter 2 of Concepts in Geostatistics, R.B. McCammon (ed.). Springer-Verlag, New York, 320 pp.

Klug, H.P. & L.E. Alexander, 1974. X-ray diffraction procedures for polycrystalline and amorphous materials. New York, Wiley. 2nd ed., 966 pp.

Lambert, A. & K.J. Hsü, 1979. Non-annual cycles of varve-like sedimentation in Walensee, Switzerland. Sedimentology 26: 453- 461.

Lanesky. D.E., B.W. Logan, R.G. Brown & A.C. Hine, 1979. A new approach to portable vibracoring underwater and on land. J. of Sed. Petrol. 49: 654-657.

Langbein, W.B., 1961. Salinity and hydrology of closed lakes. U.S. Geol. Surv. Prof. Paper 412: 1-20.

Last, W.M., 1980. Sedimentology and postglacial history of Lake Manitoba. Ph.D. thesis, Winnipeg, University of Manitoba, 686 pp.

Last, W.M. 1982. Holocene carbonate sedimentation in Lake Manitoba, Canada. Sedimentology 29: 691-704.

Last, W.M., 1983. Modern sedimentology and hydrology of lake Manitoba, Canada. Environmental geology 5: 177-190.

Last, W.M., 1984. Sedimentology of playa lakes of the northern Great Plains. Can. J. Earth Sci. 21: 107-125.

Last, W.M., 1988. Salt lakes of western Canada: a spatial and temporal geochemical perspective. p. 99-113 In: W. Nicholaichuk & H. Steppuhn (eds.) Proc. Symp. On Water Management Affecting the Wet-to-Dry Transition. Water Studies Institute, Saskatoon, Sask.

Last, W.M., 1989. Sedimentology of a saline playa in the northern Great Plains, Canada. Sedimentology 36: 109-123.

Last, W.M., 1989. Continental brines and evaporates of the northern Great Plains of Canada. Sed. Geol. 64: 207-221.

Last, W.M., 1990. Paleochemistry and paleohydrology of Ceylon lake, a salt-dominated playa basin in the northern Great Plains, Canada. J. Paleolimnology 4: 219-238.

Last, W.M., 1990. Lacustrine dolomite: an overview of modern, Holocene, and Pleistocene occurrences. Earth-Science Reviews 27: 221-263.

Last, W.M., 1992. Salt lake paleolimnology in the northern Great Plains: the facts, the fears, the future. In: R.D. Robarts and M.L. Bothwall (Eds.) Aquatic ecosystems in semi-arid regions: implications for resource management, p. 51-62.

Last, W.M., 1992. Chemical composition of saline and subsaline lakes of the northern Great Plains, western Canada. Int. J. Salt Lakes Res. 1(2): 47-76.

Last, W.M., 1993. Geolimnology of Freefight Lake: an unusual hypersaline lake in the northern Great Plains of western Canada. Sedimentology 40: 431-448.

Last, W.M., 1994. Paleohydrology of playas in the northern Great Plains: Perspectives from Palliser's Triangle. Geological Society of America Special Paper 289: 69-80.

Last, W.M., 1994. Deep-water evaporite mineral formation in lakes of Western Canada. Sedimentology and Geochemistry of Modern and Ancient Saline Lakes, SEPM Special Publication No. 50: 51-58.

Last, W.M., 1996. Bulk composition, texture, and mineralogy of Lake Winnipeg core and subsurface grab samples; in Lake Winnipeg Project: Cruise Report and Scientific Results, (ed.) B.J. Todd, C.F.M. Lewis, L.H. Thorleifson, and E. Nielson; Geological Survey of Canada, Open File 3113: 209-220.

Last, W.M. & P.D. Decker, 1992. Paleohydrology and paleochemistry of Lake Beeac, a saline palya in southern Australia. Aquatic ecosystem in semi-arid regions: implication for resource management. R.D. Robarts & M.L. Bothwell (Eds.). N.H.R.I. Symposium series 7, Environment Canada, Saskatoon, p. 63-73.

Last, W.M. & D.J. Sauchyn, 1993. Mineralogy and lithostratigraphy of Harris lake, Southwestern Saskatchewan, Canada. J. Paleolimnology 9: 23-39.

Last, W.M. & T.H. Schweyen, 1983. Sedimentology & geochemistry of saline lakes of northern Great Plains. Hydrobiologia 105: 245-263.

Last, W.M. & T.H. Schweyen, 1985. Late Holocene history of Waldsea lake, Saskatchewan, Canada. Quat. Res. 24: 219-234.

Last, W.M. & L.A. Slezak, 1986. Paleohydrology, sedimentology, and geochemistry of two meromictic saline lakes in southern Saskatchewan. Geo. Phys. Quat. 11: 5-15.

Last, W.M. & L.A. Slezak, 1987. Sodium sulphate deposits of western Canada. In Economic minerals of Saskatchewan. Sask. Geol. Soc. Spec. Publ. 8: 197-205.

Last, W.M. & L.A. Slezak, 1988. The salt lakes of western Canada: a paleolimnological overview. Hydrobiologia 158: 301-316.

Last, W.M. & J.T. Teller, 1983. Holocene climate and hydrology of the Lake Manitoba basin. In: J.T. Teller and Lee Clayton (Editors), Glacial Lake Agassiz 26: 333-353.

Last, W.M., Teller, J.T., & R.M. Forester, 1994. Paleohydrology and paleochemistry of Lake Manitoba, Canada: the isotope and ostracode records. J. Paleolimnology 12: 269-282.

Last, W. M. & D.C. Gosselin, 1997. Paleolimnology in the Great Plains of North America - special issue. Journal of Paleolimnology 17: 1-154.

Last, W. M., Vance, R. E., Wilson, S., & J. P. Smol, 1997. Early Holocene history of Clearwater Lake, Saskatchewan, Canada. Submitted to Holocene (4/97).

Last, W. M., 1999. Geolimnology of the Great Plains of western Canada. In: D.S. Lemmen and Vance, R.E. (Editors), Holocene climate and environmental change in the Palliser Triangle: a geoscientific context for evaluating the impacts of climate change on the southern Canadian Prairies, Geological Survey of Canada, Bulletin 534: 23-57.

Last, W. M. & R.E. Vance, 2000. The Holocene history of Oro Lake, one of the western Canada longest continuous lacustrine records. Sedimentary Geology (in press).

Last, W. M., 1999. Geolimnology of the Great Plains of western Canada. In Holocene Climate and Environmental Change in the Palliser Triangle: A

Geoscientific Context for Evaluating the Impacts of Climate Change on the Southern Canadian Prairies, (ed.) D.S. Lemmen and R.E. Vance; Geological Survey of Canada, Bulletin 534: 23-57.

Lemmen, D. S. (Editor), 1996. Landscapes of the Palliser Triangle. Guidebook for the Canadian Geomorphology Research Group Field Trip. Canadian Association of Geographers Annual Meeting, Saskatoon, 92 pp.

Lemmen, D. S. & R.E. Vance, 1999. An overview of the Palliser Triangle Global change project. In: D.S. Lemmen and Vance, R.E. (Editors), Holocene climate and environmental change in the Palliser Triangle: a geoscientific context for evaluating the impacts of climate change on the southern Canadian Prairies, Geological Survey of Canada, Bulletin 534: 7-22.

Lippmann, F., 1962. Benstonite, $CaBa_6(CO_3)_{13}$, a new mineral from the barite deposit in Hot Spring County, Arkansas. American Mineralogist 47: 585-598.

Lydolph, P.E., 1985. The climate of the earth. Rowman & Allanheld Publishers, 386 pp.

Madsen, B.M., 1966. Loeweite, vanthoffite, bloedite, and leonite from Southeastern New Mexico. U.S. Geol. Survey Prof. Paper 550-B: B125-B129.

McGinnety, J.A., 1972. Redetermination of the structures of potassium sulphate and potassium chromate: the effect of electrostatic crystal forces upon observed bond lengths. Acta Cryst., B28: 2845-2852.

Meyboom, P, 1966. Unsteady groundwater flow near a willow rings in hummocky moraine. Journal of Hydrology 4: 38-62.

Meneley, W.A., Christiansen, E.A. & Kupsch, W.O., 1957. Preglacial Missouri river in Saskatchewan J. Geol. 65: 441-447.

Milton C. & J. Axelrod, 1947. Fused wood-ash stones: fairchildite $K_2CO_3.CaCO_3$, buetschiliite $3K_2CO_3.2CaCO_3.6H_2O$ and calcite $CaCO_3$, their essential compositions. American mineralogist 32: 607-624.

Müller, G., 1970. High-magnesian calcite and protodolomite in Lake Balaton sediments. Nature 226: 749-750.

Müller, G., G. Irion & V. Föstner, 1972. Formation and diagenesis of inorganic Ca-Mg carbonates in the lacustrine environment. Naturwissenschaften 59: 158-164.

Multhauf, R.P., 1978. Neptune's Gift: a history of common salt. The Johns Hopkins University Press, Baltimore and London, pp. 325.

Mungoma, S., 1990. The alkaline, saline lakes of Uganda: a review. Hydrobiologia 208: 75-80.

Navrotsky, A., Putnam, R.L., Winbo, C., & Rosen E., 1997. Thermochemistry of double carbonates in the K_2CO_3-$CaCO_3$ system 82: 546-548.

Nesbitt, H.W., 1974. The study of some mineral-aqueous solution interactions: Ph.D. thesis, Baltimore, Johns Hopkins Univ. 173 pp.

Palache, C., 1938. Leightonite, a new sulphate of copper from Chile. American mineralogist 23: 34-37.

Palache, C., Berman, H., & Frondel C., 1951. Dana's system of mineralogy, 7th ed., V. II. John Wiley and Sons, Inc., New York, p. 398-452.

Plummer, L.N., Parkhurst, D.L., and Kosiur, D.R., 1976. MIX2: a computer program for modelling chemical reactions in natural waters. United States Geological Survey, Water-Resources Inventory Report 75-76, 73 p.

Plummer, L.N., Parkhurst, D.L., Fleming, G.W., and Dunkle, S.A., 1988. A computer program incorporating Pitzer's equations for calculation of geochemical reactions in brines. U.S. Geol. Survey Water-Resources Inv. Rept. 88-4153, 310 pp.

Prest, V.K., 1970. Quaternary geology, In Douglas, R.J.W. (ed.), Geology and economic minerals of Canada: Geological Survey of Canada. Economic Geology Report no. 1, p. 675-764.

Prest, V.K., 1984. The Late Wisconsinan glacier complex, in Fulton, R.J. (ed.), Quaternary stratigraphy of Canada; A Canadian contribution to IGCP Project 24: Geological Survey of Canada Paper 84-10, p. 22-36.

Price, J.S., 1993. Water level regimes in Prairies sloughs: Canadian Water Resources Journal 18: 95-107.

Quigley, R.M., 1983. Glaciolacustrine and glaciomarine clay deposition: a North American perspective, in Eyles, N. (ed.), Glacial geology-an introduction for engineers and earth scientists, p. 140-167.

Radovanovic, M., 2000. MODERN DOLOMITIC HARDGROUNDS FROM WEST BASIN LAKE, VICTORIA, AUSTRALIA. B.Sc. Hon. Thesis, University of Manitoba, 85 pp.

Radovanovic, M. D., Last, W. M., and De Deckker, P. 2000. West Basin Lake, Victoria, Australia: New Insight into the Holocene History of a Well-studied Volcanic Maar. Abstracts Volume, 8th International Paleolimnology Symposium, Queen's University.

Rawson, D.S. & G.E. Moore, 1944. The saline lakes of Saskatchewan. Can. J. Res., p. 141-20.

Reeder, S.W., Hitchon, B. And Levinson, A.A., 1972. Hydrogeochemistry of the surface waters of the Mackenzie River drainage basin, Canada-I. Factors controlling inorganic composition. Geochemica et Cosmochimica Acta 36: 825-865.

Richards, J.H. & K.I. Fung (eds.), 1969. Atlas of Saskatchewan. Univ. Saskatchewan, Saskatoon, 236 pp.

Roberts, A.C., Ansell H.G. & I.R. Jonasson, 1986. Rapidcreekite, a new hydrated calcium sulfate-carbonate from the Rapid Creek area, Yukon Territory. The Canadian Mineralogist 24: 51-53.

Roberts W.L., Campbell, T.J. and Rapp, G.R., 1990. Encyclopedia of minerals, 2rd, ed., Van Nostrand Reinhold Company, New York, 979 pp.

Rosen, M.R., 1991. Sedimentologic and geochemical constrains on the evolution of Bristol Dry Lake Basin, California, U.S.A.. Palaeogeography, Palaeoclimatology, Palaeoecology 84: 229-257.

Roulston, B.V. & D.C.E. Waugh, 1981. A borate mineral assemblage from the Penobsquis and Salt Springs evaporite deposits of southern New Brunswick. Canadian Mineralogist 19: 291-301.

Royse, Jr., C.F., J.S. Wadell & L.E. Petersen, 1971. X-ray determination of calcite-dolomite: an evaluation. J. of Sedimentary Petrology 41: 483-488.

Rueffel, P.G., 1968. Development of the largest sodium sulfate deposit in Canada. Canadian Institute of Mining and Metallurgy Bulletin 61: 1217-1228.

Rutherford, A. A., 1967. Water Quality Survey of Saskatchewan Groundwaters. Saskatchewan Research Council, Report C-66-1, 267 pp.

Rutherford, A. A., 1970. Water Quality Survey of Saskatchewan Surface Waters. Saskatchewan Research Council, Report C-66-1, 266 pp.

Sack, L.A. & W.M. Last, 1994. Lithostratigraphy and recent sedimentation history of Little Manitou Lake, Saskatchewan, Canada. J. Paleolimnology 10: 199-212.

Sanford, W.E. & W.W. Wood, 1991. Brine evolution and mineral deposition in hydrologically open evaporite basins. Amer. J. Sci. 291: 687-710.

SAS/STAT Users Guide, 1990. Version 6, Fourth Edition, Vol. 1. SAS Institute Inc., Cary, NC, USA, 670 pp.

Sauchyn, D.J., 1990. A reconstruction of Holocene geomorphology and climate, western Cypress Hills, Alberta and Saskatchewan. Can. J. Earth Sci. 27: 1504-1510.

Sauchyn, M.A. & D.J. Sauchyn, 1991. A continuous record of Holocene pollen from Harris Lake, Southwestern Saskatchewan, Canada. Palaeogeography, Palaeoclimatology, Palaeoecology. 88: 13-23.

Schwalb, A., S.M. Locke & W.E. Dean, 1995. Ostracode ^{18}O and ^{13}C evidence of Holocene environmental changes in the sediments of two Minnesota lakes. Journal of Paleolimnology 14: 281-196.

Seaman, M.T., P.J. Ashton & W.D. Williams, 1991. Inland salt waters of southern Africa. Hydrobiologia 210: 75-91.

Schmalz, R.F., 1969. Deep-water evaporite deposition: a genetic model. The American Association of Petroleum Geologists Bulletin 53: 798-823.

Schultz, L.G., 1964. Quantitative interpretation of mineralogical composition from X-ray and chemical data for the Pierre Shale. U.S. geological Survey Professional Paper 391-c, 31 pp.

Shang, Y., 1999. Mineralogy, lithostratigraphy, and inferred geochemical history of North Ingebright Lake, Saskatchewan. In Holocene Climate and Environmental Change in the Palliser Triangle: A Geoscientific Context for Evaluating the Impacts of Climate Change on the Southern Canadian Prairies, (ed.) D.S. Lemmen and R.E. Vance; Geological Survey of Canada, Bulletin 534: 95-110.

Smith, N.D. & G. Ashley, 1985. Proglacial lacustrine environment, In Ashley, G.M. et al, ed., Glacial sedimentary environment: SEPM Short Course No. 16, p. 135-216.

Smith, G.I., 1979. Subsurface stratigraphy and geochemistry of Late Quaternary evaporates, Searles Lake, California. U.S. Geological Survey Professional Paper 1043: 1-130.

Smith, G.I. & I. Friedman, 1986. Seasonal diagenetic changes in salts of Owens Lake, California, 1970-77; in Studies in Diagenesis, (ed.) F.A. Mumpton; United States Geological Survey, Bulletin 1578: 21-29.

Smoot, J.P. & T.K. Lowenstein, 1991. Depositional environments of non-marine evaporites. In: Melvin, J.L.(ed.), Evaporites, Petroleum and Mineral Resources, Elsevier, New York, p.189-348.

SIL (Societas Internationalis Limnologiae), 1959. Symposium on the classification of brackish waters. Archiv. Oceanogr. Limno. Roma 1 (Suppl.): 1-248.

Sonnenfeld, P., 1984. Brines and Evaporates. Academic Press, New York, N.Y., p. 613.

Spencer, R.J., Eugster, H.P. & B.F. Jones, 1985. Geochemistry of Great Salt Lake II: Pleistocene-Holocene evolution. Geochim. Cosmochim. Acta 49: 739-747.

Spencer, R.J., Eugster, H.P., Jones, B.F. & Rettig S.L., 1985. Geochemistry of Great Salt Lake I: Hydrochemistry since 1850. Geochim. Cosmochim. Acta 49: 723-737.

Stalker, A. M., 1976. Quaternary stratigraphy of the southwestern Canadian Prairies, in Quaternary Stratigraphy of North America, W.C., Mahaney, ed., Dowden, Hutchinson & Ross, Stroudsburg, Pa., p. 381-407.

Stewart, F.H., 1963. Marine evaporites. U.S. Geol. Survey Prof. Paper 440-Y, 53p.

Stevens, L. R., Ito, E., and Olson, D. E. L., 2000. Relationship of Mn-carbonates in varved lake-sediments to catchment vegetation in Big Watab Lake, MN, USA. J. Paleolim. 24: 199-211.

Sullivan, T.J. & D.F. Charles, 1994. The feasibility and utility of a paleolimnology/paleoclimate data cooperative for North America. J. Paleolimnology 10: 265-273.

Talbot, M.R. & K. Kelts, 1986. Primary and diagenetic carbonates in the anoxic sediments of Lake Bosumtwi, Ghana. Geology 14: 912- 916.

Teller, J.T., 1985. Glacial Agassiz and its influence on the Great Lakes, in Karrow, P.F., and Calkin, P.E., eds., Quaternary evolution of the Great Lakes: Geological Association of Canada Special Paper 30, p. 1-16.

Teller, J.T., 1987. Proglacial lakes and the southern margin of the Laurentide Ice Sheet. In "North America and Adjacent Oceans during the Last Deglaciation" (W.F. Ruddiman and H.E. Wright, Eds.), p. 39-69, Geological Society of

America, The Geology of North America, k-3.

Teller, J.T., 1990. Volume and routing of late-glacial runoff from the southern Laurentide Ice Sheet. Quaternary Research 34: 12-23.

Teller, J.T. & M.M. Fenton, 1980, Late Wisconsinan glacial stratigraphy and history of southeastern Manitoba. Canadian Journal of Earth Sciences 17: 19-35.

Teller, J.T. & W.M. Last, 1981. Late Quaternary history of Lake Manitoba, Canada. Quaternary Research 16: 97-116.

Teller, J.T. & W.M. Last, 1990. Paleohydrological indicators in playas and salt lakes, with examples from Canada, Australia, and Africa. Palaeogeography, Palaeoclimatology, Palaeoecology 76: 215-240.

Teller, J.T., S.R. Moran & L. Clayton, 1980. The Wisconsinan eglaciation of southern Saskatchewan and adjacent areas: discussion. Canadian Journal of Earth Sciences 17: 539-541.

Teller, J.T. & L. H. Thorleifson, 1983. The Lake Agassiz-Lake Superior connections; in Glacial Lake Agassiz, J.T. Teller and L. Clayton (ed.), Geological Association of Canada Special Paper 26,p. 261-290.

Truesdell, A.H. & B.F. Jones, 1974. WATEQ, a computer program for calculating chemical equilibria of natural waters. Journal of Research of the United States Geological Survey 2: 233-274.

Thorleifson, L.H. & F.J. Kristjansson, 1993. Quaternary geology and drift prospecting, Beardmore-Geraldton area, Ontario. Geological Survey of Canada Memoir 435, 146 pp.

Tomkins, R.V., 1953. Magnesium in Saskatchewan. Sask. Dep. Min. Resour., Rep. 11, 23 pp.

Tomkins, R.V., 1954. Natural sodium sulphate in Saskatchewan. Sask. Dep. Min. Resour., Rep. 6, 71 pp.

uPDSM User's Manual, 1992. Micro Powder Diffraction Search/Match. Fein-Marquart Associates. Release 4.30.

Valero-Garcés, B. & K.R. Kelts, 1995. A sedimentary facies model for perennial and meromictic saline lakes: Holocene Medicine Lake basin, South Dakota, USA. Journal of Paleolimnology 15: 123-149.

Vance, R. E., 1997. The Geological Survey of Canada's Palliser Triangle Global Change Project: a multidisciplinary geolimnological approach to predicting potential global change impacts on the Northern Great Plains. Journal of Paleolimnology 17: 3-8.

Vance, R. E. & W.M. Last, 1994. Paleolimnology and global change on the southern Canadian Prairies; in Current Research 1994-B. Geological Survey of Canada, p. 49-58

Vance, R.E., Beaudoin, A.B. & B.H. Luckman, 1995. The paleoecological record of 6 ka BP climate in the Canadian Prairie Provinces. Geographie physique et Quaternaire 49: 81- 98.

Vance, R.E., J.J. Clague & R.W. Mathewes, 1993. Holocene paleohydrology of a hypersaline lake in southeastern Alberta. J. Paleolimnology 8: 103-120.

Vance, R.E. & W.M. Last, 1994. Paleolimnology and global change on the southern Canadian Prairies. In current research 1994-B; Geological Survey of Canada, p. 49-58.

Vance, R.E., Mathewes, R.W. and J.J. Clague, 1992. 7000 year record of lake-level change on the Northern Great Plains: a high-resolution proxy of past climate. Geology 20: 879-882.

Van der Kamp, G & H. Maathuis, 1991. Annual fluctuations of groundwater levels as a result of loading by surface moisture. Journal of Hydrology 127: 137-152.

Van Doesburg, J.D., L. Vergouwen & L.V.D. Plas, 1982. Konyaite, $Na_2Mg(SO_5)_2.5H_2O$, a new mineral from the Great Konya Basin, Turkey.

American Mineralogist 67: 1035-1038.

Van Loan, P.R., 1962. An X-ray study of leightonite. The Canadian Mineralogist 7: 272-277.

Van Stempvoort, D.R., T.W.D. Edwards, M.S. Evans & W.M. Last, 1993. Plaeohydrology and paleoclimate records in a saline lake core: mineral, isotope and organic indicators. J. Paleolimnology 8: 135-147.

Vergouwen, L., 1981. Eugsterite, a new salt mineral. American Mineralogist 66: 632-636.

Vreeken, W.J., 1994. A Holocene soil-geomorphic record from the Ham site near Frontier, southwestern Saskatchewan. Canadian Journal of Earth Sciences 31: 532-543.

Wallick, E.I., 1981. Chemical evolution of groundwater in a drainage basin of Holocene age, east-central Alberta, Canada. Journal of Hydrology 54: 245-283.

Warren, J.K., 1989. Evaporite Sedimentology. Prentice-Hall, New Jersey.

Warren, J.K., 1986. Shallow water evaporitic environments and their source rock potential. Journal of Sedimentary Petrology 56:442-454.

Watson, A., 1983. Evaporite sedimentation in non-marine environments. In: A.S. Goudie and K. Pye (Editors), Chemical sediments and geomorphology: Precipitates and residua in the near-surface environment. Academic Press, London, p. 163-185.

Weare, J.H., 1987. Models of mineral solubility in concentrated brines with application to field observations. Reviews in Mineralogy 17: 143-177.

Williams, W.D., 1991. Comments on the so-called salt lakes of Greenland. Hydrobiologia 210: 67-74.

Williams, W.D., 1964. A contribution to lake typology in Victoria, Australia. Ver.

Internat. Verein. Limnol. 15: 158-163.

Wolfe, B. & J.T. Teller, 1993. Sedimentological and stratigraphic investigations of a sequence of 106 varves from glacial Lake Assiniboine, Saskatchewan. Journal of Paleolimnology 9: 257-273.

Woo, M.K., 1992. Impacts of climate variability and change on Canadian wetlands. Canadian Water Resources Journal 17: 63-69.

Wood, W.W. & W.E. Sanford, 1990. Ground-water control of evaporite deposition. Economic Geology 85: 1226-1235.

Xia, J., Haskell, B. J., Engstrom, D. R. & E. Ito, 1997. Holocene climate reconstructions from tandem trace-element and stable isotope composition of ostracodes from Coldwater Lake, North Dakota, USA. Journal of Paleolimnology 17: 85-100.

Yegorov, K.N., Ushchapovskaya, Z.F., Kashayev, A.A., Bogdanov, G.V. & Y.I. Sizykh, 1990. Zemkorite. American Mineralogist 75: 933-934.

Zuniga, L.R., V. Campos, H. Pinochet & B.Prado, 1991. A limnological reconnaissance of lake Tebenquiche,Salar de Atacama, Chile. Hydrobiologia 210: 19-24.

Appendix A Organic Matter and Carbonate Content Data

Organic Matter and Carbonate Content of North Core at North Ingenbright Lake

Depth (cm)	Organic Matter(%)	Carbonate Content(%)	Depth (cm)	Organic Matter(%)	Carbonate Content(%)
12	12.8	3.9	108	0.4	0.5
14	11.7	4.2	110	0.6	0.0
16	8.5	7.6	112	0.6	0.1
18	8.8	9.2	114	0.6	0.2
20	12.6	5.6	116	0.6	1.5
22	14.5	4.5	118	0.1	0.6
24	9.2	8.4	120	0.1	0.7
26	13.2	4.6	122	0.4	1.0
28	13.8	6.8	124	0.4	1.0
30	12.5	7.3	126	0.2	0.5
32	14.8	3.2	128	0.1	0.6
34	12.3	5.6	130	0.1	0.7
36	13.9	3.4	132	2.3	1.5
38	12.6	3.9	134	0.9	0.7
40	10.9	6.5	136	1.0	1.0
42	13.2	2.3	138	0.5	0.9
44	12.2	3.1	140	0.8	1.9
46	8.7	3.2	142	0.9	1.6
48	11.1	1.4	144	0.1	0.6
50	4.3	5.1	146	3.6	5.6
52	4.4	1.4	148	4.8	6.1
54	3.2	2.0	150	4.6	2.0
56	4.1	0.8	152	5.9	2.1
58	1.8	1.3	154	0.7	0.3
60	2.7	0.5	156	0.5	0.8
62	1.7	1.5	158	0.5	0.5
64	2.4	0.9	160	0.5	0.6
66	1.7	1.7	162	0.6	0.4
68	1.6	2.8	164	0.6	0.4
70	2.1	0.3	166	1.0	0.6
72	2.6	0.4	168	0.3	0.1
74	1.9	0.9	170	1.0	0.0
76	1.8	2.3	172	0.8	0.4
78	1.7	0.5	174	0.2	0.1
80	1.9	7.2	176	0.3	0.0
82	1.4	0.4	178	1.2	0.5
84	1.8	0.6	180	1.5	0.2
86	1.2	0.6	182	1.1	0.3
88	2.3	1.2	184	0.8	0.0
90	2.6	0.6	186	1.5	0.5
92	1.2	0.1	188	1.4	0.7
94	1.2	0.4	190	0.8	0.2
96	1.5	0.4	192	3.3	0.3
98	0.5	1.0	194	1.9	0.0
100	1.7	0.4	196	2.3	0.6
106	1.0	0.6	198	2.6	0.0
200	2.5	0.2	292	2.4	0.7
202	2.7	0.0	294	2.0	1.2
204	2.6	0.3	296	2.5	0.2
206	2.1	1.0	298	1.9	0.5
208	2.7	0.6	300	3.1	1.4

Organic Matter and Carbonate Content of North Core at North Ingenbright Lake

Depth (cm)	Organic Matter(%)	Carbonate Content(%)	Depth (cm)	Organic Matter(%)	Carbonate Content(%)
210	2.7	0.7	302	3.6	0.8
212	2.9	0.2	304	2.4	1.1
214	3.2	0.8	306	2.0	1.0
216	2.5	0.3	308	2.0	0.1
218	3.7	0.6	310	1.6	1.1
220	2.9	0.8	312	1.2	1.8
222	3.9	0.5	314	1.7	0.3
224	4.7	0.9	316	1.6	0.4
226	3.4	0.7	318	0.9	1.6
228	4.3	0.7	320	0.9	1.0
230	3.5	0.9	322	1.2	0.6
232	3.6	0.5	324	1.4	0.7
234	4.5	0.8	326	1.0	0.7
236	5.5	0.0	328	1.0	0.8
238	4.5	0.4	330	1.0	1.0
240	5.0	0.0	332	1.3	0.5
242	3.8	0.9	334	1.3	0.3
244	3.9	1.2	336	0.7	0.4
246	4.5	0.9	338	1.6	0.4
248	5.1	1.0	340	2.1	1.0
250	4.9	0.5	342	0.8	0.5
252	4.1	1.8	344	1.0	1.4
254	5.5	1.3	346	1.1	0.3
256	4.5	0.7	348	0.5	0.3
258	3.7	2.0	350	2.9	0.5
260	3.7	0.8	352	0.7	0.5
262	5.1	1.4	354	1.0	10.0
264	4.5	2.5	356	0.9	0.4
266	4.8	0.0	358	1.1	0.4
268	4.7	2.7	360	1.0	0.6
270	4.4	6.7	362	1.4	0.9
272	3.8	1.6	364	1.4	0.8
274	3.9	1.4	366	1.2	3.4
276	4.1	1.9	368	1.5	0.5
278	3.4	0.9	370	0.9	3.4
280	4.4	0.9	372	0.8	0.1
282	3.7	1.6	374	0.8	3.9
284	3.2	1.3	376	0.6	4.2
286	3.6	1.5	378	1.5	0.3
288	2.4	1.0	380	0.6	0.6
290	2.3	0.6	382	0.9	0.4
384	0.8	0.5	496	2.1	0.1
386	0.8	5.9	498	2.3	16.4
388	1.3	0.0	500	1.9	0.2
390	0.8	0.1	502	1.8	1.3
392	0.4	0.3	504	2.4	6.6
394	0.6	0.4	506	2.3	0.4
396	0.5	0.9	508	1.5	0.1
398	0.2	0.8	510	3.0	17.1
400	0.4	0.3	512	1.9	0.5
402	0.4	0.1	514	4.0	2.0

Organic Matter and Carbonate Content of North Core at North Ingenbright Lake

Depth (cm)	Organic Matter(%)	Carbonate Content(%)	Depth (cm)	Organic Matter(%)	Carbonate Content(%)
404	0.1	0.2	516	5.5	0.2
406	0.0	0.2	518	5.3	2.3
408	0.1	0.6	520	5.0	0.9
410	0.1	0.1	522	4.0	0.3
412	0.7	0.1	524	19.6	8.8
414	0.1	0.5	526	1.0	0.3
416	0.1	0.4	528	1.2	8.6
418	0.4	0.1	530	1.5	1.2
420	0.1	0.1	532	1.2	0.1
422	2.0	4.2	534	1.0	0.8
424	0.1	0.5	536	2.4	0.7
426	0.4	0.2	538	0.8	0.0
428	0.4	0.1	540	1.0	0.2
450	0.4	0.2	542	1.4	29.4
452	0.4	2.6	544	2.0	0.1
454	0.7	0.5	546	0.8	0.0
456	0.7	0.1	548	0.2	0.7
458	0.5	0.2	550	2.4	0.5
460	0.9	0.7	552	1.0	0.2
462	0.4	0.5	554	1.7	1.8
464	0.5	0.3	556	1.0	0.1
466	0.7	18.3	558	3.4	0.5
468	0.5	0.3	560	1.5	0.7
470	0.5	0.1	562	2.4	0.3
472	0.7	0.4	564	2.6	3.6
474	0.7	0.2	566	1.6	0.2
476	2.7	1.4	568	2.4	0.9
478	3.0	0.3	570	1.5	4.9
480	1.5	0.2	572	2.0	0.1
482	1.7	0.5	574	3.2	1.0
484	2.7	0.8	576	1.1	0.4
486	1.7	0.2	578	0.8	0.2
488	2.1	0.1	580	0.9	1.6
490	1.4	0.3	582	1.5	0.8
492	2.0	0.0	584	1.7	0.6
494	2.6	0.2	586	0.6	0.1
588	0.5	0.6	684	2.2	0.8
590	0.9	0.2	686	1.7	0.0
592	1.0	0.5	688	1.4	0.3
594	1.4	0.0	690	0.8	0.4
596	1.4	74.2	692	0.8	1.3
598	2.3	2.8	694	1.1	0.0
600	4.9	1.5	696	0.5	1.1
602	2.7	5.4	698	1.1	0.9
604	3.4	0.7	700	1.3	11.8
606	4.5	0.6	702	1.6	0.5
608	2.9	1.1	704	2.7	1.4
612	2.9	0.6	706	0.6	0.4
616	0.7	0.9	710	0.5	0.5
618	0.5	0.0	712	1.3	1.0
620	1.0	0.7	714	0.5	0.5

Organic Matter and Carbonate Content of North Core at North Ingenbright Lake

Depth (cm)	Organic Matter(%)	Carbonate Content(%)	Depth (cm)	Organic Matter(%).	Carbonate Content(%)
622	1.3	0.0	716	1.8	1.3
624	1.2	3.7	718	1.2	1.0
626	1.6	1.0	720	1.0	0.3
628	2.8	72.3	722	1.5	0.2
630	3.0	1.0	724	2.0	0.8
632	3.2	0.9	726	1.6	0.4
634	2.8	0.9	728	1.3	1.0
636	4.3	0.8	730	2.0	0.7
638	1.8	0.2	732	5.0	0.9
640	4.9	3.7	734	1.2	0.4
642	2.4	0.6	736	1.6	2.5
644	2.0	0.6	738	3.6	2.9
646	4.0	8.6	740	1.8	0.1
648	2.2	0.6	742	1.5	1.8
650	1.3	0.0	744	1.9	1.7
652	3.0	0.8	746	2.1	1.1
654	2.3	1.4	748	0.6	0.6
656	1.2	0.1	750	2.2	1.0
658	1.2	0.4	752	2.6	19.3
660	1.3	0.7	754	3.6	0.4
662	1.9	2.2	756	1.7	0.1
664	1.7	0.4	758	1.6	0.0
666	1.6	0.3	760	1.0	1.2
668	1.2	1.8	762	1.4	0.6
670	1.4	0.0	764	1.4	0.3
672	2.0	0.0	792	0.9	0.6
674	2.2	0.0	794	1.6	27.8
676	1.2	0.0	796	1.9	1.0
678	1.8	0.1	798	1.5	0.4
680	1.6	0.0	800	2.0	0.0
682	1.3	0.5	802	1.0	1.0
804	0.9	0.6	900	2.2	3.1
806	1.7	0.6	902	3.6	0.3
808	4.0	1.9	904	2.6	0.0
810	16.7	3.1	906	3.0	0.2
812	3.7	0.0	908	2.9	0.2
814	2.1	0.5	910	3.0	0.5
816	2.3	1.9	912	4.1	0.2
818	3.0	0.4	914	5.8	1.4
820	2.8	0.9	916	7.1	1.9
822	5.0	0.7	918	5.8	1.6
824	2.8	6.4	920	1.9	0.6
826	3.2	0.0	922	2.1	1.5
828	6.4	0.0	924	4.4	1.2
830	4.1	0.7	926	3.0	3.1
832	3.1	1.0	928	3.1	0.6
834	4.2	0.5	930	3.0	0.1
836	3.8	0.6	932	3.6	0.2
838	5.8	1.1	934	3.1	1.8
840	3.3	0.4	936	3.0	0.6
842	4.7	0.2	938	2.6	0.6

Organic Matter and Carbonate Content of North Core at North Ingenbright Lake

Depth (cm)	Organic Matter(%)	Carbonate Content(%)	Depth (cm)	Organic Matter(%)	Carbonate Content(%)
844	6.3	1.3	940	2.7	0.6
846	4.1	0.7	942	3.1	1.5
848	4.1	1.0	944	2.1	0.7
850	3.9	0.7	946	3.0	0.8
852	3.5	59.2	948	3.1	0.7
856	4.3	0.0	950	2.0	0.7
860	4.3	0.9	952	4.1	1.3
862	4.0	0.6	954	29.1	5.3
864	4.0	0.7	956	1.6	0.6
866	4.1	0.3	958	1.8	0.5
868	2.2	14.2	960	1.4	0.8
870	1.5	2.6	968	1.6	0.7
872	4.1	0.7	970	1.6	0.9
874	2.6	1.6	972	2.3	0.9
876	4.4	1.4	974	1.5	0.7
878	1.9	0.0	978	2.1	0.6
880	1.5	3.7	980	1.8	0.9
882	3.4	0.4	982	1.7	0.4
884	3.2	1.3	984	2.0	0.7
886	3.1	0.8	986	3.4	0.8
888	2.7	1.0	988	1.2	0.7
890	3.0	0.9	990	1.7	0.4
892	2.8	0.6	992	1.2	0.4
894	2.6	0.4	994	3.2	0.9
896	2.0	0.2	996	4.2	0.9
898	1.9	1.6	998	4.7	1.0
1,000	3.4	0.9	1,096	1.6	0.0
1,002	1.3	0.8	1,098	1.0	0.8
1,004	1.0	0.5	1,100	1.2	0.0
1,006	1.3	0.0	1,102	0.6	0.0
1,008	2.0	0.0	1,104	1.1	0.2
1,010	2.3	0.5	1,106	1.5	0.0
1,012	1.2	0.2	1,108	1.1	0.1
1,014	2.3	0.9	1,110	0.8	0.0
1,016	3.2	0.9	1,112	0.7	0.0
1,018	3.2	0.8	1,114	0.9	0.1
1,020	1.6	0.8	1,116	0.9	0.1
1,022	1.3	1.7	1,118	0.9	0.0
1,024	2.5	0.8	1,120	1.1	0.0
1,026	2.1	0.7	1,122	0.3	0.1
1,028	1.5	0.2	1,124	0.9	0.3
1,030	3.1	1.3	1,126	1.3	0.3
1,032	1.6	0.6	1,128	0.8	8.4
1,034	1.3	0.9	1,130	2.1	0.1
1,038	2.5	1.5	1,132	1.4	0.0
1,040	0.9	0.4	1,134	1.6	0.0
1,042	1.5	0.8	1,136	1.2	0.0
1,044	1.4	5.7	1,138	1.1	0.0
1,046	0.6	0.9	1,140	0.8	0.5
1,048	1.1	0.4	1,142	1.3	0.0
1,050	1.4	1.1	1,144	2.5	0.2

Organic Matter and Carbonate Content of North Core at North Ingenbright Lake

Depth (cm)	Organic Matter(%)	Carbonate Content(%)	Depth (cm)	Organic Matter(%)	Carbonate Content(%)
1,052	1.5	0.6	1,148	1.0	0.0
1,054	2.4	0.0	1,150	1.3	0.0
1,056	1.4	0.3	1,152	1.2	0.2
1,058	1.4	0.0	1,154	2.0	0.2
1,060	1.6	0.0	1,156	2.4	0.2
1,062	1.0	0.9	1,158	1.9	0.3
1,064	1.5	0.2	1,160	1.9	0.8
1,066	1.4	0.4	1,162	2.1	0.2
1,068	1.7	0.3	1,164	3.1	0.4
1,070	2.6	0.2	1,166	2.5	0.0
1,072	3.2	0.5	1,168	2.4	0.0
1,074	3.2	0.4	1,170	3.0	0.3
1,076	2.2	0.7	1,172	1.2	0.0
1,078	2.0	0.4	1,174	2.9	0.5
1,080	2.5	0.7	1,176	1.9	0.4
1,082	1.9	7.1	1,178	0.9	0.3
1,084	1.4	0.1	1,180	3.0	0.5
1,088	1.4	0.6	1,182	1.3	0.4
1,090	1.9	0.9	1,184	2.0	0.8
1,092	1.6	0.3	1,186	1.2	0.1
1,094	1.6	0.0	1,188	0.8	0.0
1,190	0.7	0.0	1,384	3.2	0.8
1,192	0.6	0.2	1,386	3.5	0.6
1,194	0.7	0.0	1,388	4.4	0.9
1,196	0.5	0.0	1,390	3.0	0.8
1,200	0.6	0.5	1,392	5.4	0.2
1,202	0.4	0.2	1,394	4.4	0.6
1,204	0.6	0.2	1,396	1.7	0.0
1,206	0.6	0.0	1,398	1.2	1.6
1,208	5.2	2.0	1,400	1.5	0.0
1,210	0.0	0.0	1,402	1.5	0.0
1,212	0.0	0.0	1,404	3.1	0.0
1,214	0.0	0.0	1,406	4.8	0.0
1,216	0.0	0.0	1,408	1.1	0.0
1,218	0.0	0.0	1,410	1.9	0.0
1,220	0.2	0.0	1,412	2.5	0.0
1,222	0.0	0.3	1,414	1.0	0.0
1,224	0.0	0.0	1,416	0.8	0.0
1,326	1.1	0.8	1,418	0.2	0.3
1,328	0.4	0.5	1,420	0.1	0.1
1,330	0.4	0.3	1,422	0.0	0.3
1,332	0.1	0.5	1,424	0.0	0.2
1,334	0.5	0.0	1,426	0.3	0.0
1,336	1.2	0.0	1,428	0.8	0.0
1,338	1.1	0.8	1,430	0.7	0.2
1,340	1.5	8.7	1,432	0.3	2.4
1,342	1.5	0.5	1,434	0.6	0.1
1,344	2.2	0.9	1,436	0.6	0.0
1,346	2.6	1.3	1,438	1.5	0.2
1,348	1.6	0.0	1,440	0.8	0.1
1,350	3.8	1.5	1,442	0.8	0.1

Organic Matter and Carbonate Content of North Core at North Ingenbright Lake

Depth (cm)	Organic Matter(%)	Carbonate Content(%)	Depth (cm)	Organic Matter(%)	Carbonate Content(%)
1,352	4.9	2.1	1,444	0.9	0.0
1,354	4.3	1.9	1,446	1.3	0.1
1,356	3.6	0.7	1,448	1.6	0.4
1,358	3.4	1.9	1,450	2.3	0.6
1,360	3.4	0.8	1,452	2.3	1.1
1,362	4.0	1.4	1,454	1.2	0.2
1,364	3.7	1.9	1,456	1.2	1.5
1,366	2.0	1.1	1,458	0.6	0.3
1,368	2.2	0.7	1,460	0.9	0.1
1,370	3.8	0.0	1,462	1.1	0.3
1,372	3.8	2.0	1,464	1.4	0.2
1,374	3.3	0.5	1,466	0.4	12.2
1,376	4.4	1.0	1,468	2.5	0.6
1,378	3.2	3.4	1,470	0.6	0.3
1,380	3.4	0.6	1,472	0.7	0.3
1,382	3.7	4.1	1,474	0.5	0.5
1,476	0.6	0.0	1,568	1.8	0.0
1,478	0.5	11.1	1,570	0.9	2.5
1,480	0.8	0.0	1,572	1.7	0.3
1,482	0.0	0.0	1,574	0.6	0.2
1,484	1.1	0.1	1,576	0.6	0.1
1,486	0.6	0.2	1,578	0.8	0.2
1,488	0.8	0.1	1,580	0.1	0.0
1,490	0.6	0.1	1,582	0.0	0.0
1,492	2.4	0.2	1,584	0.0	0.0
1,494	0.6	0.1	1,586	1.9	0.3
1,496	0.8	0.1	1,588	4.9	0.3
1,498	0.7	0.0	1,590	0.7	5.5
1,500	1.3	0.2	1,592	1.4	0.3
1,502	0.5	0.8	1,594	1.3	0.0
1,504	1.1	0.1	1,596	2.1	0.0
1,506	7.5	0.0	1,598	1.0	0.0
1,508	0.8	0.0	1,600	0.8	0.4
1,510	0.7	0.1	1,602	0.6	0.0
1,512	1.9	0.4	1,604	0.9	0.3
1,514	0.9	0.2	1,606	1.1	0.0
1,516	0.8	0.2	1,604	0.9	0.3
1,518	0.9	0.2	1,608	1.2	0.0
1,520	1.1	0.1	1,610	0.7	0.0
1,522	0.7	0.4	1,612	0.7	0.0
1,524	1.0	0.0	1,614	0.9	0.2
1,526	1.2	0.1	1,616	0.7	0.0
1,528	2.2	0.4	1,618	5.1	0.0
1,530	0.5	0.0	1,620	1.1	0.0
1,532	0.7	0.1	1,622	1.1	0.7
1,534	1.7	0.2	1,624	1.7	0.0
1,536	0.4	0.3	1,626	0.8	0.2
1,538	0.9	0.3	1,628	0.5	0.2
1,540	0.7	0.0	1,630	0.0	0.0
1,542	0.0	0.0	1,632	0.2	0.0
1,544	0.0	11.7	1,634	0.5	0.0

Organic Matter and Carbonate Content of North Core at North Ingenbright Lake

Depth (cm)	Organic Matter(%)	Carbonate Content(%)	Depth (cm)	Organic Matter(%)	Carbonate Content(%)
1,546	0.4	0.1	1,636	0.4	0.0
1,548	1.1	0.0	1,638	0.0	0.0
1,550	0.3	0.0	1,640	0.4	0.3
1,552	0.4	0.1	1,642	0.0	0.0
1,554	1.7	0.0	1,644	11.0	0.0
1,556	2.1	0.0	1,646	1.2	0.6
1,558	1.1	0.1	1,648	0.7	0.4
1,560	0.7	0.1	1,650	0.3	0.0
1,562	1.3	0.2	1,652	0.1	19.9
1,564	0.6	0.1	1,654	0.0	0.5
1,566	1.1	0.1	1,656	0.0	0.0
1,658	0.7	0.0	1,798	0.6	0.0
1,660	1.4	0.0	1,800	0.7	0.3
1,662	2.7	0.4	1,802	0.2	0.9
1,664	1.5	13.5	1,804	0.2	0.2
1,666	1.0	1.1	1,806	0.4	0.2
1,668	0.7	2.3	1,808	0.2	0.4
1,670	0.2	0.0	1,810	0.2	0.6
1,672	0.8	0.0	1,812	1.1	0.0
1,674	1.0	0.0	1,814	0.4	0.0
1,676	0.9	0.5	1,816	0.2	0.7
1,678	1.1	1.4	1,818	0.2	0.2
1,680	0.4	0.1	1,820	0.0	0.0
1,730	1.9	0.3	1,822	0.0	0.0
1,732	1.7	0.2	1,824	0.0	0.2
1,734	0.9	0.6	1,826	0.0	1.7
1,736	1.8	0.8	1,828	0.0	0.0
1,738	2.0	0.0	1,830	0.1	0.0
1,740	0.8	1.8	1,832	0.0	0.6
1,742	0.7	0.2	1,834	0.0	0.4
1,744	0.9	0.0	1,836	0.1	0.0
1,746	1.0	0.4	1,912	0.7	0.0
1,748	0.5	0.0	1,914	0.4	0.0
1,750	0.1	0.4	1,916	0.1	0.2
1,752	1.0	0.3	1,918	0.5	0.0
1,754	0.8	0.7	1,920	0.1	0.1
1,756	0.0	0.0	1,922	0.5	0.8
1,758	0.0	0.0	1,924	0.0	1.0
1,760	0.3	0.0	1,926	0.9	15.3
1,762	0.2	0.0	1,928	0.0	0.0
1,764	0.0	0.4	1,930	0.2	0.0
1,766	0.4	0.0	1,932	0.2	0.0
1,768	0.1	2.2	1,934	0.5	0.0
1,770	0.9	1.2	1,936	7.2	0.4
1,772	0.2	0.0	1,938	0.6	0.0
1,774	0.2	0.3	1,940	0.6	5.4
1,776	0.0	0.3	1,942	0.2	0.0
1,778	0.3	0.3	1,944	0.4	0.2
1,780	0.3	0.3	1,946	0.0	0.1
1,782	0.6	0.2	1,948	0.0	0.0
1,784	0.3	0.1	1,950	0.1	0.0

Organic Matter and Carbonate Content of North Core at North Ingenbright Lake

Depth (cm)	Organic Matter(%)	Carbonate Content(%)	Depth (cm)	Organic Matter(%)	Carbonate Content(%)
1,786	1.0	0.3	1,952	0.0	0.1
1,788	0.4	0.3	1,954	0.0	0.4
1,790	0.0	0.3	1,956	1.5	0.0
1,792	0.3	2.0	1,958	0.0	1.5
1,794	0.0	0.4	1,960	0.3	0.0
1,796	1.9	0.7	1,962	0.2	0.0
1,964	0.3	0.2	2,058	0.0	0.0
1,966	1.4	0.4	2,060	0.0	0.0
1,968	0.9	1.3	2,062	0.0	0.3
1,970	0.7	0.0	2,064	0.0	11.5
1,972	0.4	0.2	2,066	0.0	0.0
1,974	0.5	0.6	2,068	0.0	0.0
1,976	0.5	0.0	2,070	0.0	0.0
1,978	0.6	0.5	2,072	0.0	0.2
1,980	0.4	0.2	2,074	0.0	0.7
1,982	0.7	0.0	2,076	0.0	0.1
1,984	0.6	0.0	2,078	1.4	5.2
1,986	0.5	0.4	2,080	0.0	0.2
1,988	0.6	0.0	2,082	0.0	0.4
1,990	0.4	0.4	2,084	0.0	2.2
1,992	0.6	0.8	2,086	0.0	0.1
1,994	0.7	0.0	2,088	0.0	0.3
1,996	0.7	0.0	2,090	0.0	0.5
1,998	0.0	0.9	2,092	1.1	0.0
2,000	0.3	0.2	2,094	0.0	0.0
2,002	0.0	0.3	2,096	0.1	0.0
2,004	0.0	0.3	2,098	0.0	0.1
2,006	0.0	0.4	2,100	0.0	0.0
2,008	0.0	0.3	2,102	9.2	0.0
2,010	0.1	0.7	2,104	0.0	0.0
2,012	0.1	0.2	2,106	0.0	0.0
2,014	0.4	0.2	2,108	2.8	23.4
2,016	0.3	0.3	2,110	0.1	0.2
2,018	0.2	0.5	2,112	0.3	0.0
2,020	0.0	0.6	2,114	0.5	0.0
2,022	0.0	0.6	2,116	0.1	0.1
2,024	0.1	0.8	2,118	0.1	0.0
2,026	0.0	0.5	2,120	0.2	1.4
2,028	0.0	0.5	2,122	0.2	0.0
2,030	0.1	0.6	2,124	0.0	0.5
2,032	0.4	0.7	2,126	0.0	0.0
2,034	0.1	0.4	2,128	0.2	0.0
2,036	0.1	0.5	2,130	0.3	0.8
2,038	0.1	0.3	2,132	0.1	0.0
2,040	0.0	0.8	2,134	0.2	0.1
2,042	0.1	0.0	2,136	0.1	0.0
2,044	0.0	0.0	2,138	0.2	0.0
2,048	0.0	0.0	2,140	0.2	0.0
2,050	0.0	0.0	2,142	0.1	0.0
2,052	0.0	0.0	2,144	0.2	0.4
2,054	0.0	0.0	2,146	0.0	20.6

Organic Matter and Carbonate Content of North Core at North Ingenbright Lake

Depth (cm)	Organic Matter(%)	Carbonate Content(%)	Depth (cm)	Organic Matter(%)	Carbonate Content(%)
2,056	0.0	0.0	2,148	0.2	0.5
2,150	0.2	0.0	2,242	0.2	0.0
2,152	0.2	0.4	2,244	0.1	8.6
2,154	0.2	0.2	2,246	0.0	0.0
2,156	0.0	0.7	2,248	0.1	0.0
2,158	0.2	0.2	2,250	0.1	0.3
2,160	1.1	0.0	2,252	0.0	0.0
2,162	0.2	1.1	2,254	0.5	0.0
2,164	0.9	0.4	2,256	0.0	0.0
2,166	0.4	0.4	2,258	0.1	0.0
2,168	0.7	0.0	2,260	0.4	0.0
2,170	0.2	0.3	2,262	0.3	0.0
2,172	0.5	0.3	2,264	0.5	0.0
2,174	0.4	0.9	2,266	0.3	0.6
2,176	0.3	0.1	2,268	0.1	0.4
2,178	0.3	0.0	2,270	1.1	0.1
2,180	0.2	0.5	2,272	0.3	0.0
2,182	0.4	0.9	2,274	0.3	0.2
2,184	0.6	0.0	2,276	0.6	0.0
2,186	0.6	0.5	2,278	2.7	0.4
2,188	0.4	0.2	2,280	1.2	0.0
2,190	1.4	0.1	2,282	0.2	0.0
2,192	0.3	0.1	2,284	0.3	0.3
2,194	0.5	0.1	2,286	0.2	0.1
2,196	0.0	0.0	2,288	0.6	0.0
2,198	0.1	0.4	2,290	0.0	0.2
2,200	0.0	0.0	2,292	0.2	0.0
2,202	0.0	0.0	2,294	0.0	0.2
2,204	0.0	0.0			
2,206	0.0	0.0			
2,208	0.0	0.2			
2,210	0.0	0.0			
2,212	0.0	0.0			
2,214	0.0	0.0			
2,216	0.0	0.0			
2,218	0.2	0.0			
2,220	0.0	0.0			
2,222	0.0	0.0			
2,224	1.1	0.1			
2,226	0.6	0.2			
2,228	0.0	0.3			
2,230	0.0	0.0			
2,232	0.0	0.0			
2,234	0.0	0.0			
2,236	0.1	0.0			
2,238	0.2	0.2			
2,240	0.0	0.1			

Organic Matter and Carbonate Content of South Core at North Ingenbright Lake

Depth (cm)	Organic Matter(%)	Carbonate Content(%)	Depth (cm)	Organic Matter(%)	Carbonate Content(%)
16	2.9	11.8	108	0.3	0.5
18	7.6	9.4	110	0.0	0.4
20	11.3	5.5	112	0.3	0.4
22	4.8	14.0	114	0.1	0.5
24	7.6	6.2	116	0.1	0.3
26	8.7	5.3	118	0.4	0.3
28	11.7	3.7	120	0.3	0.7
30	14.6	7.6	122	0.4	2.1
32	12.3	5.1	124	0.4	0.2
34	11.5	6.1	126	0.7	0.2
36	3.1	12.6	128	0.5	0.5
38	11.6	8.2	130	0.4	0.3
40	12.3	7.0	132	0.3	0.3
42	7.4	7.9	134	0.4	0.1
44	10.5	5.4	136	0.0	0.2
46	8.5	5.3	138	0.3	1.0
48	11.3	3.5	140	0.3	0.6
50	0.5	1.2	142	0.2	0.8
52	1.7	1.0	144	0.7	0.8
54	0.3	5.1	146	0.7	0.2
56	1.1	0.1	148	0.2	0.6
58	0.5	0.5	150	0.3	0.1
60	0.1	2.3	152	0.0	0.2
62	0.0	0.0	154	0.2	0.2
64	0.0	0.0	156	0.0	0.8
66	0.0	0.0	158	0.4	0.4
68	0.1	0.0	160	0.0	0.0
70	0.1	0.5	162	0.0	0.0
72	0.0	0.3	164	0.0	0.0
74	0.0	0.3	166	0.0	0.0
76	0.0	0.2	168	0.1	0.1
78	0.0	0.0	170	0.0	0.0
80	0.0	0.1	172	0.0	0.0
82	3.6	8.2	174	0.4	0.0
84	0.0	0.0	176	0.0	0.0
86	0.3	0.0	178	0.1	0.3
88	0.0	0.2	180	0.0	0.0
90	0.0	0.3	182	0.0	0.2
92	0.2	0.4	184	0.8	0.8
94	0.2	0.3	186	0.0	0.0
96	0.1	0.0	188	0.2	0.9
98	0.2	8.1	190	0.0	0.0
100	0.4	0.0	192	0.0	0.0
102	0.2	0.7	194	0.3	0.0
104	0.4	0.0	196	0.2	0.0
106	1.0	0.0	198	0.0	1.0
200	0.3	0.0	292	2.9	0.9
202	0.2	0.1	294	3.2	1.6
204	0.5	0.9	296	2.5	0.9
206	0.7	0.6	298	2.0	0.0
208	0.0	3.0	300	1.7	1.5

Organic Matter and Carbonate Content of South Core at North Ingenbright Lake

Depth (cm)	Organic Matter(%)	Carbonate Content(%)	Depth (cm)	Organic Matter(%)	Carbonate Content(%)
210	0.6	0.0	302	1.9	0.4
212	1.4	0.0	304	1.6	1.6
214	1.6	0.0	306	3.0	0.7
216	0.9	5.7	308	2.3	1.3
218	0.8	0.0	310	0.8	1.6
220	0.8	0.1	312	0.8	0.6
222	1.0	0.6	314	1.0	0.5
224	1.0	0.1	316	0.7	0.4
226	0.6	0.2	318	1.4	1.0
228	1.2	0.2	320	1.5	1.8
230	0.7	0.5	322	0.4	2.1
232	1.3	0.0	324	0.8	0.9
234	1.8	0.0	326	2.0	0.3
236	0.5	0.6	328	1.9	2.8
238	0.2	0.2	330	0.9	1.1
240	0.7	0.0	332	1.2	0.7
242	1.1	0.0	334	1.1	0.8
244	0.9	0.6	336	0.0	1.2
246	1.4	0.0	338	1.2	0.7
248	1.0	10.8	340	0.5	0.7
250	1.8	0.0	348	1.0	0.8
252	1.3	0.0	350	0.0	0.0
254	1.2	1.2	352	0.1	0.8
256	2.8	0.0	354	1.4	0.4
258	0.9	0.0	356	0.0	0.6
260	0.6	1.2	358	0.2	0.8
262	1.4	2.4	360	2.0	0.6
264	0.6	1.5	362	0.9	0.4
266	0.1	1.5	364	1.1	0.7
268	0.5	1.0	366	1.4	0.4
270	0.9	2.0	368	1.8	0.4
272	1.3	0.8	370	2.3	0.1
274	1.4	2.7	372	0.8	0.3
276	1.5	0.6	374	0.7	0.5
278	2.0	1.1	376	1.0	0.2
280	2.0	1.6	378	1.7	0.1
282	3.2	1.7	380	1.4	0.8
284	2.9	0.5	382	1.5	0.0
286	2.0	1.1	384	2.3	0.0
288	1.9	1.5	386	1.1	0.6
290	2.3	2.1	388	1.4	0.4
390	2.0	1.1	566	3.7	2.3
392	2.3	3.3	568	2.7	1.6
394	3.2	1.3	570	3.8	0.0
396	3.4	1.3	572	3.0	3.4
398	1.7	0.6	574	3.2	3.8
400	2.7	0.0	576	2.9	0.3
402	3.2	0.6	578	3.5	2.6
404	3.3	0.4	580	3.6	1.4
406	1.7	0.8	582	3.5	0.3
408	4.1	1.9	584	4.0	0.1

Organic Matter and Carbonate Content of South Core at North Ingenbright Lake

Depth (cm)	Organic Matter(%)	Carbonate Content(%)	Depth (cm)	Organic Matter(%)	Carbonate Content(%)
410	2.2	1.4	586	4.1	0.0
412	2.6	0.2	588	3.9	0.5
414	1.7	1.0	590	3.3	0.5
416	0.7	1.0	592	0.3	2.5
500	2.5	0.9	594	2.1	1.0
502	1.0	1.4	596	1.7	2.6
504	2.7	0.9	598	2.4	2.4
506	3.3	0.1	600	3.4	1.7
508	3.4	0.1	602	3.8	0.8
510	3.6	1.4	604	4.0	0.8
512	10.8	5.4	606	3.7	5.0
514	6.8	0.0	608	3.9	1.1
516	8.6	1.1	610	2.9	0.8
518	7.3	1.5	612	1.3	1.4
520	5.2	0.7	614	3.3	1.6
522	10.7	0.0	616	2.9	5.4
524	4.0	0.7	618	0.9	0.8
526	6.3	1.3	620	2.6	4.0
528	5.1	1.1	622	2.4	2.3
530	2.3	2.9	624	1.8	3.5
532	4.9	0.4	626	5.2	4.1
534	4.8	0.7	628	2.4	4.5
536	5.3	0.8	630	1.6	2.7
538	5.9	0.9	632	2.0	1.3
540	6.6	1.4	634	2.0	1.9
542	4.4	0.4	636	2.1	1.9
546	3.5	4.1	638	1.2	1.8
548	6.2	0.7	640	1.5	1.3
550	6.2	0.2	642	1.2	1.8
552	4.8	0.4	644	1.1	1.1
554	4.3	1.5	646	0.9	0.2
556	5.0	0.0	648	1.6	0.4
558	6.3	3.7	650	3.7	1.4
560	2.9	0.0	652	1.3	0.7
562	2.3	1.9	654	0.8	0.6
564	2.7	3.2	656	1.0	0.0
658	0.3	0.2	884	23.3	1.8
660	0.0	0.4	886	20.0	3.0
662	2.4	0.5	888	18.1	4.5
664	1.8	0.2	890	20.1	2.1
666	3.5	0.4	892	17.9	4.6
668	2.8	1.1	894	19.2	3.7
670	2.5	0.8	896	22.7	1.3
672	5.1	0.9	898	23.0	1.5
674	2.7	0.9	900	25.0	1.0
676	2.1	0.1	910	20.1	3.1
678	5.8	1.2			
680	3.8	0.4			
682	3.4	4.7			
684	3.7	0.7			
686	2.7	1.1			

Organic Matter and Carbonate Content of South Core at North Ingenbright Lake

Depth (cm)	Organic Matter(%)	Carbonate Content(%)	Depth (cm)	Organic Matter(%)	Carbonate Content(%)
824	2.2	0.5			
826	0.9	1.0			
828	0.4	2.1			
830	1.6	1.2			
832	0.8	1.4			
834	0.1	4.6			
836	1.8	1.0			
838	1.8	1.3			
840	2.3	1.4			
842	0.8	5.7			
844	3.3	4.0			
846	6.1	1.5			
848	1.2	1.2			
850	1.9	2.0			
852	1.3	0.9			
854	5.3	1.2			
856	1.3	2.2			
858	1.1	1.3			
860	1.1	0.9			
862	0.6	1.0			
864	1.6	2.7			
866	3.2	1.7			
868	5.2	2.2			
870	17.8	4.8			
872	18.5	4.1			
874	19.2	2.6			
876	16.7	3.7			
878	16.2	2.2			
880	17.8	2.8			
882	14.5	4.0			

Appendix B Bulk Mineralogical Data from XRD

Mineralogical Composition of North Core at North Ingebright Lake

Depth (cm)	Quartz	K Feldspar	Plag.	Total Clay Miner.	Calcite	High Mg Calcite	Aragonite	Proto Dolomite	Dolomite
12	23.5	10.5	5.3	0.0	0.0	0.0	0.0	40.0	0.0
14	73.3	16.0	0.0	0.0	0.0	0.0	0.0	10.7	0.0
16	30.2	0.0	6.6	0.0	0.0	4.0	0.0	0.0	39.0
18	10.1	4.3	0.0	0.0	0.0	0.0	0.0	16.0	0.0
20	12.3	0.0	0.0	53.0	0.0	1.6	0.0	25.4	0.0
22	27.4	0.0	4.8	6.6	0.0	0.0	0.0	33.1	0.0
24	26.6	10.0	4.5	0.0	0.0	0.0	0.0	42.1	0.0
26	9.3	3.3	2.1	27.4	0.0	1.0	0.0	0.0	14.8
28	11.9	3.7	2.0	26.5	0.0	0.0	0.0	17.1	0.0
30	22.4	9.9	4.4	0.0	0.0	0.0	0.0	51.1	0.0
32	28.5	0.0	4.5	0.0	0.0	0.0	0.0	0.0	41.8
34	25.4	12.6	0.0	0.0	0.0	8.3	0.0	37.5	0.0
36	18.6	5.9	0.0	39.3	0.0	0.0	0.0	18.5	0.0
38	26.6	6.9	0.0	0.0	0.0	0.0	0.0	31.9	0.0
40	14.9	4.5	3.1	0.0	0.0	0.0	0.0	23.3	0.0
42	5.1	2.1	0.9	14.1	0.0	0.0	0.0	6.6	0.0
44	24.1	0.0	4.1	0.0	0.0	0.0	0.0	39.5	0.0
46	19.0	6.0	0.0	0.0	0.0	1.3	0.0	14.6	0.0
48	21.8	0.0	5.0	0.0	0.0	0.0	0.0	30.2	0.0
50	6.9	0.0	0.0	0.0	0.0	0.0	0.0	8.5	0.0
52	4.7	0.0	0.0	17.7	0.0	0.0	0.0	9.8	0.0
54	3.7	0.0	0.0	0.0	0.0	0.0	0.0	3.2	0.0
56	4.7	0.0	0.0	0.0	0.0	0.0	0.0	3.9	0.0
58	3.2	0.0	0.0	0.0	0.0	0.0	0.0	4.9	0.0
60	5.7	0.0	0.0	0.0	0.0	0.0	0.0	4.7	0.0
62	3.9	0.0	0.0	0.0	0.0	0.0	0.0	5.6	0.0
64	3.1	0.0	0.0	0.0	0.0	0.0	0.0	0.0	0.0
66	4.9	0.0	0.0	0.0	0.0	0.0	0.0	5.0	0.0
68	3.9	0.0	0.0	0.0	0.0	0.0	0.0	5.6	0.0
70	4.6	0.0	0.0	0.0	0.0	0.0	0.0	3.7	0.0
72	2.6	0.0	0.0	0.0	0.0	0.0	0.0	3.4	0.0
74	5.3	0.0	0.0	0.0	0.0	0.0	0.0	3.4	0.0
76	3.0	0.0	0.0	0.0	0.0	0.0	0.0	4.0	0.0
78	2.8	0.0	0.0	0.0	0.0	0.0	0.0	3.5	0.0
80	4.2	0.0	0.0	0.0	0.0	0.0	0.0	3.6	0.0
82	1.4	0.0	0.0	0.0	0.0	0.9	0.0	3.4	0.0
84	3.9	0.0	0.0	0.0	0.0	0.0	0.0	3.2	0.0
86	1.9	0.0	0.0	0.0	0.0	0.0	0.0	2.5	0.0
88	5.7	0.0	1.5	0.0	0.0	0.0	0.0	0.0	0.0

Mineralogical Composition of North Core at North Ingebright Lake

Depth (cm)	Quartz	K Feldspar	Plag.	Total Clay Miner.	Calcite	High Mg Calcite	Aragonite	Proto Dolomite	Dolomite
90	2.9	0.0	0.0	0.0	0.0	0.0	0.0	2.1	3.6
92	1.2	0.0	0.0	0.0	0.0	0.0	0.0	0.0	1.9
94	2.1	0.0	0.0	0.0	0.0	0.0	0.0	0.0	3.6
96	5.5	0.0	0.0	0.0	0.0	0.0	0.0	3.2	0.0
98	2.2	0.0	0.0	0.0	0.0	0.0	0.0	2.7	0.0
100	2.1	0.0	0.0	0.0	0.0	0.0	0.0	2.5	0.0
106	4.5	0.0	0.0	0.0	0.0	0.0	0.0	0.0	2.9
108	0.8	0.0	1.6	0.0	0.0	0.0	0.0	0.0	0.0
110	2.8	0.0	1.9	0.0	0.0	0.0	0.0	0.0	0.0
112	0.5	0.0	0.0	0.0	0.0	0.0	0.0	0.0	0.0
114	0.5	0.0	0.0	0.0	0.0	0.0	0.0	0.0	1.4
116	1.4	0.0	0.0	0.0	0.0	0.0	0.0	1.9	0.0
118	0.5	0.0	0.0	0.0	0.0	0.0	0.0	0.0	0.0
120	0.6	0.0	0.0	0.0	0.0	0.0	0.0	0.0	0.0
122	0.0	0.0	0.0	0.0	0.0	0.0	0.0	0.0	0.0
124	0.6	0.0	11.0	0.0	0.0	0.0	0.0	0.0	88.4
126	0.9	0.0	0.0	0.0	0.0	0.0	0.0	0.0	0.0
128	2.3	0.0	0.0	0.0	0.0	0.0	0.0	0.0	0.0
130	0.9	0.0	0.0	0.0	0.0	0.0	0.0	1.3	0.0
132	1.2	0.0	0.0	0.0	0.0	0.0	0.0	0.0	0.0
134	2.2	0.0	0.0	0.0	0.0	0.0	0.0	2.4	0.0
136	0.7	0.0	0.0	0.0	0.0	0.0	0.0	0.0	0.0
138	1.3	0.0	0.0	0.0	0.0	0.0	0.0	2.7	0.0
140	1.6	0.0	0.0	0.0	0.0	0.0	0.0	3.6	0.0
142	2.1	0.0	0.0	0.0	0.0	0.0	0.0	3.3	0.0
144	0.0	0.0	0.0	0.0	0.0	0.0	0.0	0.0	0.0
146	12.3	3.4	3.4	0.0	0.0	0.0	0.0	8.6	0.0
148	4.5	4.1	2.0	0.0	0.0	0.0	0.0	8.9	0.0
150	7.3	0.0	2.3	0.0	0.0	0.0	0.0	12.5	0.0
152	5.9	0.0	0.0	19.2	0.0	1.3	0.0	8.8	0.0
154	1.1	0.0	0.0	0.0	0.0	0.0	0.0	2.8	0.0
156	0.7	0.0	0.0	0.0	0.0	0.0	0.0	0.0	0.0
158	0.9	0.0	0.0	0.0	0.0	0.0	0.0	0.0	0.0
160	1.4	3.0	0.0	0.0	0.0	0.0	0.0	0.0	0.0
162	0.6	0.0	0.0	0.0	0.0	0.0	0.0	0.0	0.0
164	1.4	0.0	0.0	0.0	0.0	0.0	0.0	0.0	0.0
166	1.6	0.0	0.0	0.0	0.0	0.0	0.0	0.0	0.0
168	0.0	0.0	0.0	0.0	0.0	0.0	0.0	0.0	0.0
170	1.9	1.5	0.0	0.0	0.0	0.0	0.0	0.9	0.0

Mineralogical Composition of North Core at North Ingebright Lake

Depth (cm)	Quartz	K Feldspar	Plag.	Total Clay Miner.	Calcite	High Mg Calcite	Aragonite	Proto Dolomite	Dolomite
172	1.9	0.0	0.0	0.0	0.0	0.0	0.0	0.0	0.0
174	0.0	0.0	0.0	0.0	0.0	0.0	0.0	0.0	0.0
176	0.5	0.0	0.0	0.0	0.0	1.2	0.0	0.0	0.0
178	1.1	0.0	0.0	0.0	0.0	0.0	0.0	1.5	0.0
180	1.7	0.0	0.0	0.0	0.0	0.0	0.0	1.7	1.9
182	2.7	0.0	1.3	0.0	0.0	0.0	0.0	1.2	0.0
184	1.0	0.0	0.0	0.0	0.0	0.0	0.0	0.0	0.0
188	1.7	0.0	0.0	0.0	0.0	0.0	0.0	0.0	0.0
190	1.7	0.0	0.0	0.0	0.0	0.0	0.0	2.1	0.0
192	3.1	0.0	2.3	24.8	0.0	0.0	0.0	0.0	0.0
194	1.6	0.0	0.0	0.0	0.0	0.0	0.0	1.9	2.2
196	3.5	2.7	1.3	0.0	0.0	0.0	0.0	1.5	0.0
198	3.0	2.8	0.0	0.0	0.0	0.0	0.0	0.0	0.0
200	2.4	0.0	0.0	18.8	0.0	0.0	0.0	2.5	0.0
202	2.8	2.7	0.0	0.0	0.0	0.0	0.0	0.0	3.0
204	2.8	2.7	0.0	0.0	0.0	0.0	0.0	2.0	0.0
206	2.9	0.0	0.0	16.8	0.0	0.0	0.0	2.0	0.0
208	5.1	0.0	1.7	23.5	0.0	0.0	0.0	1.5	1.7
210	3.8	0.0	0.0	0.0	0.0	2.3	0.0	2.8	0.0
212	2.7	0.0	0.0	0.0	0.0	0.0	0.0	0.0	1.8
214	2.9	0.0	0.0	24.9	0.0	0.0	0.0	2.0	0.0
216	5.1	0.0	0.0	0.0	0.0	0.0	0.0	2.0	0.0
218	3.4	0.0	0.0	29.9	0.0	0.0	0.0	2.1	0.0
220	2.8	0.0	0.0	0.0	0.0	0.0	0.0	2.2	0.0
222	3.7	0.0	1.3	21.4	0.0	0.0	0.0	1.9	2.8
224	5.6	0.0	4.5	21.8	0.0	0.0	0.0	1.8	2.5
226	6.5	0.0	0.0	0.0	0.0	0.0	0.0	2.6	2.6
228	4.9	3.3	1.6	0.0	0.0	0.0	0.0	3.7	0.0
230	4.5	0.0	0.0	0.0	0.0	0.0	0.0	2.2	4.3
232	2.2	0.0	1.1	18.0	0.0	0.0	8.0	0.6	0.0
234	4.0	0.0	0.0	19.9	0.0	0.0	0.0	1.7	1.8
236	4.5	0.0	0.0	23.2	0.0	0.0	0.0	2.8	0.0
238	5.1	0.0	0.0	0.0	0.0	0.0	0.0	0.0	2.5
240	3.4	2.1	0.0	14.0	0.0	0.0	0.0	0.0	2.1
242	9.0	0.0	1.6	0.0	2.0	0.0	0.0	2.1	2.2
244	4.3	0.0	0.0	0.0	0.0	1.5	0.0	2.1	3.8
246	6.7	1.6	0.0	19.2	0.0	1.6	0.0	0.0	2.6
248	4.7	0.0	0.0	24.8	0.0	2.3	0.0	0.0	2.1
250	4.6	0.0	1.0	0.0	0.0	1.9	0.0	2.8	2.6

Mineralogical Composition of North Core at North Ingebright Lake

Depth (cm)	Quartz	K Feldspar	Plag.	Total Clay Miner.	Calcite	High Mg Calcite	Aragonite	Proto Dolomite	Dolomite
252	4.6	0.0	1.0	0.0	0.0	1.9	0.0	2.2	2.5
254	6.3	0.0	1.7	30.8	0.0	1.8	0.0	1.7	2.9
256	3.7	0.0	0.0	16.7	0.0	0.8	0.0	2.8	4.8
258	4.5	0.0	2.0	20.6	0.0	1.3	0.0	2.3	2.4
260	4.3	0.0	0.0	24.8	0.0	1.5	0.0	2.7	3.2
262	4.5	2.3	0.0	32.3	0.0	1.1	0.0	2.2	2.2
264	6.1	0.0	0.0	28.1	0.0	1.1	0.0	3.3	3.2
266	3.9	0.0	0.0	23.4	0.0	0.0	0.0	2.2	1.9
268	5.5	3.5	0.0	24.7	0.0	0.0	0.0	1.9	2.6
270	6.2	2.6	1.1	31.7	0.0	0.0	0.0	2.7	2.5
272	3.9	2.5	0.0	18.0	0.0	1.5	0.0	2.2	2.9
274	7.3	0.0	1.5	0.0	0.0	2.2	0.0	3.0	3.0
276	4.1	2.9	9.9	27.0	0.0	0.0	0.0	2.1	2.6
278	10.2	0.0	0.0	24.1	0.0	1.7	0.0	0.0	2.7
280	4.4	0.0	1.2	3.2	0.0	2.0	0.0	2.3	2.6
282	6.4	0.0	1.6	30.6	0.0	2.4	0.0	2.8	2.9
284	2.6	1.9	0.9	18.5	0.0	1.1	0.0	1.4	3.0
286	5.4	0.0	0.0	0.0	0.0	2.2	0.0	0.0	0.0
288	69.7	0.0	0.0	0.0	0.0	30.3	0.0	0.0	0.0
290	2.3	0.0	1.1	0.0	0.0	0.0	0.0	0.0	1.8
292	1.8	0.0	0.0	0.0	0.0	1.5	0.0	1.7	1.7
294	2.0	0.0	1.6	0.0	0.0	0.0	0.0	0.0	2.9
296	2.1	0.0	0.0	0.0	0.0	2.0	0.0	6.3	0.0
298	1.6	0.0	0.0	0.0	0.0	1.2	0.0	0.0	0.0
300	2.2	0.0	0.0	25.6	0.0	1.5	0.0	1.6	2.9
302	3.1	0.0	0.0	0.0	0.0	1.9	0.0	1.7	0.0
304	2.3	0.0	0.0	0.0	0.0	0.0	0.0	1.6	0.0
306	1.4	0.0	0.0	0.0	0.0	0.9	0.0	0.0	0.0
308	1.0	0.0	0.0	0.0	0.0	0.0	0.0	0.0	0.0
310	1.3	0.0	0.0	22.0	0.0	1.0	0.0	0.0	0.0
312	0.9	0.0	0.0	0.0	0.0	0.0	0.0	2.0	0.0
314	1.2	0.0	0.0	0.0	0.0	0.0	0.0	0.0	0.0
316	0.7	0.0	0.0	9.6	0.0	0.0	0.0	0.0	0.0
318	1.2	0.0	0.0	0.0	0.0	0.0	0.0	0.0	1.3
320	0.9	0.0	0.0	0.0	0.0	0.0	0.0	0.0	0.0
322	1.8	0.0	0.0	19.9	0.0	0.0	0.0	1.4	1.1
324	1.9	4.6	0.0	0.0	0.0	0.0	0.0	0.0	0.0
326	0.6	0.0	4.1	0.0	0.0	0.0	0.0	0.0	0.0
328	0.8	0.0	0.0	0.0	0.0	0.0	0.0	1.7	0.0

Mineralogical Composition of North Core at North Ingebright Lake

Depth (cm)	Quartz	K Feldspar	Plag.	Total Clay Miner.	Calcite	High Mg Calcite	Aragonite	Proto Dolomite	Dolomite
330	1.1	0.0	0.0	0.0	0.0	0.0	0.0	0.0	0.0
332	0.7	0.0	0.0	0.0	0.0	0.0	0.0	1.3	0.0
334	0.5	0.0	0.0	0.0	0.0	0.0	0.0	0.8	0.0
336	1.0	0.0	0.0	0.0	0.0	0.0	0.0	1.2	0.0
338	0.9	0.0	0.0	0.0	0.0	0.0	0.0	1.1	0.0
340	1.5	0.0	0.0	0.0	0.0	0.0	0.0	1.8	0.0
342	0.9	0.0	0.0	14.9	0.0	0.0	0.0	0.0	1.4
344	0.6	0.0	11.2	0.0	0.0	0.0	0.0	0.0	0.0
346	0.8	0.0	0.0	0.0	0.0	0.0	0.0	1.2	0.0
348	0.8	0.0	0.0	0.0	0.0	0.0	0.0	0.0	0.0
350	0.6	0.0	1.4	0.0	0.0	0.0	0.0	0.0	0.0
352	1.1	0.0	0.0	0.0	0.0	0.0	0.0	0.0	0.0
354	1.4	0.0	0.0	0.0	0.0	0.0	0.0	0.0	0.0
356	1.0	0.0	0.0	0.0	0.0	0.0	0.0	1.9	0.0
358	1.6	0.0	0.0	0.0	0.0	0.0	0.0	0.0	0.0
360	2.3	0.0	15.2	0.0	0.0	0.0	0.0	0.0	1.8
362	1.4	0.0	0.0	0.0	0.0	0.0	0.0	1.8	0.0
364	11.3	0.0	1.8	0.0	0.0	0.0	0.0	1.0	0.0
368	1.3	0.0	0.0	0.0	0.0	0.0	0.0	0.0	2.1
370	0.8	0.0	0.0	0.0	0.0	0.0	0.0	1.5	0.0
372	1.0	0.0	0.0	0.0	0.0	0.0	1.0	1.3	0.0
374	0.6	0.0	0.0	19.8	0.0	0.0	0.0	0.0	0.0
376	1.7	0.0	0.0	0.0	0.0	0.0	0.0	0.0	0.0
378	4.8	0.0	0.0	0.0	0.0	0.0	0.0	0.0	1.3
380	0.8	0.0	9.4	0.0	0.0	0.0	0.0	1.2	0.0
382	1.2	0.0	0.0	0.0	0.0	0.0	0.0	0.0	0.0
384	1.4	0.0	0.0	0.0	0.0	0.0	0.0	1.6	0.0
386	0.9	0.0	0.0	0.0	0.0	0.0	0.0	0.0	0.0
388	0.6	0.0	0.0	0.0	0.0	0.0	0.0	0.0	0.0
390	1.1	0.0	0.0	0.0	0.0	0.0	0.0	0.0	0.0
392	0.8	0.0	0.0	0.0	0.0	0.0	0.0	0.0	0.0
394	0.7	0.0	0.0	0.0	0.0	0.0	0.0	0.0	0.0
396	1.0	0.0	10.8	0.0	0.0	0.0	0.0	0.0	0.0
398	0.6	0.0	9.0	0.0	0.0	0.0	0.0	0.0	0.0
400	1.2	0.0	8.2	0.0	0.0	0.0	0.0	0.0	0.0
402	1.5	0.0	0.0	0.0	0.0	0.0	0.0	1.4	0.0
404	0.6	0.0	0.0	0.0	0.0	0.0	0.0	0.0	0.0
406	0.8	0.0	0.0	0.0	0.0	0.0	0.0	0.0	0.0
408	0.7	0.0	0.0	0.0	0.0	0.0	0.0	0.0	0.0

Mineralogical Composition of North Core at North Ingebright Lake

Depth (cm)	Quartz	K Feldspar	Plag.	Total Clay Miner.	Calcite	High Mg Calcite	Aragonite	Proto Dolomite	Dolomite
410	0.6	0.0	0.0	0.0	0.0	0.0	0.0	0.0	0.0
412	0.4	0.0	0.0	0.0	0.0	0.0	0.0	0.0	0.0
414	0.0	0.0	15.2	0.0	0.0	0.0	0.0	0.0	0.0
416	0.7	0.0	0.0	0.0	0.0	0.0	0.0	0.0	0.0
418	1.0	0.0	0.0	0.0	0.0	0.0	0.0	0.0	0.0
420	0.8	0.0	0.0	0.0	0.0	0.0	0.0	0.0	0.0
122	0.4	0.0	1.2	0.0	0.0	0.0	0.0	0.0	0.0
424	0.0	0.0	0.0	0.0	0.0	0.0	0.0	0.0	0.0
426	0.4	0.0	0.0	0.0	0.0	0.0	0.0	0.0	0.0
428	5.2	0.0	10.4	0.0	0.0	0.0	0.0	0.0	0.0
430	0.6	0.0	8.0	0.0	0.0	0.0	0.0	0.0	0.0
432	0.6	0.0	11.1	0.0	0.0	0.0	0.0	0.0	0.0
434	0.0	0.0	0.0	0.0	0.0	0.0	0.0	0.0	0.0
436	0.7	0.0	9.9	0.0	0.0	0.0	0.0	0.0	0.0
438	0.3	0.0	6.8	0.0	0.0	0.0	0.0	0.0	0.0
440	0.6	0.0	9.5	0.0	0.0	0.0	0.0	0.0	1.0
442	2.4	0.0	15.1	0.0	0.0	0.0	0.0	0.0	0.0
444	0.5	0.0	12.0	0.0	0.0	0.0	0.0	0.0	0.0
446	0.4	0.0	9.6	0.0	0.0	0.0	0.0	0.9	0.0
448	1.9	0.0	9.3	0.0	0.0	0.0	0.0	0.0	0.0
450	0.6	0.0	0.0	0.0	0.0	0.0	0.0	0.0	0.0
452	0.5	0.0	10.5	0.0	0.0	0.0	0.0	0.0	0.0
454	0.3	0.0	9.4	0.0	0.0	0.0	0.0	0.0	0.0
456	0.6	0.0	14.0	0.0	0.0	0.0	0.0	0.0	0.0
458	0.5	0.0	8.6	0.0	0.0	0.0	0.0	0.0	0.0
460	2.3	0.0	1.1	0.0	0.0	0.0	0.0	2.2	23.9
462	2.5	0.0	0.0	5.0	0.0	1.7	0.0	0.0	0.0
464	3.6	0.0	0.0	0.0	0.0	0.0	0.0	1.3	0.0
466	0.9	0.0	0.0	0.0	0.0	0.0	0.0	0.0	5.8
468	0.5	0.0	0.0	0.0	0.0	0.0	0.0	0.0	0.0
470	1.3	0.0	0.0	0.0	0.0	0.0	0.0	0.0	0.0
472	1.9	2.4	0.0	0.0	0.0	0.0	0.0	1.9	1.9
474	1.6	0.0	0.0	20.9	0.0	0.0	0.0	1.6	1.9
476	1.2	0.0	3.8	13.3	0.0	0.0	0.0	1.0	2.2
478	3.3	0.0	1.0	18.8	0.0	0.0	0.0	1.9	0.0
480	1.1	0.0	1.1	17.4	0.0	0.0	0.0	0.0	1.4
482	1.9	0.0	0.0	0.0	0.0	0.0	0.0	0.0	0.0
484	3.0	0.0	0.0	0.0	0.0	0.0	0.0	2.9	0.0
486	1.6	0.0	0.0	0.0	0.0	0.0	0.0	2.6	0.0

Mineralogical Composition of North Core at North Ingebright Lake

Depth (cm)	Quartz	K Feldspar	Plag.	Total Clay Miner.	Calcite	High Mg Calcite	Aragonite	Proto Dolomite	Dolomite
488	2.2	0.0	0.0	0.0	0.0	0.0	0.0	1.5	0.0
490	2.4	2.7	0.0	0.0	0.0	0.0	0.0	0.0	0.0
492	1.7	0.0	0.0	0.0	0.0	0.0	0.0	0.0	0.0
494	2.0	0.0	0.0	0.0	0.0	0.0	0.0	1.4	1.4
496	1.4	0.0	0.0	0.0	0.0	0.0	0.0	0.0	0.0
498	0.8	0.0	0.0	0.0	0.0	0.0	0.0	0.0	0.0
500	2.2	0.0	1.9	0.0	0.0	1.7	0.0	0.0	0.0
502	1.5	0.0	0.0	0.0	0.0	0.0	0.0	0.0	0.0
504	1.4	0.0	0.0	0.0	0.0	0.0	0.0	0.0	0.0
506	1.4	0.0	2.1	0.0	0.0	0.0	0.0	2.1	0.0
508	2.3	0.0	0.0	0.0	0.0	0.0	0.0	1.6	0.0
510	1.0	0.0	0.0	0.0	0.0	0.0	0.0	2.3	0.0
512	1.9	0.0	0.0	31.9	0.0	0.0	0.0	2.5	2.6
514	3.0	0.0	0.0	0.0	0.0	0.0	0.0	3.9	0.0
516	1.9	0.0	0.0	31.9	0.0	0.0	0.0	2.5	2.6
518	1.9	0.0	2.4	34.0	0.0	0.0	0.0	2.4	0.0
520	4.5	0.0	0.0	22.6	0.0	0.0	0.0	2.6	0.0
522	1.9	0.0	0.0	0.0	0.0	0.0	0.0	2.5	0.0
526	1.1	0.0	0.0	0.0	0.0	0.0	0.0	0.0	0.0
528	2.3	1.5	0.0	0.0	0.0	0.0	0.0	0.0	0.0
532	5.2	0.0	6.3	0.0	0.0	0.0	0.0	0.0	0.0
534	1.9	2.5	0.0	0.0	0.0	0.0	0.0	0.0	2.4
536	1.7	1.6	0.0	26.0	0.0	0.0	0.0	2.3	0.0
538	1.1	6.5	0.0	0.0	0.0	0.0	1.4	0.0	0.0
540	1.1	0.0	0.0	0.0	0.0	0.0	0.0	0.0	0.0
542	1.7	0.0	0.0	0.0	0.0	0.0	0.0	2.6	0.0
544	1.3	0.0	0.0	24.5	0.0	0.0	1.3	2.1	0.0
546	0.9	0.0	0.0	0.0	0.0	0.0	0.0	0.0	0.0
548	0.6	0.0	0.0	0.0	0.0	0.0	0.0	0.0	0.0
550	1.9	0.0	0.0	27.3	0.0	0.0	2.1	2.4	0.0
552	1.1	0.0	0.0	0.0	0.0	0.0	0.0	1.8	2.2
554	1.0	0.0	0.0	20.8	0.0	0.0	0.0	0.0	0.0
556	1.7	0.0	0.0	37.3	0.0	0.0	0.0	2.6	0.0
558	2.9	0.0	0.0	0.0	0.0	0.0	0.0	0.0	0.0
560	3.9	0.0	0.0	0.0	0.0	0.0	0.0	4.4	0.0
564	0.9	0.0	27.4	22.3	0.0	0.0	0.0	1.7	0.0
566	0.8	0.0	31.7	14.6	0.0	0.0	0.0	0.8	0.0
568	0.9	0.0	29.8	0.0	0.0	0.0	0.0	1.4	0.0
570	1.0	0.0	30.0	14.7	0.0	0.0	0.0	0.0	0.0

Mineralogical Composition of North Core at North Ingebright Lake

Depth (cm)	Quartz	K Feldspar	Plag.	Total Clay Miner.	Calcite	High Mg Calcite	Aragonite	Proto Dolomite	Dolomite
572	0.6	0.0	30.0	14.9	0.0	0.0	0.0	1.5	0.0
574	1.0	0.0	27.5	19.1	0.0	0.0	0.0	1.8	0.0
576	0.8	0.0	35.7	0.0	0.0	0.0	0.0	0.0	0.0
578	0.6	0.0	33.9	12.3	0.0	0.0	0.0	0.8	0.0
580	1.2	1.7	32.0	0.0	0.0	0.0	0.0	1.0	0.0
582	0.6	0.0	36.8	0.0	0.0	0.0	0.0	1.2	0.0
584	1.7	0.0	35.9	0.0	0.0	0.0	0.0	1.5	0.0
586	0.6	0.0	45.3	0.0	0.0	0.0	0.0	0.0	0.0
588	0.5	0.0	46.4	0.0	0.0	0.0	0.0	1.2	0.0
590	0.9	0.0	42.4	0.0	0.0	0.0	0.0	0.0	0.0
592	0.6	0.0	30.2	0.0	0.0	0.0	0.0	0.0	0.0
594	0.6	37.7	0.0	0.0	0.0	0.0	0.0	0.0	0.0
596	2.6	0.0	40.1	0.0	0.0	0.0	0.0	0.0	0.0
598	2.4	2.6	17.2	27.6	0.0	0.0	0.0	3.1	2.1
600	1.0	0.0	22.1	0.0	0.0	0.0	0.0	2.2	0.0
602	1.1	2.1	20.7	24.7	0.0	0.0	0.0	2.0	1.8
604	1.5	0.0	15.4	41.2	0.0	0.0	0.0	3.0	2.2
606	1.3	2.1	33.8	0.0	0.0	0.0	0.0	1.2	1.4
608	1.1	2.0	29.0	0.0	0.0	0.0	0.0	2.1	1.7
616	0.8	0.0	34.8	0.0	0.0	0.0	0.0	0.0	0.0
618	0.9	1.6	36.1	0.0	0.0	0.0	0.0	0.0	0.0
620	0.7	0.0	33.2	0.0	0.0	0.0	0.0	0.9	0.0
622	1.0	0.0	35.9	0.0	0.0	0.0	0.0	0.0	0.0
624	0.5	0.0	28.5	14.0	0.0	0.0	0.0	1.1	0.0
626	1.3	0.0	28.8	16.9	0.0	0.0	0.0	0.0	0.0
628	1.0	0.0	26.2	0.0	0.0	0.0	0.0	2.1	7.0
630	1.1	0.0	30.9	0.0	0.0	0.0	0.0	2.1	2.2
634	2.6	0.0	30.5	0.0	0.0	0.0	0.0	4.2	0.0
636	0.5	0.0	84.8	0.0	0.0	0.0	0.0	0.6	0.0
638	2.6	0.0	34.2	0.0	0.0	0.0	0.0	1.0	0.0
640	0.7	0.0	40.1	0.0	0.0	0.0	0.0	0.0	1.5
642	0.8	0.0	28.6	18.0	0.0	0.0	0.0	1.3	1.5
644	0.9	0.0	42.2	0.0	0.0	0.0	0.0	0.0	0.0
646	1.4	0.0	28.8	0.0	0.0	0.0	0.0	1.8	0.0
648	1.2	0.0	37.7	0.0	0.0	0.0	0.0	1.6	0.0
650	0.4	0.0	41.4	0.0	0.0	0.0	0.0	0.0	0.0
652	0.9	0.0	25.0	15.2	0.0	0.0	0.0	1.5	1.0
654	1.3	0.0	34.3	0.0	0.0	0.0	0.0	1.2	0.0
656	0.5	0.0	37.0	0.0	0.0	0.0	0.0	0.0	0.0

Mineralogical Composition of North Core at North Ingebright Lake

Depth (cm)	Quartz	K Feldspar	Plag.	Total Clay Miner.	Calcite	High Mg Calcite	Aragonite	Proto Dolomite	Dolomite
658	0.8	0.0	33.0	0.0	0.0	0.0	0.0	1.1	0.0
660	5.3	0.0	0.0	0.0	0.0	0.0	0.0	2.1	0.0
662	1.0	0.0	34.2	0.0	8.6	0.0	0.0	1.1	0.9
664	0.6	0.0	36.5	0.0	0.0	0.0	0.0	0.0	0.0
666	1.2	0.0	34.5	0.0	0.0	0.0	0.0	0.0	0.0
668	0.8	0.0	35.4	0.0	0.0	0.0	0.0	0.0	0.0
670	0.6	0.0	35.6	0.0	0.0	0.0	0.0	1.2	0.0
672	0.7	0.0	38.8	0.0	0.0	0.0	0.0	0.9	0.0
674	1.4	0.0	41.9	0.0	0.0	0.0	1.4	0.0	0.0
676	0.5	0.0	26.2	11.9	0.0	0.0	0.0	2.1	0.0
678	1.0	0.0	32.8	0.0	0.0	0.0	0.0	1.0	1.1
680	2.0	0.0	0.0	0.0	0.0	0.0	0.0	1.7	0.0
682	0.8	0.0	1.7	0.0	0.0	0.0	0.0	1.2	0.0
684	1.1	0.0	1.3	0.0	0.0	0.0	0.0	0.0	0.0
686	4.5	0.0	0.0	0.0	0.0	0.0	2.0	0.0	0.0
688	1.3	0.0	0.0	0.0	0.0	0.0	0.0	0.0	0.0
690	1.1	0.0	0.0	0.0	0.0	0.0	0.0	0.0	0.0
692	3.3	0.0	0.0	0.0	0.0	0.0	0.0	0.0	0.0
694	1.2	0.0	0.0	0.0	0.0	0.0	0.0	1.6	0.0
696	1.0	0.0	0.0	0.0	1.9	0.0	0.0	0.0	0.0
698	1.3	0.0	0.0	0.0	0.0	0.0	0.0	1.5	0.0
700	8.0	0.0	0.0	0.0	0.0	0.0	0.0	0.0	0.0
702	0.0	0.0	0.0	0.0	0.0	0.0	0.0	100.0	0.0
704	1.4	0.0	0.0	24.1	0.0	0.0	0.0	1.8	0.0
706	1.0	0.0	1.4	0.0	0.0	0.0	0.0	0.0	0.0
708	0.9	0.0	0.0	0.0	0.0	0.0	1.2	1.3	0.0
710	0.7	0.0	0.0	0.0	0.0	0.0	0.0	0.0	0.0
714	0.8	0.0	0.0	0.0	0.0	0.0	0.0	0.0	0.0
716	1.3	0.0	0.0	0.0	0.0	0.0	0.0	0.0	0.0
718	1.6	0.0	0.0	0.0	0.0	0.0	0.0	1.3	0.0
720	1.1	0.0	0.0	0.0	0.0	0.0	0.0	0.0	0.0
722	1.6	0.0	0.0	0.0	0.0	0.0	0.0	0.0	1.7
724	1.9	0.0	0.0	22.1	0.0	0.0	0.0	1.6	0.0
728	1.9	0.0	0.0	0.0	0.0	0.0	0.0	0.0	4.8
730	1.6	0.0	0.0	19.6	0.0	0.0	0.0	2.1	0.0
732	1.9	0.0	0.0	25.9	0.0	0.0	0.0	2.2	0.0
734	1.0	0.0	0.0	23.4	0.0	0.0	0.0	1.4	0.0
736	2.1	0.0	0.0	0.0	0.0	0.0	0.0	0.0	2.7
738	3.5	0.0	0.0	0.0	0.0	0.0	0.0	2.6	0.0

Mineralogical Composition of North Core at North Ingebright Lake

Depth (cm)	Quartz	K Feldspar	Plag.	Total Clay Miner.	Calcite	High Mg Calcite	Aragonite	Proto Dolomite	Dolomite
740	2.2	0.0	0.0	0.0	0.0	0.0	0.0	0.0	0.0
746	2.6	0.0	0.0	20.3	0.0	0.0	1.4	1.4	0.0
748	1.0	0.0	0.0	0.0	0.0	0.0	0.0	1.1	1.2
750	3.0	0.0	0.0	24.9	0.0	0.0	0.0	1.6	0.0
752	4.5	0.0	0.0	16.3	0.0	1.0	0.0	1.5	1.3
754	2.3	0.0	0.0	21.5	0.0	0.0	0.0	2.1	1.9
756	2.6	0.0	0.0	0.0	0.0	0.0	0.0	2.7	0.0
758	1.3	0.0	0.0	19.0	0.0	0.0	0.0	1.6	1.1
760	1.5	0.0	0.0	0.0	0.0	0.0	0.0	1.9	0.0
762	1.2	0.0	0.0	15.2	0.0	0.0	1.1	1.2	0.0
764	4.3	0.0	0.0	0.0	0.0	0.0	1.2	0.0	0.0
792	1.0	0.0	0.0	0.0	0.0	0.0	0.0	1.8	0.0
794	0.9	0.0	0.0	20.6	0.0	0.0	0.0	0.0	0.0
796	0.7	0.0	0.0	15.3	0.0	0.0	0.0	1.9	0.0
798	0.0	0.0	0.0	0.0	0.0	0.0	0.0	0.0	0.0
800	0.8	0.0	0.0	18.1	0.0	0.0	1.2	1.8	1.8
802	0.6	0.0	0.0	0.0	0.0	0.0	0.0	1.4	0.0
804	0.6	0.0	0.0	0.0	0.0	0.0	0.0	0.0	1.5
806	0.6	0.0	0.0	0.0	0.0	0.0	0.0	0.0	0.0
808	2.3	0.0	0.0	21.9	0.0	0.0	1.6	1.9	1.6
810	1.4	0.0	0.0	0.0	0.0	0.0	0.0	2.0	0.0
812	1.8	0.0	0.0	25.2	0.0	0.0	0.0	2.0	0.0
814	0.7	0.0	0.0	18.0	0.0	0.0	0.0	0.0	1.2
816	2.7	0.0	0.0	17.3	0.0	0.0	1.5	0.0	1.4
818	1.9	0.0	0.0	0.0	0.0	0.0	0.0	2.3	0.0
820	1.1	0.0	0.0	22.8	0.0	0.0	0.0	1.6	0.0
822	2.5	0.0	0.0	0.0	0.0	0.0	0.0	2.8	0.0
824	1.8	0.0	0.0	17.4	0.0	0.0	1.7	1.6	0.0
826	2.0	0.0	0.0	23.5	0.0	0.0	0.0	1.6	2.2
828	2.1	0.0	0.0	27.3	0.0	0.0	0.0	2.3	0.0
830	3.7	0.0	0.0	24.6	0.0	0.0	0.0	2.6	2.8
832	2.3	0.0	0.0	0.0	0.0	0.0	2.0	2.9	2.2
834	2.7	1.1	0.0	24.4	0.0	0.0	2.0	1.9	0.0
836	1.9	0.0	0.0	28.9	0.0	0.0	0.0	3.0	0.0
838	2.4	0.0	0.0	30.9	0.0	0.0	2.6	3.4	2.6
840	1.1	0.0	0.0	21.0	0.0	0.0	0.0	2.3	0.0
842	2.5	0.0	0.0	25.8	0.0	0.0	0.0	2.2	0.0
844	2.0	0.0	0.0	25.2	0.0	0.0	0.0	2.6	2.3
846	3.4	0.0	0.0	24.9	0.0	0.0	0.0	1.8	1.9

Mineralogical Composition of North Core at North Ingebright Lake

Depth (cm)	Quartz	K Feldspar	Plag.	Total Clay Miner.	Calcite	High Mg Calcite	Aragonite	Proto Dolomite	Dolomite
848	4.4	0.0	0.0	29.6	0.0	0.0	0.0	2.2	3.3
850	3.6	0.0	1.1	23.0	0.0	0.0	0.0	1.8	1.8
852	3.9	0.0	4.0	0.0	0.0	0.0	0.0	2.7	0.0
856	2.8	0.0	0.0	0.0	0.0	0.0	0.0	2.5	0.0
860	1.4	0.0	0.0	18.5	0.0	0.0	0.0	1.8	1.8
862	2.1	0.0	0.0	21.8	0.0	0.0	0.0	1.5	2.1
864	2.9	0.0	1.4	18.1	0.0	0.0	0.0	1.8	1.6
866	0.6	0.0	0.0	60.4	0.0	0.0	0.0	0.8	0.0
868	3.0	0.0	0.0	29.6	0.0	0.0	0.0	1.7	1.9
870	0.8	0.0	0.0	14.6	0.0	0.0	0.0	1.3	1.3
872	1.9	0.0	0.0	0.0	0.0	0.0	0.0	2.1	2.3
874	1.1	0.0	0.0	14.6	0.0	0.0	0.0	1.2	0.0
876	2.4	2.4	0.0	22.9	0.0	0.0	0.0	1.9	2.4
878	1.5	0.0	0.0	25.0	0.0	0.0	0.0	1.7	0.0
880	1.1	0.0	0.0	0.0	0.0	0.0	0.0	1.9	0.0
882	0.9	0.0	0.0	17.0	0.0	0.0	0.0	0.9	1.6
884	1.9	0.0	0.0	0.0	0.0	0.0	0.0	2.2	0.0
886	1.7	0.0	0.0	22.3	0.0	0.0	0.0	1.5	2.1
888	1.7	0.0	0.0	21.3	0.0	0.0	0.0	1.9	0.0
890	0.5	0.0	0.0	0.0	0.0	0.0	0.0	0.7	0.0
892	1.0	0.0	0.0	16.6	0.0	0.0	0.0	1.2	0.0
894	1.1	0.0	0.0	20.6	0.0	0.0	0.0	1.6	1.1
896	1.1	0.0	0.0	0.0	0.0	0.0	0.0	0.0	0.0
898	1.0	0.0	0.0	12.7	0.0	0.0	0.0	1.0	1.3
900	0.8	0.0	0.0	20.7	0.0	0.0	0.0	1.3	1.8
902	2.0	0.0	0.0	21.2	0.0	0.0	0.0	1.6	1.3
904	1.1	0.0	0.8	17.6	0.0	0.0	0.0	1.1	1.2
906	1.5	0.0	3.4	0.0	0.0	0.0	0.0	1.5	1.5
908	1.2	0.0	0.0	0.0	0.0	0.0	0.0	1.9	0.0
910	1.2	0.0	0.0	14.3	0.0	0.0	0.0	1.4	0.0
912	2.2	0.0	0.0	19.3	0.0	0.0	0.0	1.4	0.0
914	4.3	0.0	0.0	40.2	0.0	0.0	0.0	3.1	1.9
916	3.5	0.0	1.2	33.8	0.0	0.0	0.0	2.4	2.1
918	4.0	0.0	0.0	38.2	0.0	0.0	0.0	2.4	2.7
920	0.5	0.0	0.0	20.6	0.0	0.0	1.1	0.0	0.0
924	0.6	0.0	0.0	24.9	0.0	0.0	0.0	1.8	0.0
926	0.9	0.0	0.0	0.0	0.0	0.0	2.1	2.4	0.0
928	2.2	0.0	0.0	21.5	0.0	0.0	0.0	1.5	0.0
930	0.6	0.0	0.0	19.8	0.0	0.0	0.0	1.9	0.0

Mineralogical Composition of North Core at North Ingebright Lake

Depth (cm)	Quartz	K Feldspar	Plag.	Total Clay Miner.	Calcite	High Mg Calcite	Aragonite	Proto Dolomite	Dolomite
932	0.6	0.0	0.0	21.6	0.0	0.0	0.0	1.8	0.0
934	0.7	0.0	0.0	20.6	0.0	0.0	0.0	1.8	0.0
936	1.1	0.0	0.0	22.4	0.0	0.0	0.0	1.9	0.0
938	0.5	0.0	0.0	17.4	0.0	0.0	0.0	1.9	0.0
940	0.8	0.0	0.0	18.0	0.0	0.0	0.0	1.6	0.0
942	1.7	0.0	0.0	21.6	0.0	0.0	0.0	2.8	0.0
944	0.7	0.0	0.0	0.0	0.0	0.0	0.0	2.4	0.0
946	0.6	0.0	0.0	21.0	0.0	0.0	0.0	1.7	0.0
948	0.9	0.0	0.0	0.0	0.0	0.0	0.0	3.6	0.0
950	2.0	0.0	0.0	0.0	0.0	0.0	1.6	0.0	0.0
952	0.9	0.0	0.0	22.3	0.0	0.0	0.0	2.0	0.0
954	1.3	0.0	0.0	22.2	0.0	0.0	0.0	1.6	0.0
956	0.8	0.0	0.0	20.5	0.0	0.0	0.0	1.3	0.0
958	0.7	0.0	0.0	25.7	0.0	0.0	0.0	1.4	0.0
960	1.3	0.0	2.1	0.0	0.0	0.0	0.0	1.8	0.0
962	0.8	0.0	0.0	0.0	0.0	0.0	0.0	0.0	0.0
964	0.3	0.0	0.0	51.4	0.0	0.0	0.0	0.0	0.3
972	0.8	0.0	0.0	16.1	0.0	0.0	0.0	1.4	0.0
974	1.0	0.0	0.0	11.8	0.0	0.0	0.0	0.0	0.0
976	1.7	0.0	0.0	20.0	0.0	0.0	0.0	1.6	0.0
978	1.0	0.0	0.0	21.2	0.0	0.0	1.1	1.7	0.0
980	0.7	0.0	0.0	0.0	0.0	0.0	0.0	1.1	1.4
982	0.7	0.0	0.0	16.8	0.0	0.0	0.0	1.5	0.0
984	1.0	0.0	0.0	22.3	0.0	0.0	0.0	0.0	0.0
986	1.2	0.0	0.0	20.2	0.0	0.0	0.0	1.6	1.9
988	0.7	0.0	0.0	0.0	0.0	0.0	0.0	1.8	0.0
990	0.6	0.0	0.0	15.3	0.0	0.0	0.0	2.9	0.0
992	0.4	0.0	0.0	14.0	0.0	0.0	0.0	1.5	0.0
994	1.0	0.0	0.0	19.8	0.0	1.0	0.0	2.0	1.7
996	0.5	0.0	0.0	20.1	0.0	0.0	0.0	1.7	1.5
998	0.8	0.0	0.0	16.1	0.0	0.0	0.0	1.4	2.0
1,000	1.1	0.0	0.0	30.3	0.0	0.0	0.0	3.5	3.3
1,002	0.6	0.0	0.0	23.3	0.0	0.0	0.0	1.5	0.0
1,004	0.6	0.0	0.0	20.1	0.0	0.0	0.0	1.8	0.0
1,006	1.9	0.0	0.0	0.0	0.0	2.5	0.0	0.0	1.8
1,008	0.6	0.0	0.0	20.5	0.0	0.0	0.0	0.0	0.0
1,010	3.7	0.0	0.0	0.0	0.0	0.0	0.0	2.5	0.0
1,012	1.2	0.0	0.0	0.0	0.0	0.0	0.0	0.0	0.0
1,014	1.8	0.0	0.0	22.5	0.0	0.0	0.0	2.2	0.0

Mineralogical Composition of North Core at North Ingebright Lake

Depth (cm)	Quartz	K Feldspar	Plag.	Total Clay Miner.	Calcite	High Mg Calcite	Aragonite	Proto Dolomite	Dolomite
1,016	4.5	0.0	0.0	29.0	0.0	0.0	0.0	1.9	0.0
1,018	1.7	0.0	0.0	25.8	0.0	0.0	0.0	2.2	0.0
1,020	0.8	0.0	0.0	21.6	0.0	0.0	0.0	1.5	1.3
1,022	1.0	0.0	0.0	17.9	0.0	0.0	0.0	1.7	1.1
1,024	1.3	0.0	0.0	20.3	0.0	0.0	0.0	1.5	1.4
1,026	0.7	0.0	0.0	22.6	0.0	0.0	0.0	1.6	0.0
1,028	0.5	0.0	0.0	19.1	0.0	0.0	1.3	1.4	0.0
1,030	0.5	0.0	0.0	22.2	0.0	0.0	1.5	1.8	1.2
1,032	0.5	0.0	0.0	7.4	0.0	0.0	0.0	0.0	0.5
1,034	0.9	6.5	0.0	17.7	0.0	0.0	0.0	1.4	0.0
1,036	0.4	0.0	0.0	0.0	0.0	0.0	0.0	1.3	0.0
1,038	0.7	0.0	0.0	0.0	0.0	0.0	0.0	0.0	0.0
1,040	0.0	0.0	0.0	0.0	0.0	0.0	0.0	0.0	0.0
1,042	1.3	0.0	0.0	0.0	0.0	0.0	0.0	0.0	0.0
1,044	2.7	0.0	0.0	0.0	0.0	0.0	0.0	0.0	0.0
1,046	0.4	0.0	0.0	15.7	0.0	0.0	0.0	0.0	0.0
1,048	0.7	0.0	0.0	17.7	0.0	0.0	2.0	2.0	1.3
1,050	0.5	0.0	0.0	20.4	0.0	0.0	0.0	1.7	1.9
1,052	2.4	1.7	0.0	0.0	0.0	0.0	0.0	0.0	0.0
1,054	0.5	0.0	0.0	17.9	0.0	0.0	0.0	1.6	0.0
1,056	0.5	0.0	0.0	16.9	0.0	0.0	0.0	2.2	0.0
1,058	0.9	0.0	0.0	0.0	0.0	0.0	0.0	1.6	1.7
1,060	2.5	0.0	0.0	0.0	0.0	0.0	0.0	1.3	0.0
1,062	2.3	0.0	0.0	0.0	0.0	0.0	1.7	1.8	2.3
1,064	2.7	0.0	0.0	0.0	0.0	0.0	0.0	0.0	0.0
1,066	0.4	0.0	0.0	0.0	0.0	0.0	0.0	0.5	0.4
1,068	1.1	0.0	0.0	18.5	0.0	0.0	1.8	2.2	0.0
1,070	2.9	0.0	0.0	3.9	0.0	0.0	1.9	2.0	1.1
1,072	0.6	0.0	0.0	0.0	0.0	0.0	0.0	2.4	0.0
1,074	0.4	0.0	0.0	20.2	0.0	0.0	1.7	1.8	0.0
1,076	0.4	0.0	0.0	15.5	0.0	0.0	1.2	1.3	0.0
1,078	0.6	0.0	0.0	0.0	0.0	0.0	1.2	1.5	0.0
1,080	0.9	0.0	0.0	0.0	0.0	0.0	0.0	2.2	0.0
1,082	0.4	0.0	0.0	12.8	0.0	0.0	0.0	0.0	0.9
1,084	1.0	0.0	0.0	0.0	0.0	0.0	1.8	2.6	0.0
1,086	1.2	0.0	0.0	25.8	0.0	0.0	0.0	1.9	1.6
1,088	0.9	0.0	0.0	14.9	0.0	0.0	0.0	1.4	1.4
1,090	1.3	0.0	0.0	0.0	0.0	0.0	0.0	2.7	1.6
1,092	0.5	0.0	0.0	0.0	0.0	0.0	0.0	0.0	2.6

Mineralogical Composition of North Core at North Ingebright Lake

Depth (cm)	Quartz	K Feldspar	Plag.	Total Clay Miner.	Calcite	High Mg Calcite	Aragonite	Proto Dolomite	Dolomite
1,094	2.5	0.0	0.0	0.0	0.0	0.0	0.0	6.3	0.0
1,096	0.0	0.0	0.0	0.0	0.0	0.0	1.4	0.0	0.0
1,098	0.0	0.0	1.4	0.0	0.0	0.0	0.0	0.0	0.0
1,100	0.2	0.0	0.0	0.0	0.0	0.9	0.0	0.0	0.0
1,102	0.0	0.0	0.0	0.0	0.0	0.0	0.0	0.8	0.0
1,104	0.0	0.0	0.0	0.0	0.0	0.0	0.0	0.0	0.0
1,106	0.5	0.0	0.0	0.0	0.0	0.0	0.0	2.0	0.0
1,108	0.3	0.0	0.0	0.0	0.0	0.0	0.0	0.0	0.0
1,110	0.0	0.0	9.8	0.0	0.0	0.0	0.0	0.0	1.0
1,112	0.0	0.0	0.0	0.0	0.0	0.0	0.0	0.0	0.0
1,114	0.0	0.0	0.0	0.0	0.0	0.0	0.0	1.5	0.0
1,116	1.3	0.0	0.0	0.0	0.0	0.0	0.0	0.0	0.0
1,118	0.4	0.0	0.0	0.0	0.0	0.0	0.0	0.0	0.6
1,120	0.9	0.0	0.0	0.0	0.0	0.0	0.0	1.4	1.7
1,122	0.2	0.0	0.0	0.0	0.0	0.0	0.0	1.3	0.0
1,124	0.3	0.0	0.0	0.0	0.0	0.0	0.0	0.0	0.0
1,126	0.0	0.0	0.0	0.0	0.0	0.0	0.0	0.0	0.0
1,128	0.0	0.0	10.7	0.0	0.0	0.0	0.0	0.0	1.1
1,130	0.5	0.0	0.0	17.0	0.0	0.0	0.0	0.0	1.6
1,132	0.0	0.0	9.7	0.0	0.0	0.0	0.0	0.0	0.0
1,134	0.1	0.0	2.7	0.0	0.0	0.0	0.0	0.0	0.0
1,136	0.2	0.0	8.0	0.0	0.0	0.0	0.0	0.0	0.0
1,138	0.5	0.0	0.0	0.0	0.0	0.0	0.0	0.0	0.0
1,140	0.0	0.0	7.9	0.0	0.0	0.0	0.0	0.0	0.0
1,142	0.4	0.0	0.0	0.0	0.0	0.0	0.0	0.0	0.0
1,144	0.7	0.0	0.0	0.0	0.0	0.0	0.0	0.0	1.1
1,148	0.4	0.0	0.0	0.0	0.0	0.0	0.0	2.5	0.0
1,150	0.0	0.0	12.9	0.0	0.0	0.0	0.9	0.0	0.0
1,152	0.3	0.0	0.0	0.0	0.0	0.0	0.0	0.0	0.0
1,154	0.0	0.0	0.0	0.0	0.0	0.0	1.0	0.9	0.0
1,156	0.4	0.0	0.0	0.0	0.0	0.0	0.0	1.7	0.0
1,158	0.3	0.0	0.0	0.0	0.0	0.0	0.0	0.0	1.3
1,160	0.8	0.0	0.0	14.1	0.0	0.0	0.0	1.1	1.4
1,162	0.9	0.0	0.0	0.0	0.0	0.0	0.0	1.4	0.0
1,164	0.4	0.0	0.0	15.6	0.0	0.0	1.6	1.7	0.0
1,166	0.0	0.0	0.0	15.0	0.0	1.3	0.0	1.6	0.0
1,168	0.0	0.0	0.0	0.0	0.0	0.0	0.0	1.5	1.6
1,170	0.7	0.0	0.0	0.0	0.0	0.0	0.0	1.2	1.3
1,172	0.0	0.0	0.0	0.0	0.0	0.0	0.0	0.0	0.0

Mineralogical Composition of North Core at North Ingebright Lake

Depth (cm)	Quartz	K Feldspar	Plag.	Total Clay Miner.	Calcite	High Mg Calcite	Aragonite	Proto Dolomite	Dolomite
1,174	1.6	0.0	0.0	24.0	0.0	0.0	0.0	1.9	0.0
1,176	0.4	0.0	5.3	0.0	0.0	0.0	0.0	1.5	0.0
1,178	0.0	0.0	0.0	0.0	0.0	0.0	0.0	0.0	0.0
1,180	0.4	0.0	0.0	0.0	0.0	0.0	0.0	1.6	1.8
1,182	0.0	0.0	0.0	0.0	0.0	0.0	1.3	0.0	0.0
1,184	0.0	0.0	0.0	0.0	0.0	0.0	2.3	2.4	0.0
1,186	0.0	0.0	0.0	0.0	0.0	0.0	0.0	1.5	0.0
1,188	0.0	0.0	13.6	0.0	0.0	0.0	0.0	0.0	0.0
1,190	0.0	0.0	0.5	0.0	0.0	0.0	0.0	0.0	0.0
1,192	0.0	0.0	0.0	0.0	0.0	0.0	0.0	0.0	0.0
1,194	0.0	0.0	0.0	0.0	0.0	0.0	0.0	0.0	1.1
1,198	0.0	0.0	11.5	0.0	0.0	0.0	0.0	0.0	0.0
1,200	0.0	0.0	7.5	0.0	0.0	0.0	0.0	0.0	0.0
1,202	0.3	0.0	0.0	0.0	0.0	0.0	0.0	1.2	0.0
1,204	0.0	0.0	1.8	0.0	0.0	0.0	0.0	0.0	0.0
1,206	0.0	0.0	19.7	0.0	0.0	0.0	0.0	0.0	0.0
1,208	0.0	0.0	12.1	0.0	0.0	0.0	0.0	0.0	0.0
1,210	0.0	0.0	10.9	0.0	0.0	0.0	0.0	0.0	0.0
1,212	0.0	0.0	0.0	0.0	0.0	0.0	0.0	0.0	1.2
1,214	0.0	0.0	0.0	0.0	0.0	0.0	0.0	0.0	0.0
1,216	0.0	0.0	10.3	0.0	0.0	0.0	0.0	0.0	0.0
1,218	0.0	0.0	10.8	0.0	0.0	0.0	0.0	0.0	0.0
1,220	0.0	0.0	9.3	0.0	0.0	0.0	0.0	0.0	0.0
1,222	0.0	0.0	14.4	0.0	0.0	0.0	0.0	0.0	0.0
1,224	0.0	0.0	12.1	0.0	0.0	0.0	0.0	0.0	0.0
1,326	0.6	0.0	0.0	21.9	0.0	0.0	0.0	1.9	2.0
1,328	0.0	0.0	12.7	0.0	0.0	0.0	0.0	1.1	0.0
1,330	0.3	0.0	11.8	0.0	0.0	0.0	0.0	1.2	0.0
1,332	0.0	0.0	9.4	0.0	0.0	0.0	0.0	1.1	0.0
1,334	0.4	0.0	12.6	0.0	0.0	0.0	0.0	0.0	0.0
1,336	1.2	0.0	10.5	0.0	0.0	0.0	0.0	0.0	1.9
1,338	0.7	0.0	37.6	0.0	0.0	0.0	0.0	0.0	1.0
1,340	2.9	0.0	0.0	0.0	0.0	1.4	0.0	1.6	0.5
1,342	3.4	0.0	11.8	0.0	0.0	0.0	0.0	1.7	2.1
1,344	2.3	0.0	2.3	0.0	0.0	0.0	0.0	0.0	2.5
1,346	3.5	0.0	0.0	0.0	0.0	1.4	0.0	0.0	2.5
1,348	0.9	0.0	0.0	0.0	0.0	0.0	1.7	0.0	0.0
1,350	4.6	0.0	0.0	0.0	0.0	0.0	0.0	8.3	0.0
1,352	6.8	0.0	0.0	0.0	0.0	0.0	0.0	14.0	0.0

Mineralogical Composition of North Core at North Ingebright Lake

Depth (cm)	Quartz	K Feldspar	Plag.	Total Clay Miner.	Calcite	High Mg Calcite	Aragonite	Proto Dolomite	Dolomite
1,354	3.3	0.0	0.0	0.0	0.0	0.0	0.0	4.6	0.0
1,356	3.0	0.0	0.0	0.0	0.0	3.0	0.0	0.0	0.0
1,358	1.8	1.9	0.0	13.2	0.0	0.7	0.0	1.9	2.4
1,360	2.4	2.2	0.0	0.0	0.0	0.0	0.0	2.0	0.0
1,362	3.5	2.5	0.0	0.0	0.0	0.0	0.0	2.8	0.0
1,364	3.5	2.8	0.0	0.0	1.1	0.0	0.0	0.0	2.2
1,366	2.0	0.0	0.0	0.0	0.0	0.0	0.0	0.0	6.8
1,368	2.3	0.0	0.0	0.0	0.0	0.0	0.0	1.9	2.4
1,370	3.1	0.0	0.0	17.2	0.0	0.0	0.0	0.0	0.0
1,372	4.3	3.1	0.0	25.3	0.0	0.0	0.0	2.1	2.6
1,374	3.4	0.0	0.0	0.0	0.0	0.0	0.0	2.1	0.0
1,376	3.0	2.0	0.9	32.3	0.0	0.0	0.0	2.3	0.0
1,380	1.9	0.0	0.0	27.5	0.0	0.0	0.0	2.4	2.0
1,382	3.0	0.0	0.0	27.3	0.0	1.5	2.0	1.2	2.0
1,384	2.2	1.7	0.0	30.0	0.0	0.0	2.1	2.5	3.0
1,386	3.7	0.0	0.0	0.0	0.0	0.0	3.8	4.3	0.0
1,388	3.4	2.8	0.0	38.1	0.0	0.0	0.0	3.0	2.0
1,390	2.4	1.7	0.0	24.9	0.0	0.0	0.0	2.1	0.0
1,392	1.9	0.0	0.0	0.0	0.0	0.0	0.0	7.0	0.0
1,394	1.6	0.0	0.0	36.9	0.0	1.2	0.0	4.2	2.7
1,396	0.9	0.0	0.0	22.3	0.0	0.0	0.0	1.4	0.0
1,398	0.3	0.0	0.0	18.8	0.0	0.0	0.0	1.5	0.0
1,400	0.7	0.0	1.4	17.7	0.0	0.0	0.0	2.1	0.0
1,402	0.5	0.0	0.0	19.1	0.0	0.0	0.0	2.0	0.0
1,404	0.8	0.0	0.0	26.5	0.0	0.0	0.0	2.1	1.4
1,406	1.3	0.0	0.0	29.8	0.0	0.0	0.0	2.9	2.3
1,408	0.5	0.0	0.0	0.0	0.0	0.0	0.0	0.0	0.0
1,410	0.1	0.0	0.0	3.1	0.0	0.0	0.0	0.4	0.2
1,412	0.7	0.0	0.0	0.0	0.0	0.0	0.0	3.7	2.3
1,414	0.7	0.0	0.0	0.0	0.0	0.0	1.5	0.0	0.0
1,416	0.0	0.0	0.0	0.0	0.0	0.0	0.0	0.0	0.0
1,418	0.4	0.0	0.0	0.0	0.0	0.0	0.0	0.0	0.0
1,420	0.0	0.0	0.0	0.0	0.0	0.0	0.0	0.0	0.0
1,422	0.0	0.0	0.0	0.0	0.0	0.0	0.0	0.0	0.0
1,424	0.0	0.0	0.0	0.0	0.0	0.0	0.0	0.0	0.0
1,426	0.0	0.0	0.0	0.0	0.0	0.0	0.0	1.5	0.0
1,428	0.0	0.0	0.0	0.0	0.0	0.0	0.0	3.5	0.0
1,430	0.0	0.0	0.0	0.0	0.0	0.0	0.0	3.8	0.0
1,432	0.0	0.0	0.0	0.0	0.0	0.0	0.0	1.5	0.0

Mineralogical Composition of North Core at North Ingebright Lake

Depth (cm)	Quartz	K Feldspar	Plag.	Total Clay Miner.	Calcite	High Mg Calcite	Aragonite	Proto Dolomite	Dolomite
1,434	0.0	0.0	0.0	0.0	0.0	0.0	0.0	1.9	0.0
1,436	0.0	0.0	0.0	0.0	0.0	0.0	2.3	2.8	0.0
1,438	0.0	0.0	0.0	18.5	0.0	0.0	2.2	2.6	0.0
1,440	0.0	0.0	0.0	0.0	0.0	0.0	0.0	0.0	0.0
1,442	0.0	0.0	0.0	14.3	0.0	0.0	1.6	1.7	0.0
1,444	0.0	0.0	0.0	27.6	0.0	0.0	0.0	2.6	0.0
1,446	0.0	0.0	0.0	24.1	0.0	0.8	0.0	2.3	0.0
1,448	0.0	0.0	0.0	19.9	0.0	0.0	1.2	1.7	0.0
1,450	0.0	0.0	0.0	29.4	0.0	0.0	0.0	3.3	0.0
1,452	0.0	0.0	0.0	20.1	0.0	0.0	0.0	2.0	0.0
1,454	0.0	0.0	0.0	0.0	0.0	0.0	0.0	2.9	0.0
1,456	0.4	0.0	0.0	19.9	0.0	0.0	0.0	1.9	0.0
1,458	0.0	0.0	0.0	13.2	0.0	0.0	0.0	1.1	0.0
1,460	0.0	0.0	0.0	0.0	0.0	0.0	0.0	2.2	0.0
1,462	0.8	0.0	0.0	14.3	0.0	0.0	1.2	1.5	1.7
1,464	0.0	0.0	0.0	0.0	0.0	0.0	0.0	0.0	0.0
1,466	0.0	0.0	0.0	0.0	0.0	0.0	0.0	0.0	0.0
1,468	1.6	0.0	0.0	26.9	0.0	0.0	0.0	1.7	2.1
1,470	0.6	0.0	0.0	0.0	0.0	0.0	0.0	0.0	0.0
1,472	0.4	0.0	0.0	20.4	0.0	0.0	0.0	0.0	0.0
1,474	0.5	0.0	0.0	0.0	0.0	0.0	0.0	0.0	0.0
1,476	0.0	0.0	0.0	0.0	0.0	0.0	0.0	0.0	0.0
1,478	0.0	0.0	0.0	0.0	0.0	0.0	0.0	0.0	0.0
1,480	0.4	0.0	0.0	0.0	0.0	0.0	0.0	0.0	0.0
1,482	0.3	0.0	0.0	18.9	0.0	0.0	0.0	0.0	0.0
1,484	0.0	0.0	0.0	17.3	0.0	0.0	0.0	2.4	0.0
1,486	0.0	0.0	0.0	0.0	0.0	0.0	0.0	1.7	0.0
1,488	0.5	0.0	0.0	0.0	0.0	0.0	2.2	1.9	0.0
1,490	0.0	0.0	0.0	0.0	0.0	0.0	2.0	1.6	0.0
1,492	0.0	0.0	0.0	0.0	0.0	0.0	0.0	0.0	0.0
1,494	0.0	0.0	0.0	0.0	0.0	0.9	1.8	1.4	0.0
1,496	0.3	0.0	0.0	0.0	0.0	0.0	0.0	0.0	0.0
1,498	0.4	0.0	0.0	22.7	0.0	0.0	0.0	1.5	0.0
1,500	0.7	0.0	0.0	0.0	0.0	0.0	0.0	1.9	0.0
1,504	0.8	0.0	0.0	0.0	0.0	0.0	0.0	5.2	0.0
1,506	0.4	0.0	0.0	0.0	0.0	1.4	0.0	2.6	0.0
1,508	0.0	0.0	0.0	0.0	0.0	0.0	0.0	2.5	0.0
1,510	0.0	0.0	0.0	0.0	0.0	0.0	0.0	1.4	0.0
1,512	0.4	0.0	0.0	23.0	0.0	0.0	2.0	1.2	0.0

Mineralogical Composition of North Core at North Ingebright Lake

Depth (cm)	Quartz	K Feldspar	Plag.	Total Clay Miner.	Calcite	High Mg Calcite	Aragonite	Proto Dolomite	Dolomite
1,514	0.4	0.0	0.0	23.0	0.0	0.0	0.0	1.3	0.0
1,516	0.3	0.0	0.0	0.0	0.0	0.0	1.2	2.1	0.0
1,518	0.0	0.0	0.0	0.0	0.0	0.0	1.4	1.2	0.0
1,520	1.0	0.0	0.0	0.0	0.0	0.0	1.3	0.0	0.0
1,522	0.5	0.0	0.0	0.0	0.0	0.0	0.0	0.0	0.0
1,524	0.0	0.0	0.0	0.0	0.0	0.0	0.0	0.0	0.0
1,526	0.2	0.0	0.0	8.9	0.0	0.0	0.0	0.0	0.0
1,528	0.9	0.0	0.0	26.7	0.0	0.0	0.0	0.0	0.0
1,530	0.0	0.0	0.0	0.0	0.0	0.0	0.0	1.6	0.0
1,532	0.3	0.0	0.0	13.6	0.0	0.0	0.0	0.0	0.0
1,534	0.7	0.0	0.0	0.0	0.0	0.0	0.0	0.0	0.0
1,536	0.3	0.0	0.0	12.3	0.0	0.0	0.0	2.9	0.0
1,538	0.6	0.0	0.0	0.0	0.0	0.0	0.0	1.0	0.0
1,540	0.0	0.0	0.0	0.0	0.0	0.0	1.3	0.0	0.0
1,542	0.0	0.0	0.0	0.0	0.0	0.0	1.2	0.0	0.0
1,544	0.0	0.0	0.0	0.0	0.0	0.0	0.0	0.7	0.0
1,546	0.0	0.0	0.0	0.0	0.0	0.0	0.0	0.0	0.0
1,548	0.0	0.0	0.0	18.2	0.0	0.0	0.0	0.0	0.0
1,550	0.4	0.0	0.0	0.0	0.0	0.0	1.4	1.7	0.0
1,552	0.0	0.0	0.0	0.0	0.0	0.0	0.0	1.5	0.0
1,554	0.4	0.0	0.0	25.6	0.0	0.0	2.0	2.4	0.0
1,556	1.0	0.0	0.0	22.5	0.0	0.0	2.5	2.4	0.0
1,558	0.3	0.0	0.0	0.0	0.0	0.0	1.6	2.3	0.0
1,560	0.8	0.0	0.0	0.0	0.0	0.0	0.0	0.0	0.0
1,562	0.5	0.0	0.0	0.0	0.0	0.0	1.5	1.7	0.0
1,564	0.0	0.0	0.0	17.5	0.0	0.0	1.5	1.2	0.0
1,566	0.3	0.0	0.0	20.4	0.0	0.0	0.0	1.7	1.1
1,568	6.2	0.0	0.0	20.8	0.0	0.0	2.0	2.0	0.0
1,570	0.0	0.0	0.0	20.9	0.0	0.0	0.0	2.1	0.0
1,572	0.5	0.0	0.0	27.6	0.0	0.0	0.0	2.5	0.0
1,574	0.5	0.0	0.0	0.0	0.0	0.0	0.0	0.0	0.0
1,576	0.0	0.0	0.0	16.6	0.0	0.0	0.0	1.7	0.0
1,578	0.0	0.0	0.0	23.3	0.0	0.0	1.9	2.1	0.0
1,580	0.0	0.0	0.0	0.0	0.0	0.0	0.0	0.0	0.0
1,582	0.0	0.0	0.0	0.0	0.0	0.0	0.0	0.0	0.0
1,586	0.7	0.0	0.0	20.4	0.0	0.0	0.0	2.0	0.0
1,588	0.4	0.0	0.0	38.8	0.0	0.0	0.0	4.5	2.2
1,590	0.0	0.0	0.0	0.0	0.0	0.0	0.0	2.6	0.0
1,592	0.0	0.0	0.0	0.0	0.0	0.0	2.4	2.5	0.0

Mineralogical Composition of North Core at North Ingebright Lake

Depth (cm)	Quartz	K Feldspar	Plag.	Total Clay Miner.	Calcite	High Mg Calcite	Aragonite	Proto Dolomite	Dolomite
1,594	0.0	0.0	0.0	25.4	0.0	0.0	0.0	2.0	0.0
1,596	0.0	0.0	0.0	28.4	0.0	0.0	2.1	2.3	0.0
1,598	0.0	0.0	0.0	0.0	0.0	0.0	0.0	1.6	0.0
1,600	0.0	0.0	0.0	0.0	0.0	0.0	0.0	0.0	0.0
1,602	0.0	0.0	0.0	0.0	0.0	0.0	0.0	0.0	0.0
1,604	0.0	0.0	0.0	0.0	0.0	0.0	0.0	1.1	0.0
1,606	0.0	0.0	0.0	0.0	0.0	0.0	1.0	0.0	0.0
1,608	0.0	0.0	0.0	0.0	0.0	0.0	0.0	0.0	0.0
1,610	0.0	0.0	0.0	0.0	0.0	0.0	0.0	0.0	0.0
1,612	0.2	0.0	0.0	0.0	0.0	0.0	0.0	0.0	0.0
1,614	0.0	0.0	0.0	0.0	0.0	0.0	0.0	0.0	0.0
1,616	0.0	0.0	12.6	0.0	0.0	0.0	0.0	0.0	0.0
1,618	0.4	0.0	0.0	14.0	0.0	0.0	0.0	1.4	0.0
1,620	0.0	0.0	0.0	13.4	0.0	0.0	0.0	1.5	0.0
1,622	0.3	0.0	0.0	16.9	0.0	0.0	1.0	1.5	0.0
1,624	0.7	0.0	0.0	0.0	0.0	0.0	1.1	1.6	0.0
1,626	0.5	0.0	0.0	18.5	0.0	0.0	0.0	2.2	0.0
1,628	0.0	0.0	0.0	19.4	0.0	0.0	0.0	2.0	0.0
1,630	0.0	0.0	0.0	0.0	0.0	0.0	2.2	2.1	0.0
1,632	0.0	0.0	0.0	0.0	0.0	0.0	1.2	1.5	0.0
1,634	0.9	0.0	0.0	0.0	0.0	0.0	0.0	1.2	0.0
1,636	0.0	0.0	0.0	0.0	0.0	0.0	0.0	0.0	0.0
1,638	0.0	0.0	12.5	0.0	0.0	0.0	0.0	0.0	0.0
1,640	0.5	0.0	0.0	0.0	0.0	0.0	0.0	0.0	0.0
1,642	0.0	0.0	13.9	0.0	0.0	0.0	1.3	0.0	0.0
1,644	0.7	0.0	11.7	0.0	0.0	0.0	0.0	0.0	0.0
1,646	0.4	0.0	11.0	0.0	0.0	0.0	0.0	1.3	0.0
1,648	0.4	1.4	9.9	0.0	0.0	0.0	0.0	1.3	2.2
1,650	0.0	0.0	14.7	0.0	0.0	0.0	0.0	0.9	0.0
1,652	0.0	0.0	12.8	0.0	0.0	0.0	0.0	0.0	0.0
1,654	0.0	0.0	12.8	0.0	0.0	0.0	0.0	0.0	0.0
1,656	0.0	0.0	9.4	0.0	0.0	0.0	0.0	0.0	0.0
1,658	0.4	0.0	0.0	16.2	0.0	0.0	1.3	0.0	0.0
1,660	0.5	0.0	0.0	0.0	0.0	0.0	2.3	0.0	0.0
1,662	0.5	0.0	0.0	20.8	0.0	0.0	0.0	2.2	0.0
1,664	0.4	0.0	0.0	27.1	0.0	0.0	0.0	2.1	1.3
1,666	[illegible]	0.0	0.0	22.8	0.0	0.0	0.0	2.1	0.0
1,668	0.3	0.0	0.0	18.8	0.0	0.0	1.8	1.4	1.3
1,670	0.6	0.0	0.0	0.0	0.0	0.0	0.0	1.5	0.0

Mineralogical Composition of North Core at North Ingebright Lake

Depth (cm)	Quartz	K Feldspar	Plag.	Total Clay Miner.	Calcite	High Mg Calcite	Aragonite	Proto Dolomite	Dolomite
1,672	0.0	0.0	0.0	0.0	0.0	0.0	0.0	0.0	0.0
1,674	0.3	0.0	0.0	0.0	0.0	1.3	0.0	0.0	0.0
1,676	0.5	0.0	0.0	0.0	0.0	0.0	0.0	0.0	0.0
1,678	0.5	0.0	0.0	0.0	0.0	0.0	0.0	1.5	1.5
1,680	0.0	0.0	0.0	0.0	0.0	0.0	0.0	0.0	0.0
1,730	1.1	0.0	0.0	16.2	0.0	0.0	0.0	1.8	0.0
1,732	1.5	0.0	0.0	13.8	0.0	0.0	1.5	1.6	0.0
1,734	0.4	0.0	0.0	0.0	0.0	0.0	0.0	0.0	0.0
1,736	1.2	0.0	0.0	0.0	0.0	0.0	1.7	1.9	0.0
1,738	0.7	0.0	0.0	18.6	0.0	0.0	0.0	1.3	1.2
1,740	0.0	0.0	0.0	0.0	0.0	0.0	0.0	0.0	0.0
1,742	0.6	0.0	0.0	0.0	0.0	0.0	0.0	0.0	0.0
1,744	0.0	0.0	0.0	0.0	0.0	0.0	0.0	0.0	0.0
1,746	0.0	0.0	0.0	0.0	0.0	0.0	0.0	0.0	0.0
1,748	0.0	0.0	0.0	0.0	0.0	0.0	0.0	0.0	0.0
1,750	0.0	0.0	0.0	0.0	0.0	0.0	0.0	0.0	0.0
1,752	0.0	0.0	0.0	0.0	0.0	0.0	0.0	0.0	0.0
1,754	0.4	0.0	0.0	0.0	0.0	0.7	0.0	2.2	0.0
1,756	0.0	0.0	0.0	0.0	0.0	0.0	0.0	0.0	0.0
1,758	0.0	0.0	0.0	0.0	0.0	0.0	0.0	0.0	0.0
1,760	0.3	0.0	0.0	0.0	0.0	0.0	0.0	0.0	0.0
1,762	0.0	0.0	0.0	0.0	0.0	0.0	0.0	0.0	0.0
1,764	0.0	0.0	0.0	0.0	0.0	0.0	0.0	0.0	0.0
1,766	0.0	0.0	0.0	0.0	0.0	0.0	0.0	0.0	0.0
1,768	0.0	0.0	0.0	0.0	0.0	0.0	0.0	0.0	0.0
1,770	0.4	0.0	0.0	23.7	0.0	0.0	0.0	2.1	1.9
1,772	0.0	0.0	0.0	0.0	0.0	0.0	0.0	0.0	0.0
1,774	0.0	0.0	0.0	0.0	0.0	0.0	0.0	0.0	0.0
1,776	0.0	0.0	0.0	0.0	0.0	0.0	0.0	0.0	0.0
1,778	0.0	0.0	0.0	0.0	0.0	0.0	0.0	0.0	0.0
1,780	0.0	0.0	0.0	11.4	0.0	0.0	1.1	0.0	0.0
1,782	0.0	0.0	0.0	0.0	0.0	0.0	0.0	0.0	0.0
1,786	0.0	0.0	0.0	18.5	0.0	0.0	0.0	1.4	1.2
1,788	0.0	0.0	0.0	0.0	0.0	0.0	0.0	0.0	1.3
1,790	0.0	0.0	0.0	0.0	0.0	0.0	0.0	0.0	0.0
1,792	0.0	0.0	0.0	0.0	0.0	0.0	0.0	1.3	0.0
1,794	0.0	0.0	0.0	0.0	0.0	0.0	0.0	0.0	0.0
1,796	0.9	0.0	0.0	0.0	0.0	0.0	0.0	1.9	0.0
1,798	0.0	0.0	0.0	0.0	0.0	0.0	0.0	0.0	0.0

Mineralogical Composition of North Core at North Ingebright Lake

Depth (cm)	Quartz	K Feldspar	Plag.	Total Clay Miner.	Calcite	High Mg Calcite	Aragonite	Proto Dolomite	Dolomite
1,800	0.0	0.0	0.0	0.0	0.0	0.0	0.0	0.0	3.0
1,802	0.0	0.0	0.0	0.0	0.0	0.0	0.0	0.0	0.0
1,804	0.0	0.0	0.0	0.0	0.0	0.0	0.0	0.0	0.0
1,806	0.0	0.0	2.2	0.0	0.0	0.0	0.0	0.0	0.0
1,808	0.0	0.0	0.0	0.0	0.0	0.0	0.0	0.0	0.0
1,810	0.0	0.0	0.0	0.0	0.0	0.0	0.0	0.0	0.0
1,812	0.0	0.0	0.0	0.0	0.0	0.0	0.0	0.0	0.0
1,814	0.5	0.0	0.0	0.0	0.0	0.0	0.0	0.0	0.0
1,816	0.0	0.0	0.0	0.0	0.0	0.0	0.0	0.0	0.0
1,818	0.0	0.0	0.0	0.0	0.0	0.0	0.0	0.0	0.0
1,820	0.0	0.0	0.0	0.0	0.0	0.0	0.0	0.0	0.0
1,822	0.0	0.0	0.0	0.0	0.0	0.0	0.0	0.0	0.0
1,824	0.0	0.0	0.0	0.0	0.0	0.0	0.0	0.0	0.0
1,826	0.0	0.0	0.0	0.0	0.0	0.0	0.0	0.0	0.0
1,828	0.0	0.0	0.0	0.0	0.0	0.0	0.0	0.0	0.0
1,830	0.0	0.0	0.0	0.0	0.0	0.0	0.0	0.0	0.0
1,832	0.0	0.0	0.0	0.0	0.0	0.0	0.0	0.0	0.0
1,834	0.0	0.0	0.0	0.0	0.0	0.0	0.0	0.0	0.0
1,836	0.0	0.0	0.0	0.0	0.0	0.0	0.0	0.0	0.0
1,912	0.0	0.0	0.0	0.0	0.0	0.0	0.0	0.0	0.0
1,914	0.0	0.0	0.0	0.0	0.0	0.0	0.0	0.0	0.0
1,916	0.0	0.0	0.0	0.0	0.0	0.0	0.0	0.0	0.0
1,918	0.0	0.0	0.0	0.0	0.0	0.0	0.0	0.0	0.0
1,920	0.0	0.0	0.0	0.0	0.0	0.0	0.0	0.0	0.0
1,922	0.0	0.0	0.0	0.0	0.0	0.0	0.0	0.0	0.0
1,924	0.0	0.0	0.0	0.0	0.0	0.0	0.0	0.0	0.0
1,926	0.0	0.0	0.0	10.9	0.0	0.0	0.0	1.8	0.0
1,928	0.6	0.0	0.0	0.0	0.0	0.0	0.0	0.0	0.0
1,930	0.0	0.0	0.0	0.0	0.0	0.0	0.0	0.0	0.0
1,932	0.0	0.0	0.0	0.0	0.0	0.0	0.0	0.0	0.0
1,934	0.0	0.0	0.0	0.0	0.0	0.0	0.0	0.0	0.0
1,936	0.0	0.0	0.0	0.0	0.0	0.0	0.0	0.0	0.0
1,938	0.0	0.0	0.0	0.0	0.0	0.0	0.0	0.0	0.0
1,940	0.0	0.0	0.0	0.0	0.0	0.0	0.0	0.0	0.0
1,942	0.0	0.0	0.0	0.0	0.0	0.0	0.0	0.0	0.0
1,944	0.0	0.0	0.0	0.0	0.0	0.0	0.0	0.0	0.0
1,946	0.0	0.0	0.0	0.0	0.0	0.0	0.0	0.0	0.0
1,948	0.0	0.0	0.0	0.0	0.0	0.0	0.0	0.0	0.0
1,950	0.0	0.0	0.0	0.0	0.0	0.0	0.0	0.0	0.0

Mineralogical Composition of North Core at North Ingebright Lake

Depth (cm)	Quartz	K Feldspar	Plag.	Total Clay Miner.	Calcite	High Mg Calcite	Aragonite	Proto Dolomite	Dolomite
1,952	0.0	0.0	0.0	0.0	0.0	0.0	0.0	0.0	0.0
1,954	0.0	0.0	0.0	0.0	0.0	0.0	0.0	1.2	0.0
1,956	0.0	0.0	0.0	0.0	0.0	0.0	0.0	0.0	0.0
1,958	0.0	0.0	0.0	0.0	0.0	0.0	0.0	0.0	0.0
1,960	0.0	0.0	0.0	0.0	0.0	0.0	0.0	0.0	0.0
1,962	0.0	0.0	0.0	0.0	0.0	0.0	0.0	0.0	0.0
1,964	0.0	0.0	0.0	0.0	0.0	0.0	0.0	0.0	0.0
1,966	0.0	0.0	0.0	0.0	0.0	0.0	0.0	0.0	0.0
1,968	0.0	0.0	0.0	0.0	0.0	0.0	0.0	0.0	0.0
1,970	0.0	0.0	0.0	0.0	0.0	0.0	0.0	0.0	0.0
1,974	0.0	0.0	0.0	0.0	0.0	0.0	0.0	0.0	0.0
1,976	0.0	0.0	0.0	0.0	0.0	0.0	0.0	0.0	0.0
1,978	0.0	0.0	0.0	0.0	0.0	0.0	0.0	0.0	0.0
1,980	0.0	0.0	0.0	0.0	0.0	0.0	0.0	0.0	0.0
1,982	0.0	0.0	0.0	0.0	0.0	0.0	0.0	0.0	0.0
1,984	0.0	0.0	0.0	0.0	0.0	0.0	0.0	0.0	0.0
1,986	0.0	0.0	0.0	0.0	0.0	0.0	0.0	0.0	0.0
1,988	0.0	0.0	0.0	0.0	0.0	0.0	0.0	0.0	0.0
1,990	0.0	0.0	0.0	0.0	0.0	0.0	0.0	0.0	0.0
1,992	0.0	0.0	0.0	0.0	0.0	0.0	0.0	0.0	0.0
1,994	0.0	0.0	0.0	0.0	0.0	0.0	0.0	0.0	0.0
1,996	0.0	0.0	0.0	0.0	0.0	0.0	0.0	0.0	0.0
2,000	0.0	0.0	0.0	0.0	0.0	0.0	0.0	0.0	0.0
2,002	0.0	0.0	0.0	0.0	0.0	0.0	0.0	0.0	0.0
2,004	0.0	0.0	0.0	0.0	0.0	0.0	0.0	0.0	0.0
2,006	0.0	0.0	0.0	0.0	0.0	0.0	0.0	0.0	0.0
2,008	0.0	0.0	0.0	0.0	0.0	0.0	0.0	0.0	0.0
2,010	0.0	0.0	0.0	0.0	0.0	0.0	0.0	0.0	0.0
2,012	0.0	0.0	0.0	0.0	0.0	0.0	0.0	0.0	0.0
2,014	0.0	0.0	0.0	0.0	0.0	0.0	0.0	0.0	0.0
2,016	0.0	0.0	0.0	0.0	0.0	0.0	0.0	0.0	0.0
2,018	0.0	0.0	0.0	0.0	0.0	0.0	0.0	0.0	0.0
2,020	0.0	0.0	0.0	0.0	0.0	0.0	0.0	0.0	0.0
2,022	0.0	0.0	0.0	0.0	0.0	0.0	0.0	0.0	0.0
2,024	0.0	0.0	0.0	0.0	0.0	0.0	0.0	0.0	0.0
2,026	0.0	0.0	0.0	0.0	0.0	0.0	0.0	0.0	0.0
2,028	0.0	0.0	0.0	0.0	0.0	0.0	0.0	0.0	0.0
2,030	0.0	0.0	0.0	0.0	0.0	0.0	0.0	0.0	0.0
2,032	0.0	0.0	0.0	0.0	0.0	0.0	0.0	0.0	0.0

Mineralogical Composition of North Core at North Ingebright Lake

Depth (cm)	Quartz	K Feldspar	Plag.	Total Clay Miner.	Calcite	High Mg Calcite	Aragonite	Proto Dolomite	Dolomite
2,034	0.0	0.0	0.0	0.0	0.0	0.0	0.0	0.0	0.0
2,036	0.0	0.0	0.0	0.0	0.0	0.0	0.0	0.0	0.0
2,038	0.0	0.0	0.0	0.0	0.0	0.0	0.0	0.0	0.0
2,040	0.0	0.0	0.0	0.0	0.0	0.0	0.0	0.0	0.0
2,042	0.0	0.0	0.0	0.0	0.0	0.0	0.0	0.0	0.0
2,044	0.0	0.0	0.0	0.0	0.0	0.0	0.0	0.0	0.0
2,046	0.0	0.0	0.0	0.0	0.0	0.0	0.0	0.0	0.0
2,048	0.0	0.0	40.5	0.0	0.0	0.0	0.0	0.0	0.0
2,052	0.0	0.0	0.0	0.0	0.0	0.0	0.0	0.0	0.0
2,054	0.0	0.0	0.0	0.0	0.0	0.0	0.0	0.0	0.0
2,056	0.0	0.0	0.0	0.0	0.0	0.0	0.0	0.0	0.0
2,058	0.0	0.0	0.0	0.0	0.0	0.0	0.0	0.0	0.0
2,060	0.0	0.0	0.0	0.0	0.0	0.0	0.0	0.0	0.0
2,062	0.0	0.0	0.0	0.0	0.0	0.0	0.0	0.0	0.0
2,064	0.0	0.0	0.0	0.0	0.0	0.0	0.0	0.0	0.0
2,066	0.0	0.0	0.0	0.0	0.0	0.0	0.0	0.9	0.0
2,068	0.0	0.0	0.0	0.0	0.0	0.0	0.0	0.0	0.0
2,070	0.0	0.0	0.0	0.0	0.0	0.0	0.0	0.0	0.0
2,072	0.0	0.0	0.0	0.0	0.0	0.0	0.0	0.0	0.0
2,074	0.0	0.0	0.0	0.0	0.0	0.0	0.0	1.2	0.0
2,076	0.0	0.0	0.0	0.0	0.0	0.0	0.0	0.0	0.0
2,078	0.0	0.0	1.6	0.0	0.0	0.0	1.3	0.0	0.0
2,080	0.0	0.0	0.0	0.0	0.0	0.0	0.0	0.0	0.0
2,082	0.0	0.0	0.0	0.0	0.0	0.0	0.0	0.0	0.0
2,084	0.0	0.0	0.0	0.0	0.0	0.0	0.0	0.0	0.7
2,086	0.0	0.0	0.0	0.0	0.0	0.0	0.0	0.0	0.0
2,088	0.0	0.0	0.0	0.0	0.0	0.0	0.0	0.0	0.0
2,090	0.0	0.0	0.0	0.0	0.0	0.0	0.0	0.0	0.0
2,092	0.0	0.0	0.0	0.0	0.0	0.0	0.0	0.0	0.0
2,094	0.0	0.0	0.0	0.0	0.0	0.0	0.0	0.0	0.0
2,096	0.0	0.0	0.0	0.0	0.0	0.0	0.0	0.0	0.0
2,098	0.0	0.0	0.0	0.0	0.0	0.0	0.0	0.0	0.0
2,100	0.0	0.0	0.0	0.0	0.0	0.0	0.0	0.0	0.0
2,102	0.0	0.0	0.0	0.0	0.0	0.0	0.0	0.0	0.0
2,104	0.0	0.0	0.0	0.0	0.0	0.0	0.0	2.0	0.0
2,108	0.0	0.0	0.0	0.0	0.0	0.0	0.0	0.0	0.0
2,110	0.0	0.0	0.0	0.0	0.0	0.0	0.0	0.0	0.0
2,112	0.0	0.0	0.0	0.0	0.0	0.0	0.0	0.0	0.0
2,114	0.0	0.0	0.0	0.0	0.0	0.0	0.0	0.0	0.0

Mineralogical Composition of North Core at North Ingebright Lake

Depth (cm)	Quartz	K Feldspar	Plag.	Total Clay Miner.	Calcite	High Mg Calcite	Aragonite	Proto Dolomite	Dolomite
2,116	0.0	0.0	0.0	0.0	0.0	0.0	0.0	0.0	0.0
2,118	0.0	0.0	0.0	0.0	0.0	0.0	0.0	0.0	0.0
2,120	0.0	0.0	0.0	0.0	0.0	0.0	0.0	0.0	0.0
2,122	0.0	0.0	0.0	0.0	0.0	0.0	0.0	0.0	0.0
2,124	0.0	0.0	0.0	0.0	0.0	0.0	0.0	0.0	0.0
2,126	0.0	0.0	0.0	0.0	0.0	0.0	0.0	0.0	0.0
2,128	0.0	0.0	0.0	0.0	0.0	0.0	0.0	0.0	0.0
2,130	0.0	0.0	0.0	0.0	0.0	0.0	0.0	0.0	0.0
2,132	0.0	0.0	0.0	0.0	0.0	0.0	0.0	0.0	0.0
2,134	0.0	0.0	0.0	0.0	0.0	0.0	0.0	0.0	0.0
2,136	0.0	0.0	0.0	0.0	0.0	0.0	0.0	0.0	0.0
2,138	0.0	0.0	0.0	0.0	0.0	0.0	0.0	0.0	0.0
2,140	0.0	0.0	0.0	0.0	0.0	0.0	0.0	0.0	0.0
2,142	0.0	0.0	0.0	0.0	0.0	0.0	0.0	0.0	0.0
2,144	0.0	0.0	0.0	0.0	0.0	0.0	0.0	0.0	0.0
2,146	0.0	0.0	0.0	0.0	0.0	0.0	0.0	0.0	0.0
2,148	0.0	0.0	0.0	0.0	0.0	0.0	0.0	0.0	0.0
2,150	0.0	0.0	0.0	0.0	0.0	0.0	0.0	0.0	0.0
2,152	0.0	0.0	0.0	0.0	0.0	0.0	0.0	0.0	0.0
2,154	0.0	0.0	0.0	0.0	0.0	0.0	0.0	0.0	0.0
2,156	0.0	0.0	0.0	0.0	0.0	0.0	0.0	0.0	0.0
2,158	0.0	0.0	0.0	0.0	0.0	0.0	0.0	0.0	0.0
2,160	0.0	0.0	0.0	0.0	0.0	0.0	0.0	0.0	0.0
2,162	0.0	0.0	0.0	0.0	0.0	0.0	0.0	0.0	0.0
2,164	0.0	0.0	0.0	0.0	0.0	0.0	0.0	0.0	0.0
2,166	0.0	0.0	0.0	0.0	0.0	0.0	0.0	0.0	0.0
2,168	0.0	0.0	0.0	0.0	0.0	0.0	0.0	0.0	0.0
2,170	0.0	0.0	0.0	0.0	0.0	0.0	0.0	0.0	0.0
2,172	0.0	0.0	0.0	0.0	0.0	0.0	0.0	0.0	0.0
2,174	0.0	0.0	0.0	0.0	0.0	0.0	0.0	0.0	0.0
2,176	0.0	0.0	0.0	0.0	0.0	0.0	0.0	0.0	0.0
2,178	0.0	0.0	0.0	0.0	0.0	0.0	0.0	0.0	0.0
2,180	0.0	0.0	0.0	0.0	0.0	0.0	0.0	0.0	0.0
2,182	0.0	0.0	0.0	0.0	0.0	0.0	0.0	0.0	0.0
2,184	0.0	0.0	0.0	0.0	0.0	0.0	0.0	0.0	0.0
2,186	0.6	0.0	0.0	0.0	0.0	0.0	0.0	0.0	0.0
2,188	0.0	0.0	0.0	0.0	0.0	0.0	0.0	0.0	0.0
2,190	0.0	0.0	0.0	0.0	0.0	0.0	0.0	0.0	0.0
2,192	0.0	0.0	0.0	0.0	0.0	0.0	0.0	0.0	0.0

Mineralogical Composition of North Core at North Ingebright Lake

Depth (cm)	Quartz	K Feldspar	Plag.	Total Clay Miner.	Calcite	High Mg Calcite	Aragonite	Proto Dolomite	Dolomite
2,194	0.0	0.0	0.0	0.0	0.0	0.0	0.0	0.0	0.0
2,196	0.0	0.0	0.0	0.0	0.0	0.0	0.0	0.0	0.0
2,198	0.0	0.0	0.0	0.0	0.0	0.0	0.0	0.0	0.0
2,200	0.0	0.0	0.0	0.0	0.0	0.0	0.0	0.0	0.0
2,202	0.0	0.0	0.0	0.0	0.0	0.0	0.0	0.0	0.0
2,204	0.0	0.0	0.0	0.0	0.0	0.0	0.0	0.0	0.0
2,206	0.0	0.0	0.0	0.0	0.0	0.0	0.0	0.0	0.0
2,208	0.0	0.0	0.0	0.0	0.0	0.0	0.0	0.0	0.0
2,210	0.0	0.0	0.0	0.0	0.0	0.0	0.0	0.0	0.0
2,212	0.0	0.0	0.0	0.0	0.0	0.0	0.0	0.0	0.0
2,214	0.0	0.0	0.0	0.0	0.0	0.0	0.0	0.0	0.0
2,216	0.0	0.0	0.0	0.0	0.0	0.0	0.0	0.0	0.0
2,218	0.0	0.0	0.0	0.0	0.0	0.0	0.0	0.0	0.0
2,220	0.0	0.0	0.0	0.0	0.0	0.0	0.0	0.0	0.0
2,222	0.0	0.0	0.0	0.0	0.0	0.0	0.0	0.0	0.0
2,224	0.0	0.0	0.0	0.0	0.0	0.0	0.0	0.0	0.0
2,226	0.0	0.0	0.0	0.0	0.0	0.0	0.0	0.0	0.0
2,228	0.0	0.0	0.0	0.0	0.0	0.0	0.0	0.0	0.0
2,230	0.0	0.0	0.0	0.0	0.0	0.0	0.0	0.0	0.0
2,232	0.0	0.0	0.0	0.0	0.0	0.0	0.0	0.0	0.0
2,234	0.0	0.0	0.0	0.0	0.0	0.0	0.0	0.0	0.0
2,236	0.0	0.0	0.0	0.0	0.0	0.0	0.0	0.0	0.0
2,238	0.0	0.0	0.0	0.0	0.0	0.0	0.0	0.0	0.0
2,240	0.0	0.0	0.0	0.0	0.0	0.0	0.0	0.0	0.0
2,242	0.0	0.0	0.0	0.0	0.0	0.0	0.0	0.0	0.0
2,244	0.0	0.0	0.0	0.0	0.0	0.0	0.0	0.0	0.0
2,246	0.0	0.0	0.0	0.0	0.0	0.0	0.0	0.0	0.0
2,250	0.0	0.0	0.0	0.0	0.0	0.0	0.0	0.0	0.0
2,252	0.0	0.0	0.0	0.0	0.0	0.0	0.0	0.0	0.0
2,254	0.0	0.0	0.0	0.0	0.0	0.0	0.0	0.0	0.0
2,256	0.0	0.0	0.0	0.0	0.0	0.0	0.0	0.0	0.0
2,258	0.0	0.0	0.0	0.0	0.0	0.0	0.0	0.0	0.0
2,260	0.0	0.0	0.0	0.0	0.0	0.0	0.0	0.0	0.0
2,262	0.0	0.0	0.0	0.0	0.0	0.0	0.0	0.0	0.0
2,264	0.0	0.0	0.0	0.0	0.0	0.0	0.0	0.0	0.0
2,266	0.0	0.0	0.0	0.0	0.0	0.0	0.0	0.0	0.0
2,268	0.0	0.0	0.0	0.0	0.0	0.0	0.0	0.0	0.0
2,270	0.0	0.0	0.0	0.0	0.0	0.0	0.0	0.0	0.0
2,272	0.0	0.0	0.0	0.0	0.0	0.0	0.0	0.0	0.0

Mineralogical Composition of North Core at North Ingebright Lake

Depth (cm)	Quartz	K Feldspar	Plag.	Total Clay Miner.	Calcite	High Mg Calcite	Aragonite	Proto Dolomite	Dolomite
2,274	0.0	0.0	0.0	0.0	0.0	0.0	0.0	0.0	0.0
2,276	0.0	0.0	0.0	0.0	0.0	0.0	0.0	0.0	0.0
2,280	0.0	0.0	0.0	0.0	0.0	0.0	0.0	0.0	0.0
2,282	0.0	0.0	0.0	0.0	0.0	0.0	0.0	0.0	0.0
2,284	0.0	0.0	0.0	0.0	0.0	0.0	0.0	0.0	0.0
2,286	0.0	0.0	0.0	0.0	0.0	0.0	0.0	0.0	0.0
2,288	0.0	0.0	0.0	0.0	0.0	0.0	0.0	0.0	0.0
2,290	0.0	0.0	0.0	0.0	0.0	0.0	0.0	0.0	0.0
2,292	0.0	0.0	0.0	0.0	0.0	0.0	0.0	0.0	0.0
2,294	0.0	0.0	0.0	0.0	0.0	0.0	0.0	0.0	0.0
2,296	0.0	0.0	0.0	0.0	0.0	0.0	0.0	0.0	0.0

Mineralogical Composition of North Core at North Ingebright Lake

Depth (cm)	Magnesite	Gypsum	Anhydrite	Thenardite	Bloedite	Halite	Mg in High Mg Calcite	Ca in Protodolomite
12	0.0	0.0	0.0	20.6	0.0	0.0		5.6
14	0.0	0.0	0.0	0.0	0.0	0.0		71.8
16	0.0	0.0	0.0	20.3	0.0	0.0	15.9	
18	0.0	0.0	6.4	6.5	56.8	0.0		52.8
20	0.0	0.0	0.0	7.6	0.0	0.0	8.4	56.6
22	0.0	0.0	17.4	10.6	0.0	0.0		52.3
24	0.0	0.0	0.0	16.9	0.0	0.0		52.5
26	0.0	0.0	4.3	5.6	32.2	0.0	18.9	
28	0.0	0.0	0.0	4.9	34.0	0.0		54.6
30	0.0	0.0	0.0	12.2	0.0	0.0		51.9
32	0.0	11.9	0.0	13.4	0.0	0.0		
34	0.0	16.1	0.0	0.0	0.0	0.0	11.6	56.5
36	0.0	0.0	9.2	8.5	0.0	0.0		56.3
38	0.0	0.0	0.0	34.6	0.0	0.0		55.7
40	0.0	0.0	0.0	14.5	39.7	0.0		52.7
42	0.0	20.2	0.0	6.7	44.3	0.0		52.5
44	0.0	0.0	0.0	32.2	0.0	0.0		49.5
46	0.0	0.0	0.0	59.1	0.0	0.0	7.6	53.2
48	0.0	0.0	0.0	42.9	0.0	0.0		52.4
50	0.0	0.0	0.0	84.7	0.0	0.0		53.8
52	0.0	0.0	0.0	67.8	0.0	0.0		5.3
54	0.0	0.0	0.0	93.1	0.0	0.0		67.4
56	0.0	0.0	0.0	91.4	0.0	0.0		63.0
58	0.0	0.0	0.0	91.9	0.0	0.0		55.3
60	0.0	0.0	0.0	89.6	0.0	0.0		52.4
62	0.0	0.0	0.0	90.5	0.0	0.0		52.6
64	0.0	0.0	9.0	87.9	0.0	0.0		
66	0.0	0.0	0.0	90.1	0.0	0.0		54.6
68	0.0	0.0	0.0	90.4	0.0	0.0		53.7
70	0.0	0.0	0.0	91.7	0.0	0.0		51.2
72	0.0	0.0	0.0	94.0	0.0	0.0		54.6
74	0.0	0.0	0.0	91.2	0.0	0.0		55.9
76	0.0	0.0	0.0	93.0	0.0	0.0		54.6
78	0.0	0.0	0.0	93.7	0.0	0.0		5.8
80	0.0	0.0	0.0	91.2	0.0	0.0	18.5	53.3
82	0.0	0.0	0.0	95.3	0.0	0.0		56.6
84	0.0	0.0	0.0	92.9	0.0	0.0		51.4
86	0.0	0.0	0.0	95.6	0.0	0.0		51.4
88	0.0	0.0	0.0	92.8	0.0	0.0		

Mineralogical Composition of North Core at North Ingebright Lake

Depth (cm)	Magnesite	Gypsum	Anhydrite	Thenardite	Bloedite	Halite	Mg in High Mg Calcite	Ca in Protodolomite
90	0.0	0.0	0.0	91.3	0.0	0.0		61.7
92	0.0	0.0	0.0	96.8	0.0	0.0		
94	0.0	0.0	0.0	94.4	0.0	0.0		
96	0.0	0.0	0.0	91.3	0.0	0.0		5.8
98	0.0	0.0	0.0	95.1	0.0	0.0		53.7
100	0.0	0.0	0.0	95.3	0.0	0.0		51.8
106	0.0	0.0	0.0	92.6	0.0	0.0		
108	0.0	0.0	0.0	97.6	0.0	0.0		
110	0.0	0.0	0.0	95.3	0.0	0.0		
112	0.0	0.0	0.0	99.5	0.0	0.0		
114	0.0	0.0	0.0	79.7	18.4	0.0		
116	0.0	0.0	0.0	96.7	0.0	0.0		49.5
118	0.0	0.0	0.0	99.5	0.0	0.0		
120	0.0	0.0	0.0	99.4	0.0	0.0		
122	0.0	0.0	0.0	100.0	0.0	0.0		
124	0.0	0.0	0.0	0.0	0.0	0.0		
126	0.0	0.0	0.0	99.1	0.0	0.0		
128	0.0	0.0	0.0	97.7	0.0	0.0		
130	0.0	0.0	0.0	97.8	0.0	0.0		5.5
132	0.0	11.4	0.0	87.4	0.0	0.0		
134	0.0	0.0	0.0	95.5	0.0	0.0		51.5
136	0.0	10.7	0.0	88.7	0.0	0.0		
138	0.0	0.0	0.0	96.0	0.0	0.0		52.9
140	0.0	0.0	0.0	94.8	0.0	0.0		57.7
142	0.0	0.0	0.0	94.5	0.0	0.0		55.9
144	0.0	0.0	0.0	100.0	0.0	0.0		
146	0.0	0.0	0.0	72.3	0.0	0.0		52.9
148	0.0	0.0	0.0	80.5	0.0	0.0		52.4
150	0.0	0.0	0.0	78.0	0.0	0.0		52.7
152	0.0	0.0	0.0	64.8	0.0	0.0	17.3	5.8
154	0.0	0.0	0.0	96.1	0.0	0.0		49.4
156	0.0	0.0	0.0	99.3	0.0	0.0		
158	0.0	0.0	0.0	99.1	0.0	0.0		
160	0.0	0.0	0.0	95.6	0.0	0.0		
162	0.0	0.0	0.0	99.4	0.0	0.0		
164	0.0	0.0	0.0	98.6	0.0	0.0		
166	0.0	0.0	6.3	92.1	0.0	0.0		
168	0.0	0.0	0.0	100.0	0.0	0.0		
170	0.0	0.0	0.0	82.0	13.7	0.0		59.8

Mineralogical Composition of North Core at North Ingebright Lake

Depth (cm)	Magnesite	Gypsum	Anhydrite	Thenardite	Bloedite	Halite	Mg in High Mg Calcite	Ca in Protodolomite
172	0.0	0.0	0.0	98.1	0.0	0.0		
174	0.0	0.0	0.0	100.0	0.0	0.0		
176	0.0	0.0	0.0	98.2	0.0	0.0	18.8	
178	0.0	6.4	0.0	91.0	0.0	0.0		69.2
180	0.0	0.0	0.0	94.7	0.0	0.0		52.9
182	0.0	0.0	0.0	77.5	17.2	0.0		61.9
184	0.0	7.4	0.0	91.6	0.0	0.0		
188	0.0	7.1	0.0	89.0	0.0	0.0		5.8
190	0.0	19.8	0.0	78.5	0.0	0.0		
192	0.0	6.3	0.0	59.4	0.0	0.0		59.9
194	0.0	0.0	0.0	96.9	0.0	0.0		64.6
196	0.0	10.7	0.0	81.8	0.0	0.0		
198	0.0	11.3	0.0	80.4	0.0	0.0		56.5
200	0.0	10.5	0.0	65.3	0.0	0.0		
202	0.0	11.4	0.0	81.1	0.0	0.0		61.7
204	0.0	11.4	0.0	81.1	0.0	0.0		61.7
206	0.0	17.8	0.0	59.4	0.0	0.0		62.2
208	0.0	11.9	0.0	54.8	0.0	0.0		49.6
210	0.0	15.1	0.0	77.1	0.0	0.0	15.6	
212	0.0	26.1	0.0	69.2	0.0	0.0		61.8
214	0.0	12.8	0.0	57.5	0.0	0.0		6.8
216	0.0	8.6	0.0	84.2	0.0	0.0		52.4
218	0.0	7.6	0.0	56.9	0.0	0.0		62.7
220	0.0	13.2	0.0	79.4	0.0	0.0		6.6
222	2.9	15.1	0.0	51.4	0.0	0.0		63.2
224	2.6	12.2	0.0	48.1	0.0	0.0		62.9
226	0.0	0.0	0.0	89.7	0.0	0.0		63.3
228	0.0	26.8	0.0	56.8	0.0	0.0		65.2
230	0.0	0.0	0.0	86.9	0.0	0.0		
232	0.0	8.6	0.0	66.6	0.0	0.0		63.9
234	0.0	10.9	0.0	62.5	0.0	0.0		74.9
236	0.0	9.8	0.0	60.1	0.0	0.0		
238	0.0	26.4	0.0	66.4	0.0	0.0		
240	0.0	14.8	0.0	61.5	0.0	0.0		64.3
242	0.0	10.7	0.0	69.3	0.0	0.0	14.4	59.9
244	0.0	15.8	0.0	75.6	0.0	0.0	14.1	
246	0.0	15.1	0.0	55.3	0.0	0.0		
248	0.0	6.5	0.0	56.3	0.0	0.0	11.6	63.6
250	0.0	24.7	0.0	63.2	0.0	0.0	1.6	64.2

Mineralogical Composition of North Core at North Ingebright Lake

Depth (cm)	Magnesite	Gypsum	Anhydrite	Thenardite	Bloedite	Halite	Mg in High Mg Calcite	Ca in Protodolomite
252	0.0	24.7	0.0	63.2	0.0	0.0	1.6	64.2
254	0.0	0.0	0.0	54.8	0.0	0.0	12.4	74.2
256	0.0	19.8	0.0	51.3	0.0	0.0	12.7	53.3
258	0.0	9.4	0.0	57.5	0.0	0.0	11.6	63.0
260	0.0	5.5	0.0	58.1	0.0	0.0	11.6	64.2
262	0.0	13.9	0.0	41.5	0.0	0.0	13.9	67.3
264	0.0	12.3	0.0	45.9	0.0	0.0	5.9	62.7
266	0.0	12.7	0.0	55.9	0.0	0.0		66.0
268	0.0	9.0	0.0	52.7	0.0	0.0		64.5
270	0.0	5.2	0.0	47.9	0.0	0.0		64.0
272	0.0	23.6	0.0	45.3	0.0	0.0	1.1	63.9
274	0.0	18.9	0.0	64.1	0.0	0.0	1.9	62.9
276	0.0	6.4	0.0	45.1	0.0	0.0		63.1
278	0.0	0.0	0.0	61.3	0.0	0.0	13.4	
280	0.0	21.4	0.0	62.9	0.0	0.0	13.7	61.9
282	0.0	0.0	0.0	53.4	0.0	0.0	12.4	64.8
284	0.0	9.4	0.0	61.3	0.0	0.0	15.3	6.8
286	0.0	8.5	0.0	83.9	0.0	0.0	12.8	
288	0.0	0.0	0.0	0.0	0.0	0.0	11.2	
290	0.0	7.3	0.0	87.5	0.0	0.0		
292	0.0	0.0	0.0	93.3	0.0	0.0	12.2	62.3
294	0.0	0.0	0.0	93.5	0.0	0.0		
296	0.0	0.0	0.0	89.5	0.0	0.0	5.0	52.8
298	0.0	3.8	0.0	93.4	0.0	0.0	13.8	
300	0.0	0.0	0.0	66.1	0.0	0.0	14.6	52.0
302	0.0	19.3	0.0	73.9	0.0	0.0	14.8	61.9
304	0.0	18.9	0.0	77.2	0.0	0.0		63.5
306	0.0	14.7	0.0	83.0	0.0	0.0	1.4	
308	0.0	8.2	0.0	90.7	0.0	0.0		
310	0.0	6.7	0.0	69.0	0.0	0.0	4.6	
312	0.0	0.0	0.0	97.0	0.0	0.0		61.4
314	0.0	0.0	0.0	98.8	0.0	0.0		
316	0.0	0.0	0.0	89.7	0.0	0.0		
318	0.0	0.0	0.0	97.5	0.0	0.0		
320	0.0	0.0	0.0	99.1	0.0	0.0		
322	0.0	0.0	0.0	75.8	0.0	0.0		61.7
324	0.0	0.0	0.0	93.5	0.0	0.0		
326	0.0	0.4	0.0	94.9	0.0	0.0		
328	0.0	0.0	0.0	97.5	0.0	0.0		62.2

Mineralogical Composition of North Core at North Ingebright Lake

Depth (cm)	Magnesite	Gypsum	Anhydrite	Thenardite	Bloedite	Halite	Mg in High Mg Calcite	Ca in Protodolomite
330	0.0	0.0	0.0	98.9	0.0	0.0		
332	0.0	0.0	0.0	98.0	0.0	0.0		52.6
334	0.0	24.2	0.0	74.5	0.0	0.0		62.0
336	0.0	0.0	0.0	97.8	0.0	0.0		62.5
338	0.0	0.0	0.0	98.0	0.0	0.0		61.7
340	0.0	0.0	0.0	96.7	0.0	0.0		58.5
342	0.0	0.0	0.0	82.8	0.0	0.0		
344	0.0	0.0	0.0	88.2	0.0	0.0		
346	0.0	0.0	0.0	98.0	0.0	0.0		59.8
348	0.0	0.0	0.0	99.2	0.0	0.0		
350	0.0	0.0	0.0	98.0	0.0	0.0		
352	0.0	0.0	0.0	98.9	0.0	0.0		
354	0.0	0.0	0.0	98.6	0.0	0.0		
356	0.0	0.0	0.0	97.1	0.0	0.0		66.7
358	0.0	0.0	0.0	98.4	0.0	0.0		
360	0.0	0.0	0.0	80.7	0.0	0.0		
362	0.0	0.0	0.0	96.9	0.0	0.0		64.7
364	0.0	0.0	0.0	85.9	0.0	0.0		6.4
368	0.0	0.0	0.0	96.6	0.0	0.0		
370	0.0	0.0	0.0	97.7	0.0	0.0		65.2
372	0.0	15.1	0.0	81.5	0.0	0.0		6.7
374	0.0	6.0	0.0	73.7	0.0	0.0		
376	0.0	0.0	0.0	98.3	0.0	0.0		
378	0.0	0.0	0.0	93.9	0.0	0.0		
380	0.0	0.0	0.0	88.6	0.0	0.0		59.1
382	0.0	0.0	0.0	98.8	0.0	0.0		
384	0.0	0.0	0.0	97.0	0.0	0.0		6.6
386	0.0	0.0	0.0	99.1	0.0	0.0		
388	0.0	0.0	0.0	99.4	0.0	0.0		
390	0.0	0.0	0.0	98.9	0.0	0.0		
392	0.0	0.0	0.0	99.2	0.0	0.0		
394	0.0	0.0	0.0	99.3	0.0	0.0		
396	0.0	5.3	0.0	82.8	0.0	0.0		
398	0.0	0.0	0.0	90.4	0.0	0.0		
400	0.0	0.0	0.0	90.6	0.0	0.0		
402	0.0	0.0	0.0	97.1	0.0	0.0		53.2
404	0.0	0.0	0.0	99.4	0.0	0.0		
406	0.0	0.0	0.0	99.2	0.0	0.0		
408	0.0	0.0	0.0	99.3	0.0	0.0		

Mineralogical Composition of North Core at North Ingebright Lake

Depth (cm)	Magnesite	Gypsum	Anhydrite	Thenardite	Bloedite	Halite	Mg in High Mg Calcite	Ca in Protodolomite
410	0.0	0.0	0.0	99.4	0.0	0.0		
412	0.0	0.0	0.0	99.6	0.0	0.0		
414	0.0	0.0	0.0	84.8	0.0	0.0		
416	0.0	0.0	0.0	99.3	0.0	0.0		
418	0.0	0.0	0.0	99.0	0.0	0.0		
420	0.0	0.0	0.0	99.2	0.0	0.0		
422	0.0	5.0	0.0	93.5	0.0	0.0		
424	0.0	0.0	0.0	100.0	0.0	0.0		
426	0.0	0.0	0.0	99.6	0.0	0.0		
428	0.0	0.0	0.0	84.4	0.0	0.0		
430	0.0	0.0	0.0	91.5	0.0	0.0		
432	0.0	0.0	0.0	88.3	0.0	0.0		
434	0.0	0.0	0.0	100.0	0.0	0.0		
436	0.0	0.0	0.0	89.4	0.0	0.0		
438	0.0	0.0	0.0	92.9	0.0	0.0		
440	0.0	0.0	0.0	89.0	0.0	0.0		
442	0.0	0.0	0.0	82.5	0.0	0.0		
444	0.0	0.0	0.0	87.5	0.0	0.0		
446	0.0	0.0	0.0	89.1	0.0	0.0		54.4
448	0.0	0.0	0.0	88.8	0.0	0.0		
450	0.0	0.0	0.0	99.4	0.0	0.0		
452	0.0	0.0	0.0	89.0	0.0	0.0		
454	0.0	7.3	0.0	83.0	0.0	0.0		
456	0.0	0.0	0.0	85.5	0.0	0.0		
458	0.0	6.7	0.0	84.2	0.0	0.0		
460	0.0	0.0	0.0	70.5	0.0	0.0		67.0
462	0.0	10.1	0.0	80.7	0.0	0.0	9.2	
464	0.0	7.3	0.0	87.9	0.0	0.0		77.6
466	0.0	11.7	0.0	81.5	0.0	0.0		
468	0.0	0.0	0.0	99.5	0.0	0.0		
470	0.0	0.0	0.0	98.7	0.0	0.0		
472	0.0	8.3	0.0	83.7	0.0	0.0		62.8
474	0.0	0.0	0.0	74.0	0.0	0.0		61.1
476	0.0	33.1	0.0	45.2	0.0	0.0		6.4
478	3.2	6.5	0.0	65.3	0.0	0.0		63.4
480	2.5	0.0	0.0	76.5	0.0	0.0		
482	0.0	11.4	0.0	86.7	0.0	0.0		
484	0.0	11.2	0.0	83.0	0.0	0.0		6.5
486	0.0	0.0	0.0	95.8	0.0	0.0		69.2

Mineralogical Composition of North Core at North Ingebright Lake

Depth (cm)	Magnesite	Gypsum	Anhydrite	Thenardite	Bloedite	Halite	Mg in High Mg Calcite	Ca in Protodolomite
488	0.0	33.6	0.0	62.7	0.0	0.0		63.4
490	0.0	8.6	0.0	86.3	0.0	0.0		
492	0.0	0.0	0.0	98.3	0.0	0.0		
494	0.0	7.8	0.0	87.4	0.0	0.0		6.7
496	0.0	5.9	0.0	92.7	0.0	0.0		
498	0.0	20.3	0.0	78.9	0.0	0.0		
500	0.0	0.0	0.0	94.3	0.0	0.0	9.9	
502	0.0	32.4	0.0	66.1	0.0	0.0		
504	0.0	0.0	0.0	98.6	0.0	0.0		
506	0.0	0.0	0.0	94.5	0.0	0.0		6.7
508	0.0	22.8	0.0	73.3	0.0	0.0		62.9
510	0.0	12.7	0.0	84.0	0.0	0.0		5.6
512	0.0	9.1	0.0	52.0	0.0	0.0		62.9
514	0.0	15.9	0.0	77.2	0.0	0.0		52.8
516	0.0	9.1	0.0	52.0	0.0	0.0		62.9
518	0.0	10.1	0.0	49.1	0.0	0.0		62.5
520	0.0	11.9	0.0	58.4	0.0	0.0		62.6
522	0.0	16.0	0.0	79.7	0.0	0.0		61.7
526	0.0	8.5	0.0	90.4	0.0	0.0		
528	0.0	0.0	0.0	96.2	0.0	0.0		
532	0.0	0.0	0.0	88.5	0.0	0.0		
534	0.0	0.0	0.0	93.2	0.0	0.0		
536	0.0	0.0	0.0	68.4	0.0	0.0		64.9
538	0.0	0.0	0.0	91.0	0.0	0.0		
540	0.0	0.0	0.0	98.9	0.0	0.0		
542	0.0	0.0	0.0	95.6	0.0	0.0		65.7
544	0.0	0.0	0.0	70.8	0.0	0.0		58.7
546	0.0	7.1	0.0	91.9	0.0	0.0		
548	0.0	6.7	0.0	92.7	0.0	0.0		
550	0.0	0.0	0.0	66.4	0.0	0.0		62.5
552	0.0	8.2	0.0	86.7	0.0	0.0		6.6
554	3.1	6.0	0.0	69.1	0.0	0.0		
556	0.0	0.0	0.0	58.4	0.0	0.0		65.4
558	0.0	0.0	0.0	97.1	0.0	0.0		
560	0.0	0.0	0.0	91.7	0.0	0.0		62.4
564	2.6	0.0	0.0	45.2	0.0	0.0		61.9
566	0.0	0.0	0.0	52.1	0.0	0.0		63.7
568	0.0	15.4	0.0	52.5	0.0	0.0		62.1
570	0.0	3.9	0.0	50.4	0.0	0.0		

Mineralogical Composition of North Core at North Ingebright Lake

Depth (cm)	Magnesite	Gypsum	Anhydrite	Thenardite	Bloedite	Halite	Mg in High Mg Calcite	Ca in Protodolomite
572	0.0	4.5	0.0	48.5	0.0	0.0		6.8
574	0.0	7.0	0.0	43.7	0.0	0.0		61.3
576	0.0	3.4	0.0	60.1	0.0	0.0		
578	0.0	3.4	0.0	48.8	0.0	0.0		64.9
580	0.0	0.0	0.0	64.1	0.0	0.0		60.0
582	0.0	0.0	0.0	61.3	0.0	0.0		63.7
584	0.0	0.0	0.0	60.9	0.0	0.0		66.3
586	0.0	0.0	0.0	54.1	0.0	0.0		
588	0.0	0.0	0.0	51.8	0.0	0.0		62.3
590	0.0	0.0	0.0	56.6	0.0	0.0		
592	0.0	0.0	0.0	69.1	0.0	0.0		
594	0.0	9.8	0.0	51.9	0.0	0.0		
596	0.0	0.0	0.0	57.3	0.0	0.0		
598	4.2	6.3	0.0	34.5	0.0	0.0		63.7
600	3.3	10.0	0.0	61.4	0.0	0.0		67.9
602	0.0	6.2	0.0	41.4	0.0	0.0		61.4
604	5.1	0.0	0.0	31.5	0.0	0.0		65.4
606	3.6	7.4	0.0	49.1	0.0	0.0		75.3
608	4.0	4.4	0.0	55.8	0.0	0.0		6.3
616	0.0	5.7	0.0	58.7	0.0	0.0		
618	0.0	0.0	0.0	61.4	0.0	0.0		
620	0.0	0.0	0.0	65.2	0.0	0.0		64.2
622	0.0	7.5	0.0	55.6	0.0	0.0		
624	0.0	5.0	0.0	50.9	0.0	0.0		61.3
626	0.0	0.0	0.0	53.0	0.0	0.0		
628	0.0	6.2	0.0	57.4	0.0	0.0		65.4
630	0.0	8.3	0.0	55.4	0.0	0.0		63.8
634	0.0	10.7	0.0	52.0	0.0	0.0		61.9
636	0.0	0.0	0.0	14.1	0.0	0.0		66.9
638	0.0	0.0	0.0	62.2	0.0	0.0		63.5
640	0.0	0.0	0.0	57.8	0.0	0.0		
642	0.0	0.0	0.0	49.8	0.0	0.0		63.2
644	0.0	0.0	0.0	56.9	0.0	0.0		
646	0.0	16.3	0.0	51.8	0.0	0.0		63.6
648	0.0	6.9	0.0	52.7	0.0	0.0		65.3
650	0.0	0.0	0.0	58.2	0.0	0.0		
652	0.0	6.7	0.0	49.7	0.0	0.0		61.8
654	0.0	9.1	0.0	54.1	0.0	0.0		62.7
656	0.0	0.0	0.0	62.4	0.0	0.0		

Mineralogical Composition of North Core at North Ingebright Lake

Depth (cm)	Magnesite	Gypsum	Anhydrite	Thenardite	Bloedite	Halite	Mg in High Mg Calcite	Ca in Protodolomite
658	0.0	0.0	0.0	65.1	0.0	0.0		56.7
660	0.0	0.0	0.0	92.5	0.0	0.0		64.9
662	0.0	4.4	0.0	49.8	0.0	0.0		6.8
664	0.0	0.0	0.0	62.9	0.0	0.0		
666	0.0	6.4	0.0	57.9	0.0	0.0		
668	0.0	6.3	0.0	57.5	0.0	0.0		
670	0.0	4.2	0.0	58.4	0.0	0.0		6.9
672	0.0	0.0	0.0	59.5	0.0	0.0		65.7
674	0.0	0.0	0.0	55.3	0.0	0.0		
676	0.0	4.0	0.0	55.3	0.0	0.0		61.5
678	0.0	5.6	0.0	58.5	0.0	0.0		65.5
680	0.0	12.6	0.0	83.7	0.0	0.0		61.3
682	0.0	0.0	0.0	96.3	0.0	0.0		62.8
684	0.0	0.0	0.0	97.7	0.0	0.0		
686	0.0	0.0	0.0	93.4	0.0	0.0		
688	0.0	72.4	0.0	26.3	0.0	0.0		
690	0.0	0.0	0.0	98.9	0.0	0.0		
692	0.0	7.6	0.0	89.1	0.0	0.0		
694	0.0	11.1	0.0	86.1	0.0	0.0		64.7
696	0.0	0.0	0.0	97.1	0.0	0.0		
698	0.0	0.0	0.0	97.2	0.0	0.0		68.9
700	0.0	0.0	0.0	92.0	0.0	0.0		
702	0.0	0.0	0.0	0.0	0.0	0.0		64.7
704	0.0	0.0	0.0	72.7	0.0	0.0		67.0
706	0.0	0.0	0.0	97.6	0.0	0.0		
708	0.0	11.9	0.0	84.8	0.0	0.0		62.5
710	0.0	0.0	0.0	99.3	0.0	0.0		
714	0.0	13.9	0.0	85.3	0.0	0.0		
716	0.0	0.0	0.0	98.7	0.0	0.0		
718	0.0	16.5	0.0	80.6	0.0	0.0		64.4
720	0.0	0.0	0.0	98.9	0.0	0.0		
722	0.0	6.0	0.0	90.6	0.0	0.0		
724	0.0	0.0	0.0	74.4	0.0	0.0		54.5
728	0.0	0.0	0.0	93.3	0.0	0.0		
730	0.0	12.2	0.0	64.4	0.0	0.0		68.7
732	0.0	7.8	0.0	62.2	0.0	0.0		63.8
734	0.0	0.0	0.0	74.2	0.0	0.0		53.2
736	0.0	7.6	0.0	87.6	0.0	0.0		
738	3.6	19.9	0.0	70.5	0.0	0.0		64.3

Mineralogical Composition of North Core at North Ingebright Lake

Depth (cm)	Magnesite	Gypsum	Anhydrite	Thenardite	Bloedite	Halite	Mg in High Mg Calcite	Ca in Protodolomite
740	0.0	0.0	0.0	97.8	0.0	0.0		
746	0.0	8.5	0.0	65.8	0.0	0.0		65.9
748	0.0	0.0	0.0	96.7	0.0	0.0		63.6
750	0.0	6.2	0.0	64.4	0.0	0.0		65.4
752	2.6	8.0	0.0	65.0	0.0	0.0	9.1	66.2
754	0.0	13.6	0.0	58.7	0.0	0.0		66.6
756	4.2	0.0	0.0	90.6	0.0	0.0		67.5
758	0.0	5.3	0.0	71.8	0.0	0.0		62.8
760	6.2	0.0	0.0	90.3	0.0	0.0		61.7
762	0.0	9.4	0.0	71.9	0.0	0.0		61.7
764	0.0	6.2	0.0	88.3	0.0	0.0		
792	0.0	6.5	0.0	90.8	0.0	0.0		62.9
794	0.0	0.0	0.0	78.4	0.0	0.0		
796	0.0	6.7	0.0	75.4	0.0	0.0		66.4
798	2.3	0.0	0.0	97.7	0.0	0.0		
800	0.0	8.4	0.0	67.9	0.0	0.0		61.7
802	0.0	8.5	0.0	89.5	0.0	0.0		64.0
804	0.0	8.2	0.0	89.7	0.0	0.0		
806	0.0	12.3	0.0	87.1	0.0	0.0		
808	3.2	6.0	0.0	61.6	0.0	0.0		63.9
810	0.0	9.2	0.0	87.4	0.0	0.0		68.6
812	0.0	0.0	0.0	70.9	0.0	0.0		63.9
814	0.0	11.2	0.0	68.9	0.0	0.0		
816	0.0	0.0	0.0	77.2	0.0	0.0		
818	3.5	7.6	0.0	84.6	0.0	0.0		62.3
820	0.0	8.9	0.0	65.7	0.0	0.0		66.9
822	5.2	31.9	0.0	57.6	0.0	0.0		68.7
824	0.0	20.2	0.0	57.2	0.0	0.0		62.6
826	2.4	10.2	0.0	58.2	0.0	0.0		65.3
828	4.6	9.9	0.0	53.8	0.0	0.0		67.6
830	4.2	10.5	0.0	51.5	0.0	0.0		65.6
832	0.0	11.4	0.0	79.3	0.0	0.0		62.8
834	3.2	7.9	0.0	56.9	0.0	0.0		63.9
836	4.3	12.5	0.0	49.5	0.0	0.0		64.1
838	5.1	9.6	0.0	43.5	0.0	0.0		62.7
840	0.0	9.0	0.0	66.5	0.0	0.0		62.8
842	0.0	10.3	0.0	59.2	0.0	0.0		64.0
844	3.6	12.5	0.0	51.9	0.0	0.0		62.8
846	3.2	6.9	8.2	49.7	0.0	0.0		66.6

Mineralogical Composition of North Core at North Ingebright Lake

Depth (cm)	Magnesite	Gypsum	Anhydrite	Thenardite	Bloedite	Halite	Mg in High Mg Calcite	Ca in Protodolomite
848	0.0	8.0	0.0	52.5	0.0	0.0		62.9
850	0.0	17.5	0.0	51.2	0.0	0.0		62.6
852	0.0	11.9	0.0	77.5	0.0	0.0		6.7
856	0.0	22.2	0.0	72.4	0.0	0.0		64.7
860	0.0	17.3	0.0	59.2	0.0	0.0		65.3
862	0.0	14.4	0.0	58.2	0.0	0.0		64.5
864	2.8	26.2	0.0	45.3	0.0	0.0		64.2
866	0.0	17.8	0.0	20.4	0.0	0.0		66.4
868	3.4	15.8	0.0	44.6	0.0	0.0		68.9
870	0.0	17.3	0.0	45.1	19.6	0.0		65.3
872	0.0	36.9	0.0	56.9	0.0	0.0		67.7
874	0.0	14.7	0.0	68.3	0.0	0.0		62.7
876	0.0	20.0	0.0	48.0	0.0	0.0		64.6
878	0.0	16.5	0.0	55.3	0.0	0.0		63.9
880	0.0	31.5	0.0	65.5	0.0	0.0		66.5
882	0.0	14.9	0.0	64.8	0.0	0.0		64.9
884	0.0	21.0	0.0	74.9	0.0	0.0		65.4
886	0.0	11.6	0.0	60.7	0.0	0.0		67.6
888	0.0	19.6	0.0	55.5	0.0	0.0		65.5
890	0.0	78.0	0.0	20.8	0.0	0.0		63.6
892	0.0	19.6	0.0	61.6	0.0	0.0		65.4
894	0.0	7.1	0.0	68.5	0.0	0.0		64.4
896	2.6	20.6	0.0	75.8	0.0	0.0		
898	1.5	51.9	0.0	30.6	0.0	0.0		65.6
900	2.3	9.3	0.0	63.8	0.0	0.0		64.6
902	0.0	17.4	0.0	56.5	0.0	0.0		63.9
904	0.0	20.3	0.0	57.9	0.0	0.0		62.7
906	0.0	23.9	0.0	68.2	0.0	0.0		62.5
908	3.5	20.6	0.0	72.8	0.0	0.0		63.7
910	0.0	18.0	0.0	65.2	0.0	0.0		67.3
912	0.0	15.7	0.0	61.4	0.0	0.0		66.5
914	5.3	0.0	0.0	45.2	0.0	0.0		64.6
916	4.4	17.0	0.0	35.6	0.0	0.0		64.4
918	0.0	0.0	0.0	52.6	0.0	0.0		65.2
920	0.0	0.0	0.0	77.8	0.0	0.0		
924	3.2	31.8	0.0	37.7	0.0	0.0		62.8
926	0.0	21.2	0.0	73.3	0.0	0.0		61.8
928	0.0	15.4	0.0	59.4	0.0	0.0		65.6
930	3.1	16.4	0.0	58.2	0.0	0.0		63.7

Mineralogical Composition of North Core at North Ingebright Lake

Depth (cm)	Magnesite	Gypsum	Anhydrite	Thenardite	Bloedite	Halite	Mg in High Mg Calcite	Ca in Protodolomite
932	0.0	15.8	0.0	60.2	0.0	0.0		65.8
934	0.0	15.5	0.0	61.3	0.0	0.0		64.3
936	3.2	12.9	0.0	58.4	0.0	0.0		64.8
938	0.0	23.4	0.0	56.8	0.0	0.0		68.7
940	3.3	9.8	0.0	66.4	0.0	0.0		63.4
942	0.0	0.0	0.0	73.8	0.0	0.0		62.9
944	0.0	0.7	0.0	96.2	0.0	0.0		64.5
946	0.0	5.5	0.0	71.1	0.0	0.0		63.7
948	0.0	10.7	0.0	84.8	0.0	0.0		66.3
950	0.0	0.0	0.0	96.4	0.0	0.0		
952	0.0	0.0	0.0	74.8	0.0	0.0		64.1
954	0.0	5.3	0.0	69.5	0.0	0.0		63.3
956	0.0	8.0	0.0	69.4	0.0	0.0		65.2
958	0.0	0.0	0.0	72.2	0.0	0.0		67.1
960	0.0	10.9	0.0	84.0	0.0	0.0		6.9
962	0.0	24.9	0.0	74.3	0.0	0.0		
964	0.0	15.1	0.0	32.9	0.0	0.0		
972	0.0	22.1	0.0	59.6	0.0	0.0		62.8
974	0.0	46.0	0.0	41.2	0.0	0.0		
976	2.6	10.9	0.0	63.2	0.0	0.0		62.8
978	0.0	20.8	0.0	54.3	0.0	0.0		61.2
980	0.0	13.3	0.0	83.5	0.0	0.0		62.5
982	0.0	12.8	0.0	68.2	0.0	0.0		61.5
984	0.0	11.8	0.0	64.9	0.0	0.0		
986	3.1	11.3	0.0	60.7	0.0	0.0		64.3
988	0.0	10.4	0.0	87.1	0.0	0.0		64.4
990	3.7	6.6	0.0	70.9	0.0	0.0		63.4
992	0.0	29.8	0.0	54.3	0.0	0.0		63.9
994	2.7	24.0	0.0	47.8	0.0	0.0	4.7	64.4
996	2.8	45.9	0.0	27.6	0.0	0.0		62.0
998	2.7	43.2	0.0	33.9	0.0	0.0		66.4
1,000	4.3	13.2	0.0	44.4	0.0	0.0		63.9
1,002	0.0	8.6	0.0	66.0	0.0	0.0		65.8
1,004	0.0	13.4	0.0	64.1	0.0	0.0		6.8
1,006	0.0	9.5	0.0	84.3	0.0	0.0	6.0	
1,008	2.5	15.7	0.0	60.8	0.0	0.0		
1,010	0.0	0.0	0.0	93.8	0.0	0.0		65.6
1,012	3.2	9.8	0.0	82.3	0.0	3.6		
1,014	4.0	14.9	0.0	54.6	0.0	0.0		6.6

Mineralogical Composition of North Core at North Ingebright Lake

Depth (cm)	Magnesite	Gypsum	Anhydrite	Thenardite	Bloedite	Halite	Mg in High Mg Calcite	Ca in Protodolomite
1,016	4.4	8.2	0.0	50.0	0.0	2.1		62.7
1,018	4.3	0.0	0.0	65.9	0.0	0.0		68.7
1,020	2.6	16.3	0.0	55.8	0.0	0.0		62.7
1,022	0.0	6.6	0.0	71.8	0.0	0.0		61.6
1,024	3.0	15.5	0.0	57.0	0.0	0.0		63.3
1,026	2.7	9.4	0.0	63.1	0.0	0.0		63.9
1,028	0.0	16.0	0.0	61.7	0.0	0.0		61.3
1,030	3.2	17.4	0.0	52.2	0.0	0.0		62.1
1,032	0.0	39.4	0.0	52.2	0.0	0.0		
1,034	3.3	9.0	0.0	61.3	0.0	0.0		64.9
1,036	0.0	11.6	0.0	86.7	0.0	0.0		63.6
1,038	0.0	18.9	0.0	80.5	0.0	0.0		
1,040	0.0	8.2	0.0	91.8	0.0	0.0		
1,042	0.0	18.8	0.0	79.8	0.0	0.0		
1,044	1.9	5.7	0.0	89.7	0.0	0.0		
1,046	1.4	11.4	0.0	71.1	0.0	0.0		
1,048	3.2	8.5	0.0	64.6	0.0	0.0		6.0
1,050	4.1	5.8	0.0	65.6	0.0	0.0		62.7
1,052	0.0	12.0	0.0	83.9	0.0	0.0		
1,054	3.4	12.8	0.0	63.7	0.0	0.0		64.2
1,056	3.4	13.7	0.0	63.3	0.0	0.0		62.6
1,058	0.0	14.9	0.0	80.9	0.0	0.0		63.4
1,060	0.0	16.5	0.0	79.6	0.0	0.0		6.7
1,062	0.0	9.5	0.0	82.4	0.0	0.0		59.8
1,064	0.0	24.7	0.0	72.6	0.0	0.0		
1,066	0.0	79.9	0.0	18.8	0.0	0.0		6.2
1,068	0.0	9.7	0.0	66.7	0.0	0.0		59.5
1,070	0.0	23.6	0.0	64.6	0.0	0.0		62.2
1,072	0.0	18.9	0.0	78.0	0.0	0.0		67.7
1,074	0.0	15.2	0.0	60.6	0.0	0.0		6.4
1,076	0.0	18.5	0.0	63.1	0.0	0.0		61.3
1,078	0.0	11.7	0.0	85.1	0.0	0.0		61.7
1,080	0.0	9.7	0.0	87.2	0.0	0.0		67.7
1,082	0.0	20.2	0.0	65.7	0.0	0.0		
1,084	0.0	0.0	0.0	94.6	0.0	0.0		62.3
1,086	4.2	6.5	0.0	58.9	0.0	0.0		65.2
1,088	0.0	33.0	0.0	48.3	0.0	0.0		63.5
1,090	4.8	11.4	0.0	78.1	0.0	0.0		68.2
1,092	0.0	13.2	0.0	83.7	0.0	0.0		

Mineralogical Composition of North Core at North Ingebright Lake

Depth (cm)	Magnesite	Gypsum	Anhydrite	Thenardite	Bloedite	Halite	Mg in High Mg Calcite	Ca in Protodolomite
1,094	11.9	67.7	0.0	11.6	0.0	0.0		63.6
1,096	0.0	10.1	0.0	88.5	0.0	0.0		
1,098	0.0	14.8	0.0	83.9	0.0	0.0		
1,100	0.0	0.0	0.0	98.9	0.0	0.0	4.8	
1,102	0.0	10.1	0.0	89.2	0.0	0.0		77.6
1,104	0.0	0.0	0.0	100.0	0.0	0.0		
1,106	0.0	10.7	0.0	86.8	0.0	0.0		64.6
1,108	0.0	14.9	0.0	80.6	0.0	3.2		
1,110	0.0	0.0	0.0	90.2	0.0	0.0		
1,112	0.0	17.4	0.0	81.1	0.0	0.0		65.3
1,114	0.0	31.5	0.0	68.5	0.0	0.0		
1,116	0.0	46.6	0.0	51.6	0.0	0.0		
1,118	0.0	16.0	0.0	80.5	0.0	0.0		6.5
1,120	0.0	10.8	0.0	87.0	0.0	0.0		64.4
1,122	0.0	36.9	0.0	62.8	0.0	0.0		
1,124	0.0	33.3	0.0	66.5	0.0	0.0		
1,126	0.0	16.9	0.0	83.1	0.0	0.0		
1,128	0.0	50.7	0.0	37.6	0.0	0.0		
1,130	2.8	17.2	0.0	60.9	0.0	0.0		
1,132	0.0	18.9	0.0	71.3	0.0	0.0		
1,134	0.0	62.6	0.0	34.6	0.0	0.0		
1,136	0.0	20.0	0.0	71.8	0.0	0.0		
1,138	0.0	11.5	0.0	88.1	0.0	0.0		
1,140	0.0	41.1	0.0	50.9	0.0	0.0		
1,142	0.0	16.0	0.0	82.4	0.0	0.0		
1,144	0.0	0.0	0.0	96.9	0.0	0.0		68.5
1,148	0.0	14.3	0.0	84.5	0.0	0.0		
1,150	0.0	10.0	0.0	77.0	0.0	0.0		
1,152	0.0	29.1	0.0	70.6	0.0	0.0		
1,154	0.0	41.1	0.0	57.0	0.0	0.0		62.3
1,156	0.0	20.1	0.0	77.9	0.0	0.0		65.2
1,158	0.0	12.3	0.0	86.2	0.0	0.0		
1,160	0.0	18.4	0.0	64.3	0.0	0.0		61.7
1,162	0.0	19.4	0.0	78.3	0.0	0.0		61.2
1,164	0.0	24.7	0.0	56.0	0.0	0.0		61.8
1,166	0.0	10.0	0.0	72.1	0.0	0.0	9.7	59.5
1,168	0.0	11.6	0.0	85.3	0.0	0.0		63.9
1,170	0.0	33.8	0.0	63.0	0.0	0.0		61.2
1,172	0.0	9.6	0.0	90.4	0.0	0.0		

Mineralogical Composition of North Core at North Ingebright Lake

Depth (cm)	Magnesite	Gypsum	Anhydrite	Thenardite	Bloedite	Halite	Mg in High Mg Calcite	Ca in Protodolomite
1,174	3.1	11.8	0.0	57.6	0.0	0.0		62.2
1,176	0.0	27.9	0.0	64.9	0.0	0.0		61.6
1,178	0.0	17.6	0.0	82.4	0.0	0.0		
1,180	0.0	23.6	0.0	72.7	0.0	0.0		66.6
1,182	0.0	28.5	0.0	70.2	0.0	0.0		
1,184	0.0	10.2	0.0	85.0	0.0	0.0		62.3
1,186	0.0	7.1	0.0	91.4	0.0	0.0		61.8
1,188	0.0	0.0	0.0	86.4	0.0	0.0		
1,190	0.0	8.2	0.0	91.3	0.0	0.0		
1,192	0.0	20.9	0.0	79.1	0.0	0.0		
1,194	0.0	0.0	0.0	98.9	0.0	0.0		
1,198	0.0	0.0	0.0	88.5	0.0	0.0		
1,200	0.0	0.0	0.0	92.5	0.0	0.0		
1,202	0.0	0.0	0.0	98.4	0.0	0.0		61.9
1,204	0.0	0.0	0.0	98.2	0.0	0.0		
1,206	0.0	5.2	0.0	75.1	0.0	0.0		
1,208	0.0	7.5	0.0	80.5	0.0	0.0		
1,210	1.8	0.0	0.0	87.3	0.0	0.0		
1,212	0.0	0.0	0.0	98.8	0.0	0.0		
1,214	0.0	0.0	0.0	100.0	0.0	0.0		
1,216	0.0	0.0	0.0	89.7	0.0	0.0		
1,218	0.0	0.0	0.0	89.2	0.0	0.0		
1,220	0.0	6.0	0.0	84.7	0.0	0.0		
1,222	0.0	0.0	0.0	85.6	0.0	0.0		
1,224	0.0	0.0	0.0	87.9	0.0	0.0		
1,326	0.0	0.0	0.0	73.6	0.0	0.0		62.8
1,328	0.0	0.0	0.0	86.2	0.0	0.0		62.0
1,330	0.0	9.0	0.0	77.8	0.0	0.0		6.6
1,332	0.0	0.0	0.0	89.5	0.0	0.0		58.7
1,334	0.0	0.0	0.0	87.0	0.0	0.0		
1,336	0.0	6.1	0.0	80.4	0.0	0.0		
1,338	1.5	0.0	0.0	59.2	0.0	0.0		
1,340	0.0	13.9	0.0	79.8	0.0	0.0	7.3	59.5
1,342	0.0	0.0	0.0	81.0	0.0	0.0		61.7
1,344	0.0	18.4	0.0	74.5	0.0	0.0		
1,346	0.0	34.7	0.0	57.9	0.0	0.0	7.2	
1,348	0.0	9.4	0.0	88.0	0.0	0.0		
1,350	0.0	0.0	0.0	87.1	0.0	0.0		53.2
1,352	0.0	0.0	0.0	79.2	0.0	0.0		56.4

Mineralogical Composition of North Core at North Ingebright Lake

Depth (cm)	Magnesite	Gypsum	Anhydrite	Thenardite	Bloedite	Halite	Mg in High Mg Calcite	Ca in Protodolomite
1,354	0.0	12.5	0.0	79.6	0.0	0.0		57.3
1,356	4.1	8.8	0.0	81.2	0.0	0.0	3.8	
1,358	0.0	16.6	0.0	40.3	21.2	0.0	14.3	52.6
1,360	0.0	22.3	0.0	51.8	19.4	0.0		54.3
1,362	0.0	25.0	0.0	63.1	0.0	3.0		51.7
1,364	0.0	22.8	0.0	45.1	22.6	0.0		
1,366	0.0	9.0	0.0	82.2	0.0	0.0		
1,368	3.0	21.7	0.0	68.8	0.0	0.0		61.6
1,370	0.0	7.4	0.0	45.2	27.1	0.0		
1,372	0.0	9.2	0.0	50.0	0.0	3.3		63.8
1,374	0.0	13.2	0.0	81.3	0.0	0.0		55.4
1,376	4.5	7.6	0.0	47.3	0.0	0.0		65.9
1,380	4.1	7.2	0.0	54.9	0.0	0.0		66.0
1,382	4.7	10.1	0.0	48.1	0.0	0.0	11.4	75.9
1,384	3.0	4.9	0.0	50.5	0.0	0.0		61.6
1,386	6.9	8.7	0.0	72.6	0.0	0.0		62.6
1,388	4.8	6.1	0.0	39.9	0.0	0.0		65.9
1,390	4.0	10.8	0.0	54.1	0.0	0.0		64.9
1,392	9.7	16.0	0.0	65.3	0.0	0.0		69.8
1,394	5.9	5.8	0.0	41.8	0.0	0.0	6.4	61.5
1,396	3.1	7.2	0.0	65.1	0.0	0.0		65.5
1,398	3.4	0.0	0.0	75.9	0.0	0.0		63.5
1,400	3.2	13.8	0.0	61.0	0.0	0.0		6.5
1,402	0.0	6.1	0.0	72.3	0.0	0.0		64.6
1,404	3.0	5.4	0.0	60.8	0.0	0.0		64.7
1,406	5.1	12.0	0.0	46.6	0.0	0.0		63.5
1,408	0.0	0.0	0.0	99.5	0.0	0.0		
1,410	0.5	4.0	0.0	91.8	0.0	0.0		63.3
1,412	5.8	0.0	0.0	87.5	0.0	0.0		67.4
1,414	0.0	0.0	0.0	97.8	0.0	0.0		
1,416	0.0	0.0	0.0	100.0	0.0	0.0		
1,418	0.0	0.0	0.0	99.6	0.0	0.0		
1,420	0.0	0.0	0.0	100.0	0.0	0.0		
1,422	0.0	0.0	0.0	100.0	0.0	0.0		
1,424	0.0	0.0	0.0	100.0	0.0	0.0		
1,426	0.0	0.0	0.0	98.5	0.0	0.0		6.8
1,428	6.8	0.0	0.0	89.7	0.0	0.0		67.8
1,430	0.0	0.0	0.0	96.2	0.0	0.0		72.8
1,432	0.0	0.0	0.0	98.5	0.0	0.0		62.2

Mineralogical Composition of North Core at North Ingebright Lake

Depth (cm)	Magnesite	Gypsum	Anhydrite	Thenardite	Bloedite	Halite	Mg in High Mg Calcite	Ca in Protodolomite
1,434	0.0	0.0	0.0	98.1	0.0	0.0		68.7
1,436	5.0	0.0	0.0	89.9	0.0	0.0		58.1
1,438	0.0	0.0	0.0	76.7	0.0	0.0		6.4
1,440	0.0	0.0	0.0	100.0	0.0	0.0		
1,442	0.0	0.0	0.0	82.4	0.0	0.0		61.8
1,444	0.0	0.0	0.0	69.8	0.0	0.0		67.9
1,446	3.3	0.0	0.0	69.5	0.0	0.0	16.9	65.8
1,448	0.0	0.0	0.0	77.2	0.0	0.0		61.6
1,450	0.0	0.0	0.0	67.3	0.0	0.0		62.2
1,452	3.0	0.0	0.0	74.9	0.0	0.0		62.7
1,454	0.0	0.0	0.0	97.1	0.0	0.0		62.9
1,456	0.0	0.0	0.0	77.8	0.0	0.0		61.4
1,458	0.0	4.9	0.0	80.9	0.0	0.0		64.4
1,460	0.0	0.0	0.0	97.8	0.0	0.0		66.7
1,462	0.0	0.0	0.0	80.4	0.0	0.0		59.0
1,464	0.0	0.0	0.0	100.0	0.0	0.0		
1,466	0.0	0.0	0.0	100.0	0.0	0.0		
1,468	4.4	0.0	0.0	63.3	0.0	0.0		58.9
1,470	0.0	0.0	0.0	99.4	0.0	0.0		
1,472	0.0	0.0	0.0	79.2	0.0	0.0		
1,474	0.0	0.0	0.0	99.5	0.0	0.0		
1,476	0.0	0.0	0.0	100.0	0.0	0.0		
1,478	2.0	0.0	0.0	98.0	0.0	0.0		
1,480	0.0	0.0	0.0	99.6	0.0	0.0		
1,482	4.8	0.0	0.0	73.6	0.0	0.0		63.4
1,484	2.7	0.0	0.0	78.3	0.0	0.0		65.5
1,486	3.9	0.0	0.0	92.0	0.0	0.0		6.3
1,488	0.0	4.2	0.0	91.7	0.0	0.0		64.6
1,490	0.0	0.0	0.0	100.0	0.0	0.0		
1,492	0.0	0.0	0.0	95.9	0.0	0.0	17.3	62.8
1,494	0.0	0.0	0.0	100.0	0.0	0.0		
1,496	0.0	0.0	0.0	98.2	0.0	0.0		65.7
1,498	0.0	0.0	0.0	74.9	0.0	0.0		61.7
1,500	6.7	0.0	0.0	87.4	0.0	0.0		53.7
1,504	0.0	0.0	0.0	95.2	0.0	0.0	6.9	61.7
1,506	0.0	5.8	0.0	91.3	0.0	0.0		63.6
1,508	0.0	0.0	0.0	98.6	0.0	0.0		61.7
1,510	0.0	0.0	0.0	98.8	0.0	0.0		63.6
1,512	4.3	0.0	0.0	68.1	0.0	0.0		62.3

Mineralogical Composition of North Core at North Ingebright Lake

Depth (cm)	Magnesite	Gypsum	Anhydrite	Thenardite	Bloedite	Halite	Mg in High Mg Calcite	Ca in Protodolomite
1,514	0.0	0.0	0.0	75.3	0.0	0.0		67.7
1,516	0.0	0.0	0.0	96.4	0.0	0.0		6.5
1,518	3.0	0.0	0.0	94.3	0.0	0.0		63.2
1,520	0.0	0.0	0.0	97.7	0.0	0.0		
1,522	0.0	24.4	0.0	75.2	0.0	0.0		
1,524	0.0	0.0	0.0	100.0	0.0	0.0		
1,526	0.0	0.0	0.0	90.9	0.0	0.0		
1,528	0.0	4.2	0.0	66.6	0.0	0.0		63.9
1,530	0.0	0.0	0.0	100.0	0.0	0.0		
1,532	0.0	0.0	0.0	86.2	0.0	0.0		
1,534	4.7	6.1	0.0	85.7	0.0	0.0		63.1
1,536	0.0	0.0	0.0	86.4	0.0	0.0		62.1
1,538	0.0	0.0	0.0	98.1	0.0	0.0		
1,540	0.0	0.0	0.0	96.1	0.0	0.0		
1,542	0.0	0.0	0.0	97.2	0.0	0.0		54.5
1,544	0.0	6.0	0.0	94.0	0.0	0.0		
1,546	0.0	0.0	0.0	81.8	0.0	0.0		
1,548	0.0	0.0	0.0	96.5	0.0	0.0		63.4
1,550	0.0	0.0	0.0	98.5	0.0	0.0		62.9
1,552	0.0	0.0	0.0	100.0	0.0	0.0		
1,554	4.2	0.0	0.0	65.5	0.0	0.0		62.9
1,556	4.0	0.0	0.0	67.6	0.0	0.0		62.8
1,558	3.2	0.0	0.0	92.6	0.0	0.0		61.8
1,560	0.0	0.0	0.0	99.2	0.0	0.0		
1,562	3.3	0.0	0.0	93.0	0.0	0.0		62.2
1,564	0.0	0.0	0.0	79.8	0.0	0.0		63.5
1,566	2.5	0.0	0.0	74.0	0.0	0.0		62.7
1,568	3.3	0.0	0.0	65.8	0.0	0.0		6.7
1,570	0.0	0.0	0.0	77.0	0.0	0.0		64.4
1,572	4.0	0.0	0.0	65.3	0.0	0.0		63.2
1,574	0.0	5.2	0.0	94.3	0.0	0.0		
1,576	3.1	0.0	0.0	78.6	0.0	0.0		63.4
1,578	3.1	0.0	0.0	69.6	0.0	0.0		6.5
1,580	0.0	0.0	0.0	100.0	0.0	0.0		
1,582	0.0	0.0	0.0	100.0	0.0	0.0		
1,586	4.2	0.0	0.0	72.6	0.0	0.0		63.4
1,588	6.6	0.0	0.0	47.4	0.0	0.0		62.7
1,590	0.0	0.0	0.0	97.4	0.0	0.0		66.5
1,592	0.0	0.0	0.0	95.1	0.0	0.0		63.6

Mineralogical Composition of North Core at North Ingebright Lake

Depth (cm)	Magnesite	Gypsum	Anhydrite	Thenardite	Bloedite	Halite	Mg in High Mg Calcite	Ca in Protodolomite
1,594	3.3	0.0	0.0	69.3	0.0	0.0		64.0
1,596	4.3	0.0	0.0	62.9	0.0	0.0		63.2
1,598	0.0	0.0	0.0	98.4	0.0	0.0		64.2
1,600	0.0	0.0	0.0	100.0	0.0	0.0		
1,602	0.0	0.0	0.0	100.0	0.0	0.0		
1,604	0.0	0.0	0.0	98.9	0.0	0.0		62.7
1,606	0.0	0.0	0.0	99.0	0.0	0.0		
1,608	1.7	0.0	0.0	98.3	0.0	0.0		
1,610	0.0	0.0	0.0	100.0	0.0	0.0		
1,612	0.0	0.0	0.0	99.8	0.0	0.0		
1,614	0.0	0.0	0.0	100.0	0.0	0.0		
1,616	0.0	0.0	0.0	86.0	0.0	0.0		58.3
1,618	0.0	0.0	0.0	84.1	0.0	0.0		62.9
1,620	0.0	0.0	0.0	84.0	0.0	0.0		62.7
1,622	0.0	0.0	0.0	80.0	0.0	0.0		61.2
1,624	5.1	0.0	0.0	91.9	0.0	0.0		65.8
1,626	3.3	0.0	0.0	75.8	0.0	0.0		64.5
1,628	0.0	0.0	0.0	76.3	0.0	0.0		63.5
1,630	0.0	0.0	0.0	97.2	0.0	0.0		62.4
1,632	0.0	0.0	0.0	98.8	0.0	0.0		65.6
1,634	0.0	0.0	0.0	99.1	0.0	0.0		
1,636	0.0	0.0	0.0	100.0	0.0	0.0		
1,638	0.0	0.0	0.0	87.5	0.0	0.0		
1,640	0.0	0.0	0.0	98.2	0.0	0.0		
1,642	0.0	0.0	0.0	86.1	0.0	0.0		
1,644	0.0	0.0	0.0	86.2	0.0	0.0		64.6
1,646	0.0	7.6	0.0	77.4	0.0	0.0		62.7
1,648	0.0	0.0	0.0	87.4	0.0	0.0		6.8
1,650	0.0	0.0	0.0	85.3	0.0	0.0		
1,652	0.0	6.3	0.0	80.8	0.0	0.0		
1,654	0.0	0.0	0.0	87.2	0.0	0.0		
1,656	0.0	0.0	0.0	90.6	0.0	0.0		
1,658	0.0	0.0	0.0	82.1	0.0	0.0		
1,660	3.2	7.2	0.0	84.7	0.0	0.0		63.2
1,662	3.9	4.3	0.0	67.1	0.0	0.0		65.3
1,664	4.2	0.0	0.0	66.2	0.0	0.0		64.6
1,666	0.0	0.0	0.0	72.7	0.0	0.0		63.5
1,668	0.0	0.0	0.0	79.4	0.0	0.0		66.0
1,670	0.0	0.0	0.0	99.4	0.0	0.0		

Mineralogical Composition of North Core at North Ingebright Lake

Depth (cm)	Magnesite	Gypsum	Anhydrite	Thenardite	Bloedite	Halite	Mg in High Mg Calcite	Ca in Protodolomite
1,672	0.0	0.0	0.0	100.0	0.0	0.0		
1,674	0.0	0.0	0.0	98.4	0.0	0.0	5.6	
1,676	0.0	0.0	0.0	99.5	0.0	0.0		
1,678	0.0	0.0	0.0	96.5	0.0	0.0		63.9
1,680	0.0	0.0	0.0	100.0	0.0	0.0		
1,730	3.3	10.0	0.0	67.7	0.0	0.0		63.2
1,732	2.3	14.0	0.0	65.2	0.0	0.0		62.3
1,734	0.0	10.5	0.0	89.1	0.0	0.0		
1,736	2.7	11.4	0.0	81.0	0.0	0.0		62.3
1,738	2.1	10.7	0.0	65.5	0.0	0.0		64.2
1,740	0.0	0.0	0.0	100.0	0.0	0.0		
1,742	0.0	0.0	0.0	99.4	0.0	0.0		
1,744	0.0	0.0	0.0	100.0	0.0	0.0		
1,746	0.0	0.0	0.0	100.0	0.0	0.0		
1,748	0.0	0.0	0.0	100.0	0.0	0.0		
1,750	0.0	0.0	0.0	100.0	0.0	0.0		
1,752	0.0	0.0	0.0	100.0	0.0	0.0		
1,754	0.0	0.0	0.0	96.7	0.0	0.0	7.3	64.0
1,756	0.0	0.0	0.0	100.0	0.0	0.0		
1,758	0.0	0.0	0.0	100.0	0.0	0.0		
1,760	0.0	0.0	0.0	99.7	0.0	0.0		
1,762	0.0	0.0	0.0	100.0	0.0	0.0		
1,764	0.0	0.0	0.0	100.0	0.0	0.0		
1,766	0.0	0.0	0.0	98.3	0.0	1.7		
1,768	0.0	0.0	0.0	100.0	0.0	0.0		
1,770	4.1	0.0	0.0	67.9	0.0	0.0		64.2
1,772	0.0	0.0	0.0	100.0	0.0	0.0		
1,774	0.0	0.0	0.0	100.0	0.0	0.0		
1,776	0.0	0.0	0.0	100.0	0.0	0.0		
1,778	0.0	6.6	0.0	93.4	0.0	0.0		
1,780	0.0	0.0	0.0	87.5	0.0	0.0		
1,782	0.0	0.0	0.0	100.0	0.0	0.0		
1,786	0.0	0.0	0.0	78.9	0.0	0.0		62.3
1,788	0.0	0.0	0.0	98.7	0.0	0.0		
1,790	0.0	0.0	0.0	100.0	0.0	0.0		
1,792	0.0	0.0	0.0	98.7	0.0	0.0		52.0
1,794	0.0	0.0	0.0	100.0	0.0	0.0		
1,796	0.0	18.2	0.0	79.1	0.0	0.0		63.3
1,798	0.0	8.8	0.0	91.2	0.0	0.0		

Mineralogical Composition of North Core at North Ingebright Lake

Depth (cm)	Magnesite	Gypsum	Anhydrite	Thenardite	Bloedite	Halite	Mg in High Mg Calcite	Ca in Protodolomite
1,800	0.0	0.0	0.0	97.0	0.0	0.0		
1,802	0.0	0.0	0.0	100.0	0.0	0.0		
1,804	0.0	0.0	0.0	100.0	0.0	0.0		
1,806	0.0	0.0	0.0	97.8	0.0	0.0		
1,808	0.0	0.0	0.0	100.0	0.0	0.0		
1,810	0.0	0.0	0.0	100.0	0.0	0.0		
1,812	0.0	0.0	0.0	100.0	0.0	0.0		
1,814	0.0	5.2	0.0	94.3	0.0	0.0		
1,816	0.0	0.0	0.0	100.0	0.0	0.0		
1,818	0.0	0.0	0.0	100.0	0.0	0.0		
1,820	0.0	0.0	0.0	100.0	0.0	0.0		
1,822	0.0	0.0	0.0	80.6	19.4	0.0		
1,824	0.0	0.0	0.0	100.0	0.0	0.0		
1,826	0.0	0.0	0.0	100.0	0.0	0.0		
1,828	0.0	9.4	0.0	90.6	0.0	0.0		
1,830	0.0	0.0	0.0	100.0	0.0	0.0		
1,832	0.0	0.0	0.0	100.0	0.0	0.0		
1,834	0.0	0.0	0.0	100.0	0.0	0.0		
1,836	0.0	0.0	0.0	100.0	0.0	0.0		
1,912	0.0	0.0	0.0	100.0	0.0	0.0		
1,914	0.0	0.0	0.0	100.0	0.0	0.0		
1,916	0.0	0.0	0.0	100.0	0.0	0.0		
1,918	0.0	0.0	0.0	100.0	0.0	0.0		
1,920	0.0	0.0	0.0	100.0	0.0	0.0		
1,922	0.0	0.0	0.0	100.0	0.0	0.0		
1,924	0.0	0.0	0.0	100.0	0.0	0.0		
1,926	0.0	5.0	0.0	82.4	0.0	0.0		61.2
1,928	0.0	0.0	0.0	99.4	0.0	0.0		
1,930	0.0	0.0	0.0	100.0	0.0	0.0		
1,932	0.0	0.0	0.0	100.0	0.0	0.0		
1,934	0.0	0.0	0.0	100.0	0.0	0.0		
1,936	0.0	0.0	0.0	100.0	0.0	0.0		
1,938	0.0	0.0	0.0	100.0	0.0	0.0		
1,940	0.0	0.0	0.0	100.0	0.0	0.0		
1,942	0.0	0.0	0.0	100.0	0.0	0.0		
1,944	0.0	0.0	0.0	100.0	0.0	0.0		
1,946	0.0	0.0	0.0	100.0	0.0	0.0		
1,948	0.0	0.0	0.0	100.0	0.0	0.0		
1,950	0.0	0.0	0.0	100.0	0.0	0.0		

Mineralogical Composition of North Core at North Ingebright Lake

Depth (cm)	Magnesite	Gypsum	Anhydrite	Thenardite	Bloedite	Halite	Mg in High Mg Calcite	Ca in Protodolomite
1,952	0.0	0.0	0.0	100.0	0.0	0.0		
1,954	0.0	0.0	0.0	98.8	0.0	0.0		7.8
1,956	0.0	0.0	0.0	100.0	0.0	0.0		
1,958	0.0	0.0	0.0	100.0	0.0	0.0		
1,960	0.0	0.0	0.0	100.0	0.0	0.0		
1,962	0.0	0.0	0.0	100.0	0.0	0.0		
1,964	0.0	0.0	0.0	100.0	0.0	0.0		
1,966	0.0	0.0	0.0	100.0	0.0	0.0		
1,968	0.0	0.0	0.0	100.0	0.0	0.0		
1,970	0.0	0.0	0.0	100.0	0.0	0.0		
1,974	0.0	0.0	0.0	100.0	0.0	0.0		
1,976	0.0	0.0	0.0	100.0	0.0	0.0		
1,978	0.0	0.0	0.0	100.0	0.0	0.0		
1,980	0.0	0.0	0.0	100.0	0.0	0.0		
1,982	0.0	0.0	0.0	100.0	0.0	0.0		
1,984	0.0	0.0	0.0	100.0	0.0	0.0		
1,986	0.0	0.0	0.0	100.0	0.0	0.0		
1,988	0.0	0.0	0.0	100.0	0.0	0.0		
1,990	0.0	0.0	0.0	100.0	0.0	0.0		
1,992	0.0	0.0	0.0	100.0	0.0	0.0		
1,994	0.0	0.0	0.0	100.0	0.0	0.0		
1,996	0.0	0.0	0.0	100.0	0.0	0.0		
2,000	0.0	0.0	0.0	100.0	0.0	0.0		
2,002	0.0	0.0	0.0	100.0	0.0	0.0		
2,004	0.0	0.0	0.0	100.0	0.0	0.0		
2,006	0.0	0.0	0.0	100.0	0.0	0.0		
2,008	0.0	0.0	0.0	100.0	0.0	0.0		
2,010	0.0	0.0	0.0	100.0	0.0	0.0		
2,012	0.0	0.0	0.0	100.0	0.0	0.0		
2,014	0.0	0.0	0.0	100.0	0.0	0.0		
2,016	0.0	0.0	0.0	100.0	0.0	0.0		
2,018	0.0	0.0	0.0	100.0	0.0	0.0		
2,020	0.0	0.0	0.0	100.0	0.0	0.0		
2,022	0.0	0.0	0.0	100.0	0.0	0.0		
2,024	0.0	0.0	0.0	100.0	0.0	0.0		
2,026	0.0	0.0	0.0	100.0	0.0	0.0		
2,028	0.0	0.0	0.0	100.0	0.0	0.0		
2,030	0.0	0.0	0.0	100.0	0.0	0.0		
2,032	0.0	0.0	0.0	100.0	0.0	0.0		

Mineralogical Composition of North Core at North Ingebright Lake

Depth (cm)	Magnesite	Gypsum	Anhydrite	Thenardite	Bloedite	Halite	Mg in High Mg Calcite	Ca in Protodolomite
2,034	0.0	0.0	0.0	100.0	0.0	0.0		
2,036	0.0	0.0	0.0	100.0	0.0	0.0		
2,038	0.0	0.0	0.0	98.3	0.0	1.7		
2,040	0.0	0.0	0.0	100.0	0.0	0.0		
2,042	0.0	0.0	0.0	100.0	0.0	0.0		
2,044	0.0	0.0	0.0	100.0	0.0	0.0		
2,046	0.0	0.0	0.0	100.0	0.0	0.0		
2,048	0.0	3.4	0.0	56.1	0.0	0.0		
2,052	0.0	0.0	0.0	100.0	0.0	0.0		
2,054	0.0	0.0	0.0	100.0	0.0	0.0		
2,056	0.0	0.0	0.0	100.0	0.0	0.0		
2,058	0.0	0.0	0.0	100.0	0.0	0.0		
2,060	0.0	0.0	0.0	100.0	0.0	0.0		
2,062	0.0	0.0	0.0	100.0	0.0	0.0		
2,064	0.0	0.0	0.0	100.0	0.0	0.0		
2,066	0.0	0.0	0.0	99.1	0.0	0.0		54.0
2,068	0.0	0.0	0.0	100.0	0.0	0.0		
2,070	0.0	0.0	0.0	100.0	0.0	0.0		
2,072	0.0	0.0	0.0	100.0	0.0	0.0		
2,074	0.0	0.0	0.0	98.8	0.0	0.0		70.0
2,076	0.0	0.0	0.0	100.0	0.0	0.0		
2,078	0.0	0.0	0.0	80.1	16.9	0.0		
2,080	0.0	0.0	0.0	100.0	0.0	0.0		
2,082	0.0	0.0	0.0	100.0	0.0	0.0		
2,084	0.0	0.0	0.0	99.3	0.0	0.0		
2,086	0.0	0.0	0.0	100.0	0.0	0.0		
2,088	0.0	0.0	0.0	100.0	0.0	0.0		
2,090	0.0	0.0	0.0	100.0	0.0	0.0		
2,092	0.0	0.0	0.0	100.0	0.0	0.0		
2,094	0.0	0.0	0.0	100.0	0.0	0.0		
2,096	0.0	0.0	0.0	100.0	0.0	0.0		
2,098	0.0	0.0	0.0	100.0	0.0	0.0		
2,100	0.0	0.0	0.0	100.0	0.0	0.0		
2,102	0.0	0.0	0.0	100.0	0.0	0.0		
2,104	0.0	0.0	0.0	98.0	0.0	0.0		64.2
2,108	0.0	0.0	0.0	100.0	0.0	0.0		
2,110	0.0	0.0	0.0	100.0	0.0	0.0		
2,112	0.0	0.0	0.0	100.0	0.0	0.0		
2,114	0.0	0.0	0.0	100.0	0.0	0.0		

Mineralogical Composition of North Core at North Ingebright Lake

Depth (cm)	Magnesite	Gypsum	Anhydrite	Thenardite	Bloedite	Halite	Mg in High Mg Calcite	Ca in Protodolomite
2,116	0.0	0.0	0.0	100.0	0.0	0.0		
2,118	0.0	0.0	0.0	100.0	0.0	0.0		
2,120	0.0	0.0	0.0	100.0	0.0	0.0		
2,122	0.0	0.0	0.0	100.0	0.0	0.0		
2,124	0.0	0.0	0.0	100.0	0.0	0.0		
2,126	0.0	0.0	0.0	100.0	0.0	0.0		
2,128	0.0	0.0	0.0	100.0	0.0	0.0		
2,130	0.0	0.0	0.0	100.0	0.0	0.0		
2,132	0.0	0.0	0.0	100.0	0.0	0.0		
2,134	0.0	0.0	0.0	100.0	0.0	0.0		
2,136	0.0	0.0	0.0	100.0	0.0	0.0		
2,138	0.0	0.0	0.0	100.0	0.0	0.0		
2,140	0.0	0.0	0.0	100.0	0.0	0.0		
2,142	0.0	0.0	0.0	100.0	0.0	0.0		
2,144	0.0	0.0	0.0	100.0	0.0	0.0		
2,146	0.0	0.0	0.0	100.0	0.0	0.0		
2,148	0.0	0.0	0.0	100.0	0.0	0.0		
2,150	0.0	0.0	0.0	100.0	0.0	0.0		
2,152	0.0	0.0	0.0	100.0	0.0	0.0		
2,154	0.0	0.0	0.0	100.0	0.0	0.0		
2,156	0.0	0.0	0.0	100.0	0.0	0.0		
2,158	0.0	0.0	0.0	100.0	0.0	0.0		
2,160	0.0	0.0	0.0	100.0	0.0	0.0		
2,162	0.0	0.0	0.0	100.0	0.0	0.0		
2,164	0.0	0.0	0.0	100.0	0.0	0.0		
2,166	0.0	0.0	0.0	100.0	0.0	0.0		
2,168	0.0	0.0	0.0	100.0	0.0	0.0		
2,170	0.0	0.0	0.0	100.0	0.0	0.0		
2,172	0.0	0.0	0.0	100.0	0.0	0.0		
2,174	0.0	0.0	0.0	100.0	0.0	0.0		
2,176	0.0	0.0	0.0	100.0	0.0	0.0		
2,178	0.0	0.0	0.0	100.0	0.0	0.0		
2,180	0.0	0.0	0.0	100.0	0.0	0.0		
2,182	0.0	0.0	0.0	100.0	0.0	0.0		
2,184	0.0	0.0	0.0	100.0	0.0	0.0		
2,186	0.0	0.0	0.0	99.4	0.0	0.0		
2,188	0.0	0.0	0.0	100.0	0.0	0.0		
2,190	0.0	0.0	0.0	100.0	0.0	0.0		
2,192	0.0	0.0	0.0	100.0	0.0	0.0		

Mineralogical Composition of North Core at North Ingebright Lake

Depth (cm)	Magnesite	Gypsum	Anhydrite	Thenardite	Bloedite	Halite	Mg in High Mg Calcite	Ca in Protodolomite
2,194	0.0	0.0	0.0	100.0	0.0	0.0		
2,196	0.0	0.0	0.0	100.0	0.0	0.0		
2,198	0.0	0.0	0.0	100.0	0.0	0.0		
2,200	0.0	6.0	0.0	94.0	0.0	0.0		
2,202	0.0	0.0	0.0	100.0	0.0	0.0		
2,204	0.0	0.0	0.0	100.0	0.0	0.0		
2,206	0.0	0.0	0.0	100.0	0.0	0.0		
2,208	0.0	0.0	0.0	100.0	0.0	0.0		
2,210	0.0	0.0	0.0	100.0	0.0	0.0		
2,212	0.0	0.0	0.0	100.0	0.0	0.0		
2,214	0.0	0.0	0.0	100.0	0.0	0.0		
2,216	0.0	0.0	0.0	100.0	0.0	0.0		
2,218	0.0	0.0	0.0	100.0	0.0	0.0		
2,220	0.0	5.3	0.0	94.7	0.0	0.0		
2,222	0.0	0.0	0.0	100.0	0.0	0.0		
2,224	0.0	0.0	0.0	100.0	0.0	0.0		
2,226	0.0	0.0	0.0	100.0	0.0	0.0		
2,228	0.0	0.0	0.0	100.0	0.0	0.0		
2,230	0.0	0.0	0.0	100.0	0.0	0.0		
2,232	0.0	0.0	0.0	100.0	0.0	0.0		
2,234	0.0	0.0	0.0	100.0	0.0	0.0		
2,236	0.0	0.0	0.0	100.0	0.0	0.0		
2,238	0.0	0.0	0.0	100.0	0.0	0.0		
2,240	0.0	0.0	0.0	100.0	0.0	0.0		
2,242	0.0	0.0	0.0	100.0	0.0	0.0		
2,244	0.0	0.0	0.0	100.0	0.0	0.0		
2,246	0.0	0.0	0.0	100.0	0.0	0.0		
2,250	0.0	0.0	0.0	100.0	0.0	0.0		
2,252	0.0	0.0	0.0	100.0	0.0	0.0		
2,254	0.0	0.0	0.0	100.0	0.0	0.0		
2,256	0.0	0.0	0.0	100.0	0.0	0.0		
2,258	0.0	0.0	0.0	100.0	0.0	0.0		
2,260	0.0	0.0	0.0	100.0	0.0	0.0		
2,262	0.0	0.0	0.0	100.0	0.0	0.0		
2,264	0.0	0.0	0.0	100.0	0.0	0.0		
2,266	0.0	0.0	0.0	100.0	0.0	0.0		
2,268	0.0	0.0	0.0	100.0	0.0	0.0		
2,270	0.0	0.0	0.0	100.0	0.0	0.0		
2,272	0.0	0.0	0.0	100.0	0.0	0.0		

Mineralogical Composition of North Core at North Ingebright Lake

Depth (cm)	Magnesite	Gypsum	Anhydrite	Thenardite	Bloedite	Halite	Mg in High Mg Calcite	Ca in Protodolomite
2,274	0.0	0.0	0.0	100.0	0.0	0.0		
2,276	0.0	0.0	0.0	100.0	0.0	0.0		
2,280	0.0	0.0	0.0	100.0	0.0	0.0		
2,282	0.0	0.0	0.0	100.0	0.0	0.0		
2,284	0.0	0.0	0.0	100.0	0.0	0.0		
2,286	0.0	0.0	0.0	100.0	0.0	0.0		
2,288	0.0	0.0	0.0	100.0	0.0	0.0		
2,290	0.0	0.0	0.0	100.0	0.0	0.0		
2,292	0.0	0.0	0.0	100.0	0.0	0.0		
2,294	0.0	0.0	0.0	100.0	0.0	0.0		
2,296	0.0	0.0	0.0	100.0	0.0	0.0		

Mineralogical Composition of South Core at North Ingebright Lake

Depth (cm)	Quartz	K-Feldspar	Plag.	Total Clay Miner.	Calcite	Aragonite	High-Mg Calcite	Proto Dolomite	Dolomite
10	11.2	0.0	2.8	0.0	0.0	0.0	0.0	0.0	22.2
12	6.4	0.0	1.6	0.0	0.0	0.0	0.0	12.1	0.0
14	11.5	0.0	2.5	38.0	0.0	0.0	0.0	0.0	19.8
16	11.5	0.0	2.4	38.9	0.0	0.0	0.0	0.0	19.8
18	15.0	0.0	3.0	0.0	0.0	0.0	1.8	0.0	26.1
20	9.3	5.6	2.0	34.8	0.0	0.0	0.0	0.0	15.0
22	11.6	6.0	4.3	44.8	0.0	0.0	1.6	20.6	0.0
24	8.5	0.0	3.1	39.9	0.0	0.0	0.0	0.0	21.1
26	9.7	4.7	3.3	39.8	0.0	0.0	2.5	0.0	17.7
28	15.0	12.9	4.1	0.0	0.0	0.0	0.0	34.9	0.0
30	21.3	0.0	0.0	52.9	0.0	0.0	0.0	25.8	0.0
32	15.3	5.2	2.8	44.3	0.0	0.0	0.0	19.8	0.0
34	30.5	0.0	8.1	0.0	0.0	0.0	0.0	0.0	36.7
36	24.1	0.0	5.4	0.0	0.0	0.0	0.0	0.0	39.0
38	15.1	4.9	10.6	47.8	0.0	0.0	0.0	19.2	0.0
40	42.7	0.0	8.2	0.0	0.0	0.0	0.0	0.0	49.2
42	27.0	0.0	6.0	0.0	0.0	0.0	0.0	0.0	40.4
44	26.9	0.0	9.7	0.0	0.0	0.0	0.0	0.0	39.3
46	19.1	4.9	3.1	37.1	0.0	0.0	2.0	0.0	14.4
48	11.6	5.0	12.5	44.0	0.0	0.0	1.5	0.0	12.5
50	1.9	0.0	1.4	0.0	32.1	0.0	0.0	0.0	1.7
52	6.2	0.0	0.0	0.0	0.0	0.0	0.0	0.0	2.5
54	2.2	0.0	1.8	15.1	0.0	0.0	25.7	0.0	0.0
56	3.0	0.0	0.0	0.0	0.0	0.0	0.0	1.2	0.0
58	0.6	0.0	0.0	0.0	0.0	0.0	0.7	0.0	0.0
60	1.3	0.0	0.0	0.0	0.0	0.0	0.0	0.0	2.2
62	0.0	0.0	0.0	0.0	0.0	0.0	0.0	0.0	0.0
64	0.0	0.0	0.0	0.0	0.0	0.0	0.0	100.0	0.0
66	0.0	0.0	0.0	0.0	0.0	0.0	0.0	0.0	1.0
68	0.0	0.0	0.0	0.0	0.0	0.0	0.0	0.0	0.0
70	0.6	0.0	0.0	0.0	0.0	0.0	0.0	0.0	0.0
72	0.5	0.0	0.0	0.0	0.0	0.0	0.0	0.0	0.0
74	0.0	0.0	0.0	0.0	0.0	0.0	0.0	0.0	0.0
76	0.4	0.0	0.0	0.0	0.0	0.0	0.0	0.0	0.0
78	0.3	0.0	0.0	0.0	0.0	0.0	0.0	0.0	0.0

Mineralogical Composition of South Core at North Ingebright Lake

Depth (cm)	Quartz	K-Feldspar	Plag.	Total Clay Miner.	Calcite	Aragonite	High-Mg Calcite	Proto Dolomite	Dolomite
80	0.5	0.0	0.0	0.0	0.0	0.0	0.0	0.0	0.0
82	0.4	0.0	0.0	0.0	0.0	0.0	0.0	0.0	0.0
84	0.8	0.0	0.0	0.0	0.0	0.0	0.0	0.0	0.0
86	1.1	0.0	0.0	0.0	0.0	0.0	0.0	0.0	0.0
88	0.5	0.0	0.0	0.0	0.0	0.0	0.0	0.0	0.0
90	0.0	0.0	0.0	0.0	0.0	0.0	0.0	0.0	0.0
92	1.0	0.0	0.0	0.0	0.0	0.0	0.0	0.0	0.0
94	0.7	0.0	1.6	0.0	0.0	0.0	0.0	0.0	0.0
96	0.6	0.0	0.0	0.0	0.0	0.0	0.0	0.0	0.0
98	0.3	0.0	0.0	0.0	0.0	0.0	0.0	0.0	0.0
100	0.4	0.0	0.0	0.0	0.0	0.0	0.0	0.0	0.0
102	0.6	0.0	0.0	0.0	0.0	0.0	0.0	0.0	0.0
104	0.0	0.0	0.0	0.0	0.0	0.0	0.0	0.0	0.0
106	0.4	0.0	0.0	0.0	0.0	0.0	0.0	0.0	0.0
108	0.4	0.0	0.0	0.0	0.0	0.0	0.0	0.0	0.0
110	0.0	0.0	0.0	0.0	0.0	0.0	0.0	0.0	1.1
112	0.4	0.0	0.0	0.0	0.0	0.0	0.0	0.0	0.0
114	0.0	0.0	0.0	0.0	0.0	0.0	0.0	0.0	0.0
116	0.0	0.0	0.0	0.0	0.0	0.0	0.0	0.0	0.0
118	0.4	0.0	0.0	0.0	0.0	0.0	0.0	0.0	0.0
120	2.0	0.0	0.0	0.0	0.0	0.0	0.0	0.0	0.0
122	0.9	0.0	0.0	0.0	0.0	0.0	0.0	0.0	0.0
124	0.0	0.0	0.0	0.0	0.0	0.0	0.0	0.0	0.0
126	0.5	0.0	0.0	0.0	0.0	0.0	0.0	0.0	0.0
128	0.6	0.0	0.0	0.0	0.0	0.0	0.0	0.0	0.0
130	0.8	0.0	0.0	0.0	0.0	0.0	0.0	0.0	0.0
132	1.0	0.0	0.0	0.0	0.0	0.0	0.0	0.0	0.0
134	1.0	0.0	0.0	0.0	1.6	0.0	0.0	0.0	0.0
136	0.7	0.0	0.0	0.0	0.0	0.0	0.0	0.0	0.0
138	2.0	0.0	0.0	0.0	0.0	0.0	0.0	0.0	0.0
140	0.9	0.0	0.0	0.0	0.0	0.0	0.0	0.0	0.0
142	1.0	0.0	0.0	0.0	0.0	0.0	0.0	0.0	0.0
144	1.6	0.0	0.0	0.0	0.0	0.0	0.0	0.0	0.0
146	0.0	0.0	0.0	0.0	0.0	0.0	0.0	0.0	0.0
148	0.5	0.0	0.0	0.0	0.0	0.0	0.0	0.0	0.0

Mineralogical Composition of South Core at North Ingebright Lake

Depth (cm)	Quartz	K-Feldspar	Plag.	Total Clay Miner.	Calcite	Aragonite	High-Mg Calcite	Proto Dolomite	Dolomite
150	0.3	0.0	0.0	0.0	0.0	0.0	0.0	0.0	0.0
152	0.5	0.0	0.0	0.0	0.0	0.0	0.0	0.0	0.0
154	1.1	0.0	0.0	0.0	0.0	0.0	0.0	0.0	0.0
156	0.6	0.0	0.0	0.0	0.0	0.0	0.0	0.0	0.0
158	2.2	0.0	0.0	0.0	0.0	0.0	0.0	0.0	0.8
160	0.0	0.0	0.0	0.0	0.0	0.0	0.0	0.0	0.0
162	0.6	0.0	0.0	0.0	0.0	0.0	0.0	0.0	0.0
164	0.8	0.0	0.0	0.0	0.0	0.0	0.0	0.0	0.0
166	0.3	0.0	0.0	0.0	0.0	0.0	0.0	0.0	0.0
168	0.7	0.0	0.0	0.0	0.0	0.0	0.0	0.0	0.0
170	1.1	0.0	0.0	0.0	0.0	0.0	0.0	0.0	0.0
172	0.8	0.0	0.0	0.0	0.0	0.0	0.0	0.0	0.0
174	0.6	0.0	0.0	0.0	0.0	0.0	0.0	0.0	0.0
176	0.9	0.0	0.0	0.0	0.0	0.0	0.0	0.0	0.0
178	0.8	0.0	0.0	0.0	0.0	0.0	0.0	0.0	0.0
180	0.4	0.0	0.0	0.0	0.0	0.0	0.0	0.0	0.0
182	2.9	0.0	0.0	0.0	0.0	0.0	0.0	1.0	0.0
184	0.8	0.0	0.0	0.0	0.0	0.0	0.0	0.0	0.0
186	0.0	0.0	0.0	0.0	0.0	0.0	0.0	0.0	0.0
188	0.5	0.0	0.0	0.0	0.0	0.0	0.0	0.0	0.0
190	0.0	0.0	0.0	0.0	0.0	1.6	0.0	0.0	1.7
192	1.3	0.0	0.0	0.0	0.0	0.0	0.0	0.0	0.0
194	0.8	0.0	0.0	0.0	0.0	0.0	0.0	0.0	0.0
196	1.0	0.0	0.0	0.0	0.0	0.0	0.0	0.0	0.0
198	0.6	0.0	0.0	0.0	0.0	0.0	0.0	0.0	0.0
200	0.4	0.0	0.0	0.0	0.0	0.0	1.2	0.0	0.0
202	0.8	0.0	0.0	0.0	0.0	0.0	0.0	0.0	0.0
204	1.5	0.0	0.0	0.0	0.0	0.0	0.0	0.0	0.0
226	0.5	0.0	0.0	0.0	0.0	0.0	0.0	0.0	0.0
228	2.0	0.0	0.0	0.0	0.0	0.0	0.0	0.0	0.0
230	8.6	0.0	0.0	0.0	0.0	0.0	0.0	0.0	0.0
232	0.9	0.0	0.0	0.0	0.0	0.0	0.0	0.0	0.0
234	0.7	0.0	0.0	0.0	0.0	0.0	0.0	0.0	0.0
236	0.6	0.0	0.0	0.0	0.0	0.0	0.0	0.0	0.0
238	0.6	0.0	0.0	0.0	0.0	0.0	0.0	0.0	0.0

Mineralogical Composition of South Core at North Ingebright Lake

Depth (cm)	Quartz	K-Feldspar	Plag.	Total Clay Miner.	Calcite	Aragonite	High-Mg Calcite	Proto Dolomite	Dolomite
240	0.6	0.0	0.0	0.0	0.0	0.0	0.0	0.0	0.0
242	0.9	0.0	0.0	0.0	0.0	0.0	0.0	0.0	0.0
244	1.1	0.0	0.0	0.0	0.0	0.0	0.0	0.0	0.0
246	1.1	0.0	0.0	0.0	0.0	0.0	0.0	0.0	1.7
248	1.2	0.0	2.6	0.0	0.0	0.0	0.0	0.0	0.0
250	1.2	0.0	0.0	0.0	0.0	0.0	0.0	1.7	0.0
252	2.4	0.0	0.0	0.0	0.0	0.0	0.0	0.0	0.0
254	1.1	0.0	0.0	0.0	0.0	0.0	0.0	0.0	0.0
256	1.3	0.0	0.0	0.0	0.0	0.0	0.0	0.0	0.0
258	0.5	0.0	0.0	0.0	0.0	0.0	0.0	0.0	0.0
260	1.6	0.0	0.0	0.0	0.0	0.0	0.0	0.0	0.0
262	2.0	0.0	0.0	0.0	0.0	0.0	0.0	0.0	1.5
264	2.6	0.0	0.0	0.0	0.0	0.0	0.0	0.0	0.0
266	1.7	0.0	0.0	0.0	0.0	1.4	0.0	0.0	0.0
268	1.0	2.9	0.0	0.0	0.0	0.0	0.0	0.0	0.0
270	1.5	0.0	0.0	23.3	0.0	0.0	0.0	0.0	0.0
272	1.6	0.0	0.0	22.5	0.0	1.2	0.0	0.0	0.0
274	2.4	0.0	0.0	0.0	0.0	0.0	0.0	0.0	0.0
276	1.6	0.0	0.0	0.0	0.0	1.7	0.0	0.0	0.0
278	2.1	0.0	1.6	24.0	0.0	1.7	0.0	1.5	0.0
280	1.4	0.0	0.0	19.5	0.0	0.0	0.0	0.0	0.0
282	3.4	0.0	0.0	0.0	0.0	0.0	0.0	1.7	3.0
284	3.4	0.0	0.0	0.0	0.0	0.0	0.0	0.0	0.0
286	3.2	0.0	0.0	0.0	0.0	0.0	0.0	2.0	0.0
288	3.3	0.0	0.0	0.0	0.0	0.0	0.0	0.0	2.1
290	3.0	2.7	0.0	30.9	0.0	0.0	0.0	1.7	0.0
292	3.4	3.2	0.0	27.0	0.0	0.0	0.0	1.5	2.1
294	4.7	0.0	1.7	28.8	0.0	0.0	1.9	2.3	2.6
296	3.4	0.0	0.0	0.0	0.0	0.0	0.0	0.0	2.2
298	1.7	0.0	0.0	18.9	0.0	0.0	0.0	0.0	0.0
300	2.2	0.0	2.2	0.0	0.0	0.0	0.0	0.0	2.9
302	1.7	0.0	0.0	20.2	0.0	0.0	0.0	1.7	0.0
304	1.5	0.0	0.0	20.4	0.0	0.0	0.0	1.9	1.3
306	3.0	0.0	0.0	0.0	0.0	0.0	0.0	2.0	0.0
308	1.5	0.0	0.0	19.4	0.0	0.0	0.0	0.0	0.0

Mineralogical Composition of South Core at North Ingebright Lake

Depth (cm)	Quartz	K-Feldspar	Plag.	Total Clay Miner.	Calcite	Aragonite	High-Mg Calcite	Proto Dolomite	Dolomite
310	1.5	0.0	0.0	0.0	0.0	0.0	0.0	0.0	0.0
312	1.6	0.0	1.0	0.0	0.0	0.0	0.0	0.0	0.0
314	2.7	0.0	0.0	0.0	0.0	0.0	0.0	1.8	0.0
316	2.1	0.0	0.0	0.0	0.0	0.0	0.0	2.0	0.0
318	2.8	0.0	0.0	0.0	0.0	0.0	0.0	2.5	2.3
320	2.7	0.0	0.0	23.2	0.0	0.0	1.3	2.2	2.0
322	1.8	0.0	0.0	19.2	0.0	0.0	0.0	1.9	1.5
324	1.4	0.0	0.0	22.1	0.0	0.0	0.0	1.5	0.0
326	4.7	0.0	0.0	39.7	0.0	0.0	0.0	3.0	2.0
328	2.5	0.0	1.2	34.8	0.0	0.0	1.2	2.2	0.0
330	2.3	0.0	0.0	27.5	0.0	0.0	0.0	1.9	2.0
332	1.6	0.0	0.0	0.0	0.0	0.0	0.0	0.0	2.2
334	2.4	0.0	0.0	0.0	0.0	0.0	0.0	2.5	2.6
336	2.2	0.0	1.9	0.0	0.0	0.0	0.0	2.7	1.8
338	3.1	0.0	1.4	27.1	0.0	0.0	0.0	1.9	0.0
340	1.0	0.0	0.0	0.0	0.0	0.0	0.0	1.5	0.0
342	2.3	0.0	0.0	0.0	0.0	0.0	0.0	2.7	2.3
344	1.5	0.0	0.0	21.1	0.0	0.0	0.0	1.8	0.0
346	2.2	0.0	0.0	27.7	0.0	0.0	1.2	1.6	1.8
348	2.0	0.0	0.0	24.9	0.0	0.0	0.0	1.3	0.0
350	1.4	0.0	0.0	0.0	0.0	0.0	0.0	0.0	0.0
352	1.3	0.0	0.0	0.0	0.0	0.0	0.0	0.0	0.0
354	2.7	0.0	0.0	0.0	0.0	0.0	0.0	1.4	3.4
356	1.3	0.0	0.0	0.0	0.0	0.0	0.0	0.0	0.0
358	1.9	0.0	0.0	0.0	0.0	0.0	0.0	0.0	0.0
360	6.1	0.0	0.0	0.0	0.0	0.0	0.0	2.0	0.0
362	1.5	0.0	0.0	25.2	0.0	0.0	0.0	0.0	0.0
364	1.9	0.0	0.0	0.0	0.0	0.0	0.0	2.0	0.0
366	2.6	0.0	0.0	0.0	0.0	0.0	0.0	0.0	2.8
368	1.4	0.0	0.0	0.0	0.0	0.0	0.0	0.0	0.0
370	1.5	0.0	1.2	0.0	0.0	0.0	0.0	0.0	1.9
372	1.6	0.0	0.0	0.0	0.0	0.0	0.0	1.4	0.0
374	1.0	0.0	0.0	0.0	0.0	0.0	0.0	2.0	0.0
376	2.0	0.0	0.0	0.0	0.0	0.0	0.0	0.0	0.0
378	0.9	0.0	0.0	0.0	0.0	0.0	0.0	0.0	0.0

Mineralogical Composition of South Core at North Ingebright Lake

Depth (cm)	Quartz	K-Feldspar	Plag.	Total Clay Miner.	Calcite	Aragonite	High-Mg Calcite	Proto Dolomite	Dolomite
380	1.8	0.0	0.0	0.0	0.0	0.0	0.0	2.8	2.2
382	1.0	0.0	0.0	0.0	0.0	0.0	0.0	0.0	1.8
384	1.1	0.0	0.0	0.0	0.0	0.0	0.0	0.0	2.2
386	1.3	0.0	0.0	0.0	0.0	0.0	0.0	0.0	0.0
388	2.3	0.0	0.0	0.0	0.0	0.0	0.0	0.0	0.0
390	1.6	0.0	0.0	0.0	0.0	0.0	0.0	0.0	0.0
392	1.4	0.0	0.0	20.2	0.0	0.0	0.0	1.4	0.0
394	2.9	0.0	0.0	0.0	0.0	0.0	0.0	0.0	2.9
396	2.8	0.0	5.1	0.0	0.0	0.0	0.0	2.5	0.0
398	2.4	0.0	0.0	0.0	0.0	0.0	0.0	2.4	0.0
400	2.6	0.0	0.0	0.0	0.0	0.0	0.0	1.6	1.8
402	2.3	0.0	0.0	28.9	0.0	0.0	0.0	3.6	0.0
404	2.6	0.0	0.0	28.7	0.0	0.0	0.0	0.0	2.1
406	1.4	0.0	0.0	0.0	0.0	0.0	0.0	1.7	0.0
408	3.0	0.0	0.0	21.2	0.0	1.3	0.0	2.0	2.2
410	2.1	0.0	0.0	26.9	0.0	0.0	0.0	0.0	0.0
412	2.4	0.0	0.0	27.9	0.0	1.3	0.0	0.0	0.0
414	2.5	0.0	0.0	0.0	0.0	1.9	1.7	2.3	2.3
416	1.2	0.0	0.0	19.2	0.0	0.0	0.0	1.3	1.8
500	2.3	0.0	2.7	34.6	0.0	0.0	0.0	2.5	2.2
502	4.7	0.0	0.0	0.0	0.0	0.0	0.0	0.0	0.0
504	2.1	0.0	3.3	0.0	0.0	0.0	2.0	0.0	0.0
508	1.9	0.0	0.0	30.9	0.0	0.0	0.0	2.9	0.0
510	2.9	0.0	0.0	38.7	0.0	0.0	0.0	2.8	3.0
512	4.8	0.0	3.4	41.6	0.0	0.0	0.0	2.4	0.3
514	3.3	0.0	0.0	29.1	0.0	0.0	0.0	2.3	3.0
516	4.3	0.0	1.9	44.5	0.0	0.0	0.0	2.6	2.2
518	3.7	0.0	1.3	28.4	0.0	0.0	0.0	2.7	17.0
520	3.7	0.0	1.3	25.7	0.0	0.0	0.0	1.8	0.0
522	1.8	0.0	0.0	24.1	0.0	0.0	0.0	2.0	3.0
524	3.0	0.0	0.0	24.4	0.0	0.0	0.0	2.4	1.9
526	2.4	0.0	0.0	38.4	0.0	0.0	0.0	2.9	2.1
528	5.6	0.0	0.0	36.5	0.0	0.0	0.0	2.7	2.7
530	2.9	0.0	0.0	30.9	0.0	0.0	0.0	1.7	2.7
532	6.7	0.0	0.0	24.3	0.0	0.0	0.0	0.0	1.4

Mineralogical Composition of South Core at North Ingebright Lake

Depth (cm)	Quartz	K-Feldspar	Plag.	Total Clay Miner.	Calcite	Aragonite	High-Mg Calcite	Proto Dolomite	Dolomite
534	2.8	0.0	0.0	18.7	0.0	0.0	0.0	1.6	1.6
536	2.0	0.0	1.5	26.6	0.0	0.0	0.0	2.3	0.0
538	2.8	0.0	0.0	26.7	0.0	0.0	0.0	1.8	0.0
540	3.4	0.0	0.0	27.4	0.0	0.0	0.0	2.2	2.2
542	2.5	0.0	0.0	27.5	0.0	0.0	0.0	2.2	3.1
544	2.7	1.8	0.0	22.6	0.0	0.0	0.0	2.4	2.0
546	3.0	0.0	0.0	37.0	0.0	0.0	0.0	3.2	2.1
548	2.7	0.0	0.0	29.8	0.0	0.0	0.0	2.9	2.6
550	2.1	0.0	0.0	36.4	0.0	0.0	0.0	2.9	0.0
552	2.1	0.0	0.0	27.5	0.0	0.0	0.0	1.8	2.2
554	4.2	0.0	0.0	0.0	0.0	0.0	0.0	2.6	0.0
556	1.8	2.0	0.0	27.4	0.0	0.0	0.0	2.1	2.0
558	2.0	1.7	0.0	25.5	0.0	0.0	0.0	2.4	0.0
560	1.5	0.0	0.0	27.2	0.0	0.0	0.0	2.2	2.7
562	1.7	0.0	0.0	35.2	0.0	0.0	0.0	3.0	0.0
564	1.5	0.0	0.0	26.1	0.0	0.0	0.0	1.6	0.0
566	2.3	0.0	0.0	28.3	0.0	0.0	0.0	1.9	1.8
568	1.8	0.0	0.0	19.4	0.0	0.0	0.0	2.0	0.0
570	1.1	0.0	0.0	18.6	0.0	0.0	0.0	1.6	1.6
572	3.0	0.0	0.0	23.8	0.0	0.0	0.0	1.6	0.0
574	2.3	0.0	0.0	0.0	0.0	0.0	0.0	2.4	0.0
576	1.4	0.0	0.0	19.6	0.0	0.0	0.0	1.8	2.1
578	1.8	0.0	1.3	24.1	0.0	0.0	0.0	2.0	2.9
580	1.4	0.0	0.0	21.3	0.0	0.0	0.0	1.7	2.3
582	1.1	0.0	0.4	20.1	0.0	0.0	0.0	1.6	0.0
584	1.2	1.9	0.0	0.0	0.0	0.0	0.0	2.2	0.0
586	0.8	0.0	0.0	6.5	0.0	0.0	1.5	0.0	0.0
588	1.8	0.0	0.0	20.4	0.0	0.0	0.0	1.3	1.2
590	1.4	0.0	0.8	16.7	0.0	0.0	0.0	1.5	4.4
592	1.0	0.0	0.0	17.3	0.0	0.0	0.4	1.3	2.4
594	0.9	0.0	0.0	16.3	0.0	0.0	0.7	1.7	0.0
596	1.4	0.0	0.0	17.8	0.0	0.0	0.0	1.6	1.6
598	0.8	0.9	0.0	19.6	0.0	0.0	0.0	0.0	1.0
600	1.0	0.0	0.0	24.9	0.0	0.0	0.0	2.7	1.8
602	1.2	0.0	0.0	18.7	0.0	0.0	0.0	1.5	1.7

Mineralogical Composition of South Core at North Ingebright Lake

Depth (cm)	Quartz	K-Feldspar	Plag.	Total Clay Miner.	Calcite	Aragonite	High-Mg Calcite	Proto Dolomite	Dolomite
604	1.3	1.6	0.0	29.3	0.0	0.0	0.0	2.2	0.0
606	1.1	0.0	0.0	18.9	0.0	0.0	0.0	1.6	1.5
608	0.9	0.0	0.0	20.7	0.0	0.0	0.0	1.6	1.9
610	0.8	0.0	0.0	18.9	0.0	0.0	0.0	1.9	0.0
612	0.8	0.0	0.0	0.0	0.0	0.0	0.0	1.3	0.0
614	2.1	0.0	0.0	0.0	0.0	0.0	0.0	1.7	1.9
616	1.9	0.0	0.0	20.0	0.0	2.0	1.1	0.0	1.9
618	1.0	0.0	0.0	0.0	0.0	1.5	0.0	0.0	0.0
620	3.5	0.0	1.8	0.0	0.0	4.2	2.2	0.0	2.9
622	2.3	0.0	0.0	0.0	1.7	3.2	0.0	0.0	2.8
624	2.2	0.0	0.0	0.0	0.0	0.0	0.0	0.3	0.0
626	1.7	0.0	0.9	15.4	0.0	2.1	0.9	1.3	1.4
628	3.3	0.0	0.0	0.0	3.3	4.0	0.0	0.0	2.3
630	1.8	0.0	0.0	17.6	0.0	2.6	0.0	0.0	1.9
632	1.7	0.0	0.0	0.0	0.0	2.1	1.5	0.0	2.7
634	1.7	0.0	0.0	0.0	0.0	2.0	1.2	0.0	1.7
636	1.4	0.0	0.0	0.0	0.0	1.2	0.0	0.0	0.0
638	3.7	0.0	0.0	0.0	0.0	2.3	0.0	2.3	2.4
640	2.0	0.0	0.0	17.3	0.0	2.0	0.0	1.7	0.0
642	4.5	3.0	0.0	0.0	0.0	2.8	2.5	0.0	2.7
644	2.6	0.0	0.0	0.0	0.0	1.8	1.4	1.1	1.6
646	0.4	0.0	0.0	13.7	0.0	0.0	0.0	1.6	0.0
648	1.1	0.0	0.0	0.0	0.0	1.7	0.0	1.8	0.0
650	1.6	0.0	0.0	22.9	0.0	0.0	1.2	1.3	1.7
652	1.6	0.0	0.0	0.0	0.0	2.2	0.0	0.0	2.3
654	0.4	0.0	0.7	0.0	0.0	0.0	0.0	0.0	0.0
656	0.5	0.0	0.0	0.0	0.0	0.0	0.0	0.0	0.0
658	0.4	0.0	0.0	0.0	0.0	0.0	0.0	0.0	0.0
660	0.0	0.0	0.0	0.0	0.0	0.0	0.0	0.0	0.0
662	0.4	0.9	0.0	0.0	0.0	0.0	0.0	0.0	0.0
664	0.6	0.0	0.0	0.0	0.0	0.0	0.0	0.0	0.7
666	1.0	0.0	0.0	0.0	0.0	0.0	0.0	1.2	1.3
668	2.0	2.3	2.3	0.0	0.0	0.0	0.0	0.0	0.0
670	1.2	0.0	0.0	0.0	0.0	0.0	0.0	1.5	1.8
672	0.9	0.0	0.0	0.0	0.0	1.2	0.0	0.0	1.4

Mineralogical Composition of South Core at North Ingebright Lake

Depth (cm)	Quartz	K-Feldspar	Plag.	Total Clay Miner.	Calcite	Aragonite	High-Mg Calcite	Proto Dolomite	Dolomite
674	0.5	0.0	2.0	0.0	0.0	0.0	0.0	0.0	0.0
676	0.5	0.0	0.0	0.0	0.0	0.0	0.0	1.3	0.0
678	0.9	0.0	0.0	15.0	0.0	1.3	0.0	1.2	1.8
680	1.3	0.0	0.0	20.7	0.0	0.0	0.0	1.7	0.0
682	1.3	0.0	0.0	0.0	0.0	0.0	0.0	1.8	2.2
684	0.7	0.0	0.0	12.9	0.0	0.0	0.0	1.3	2.0
686	0.5	0.0	0.0	15.9	0.0	0.0	0.0	1.6	0.0
824	0.3	0.0	0.0	0.0	0.0	0.0	0.0	0.0	0.0
826	0.9	0.0	0.0	0.0	0.0	0.0	0.0	0.0	0.0
828	0.6	0.0	0.0	0.0	0.0	0.0	0.0	0.0	1.8
830	1.7	0.0	0.0	0.0	0.0	0.0	0.0	0.0	2.1
832	0.6	0.0	0.0	14.6	0.0	0.0	0.0	0.0	0.0
834	1.4	0.0	0.0	0.0	0.0	0.0	0.0	0.0	0.0
836	1.2	0.0	0.0	29.9	0.0	0.0	0.0	1.7	0.0
838	1.5	0.0	0.0	24.9	0.0	0.0	0.0	0.0	0.0
840	2.0	0.0	0.0	33.1	0.0	0.0	0.0	1.9	0.0
842	1.4	0.0	0.0	0.0	0.0	0.0	0.0	0.0	0.0
844	1.4	2.4	0.0	33.4	0.0	0.0	0.0	2.9	1.9
846	1.5	0.0	0.0	32.6	0.0	0.0	0.0	3.5	2.4
848	0.6	0.0	0.0	0.0	0.0	0.0	0.0	0.0	0.0
850	1.4	0.0	0.0	28.6	0.0	0.0	0.8	1.7	1.6
852	1.5	0.0	1.8	0.0	0.0	1.9	0.0	2.6	1.7
854	0.9	0.8	0.0	17.3	0.0	0.0	0.0	1.4	0.0
856	0.7	0.0	0.0	23.9	0.0	0.0	0.0	2.3	0.0
858	0.5	0.0	0.0	25.9	0.0	0.0	0.0	2.2	0.0
860	0.5	0.0	0.0	0.0	0.0	0.0	0.0	1.4	2.5
862	0.5	0.0	0.0	0.0	0.0	0.0	0.0	1.4	0.0
864	0.6	0.0	0.0	21.3	0.0	0.0	0.0	2.0	0.0
866	0.8	0.0	0.0	29.5	0.0	0.0	0.0	2.7	0.0
868	0.3	0.0	0.5	61.4	0.0	0.0	0.0	1.4	1.6
870	5.0	2.4	1.7	0.0	0.0	0.0	1.2	0.0	7.4
872	2.3	1.2	0.0	14.5	0.0	0.0	0.0	1.0	2.3
874	3.0	1.1	0.8	0.0	0.0	0.0	0.0	0.0	2.0
876	4.1	2.5	1.2	18.8	0.9	0.0	0.0	0.0	1.5
878	5.4	0.0	1.4	0.0	0.0	0.0	1.4	0.0	3.0

Mineralogical Composition of South Core at North Ingebright Lake

Depth (cm)	Quartz	K-Feldspar	Plag.	Total Clay Miner.	Calcite	Aragonite	High-Mg Calcite	Proto Dolomite	Dolomite
880	2.3	0.0	0.6	11.6	0.0	0.0	0.0	0.0	3.1
882	5.5	0.0	0.0	20.8	1.4	0.0	0.0	1.0	2.8
884	3.0	1.8	0.0	19.0	0.0	0.0	0.0	0.0	3.4
886	2.5	0.0	0.7	0.0	0.6	0.0	0.0	0.7	2.0
888	1.7	2.0	0.9	9.7	0.6	0.0	0.0	1.1	1.4
890	8.0	7.0	0.0	15.0	0.5	0.0	0.0	0.0	0.7
892	1.9	0.0	0.9	12.5	0.7	0.0	0.0	0.0	1.8
894	1.6	0.0	4.0	15.0	0.6	0.0	0.3	0.0	2.2
896	1.7	1.4	1.1	12.2	0.8	0.0	0.0	0.0	0.0
898	26.3	0.0	15.0	40.9	0.0	0.0	0.0	0.0	5.8
900	24.1	0.0	5.4	35.0	0.0	0.0	0.0	0.0	4.0
910	25.1	4.9	18.6	37.8	0.0	0.0	0.0	1.2	2.5

Mineralogical Composition of South Core at North Ingebright Lake

Depth (cm)	Magnesite	Gypsum	Anhydrite	Thenardite	Bloedite	Halite	Mg in High Mg Calcite	Ca in Protodolomite
10	0.0	0.0	0.0	63.7	0.0	0.0		
12	0.0	0.0	7.4	19.3	53.2	0.0		53.3
14	0.0	0.0	0.0	28.1	0.0	0.0		
16	0.0	0.0	0.0	27.5	0.0	0.0		
18	0.0	0.0	0.0	54.0	0.0	0.0	8.0	
20	0.0	0.0	0.0	33.4	0.0	0.0		
22	0.0	0.0	0.0	11.1	0.0	0.0	2.0	52.3
24	0.0	0.0	0.0	27.4	0.0	0.0		
26	0.0	0.0	0.0	22.4	0.0	0.0	15.8	
28	0.0	0.0	0.0	33.1	0.0	0.0		52.8
30	0.0	0.0	0.0	0.0	0.0	0.0		54.8
32	0.0	0.0	0.0	12.5	0.0	0.0		53.8
34	0.0	0.0	0.0	24.7	0.0	0.0		
36	0.0	0.0	0.0	31.4	0.0	0.0		
38	0.0	0.0	0.0	0.0	0.0	2.5		52.0
40	0.0	0.0	0.0	0.0	0.0	0.0		
42	0.0	0.0	0.0	26.7	0.0	0.0		
44	0.0	0.0	0.0	24.0	0.0	0.0		
46	0.0	0.0	0.0	19.3	0.0	0.0	16.8	
48	0.0	0.0	0.0	13.0	0.0	0.0	16.8	
50	0.0	0.0	0.0	62.9	0.0	0.0		
52	0.0	0.0	0.0	91.3	0.0	0.0		
54	0.0	0.0	0.0	55.2	0.0	0.0		
56	0.0	0.0	0.0	95.8	0.0	0.0		52.7
58	0.0	0.0	0.0	98.7	0.0	0.0	4.5	
60	0.0	0.0	0.0	96.4	0.0	0.0		
62	0.0	0.0	0.0	100.0	0.0	0.0		
64	0.0	0.0	0.0	0.0	0.0	0.0		80.0
66	0.0	0.0	0.0	99.0	0.0	0.0		
68	0.0	0.0	0.0	100.0	0.0	0.0		
70	0.0	0.0	0.0	99.4	0.0	0.0		
72	0.0	0.0	0.0	99.5	0.0	0.0		
74	0.0	0.0	0.0	100.0	0.0	0.0		
76	0.0	0.0	0.0	99.6	0.0	0.0		
78	0.0	0.0	0.0	99.7	0.0	0.0		

Mineralogical Composition of South Core at North Ingebright Lake

Depth (cm)	Magnesite	Gypsum	Anhydrite	Thenardite	Bloedite	Halite	Mg in High Mg Calcite	Ca in Protodolomite
80	0.0	0.0	0.0	99.5	0.0	0.0		
82	0.0	0.0	0.0	99.6	0.0	0.0		
84	0.0	0.0	0.0	99.2	0.0	0.0		
86	0.0	0.0	0.0	98.9	0.0	0.0		
88	0.0	0.0	0.0	99.5	0.0	0.0		
90	0.0	0.0	0.0	100.0	0.0	0.0		
92	0.0	0.0	0.0	99.0	0.0	0.0		
94	0.0	0.0	0.0	97.7	0.0	0.0		
96	0.0	0.0	0.0	99.4	0.0	0.0		
98	0.0	0.0	0.0	99.7	0.0	0.0		
100	0.0	0.0	0.0	99.6	0.0	0.0		
102	0.0	0.0	0.0	99.4	0.0	0.0		
104	0.0	0.0	0.0	100.0	0.0	0.0		
106	0.0	0.0	0.0	99.6	0.0	0.0		
108	0.0	0.0	0.0	99.6	0.0	0.0		
110	0.0	0.0	0.0	98.9	0.0	0.0		
112	0.0	0.0	0.0	99.6	0.0	0.0		
114	0.0	0.0	0.0	100.0	0.0	0.0		
116	0.0	0.0	0.0	100.0	0.0	0.0		
118	0.0	0.0	0.0	99.6	0.0	0.0		
120	0.0	0.0	0.0	98.0	0.0	0.0		
122	0.0	0.0	0.0	99.1	0.0	0.0		
124	0.0	0.0	0.0	100.0	0.0	0.0		
126	0.0	0.0	0.0	99.5	0.0	0.0		
128	0.0	0.0	0.0	99.4	0.0	0.0		
130	0.0	5.1	0.0	94.1	0.0	0.0		
132	0.0	0.0	0.0	99.0	0.0	0.0		
134	0.0	0.0	0.0	97.4	0.0	0.0		
136	0.0	0.0	0.0	99.3	0.0	0.0		
138	0.0	0.0	0.0	98.0	0.0	0.0		
140	0.0	0.0	0.0	99.1	0.0	0.0		
142	0.0	0.0	0.0	99.0	0.0	0.0		
144	0.0	0.0	0.0	98.4	0.0	0.0		
146	0.0	0.0	0.0	100.0	0.0	0.0		
148	0.0	0.0	0.0	99.5	0.0	0.0		

Mineralogical Composition of South Core at North Ingebright Lake

Depth (cm)	Magnesite	Gypsum	Anhydrite	Thenardite	Bloedite	Halite	Mg in High Mg Calcite	Ca in Protodolomite
150	0.0	0.0	0.0	99.7	0.0	0.0		
152	0.0	0.0	0.0	99.5	0.0	0.0		
154	0.0	0.0	0.0	98.9	0.0	0.0		
156	0.0	4.8	0.0	94.7	0.0	0.0		
158	0.0	0.0	0.0	97.1	0.0	0.0		
160	0.0	0.0	0.0	100.0	0.0	0.0		
162	0.0	0.0	0.0	99.4	0.0	0.0		
164	0.0	0.0	0.0	99.2	0.0	0.0		
166	0.0	0.0	0.0	99.7	0.0	0.0		
168	0.0	0.0	0.0	99.3	0.0	0.0		
170	0.0	0.0	0.0	98.9	0.0	0.0		
172	0.0	0.0	0.0	99.2	0.0	0.0		
174	0.0	0.0	0.0	99.4	0.0	0.0		
176	0.0	0.0	0.0	99.1	0.0	0.0		
178	0.0	0.0	0.0	99.2	0.0	0.0		
180	0.0	4.7	0.0	94.9	0.0	0.0		
182	0.0	0.0	0.0	96.2	0.0	0.0		63.8
184	0.0	0.0	0.0	99.2	0.0	0.0		
186	0.0	0.0	0.0	100.0	0.0	0.0		
188	0.0	0.0	0.0	99.5	0.0	0.0		
190	0.0	0.0	0.0	96.8	0.0	0.0		
192	0.0	0.0	0.0	98.7	0.0	0.0		
194	0.0	0.0	0.0	99.2	0.0	0.0		
196	0.0	0.0	0.0	99.0	0.0	0.0		
198	0.0	0.0	0.0	99.4	0.0	0.0		
200	0.0	14.5	0.0	83.8	0.0	0.0	4.4	
202	0.0	0.0	0.0	99.2	0.0	0.0		
204	0.0	0.0	0.0	98.5	0.0	0.0		
226	0.0	0.0	0.0	99.5	0.0	0.0		
228	0.0	0.0	0.0	98.0	0.0	0.0		
230	0.0	0.0	0.0	91.4	0.0	0.0		
232	0.0	0.0	0.0	99.1	0.0	0.0		
234	0.0	0.0	0.0	99.3	0.0	0.0		
236	0.0	8.3	0.0	91.0	0.0	0.0		
238	0.0	0.0	0.0	99.4	0.0	0.0		

Mineralogical Composition of South Core at North Ingebright Lake

Depth (cm)	Magnesite	Gypsum	Anhydrite	Thenardite	Bloedite	Halite	Mg in High Mg Calcite	Ca in Protodolomite
240	0.0	0.0	0.0	99.4	0.0	0.0		
242	0.0	0.0	0.0	99.1	0.0	0.0		
244	0.0	12.1	0.0	86.8	0.0	0.0		
246	0.0	12.5	0.0	84.8	0.0	0.0		
248	0.0	8.9	0.0	87.2	0.0	0.0		
250	0.0	0.0	0.0	97.0	0.0	0.0		62.9
252	0.0	9.6	0.0	88.1	0.0	0.0		
254	0.0	0.0	0.0	98.9	0.0	0.0		
256	0.0	0.0	0.0	98.7	0.0	0.0		
258	0.0	6.5	0.0	93.0	0.0	0.0		
260	0.0	8.2	0.0	90.2	0.0	0.0		
262	0.0	17.6	0.0	78.9	0.0	0.0		
264	0.0	11.3	0.0	86.1	0.0	0.0		
266	0.0	10.6	0.0	86.4	0.0	0.0		
268	0.0	13.3	0.0	82.9	0.0	0.0		
270	0.0	0.0	0.0	75.2	0.0	0.0		
272	0.0	0.0	0.0	74.7	0.0	0.0		
274	0.0	0.0	0.0	97.6	0.0	0.0		
276	0.0	0.0	0.0	96.7	0.0	0.0		
278	0.0	0.0	0.0	69.1	0.0	0.0		59.7
280	0.0	10.9	0.0	68.2	0.0	0.0		
282	3.1	20.8	0.0	68.0	0.0	0.0		64.2
284	0.0	17.2	0.0	79.4	0.0	0.0		
286	0.0	0.0	0.0	94.8	0.0	0.0		64.7
288	0.0	9.1	0.0	85.4	0.0	0.0		
290	2.5	7.3	0.0	51.9	0.0	0.0		61.6
292	0.0	6.0	0.0	56.7	0.0	0.0		58.3
294	0.0	0.0	0.0	58.1	0.0	0.0	7.4	6.7
296	0.0	12.2	0.0	82.2	0.0	0.0		
298	2.2	7.7	0.0	69.5	0.0	0.0		
300	0.0	0.0	0.0	92.7	0.0	0.0		
302	0.0	6.5	0.0	69.9	0.0	0.0		46.4
304	0.0	0.0	0.0	74.9	0.0	0.0		65.6
306	0.0	0.0	0.0	95.0	0.0	0.0		63.4
308	0.0	6.1	0.0	73.0	0.0	0.0		

Mineralogical Composition of South Core at North Ingebright Lake

Depth (cm)	Magnesite	Gypsum	Anhydrite	Thenardite	Bloedite	Halite	Mg in High Mg Calcite	Ca in Protodolomite
310	0.0	7.7	0.0	90.8	0.0	0.0		
312	0.0	0.0	0.0	97.4	0.0	0.0		
314	0.0	6.8	0.0	88.7	0.0	0.0		63.2
316	0.0	10.2	0.0	85.7	0.0	0.0		64.7
318	0.0	0.0	0.0	92.3	0.0	0.0		63.7
320	0.0	0.0	0.0	68.5	0.0	0.0	5.7	6.4
322	0.0	5.7	0.0	69.9	0.0	0.0		62.7
324	0.0	0.0	0.0	75.0	0.0	0.0		62.3
326	0.0	0.0	0.0	50.6	0.0	0.0		63.7
328	0.0	0.0	0.0	58.1	0.0	0.0	5.7	61.5
330	3.0	0.0	0.0	63.3	0.0	0.0		60.0
332	0.0	0.0	0.0	76.5	19.7	0.0		
334	0.0	5.3	0.0	87.2	0.0	0.0		6.2
336	0.0	0.0	0.0	91.4	0.0	0.0		62.5
338	0.0	0.0	0.0	66.4	0.0	0.0		62.3
340	0.0	8.1	0.0	89.4	0.0	0.0		66.9
342	0.0	0.0	0.0	92.7	0.0	0.0		6.7
344	2.5	0.0	0.0	73.0	0.0	0.0		62.3
346	3.1	0.0	0.0	62.4	0.0	0.0	6.0	62.6
348	0.0	5.0	0.0	66.8	0.0	0.0		66.0
350	0.0	0.0	0.0	98.6	0.0	0.0		
352	0.0	0.0	0.0	98.7	0.0	0.0		
354	0.0	6.9	0.0	85.5	0.0	0.0		61.6
356	0.0	0.0	0.0	98.7	0.0	0.0		
358	0.0	0.0	0.0	98.1	0.0	0.0		
360	0.0	0.0	0.0	91.8	0.0	0.0		62.8
362	0.0	0.0	0.0	73.3	0.0	0.0		
364	0.0	0.0	0.0	96.1	0.0	0.0		62.9
366	0.0	0.0	0.0	94.6	0.0	0.0		
368	0.0	5.1	0.0	93.5	0.0	0.0		
370	0.0	0.0	0.0	81.4	13.9	0.0		
372	0.0	0.0	0.0	97.0	0.0	0.0		63.7
374	0.0	4.8	0.0	92.2	0.0	0.0		6.3
376	0.0	0.0	0.0	98.0	0.0	0.0		
378	0.0	0.0	0.0	99.1	0.0	0.0		

Mineralogical Composition of South Core at North Ingebright Lake

Depth (cm)	Magnesite	Gypsum	Anhydrite	Thenardite	Bloedite	Halite	Mg in High Mg Calcite	Ca in Protodolomite
380	0.0	0.0	0.0	93.2	0.0	0.0		68.9
382	0.0	6.2	0.0	91.0	0.0	0.0		
384	0.0	8.7	0.0	88.0	0.0	0.0		
386	0.0	0.0	0.0	98.7	0.0	0.0		
388	0.0	0.0	0.0	97.7	0.0	0.0		
390	0.0	0.0	0.0	98.4	0.0	0.0		
392	0.0	0.0	0.0	77.1	0.0	0.0		62.3
394	0.0	0.0	0.0	94.1	0.0	0.0		
396	3.8	10.0	0.0	75.7	0.0	0.0		63.7
398	0.0	8.9	0.0	86.3	0.0	0.0		62.3
400	2.6	16.2	0.0	75.2	0.0	0.0		65.5
402	0.0	7.4	0.0	57.8	0.0	0.0		68.4
404	0.0	6.4	0.0	60.1	0.0	0.0		
406	0.0	0.0	0.0	96.9	0.0	0.0		62.6
408	0.0	5.3	0.0	64.9	0.0	0.0		61.9
410	2.6	0.0	0.0	68.3	0.0	0.0		
412	2.2	6.5	0.0	59.6	0.0	0.0		
414	3.1	7.9	0.0	78.3	0.0	0.0	4.6	63.5
416	0.0	0.0	0.0	76.4	0.0	0.0		59.3
500	3.3	0.0	0.0	52.4	0.0	0.0		63.9
502	0.0	8.9	0.0	86.4	0.0	0.0		
504	0.0	0.0	0.0	68.1	24.5	0.0	4.9	
508	0.0	5.8	0.0	58.5	0.0	0.0		66.0
510	0.0	0.0	0.0	52.5	0.0	0.0		62.4
512	0.0	15.6	0.0	31.9	0.0	0.0		63.3
514	0.0	8.8	0.0	53.5	0.0	0.0		63.6
516	0.0	13.6	0.0	30.9	0.0	0.0		63.9
518	3.5	14.0	0.0	29.3	0.0	0.0		62.4
520	0.0	10.8	0.0	56.7	0.0	0.0		64.3
522	3.1	9.1	0.0	56.8	0.0	0.0		63.8
524	4.4	6.6	0.0	57.2	0.0	0.0		62.9
526	4.7	10.6	0.0	38.9	0.0	0.0		64.3
528	0.0	0.0	0.0	52.6	0.0	0.0		63.9
530	0.0	0.0	0.0	61.8	0.0	0.0		67.4
532	3.0	7.3	0.0	57.4	0.0	0.0		

Mineralogical Composition of South Core at North Ingebright Lake

Depth (cm)	Magnesite	Gypsum	Anhydrite	Thenardite	Bloedite	Halite	Mg in High Mg Calcite	Ca in Protodolomite
534	0.0	9.0	0.0	66.3	0.0	0.0		63.7
536	0.0	15.9	0.0	51.6	0.0	0.0		62.5
538	3.2	14.2	0.0	51.3	0.0	0.0		64.4
540	4.0	25.4	0.0	35.5	0.0	0.0		64.4
542	3.9	14.4	0.0	46.3	0.0	0.0		64.5
544	3.9	22.5	0.0	42.1	0.0	0.0		62.7
546	4.8	16.5	0.0	33.5	0.0	0.0		61.9
548	4.4	19.5	0.0	38.2	0.0	0.0		61.2
550	4.9	9.4	0.0	44.3	0.0	0.0		63.9
552	4.2	9.2	0.0	52.8	0.0	0.0		62.5
554	0.0	15.3	0.0	77.9	0.0	0.0		61.1
556	0.0	22.5	0.0	42.1	0.0	0.0		63.7
558	4.5	16.5	0.0	47.3	0.0	0.0		63.5
560	0.0	8.8	0.0	57.6	0.0	0.0		62.7
562	0.0	11.6	0.0	48.6	0.0	0.0		63.6
564	0.0	13.5	0.0	57.4	0.0	0.0		63.4
566	3.3	10.3	0.0	52.2	0.0	0.0		63.7
568	2.3	24.9	0.0	49.6	0.0	0.0		65.3
570	2.1	17.3	0.0	57.8	0.0	0.0		65.2
572	0.0	0.0	0.0	71.5	0.0	0.0		66.2
574	4.1	14.5	0.0	76.7	0.0	0.0		64.5
576	3.3	13.6	0.0	58.2	0.0	0.0		63.2
578	3.7	8.9	0.0	55.3	0.0	0.0		62.5
580	0.0	19.4	0.0	53.9	0.0	0.0		62.4
582	0.0	19.7	0.0	57.1	0.0	0.0		63.6
584	3.1	19.8	0.0	71.8	0.0	0.0		68.7
586	0.0	29.5	0.0	61.8	0.0	0.0	3.3	
588	3.4	22.9	0.0	49.1	0.0	0.0		62.6
590	0.0	15.6	0.0	59.7	0.0	0.0		63.2
592	0.0	18.9	0.0	58.8	0.0	0.0	12.6	61.7
594	0.0	9.8	0.0	70.7	0.0	0.0	18.1	64.6
596	0.0	18.3	0.0	59.3	0.0	0.0		6.6
598	2.7	25.1	0.0	44.2	5.7	0.0		
600	0.0	12.8	0.0	56.7	0.0	0.0		62.9
602	4.1	11.4	0.0	61.4	0.0	0.0		62.6

Mineralogical Composition of South Core at North Ingebright Lake

Depth (cm)	Magnesite	Gypsum	Anhydrite	Thenardite	Bloedite	Halite	Mg in High Mg Calcite	Ca in Protodolomite
604	0.0	8.4	0.0	57.2	0.0	0.0		65.2
606	3.8	14.9	0.0	58.1	0.0	0.0		63.3
608	0.0	17.0	0.0	57.9	0.0	0.0		63.9
610	2.7	12.3	0.0	63.5	0.0	0.0		63.9
612	0.0	15.1	0.0	82.9	0.0	0.0		62.7
614	0.0	0.0	0.0	94.4	0.0	0.0		63.0
616	0.0	21.7	0.0	51.3	0.0	0.0	5.3	
618	0.0	27.9	0.0	69.6	0.0	0.0		
620	0.0	18.9	0.0	66.6	0.0	0.0	4.7	
622	0.0	21.3	0.0	68.7	0.0	0.0		
624	0.0	20.3	0.0	77.1	0.0	0.0		6.8
626	0.0	34.7	0.0	41.7	0.0	0.0	3.9	63.9
628	0.0	17.4	0.0	69.7	0.0	0.0		
630	0.0	7.9	0.0	45.5	22.9	0.0		
632	0.0	18.7	0.0	73.2	0.0	0.0	4.8	
634	0.0	13.7	0.0	58.6	21.0	0.0	4.5	
636	0.0	4.3	0.0	93.1	0.0	0.0		
638	0.0	0.0	0.0	89.2	0.0	0.0		64.6
640	0.0	9.4	0.0	67.6	0.0	0.0		66.2
642	0.0	0.0	0.0	84.6	0.0	0.0	4.4	
644	5.6	0.0	0.0	65.4	20.5	0.0	4.5	61.4
646	0.0	24.3	0.0	60.0	0.0	0.0		61.5
648	0.0	10.6	0.0	84.7	0.0	0.0		62.5
650	0.0	7.3	0.0	63.9	0.0	0.0	7.5	6.5
652	0.0	9.8	0.0	84.2	0.0	0.0		
654	0.0	11.1	0.0	87.8	0.0	0.0		
656	0.0	10.9	0.0	88.6	0.0	0.0		
658	0.0	6.7	0.0	92.9	0.0	0.0		
660	0.0	0.0	0.0	100.0	0.0	0.0		
662	0.0	61.4	0.0	36.6	0.0	0.0		
664	0.0	24.4	0.0	75.0	0.0	0.0		
666	0.0	51.8	0.0	44.8	0.0	0.0		62.8
668	0.0	31.3	0.0	62.1	0.0	0.0		
670	0.0	38.7	0.0	56.8	0.0	0.0		61.6
672	1.6	69.6	0.0	25.3	0.0	0.0		

Mineralogical Composition of South Core at North Ingebright Lake

Depth (cm)	Magnesite	Gypsum	Anhydrite	Thenardite	Bloedite	Halite	Mg in High Mg Calcite	Ca in Protodolomite
674	0.0	38.7	0.0	58.8	0.0	0.0		
676	0.0	37.9	0.0	60.2	0.0	0.0		6.2
678	0.0	44.9	0.0	34.8	0.0	0.0		63.9
680	0.0	18.6	0.0	57.6	0.0	0.0		61.3
682	0.0	65.6	0.0	29.1	0.0	0.0		61.9
684	0.0	32.6	0.0	50.5	0.0	0.0		62.6
686	0.0	17.7	0.0	64.3	0.0	0.0		62.3
824	0.0	16.9	0.0	82.8	0.0	0.0		
826	0.0	26.3	0.0	72.8	0.0	0.0		
828	0.0	29.7	0.0	67.9	0.0	0.0		
830	0.0	11.5	0.0	84.7	0.0	0.0		
832	0.0	38.6	0.0	46.2	0.0	0.0		
834	0.0	10.0	0.0	88.6	0.0	0.0		
836	0.0	11.0	0.0	56.2	0.0	0.0		65.7
838	0.0	0.0	0.0	73.6	0.0	0.0		
840	0.0	0.0	0.0	63.1	0.0	0.0		61.3
842	1.4	0.0	0.0	97.2	0.0	0.0		
844	4.2	14.5	0.0	39.4	0.0	0.0		63.9
846	4.9	23.6	0.0	31.4	0.0	0.0		62.8
848	0.0	7.2	0.0	92.1	0.0	0.0		
850	0.0	5.8	0.0	60.1	0.0	0.0	15.3	65.7
852	0.0	0.0	0.0	90.5	0.0	0.0		62.8
854	1.8	63.6	0.0	14.3	0.0	0.0		64.2
856	0.0	6.1	0.0	67.0	0.0	0.0		62.7
858	0.0	0.0	0.0	71.5	0.0	0.0		63.5
860	0.0	27.2	0.0	68.3	0.0	0.0		63.2
862	0.0	8.5	0.0	89.5	0.0	0.0		62.6
864	3.2	17.8	0.0	55.1	0.0	0.0		61.8
866	3.9	17.7	0.0	45.4	0.0	0.0		61.5
868	2.1	18.1	0.0	14.6	0.0	0.0		62.9
870	0.0	77.5	0.0	4.8	0.0	0.0	4.7	
872	3.5	71.7	0.0	3.5	0.0	0.0		
874	0.0	86.5	0.0	6.5	0.0	0.0		
876	0.0	66.1	0.0	4.9	0.0	0.0		
878	0.0	85.9	0.0	2.9	0.0	0.0	3.8	

Mineralogical Composition of South Core at North Ingebright Lake

Depth (cm)	Magnesite	Gypsum	Anhydrite	Thenardite	Bloedite	Halite	Mg in High Mg Calcite	Ca in Protodolomite
880	0.0	80.7	0.0	1.7	0.0	0.0		
882	0.0	64.4	0.0	4.1	0.0	0.0		65.4
884	0.0	61.7	0.0	11.0	0.0	0.0		
886	0.0	88.2	0.0	5.4	0.0	0.0		63.7
888	0.0	78.4	0.0	4.2	0.0	0.0		49.7
890	0.0	55.0	0.0	1.6	0.0	0.0		
892	0.0	79.8	0.0	2.4	0.0	0.0		
894	0.0	50.0	0.0	1.9	0.0	0.0	19.0	
896	0.0	78.8	0.0	4.1	0.0	0.0		
898	0.0	5.6	0.0	6.4	0.0	0.0		
900	0.0	0.0	0.0	31.4	0.0	0.0		
910	0.0	4.0	0.0	6.8	0.0	0.0		

Appendix C Detailed Evaporite Mineralogy from μPDSM

Detailed Evaporite Mineralogy (North Core)

Depth (cm)	Ankerite $Ca(Fe,Mg)(CO_3)_2$	Benstonite $Ca_7Ba_6(CO_3)_{13}$	Fairchildite $K_2Ca(CO_3)_2$	Gaylussite $Na_2Ca(CO_3)_2 \cdot 5H_2O$	Arcanite $(K,NH_4)_2SO_4$	Epsomite $MgSO_4 \cdot 7H_2O$	Eugsterite $Na_2Ca(SO_4)_3 \cdot 2H_2O$	Gorgeyite $K_2Ca_5(SO_4)_6 \cdot 2H_2O$	Krausite $KFe(SO_4)_2 \cdot H_2O$	Leightonite $K_2Ca_2Cu(SO_4)_4 \cdot 2H_2O$	Mercallite $KHSO_4$	Polyhalite $K_2Ca_2Mg(SO_4)_4 \cdot 2H_2O$	Starkeyite $MgSO_4 \cdot 2H_2O$	Wattevilleite $Na_2Ca(SO_4)_2 \cdot 4H_2O$
12										X				
14														
16					X								X	
18										X				
20														
22														
24										X				
26														
28														
30					X									
32		X												
34														
36	X													
38														
40														
42														
44														
46	X								X					
48	X													
50														
52														
54														
56	X													
58										X				
60														
62														
64														
66														
68										X				
70														
72														
74										X				
76										X				
78														
80														
82														

Detailed Evaporite Mineralogy (North Core)

Depth (cm)	Ankerite $Ca(Fe,Mg)(CO_3)_2$	Benstonite $Ca_7Ba_6(CO_3)_{13}$	Fairchildite $K_2Ca(CO_3)_2$	Gaylussite $Na_2Ca(CO_3)_2 5H_2O$	Arcanite $(K,NH_4)_2SO_4$	Epsomite $MgSO_4 7H_2O$	Eugsterite $Na_2Ca(SO_4)_3 2H_2O$	Gorgeyite $K_2Ca_5(SO_4)_6 2H_2O$	Krausite $KFe(SO_4)_2 H_2O$	Leightonite $K_2Ca_2Cu(SO_4)_4 2H_2O$	Mercallite $KHSO_4$	Polyhalite $K_2Ca_2Mg(SO_4)_4 2H_2O$	Starkeyite $MgSO_4 2H_2O$	Wattevilleite $Na_2Ca(SO_4)_2 4H_2O$
84														
86														
88														
90														
92														
94														
96														
98														
100														
106														
108														
110														
112														
114														
116														
118														
120														
122														
124														
126														
128														
130														
132														
134														
136														
138														
140														
142										X				
144														
146														
148														
150														
152					X									
154														
156														
158														

Detailed Evaporite Mineralogy (North Core)

Depth (cm)	Ankerite $Ca(Fe,Mg)(CO_3)_2$	Benstonite $Ca_7Ba_6(CO_3)_{13}$	Fairchildite $K_2Ca(CO_3)_2$	Gaylussite $Na_2Ca(CO_3)_2 5H_2O$	Arcanite $(K,NH_4)_2SO_4$	Epsomite $MgSO_4 7H_2O$	Eugsterite $Na_2Ca(SO_4)_3 2H_2O$	Gorgeyite $K_2Ca_5(SO_4)_6 2H_2O$	Krausite $KFe(SO_4)_2 H_2O$	Leightonite $K_2Ca_2Cu(SO_4)_4 2H_2O$	Mercallite $KHSO_4$	Polyhalite $K_2Ca_2Mg(SO_4)_4 2H_2O$	Starkeyite $MgSO_4 2H_2O$	Wattevilleite $Na_2Ca(SO_4)_2 4H_2O$
160														
162														
164														
166														
168														
170														
172														
174														
176														
178														
180														
182														
184														
188														
190														
192														
194														
196														
198										X				
200														
202														
204														
206									X					
208														
210														
212														
214											X			
216														
218														
220														
222					X									
224					X									
226														
228														
230														
232		X												

Detailed Evaporite Mineralogy (North Core)

Depth (cm)	Ankerite $Ca(Fe,Mg)(CO_3)_2$	Benstonite $Ca_7Ba_6(CO_3)_{13}$	Fairchildite $K_2Ca(CO_3)_2$	Gaylussite $Na_2Ca(CO_3)_2 \cdot 5H_2O$	Arcanite $(K,NH_4)_2SO_4$	Epsomite $MgSO_4 \cdot 7H_2O$	Eugsterite $Na_2Ca(SO_4)_3 \cdot 2H_2O$	Gorgeyite $K_2Ca_5(SO_4)_6 \cdot 2H_2O$	Krausite $KFe(SO_4)_2 \cdot H_2O$	Leightonite $K_2Ca_2Cu(SO_4)_4 \cdot 2H_2O$	Mercallite $KHSO_4$	Polyhalite $K_2Ca_2Mg(SO_4)_4 \cdot 2H_2O$	Starkeyite $MgSO_4 \cdot 2H_2O$	Wattevilleite $Na_2Ca(SO_4)_2 \cdot 4H_2O$
234														
236														
238														
234														
242											X			
244					X									
246														
248												X		
250						X						X		
252												X		
254					X	X						X		
256											X	X		
258						X						X		
260								X						
262														
264					X						X			
266														
268												X		
270														
272												X		
274												X		
276											X	X		
278														
280												X		
282		X												
284														
286														
288												X		
290														
292														
294														
296										X				
298														
300												X		
302												X		
304														

Detailed Evaporite Mineralogy (North Core)

Depth (cm)	Ankerite $Ca(Fe,Mg)(CO_3)_2$	Benstonite $Ca_7Ba_6(CO_3)_{13}$	Fairchildite $K_2Ca(CO_3)_2$	Gaylussite $Na_2Ca(CO_3)_2\,5H_2O$	Arcanite $(K,NH_4)_2SO_4$	Epsomite $MgSO_4\,7H_2O$	Eugsterite $Na_2Ca(SO_4)_3\,2H_2O$	Gorgeyite $K_2Ca_5(SO_4)_6\,2H_2O$	Krausite $KFe(SO_4)_2\,H_2O$	Leightonite $K_2Ca_2Cu(SO_4)_4\,2H_2O$	Mercallite $KHSO_4$	Polyhalite $K_2Ca_2Mg(SO_4)_4\,2H_2O$	Starkeyite $MgSO_4\,2H_2O$	Wattevilleite $Na_2Ca(SO_4)_2\,4H_2O$
306														
308														
310								X						
312														
314														
316														
318														
320														
322														
324														
326														
328			X											
330														
332														
334														
336														
338														
340														
342														
344														
346														
348														
350														
352														
354														
356														
358														
360														
362														
364														
368														
370														
372														
374														
376														
378														

Detailed Evaporite Mineralogy (North Core)

Depth (cm)	Ankerite $Ca(Fe,Mg)(CO_3)_2$	Benstonite $Ca_7Ba_6(CO_3)_{13}$	Fairchildite $K_2Ca(CO_3)_2$	Gaylussite $Na_2Ca(CO_3)_2 5H_2O$	Arcanite $(K,NH_4)_2SO_4$	Epsomite $MgSO_4 7H_2O$	Eugsterite $Na_2Ca(SO_4)_3 2H_2O$	Gorgeyite $K_2Ca_5(SO_4)_6 2H_2O$	Krausite $KFe(SO_4)_2 H_2O$	Leightonite $K_2Ca_2Cu(SO_4)_4 2H_2O$	Mercallite $KHSO_4$	Polyhalite $K_2Ca_2Mg(SO_4)_4 2H_2O$	Starkeyite $MgSO_4 2H_2O$	Wattevilleite $Na_2Ca(SO_4)_2 4H_2O$
380														
382														
384														
386														
388														
390														
392														
394														
396														
398														
400														
402														
404														
406														
408														
410														
412														
414														
416														
418														
420														
422														
424														
426														
428														
430														
432			X											
434														
436														
438														
440														
442														
444														
446														
448														
450														

Detailed Evaporite Mineralogy (North Core)

Depth (cm)	Ankerite $Ca(Fe,Mg)(CO_3)_2$	Benstonite $Ca_7Ba_6(CO_3)_{13}$	Fairchildite $K_2Ca(CO_3)_2$	Gaylussite $Na_2Ca(CO_3)_2$ $5H_2O$	Arcanite $(K,NH_4)_2SO_4$	Epsomite $MgSO_4$ $7H_2O$	Eugsterite $Na_2Ca(SO_4)_3$ $2H_2O$	Gorgeyite $K_2Ca_5(SO_4)_6$ $2H_2O$	Krausite $KFe(SO_4)_2$ H_2O	Leightonite $K_2Ca_2Cu(SO_4)_4$ $2H_2O$	Mercallite $KHSO_4$	Polyhalite $K_2Ca_2Mg(SO_4)_4$ $2H_2O$	Starkeyite $MgSO_4$ $2H_2O$	Wattevilleite $Na_2Ca(SO_4)_2$ $4H_2O$
452														
454														
456														
458														
460														
462								X						
464														
466														
468														
470														
472														
474														
476														
478														
480														
482														
484														
486														
488														
490														
492														
494					X									
496														
498														
500														
502														
504														
506														
508														
510														
512														
514														
516														
518														
520					X									
522														

Detailed Evaporite Mineralogy (North Core)

Depth (cm)	Ankerite $Ca(Fe,Mg)(CO_3)_2$	Benstonite $Ca_7Ba_6(CO_3)_{13}$	Fairchildite $K_2Ca(CO_3)_2$	Gaylussite $Na_2Ca(CO_3)_2$ $5H_2O$	Arcanite $(K,NH_4)_2SO_4$	Epsomite $MgSO_4$ $7H_2O$	Eugsterite $Na_2Ca(SO_4)_3$ $2H_2O$	Gorgeyite $K_2Ca_5(SO_4)_6$ $2H_2O$	Krausite $KFe(SO_4)_2$ H_2O	Leightonite $K_2Ca_2Cu(SO_4)_4$ $2H_2O$	Mercallite $KHSO_4$	Polyhalite $K_2Ca_2Mg(SO_4)_4$ $2H_2O$	Starkeyite $MgSO_4$ $2H_2O$	Wattevilleite $Na_2Ca(SO_4)_2$ $4H_2O$
526														
528														
532														
534														
536														
538														
540														
542														
544														
546														
548														
550														
552					X									
554														
556														
558														
560														
564														
566														
568														
570														
572														
574				X										X
576														
578														
580														
582														
584			X											
586														
588														
590														
592														
594														
596														
598														
600					X									

Detailed Evaporite Mineralogy (North Core)

Depth (cm)	Ankerite $Ca(Fe,Mg)(CO_3)_2$	Benstonite $Ca_7Ba_6(CO_3)_{13}$	Fairchildite $K_2Ca(CO_3)_2$	Gaylussite $Na_2Ca(CO_3)_2$ $5H_2O$	Arcanite $(K,NH_4)_2SO_4$	Epsomite $MgSO_4$ $7H_2O$	Eugsterite $Na_2Ca(SO_4)_3$ $2H_2O$	Gorgeyite $K_2Ca_5(SO_4)_6$ $2H_2O$	Krausite $KFe(SO_4)_2$ H_2O	Leightonite $K_2Ca_2Cu(SO_4)_4$ $2H_2O$	Mercallite $KHSO_4$	Polyhalite $K_2Ca_2Mg(SO_4)_4$ $2H_2O$	Starkeyite $MgSO_4$ $2H_2O$	Wattevilleite $Na_2Ca(SO_4)_2$ $4H_2O$
602														
604														
606														
608														
616														
618														
620														
622														
624														
626														
628														
630														
634					X									
636														
638														
640														
642														
644														
646														
648														
650														
652														
654														
656														
658														
660														
662												X		
664														
666														
668														
670														
672														
674														
676														
678														
680														

Detailed Evaporite Mineralogy (North Core)

Depth (cm)	Ankerite $Ca(Fe,Mg)(CO_3)_2$	Benstonite $Ca_7Ba_6(CO_3)_{13}$	Fairchildite $K_2Ca(CO_3)_2$	Gaylussite $Na_2Ca(CO_3)_2$ $5H_2O$	Arcanite $(K,NH_4)_2SO_4$	Epsomite $MgSO_4$ $7H_2O$	Eugsterite $Na_2Ca(SO_4)_3$ $2H_2O$	Gorgeyite $K_2Ca_5(SO_4)_6$ $2H_2O$	Krausite $KFe(SO_4)_2$ H_2O	Leightonite $K_2Ca_2Cu(SO_4)_4$ $2H_2O$	Mercallite $KHSO_4$	Polyhalite $K_2Ca_2Mg(SO_4)_4$ $2H_2O$	Starkeyite $MgSO_4$ $2H_2O$	Wattevilleite $Na_2Ca(SO_4)_2$ $4H_2O$
682														
684														
686														
688			X											
690														
692														
694														
696														
698			X											
700														
702														
704														
706														
708			X											
710														
714														
716														
718														
720														
722														
724														
728														
730														
732														
734														
736														
738			X											
740														
746														
748														
750														
752								X						
754														
756														
758														
760														

Detailed Evaporite Mineralogy (North Core)

Depth (cm)	Ankerite $Ca(Fe,Mg)(CO_3)_2$	Benstonite $Ca_7Ba_6(CO_3)_{13}$	Fairchildite $K_2Ca(CO_3)_2$	Gaylussite $Na_2Ca(CO_3)_2$ $5H_2O$	Arcanite $(K,NH_4)_2SO_4$	Epsomite $MgSO_4$ $7H_2O$	Eugsterite $Na_2Ca(SO_4)_3$ $2H_2O$	Gorgeyite $K_2Ca_5(SO_4)_6$ $2H_2O$	Krausite $KFe(SO_4)_2$ H_2O	Leightonite $K_2Ca_2Cu(SO_4)_4$ $2H_2O$	Mercallite $KHSO_4$	Polyhalite $K_2Ca_2Mg(SO_4)_4$ $2H_2O$	Starkeyite $MgSO_4$ $2H_2O$	Wattevilleite $Na_2Ca(SO_4)_2$ $4H_2O$
762														
764														
792														
794														
796														
798														
800														
802														
804														
806														
808						X								
810														
812														
814														
816													X	
818														
820														
822														
824														
826														
828														
830														
832												X		
834											X			
836					X									
838					X									
840														
842														
844														
846														
848														
850														
852														
856														
860														
862														

Detailed Evaporite Mineralogy (North Core)

Depth (cm)	Ankerite $Ca(Fe,Mg)(CO_3)_2$	Benstonite $Ca_7Ba_6(CO_3)_{13}$	Fairchildite $K_2Ca(CO_3)_2$	Gaylussite $Na_2Ca(CO_3)_2$ $5H_2O$	Arcanite $(K,NH_4)_2SO_4$	Epsomite $MgSO_4$ $7H_2O$	Eugsterite $Na_2Ca(SO_4)_3$ $2H_2O$	Gorgeyite $K_2Ca_5(SO_4)_6$ $2H_2O$	Krausite $KFe(SO_4)_2$ H_2O	Leightonite $K_2Ca_2Cu(SO_4)_4$ $2H_2O$	Mercallite $KHSO_4$	Polyhalite $K_2Ca_2Mg(SO_4)_4$ $2H_2O$	Starkeyite $MgSO_4$ $2H_2O$	Wattevilleite $Na_2Ca(SO_4)_2$ $4H_2O$
864														
866														
868														
870														
872														
874														
876														
878														
880														
882														
884														
886														
888														
890														
892														
894														
896														
898														
900														
902														
904												X		
906														
908														
910														
912														
914														
916														
918												X		
920												X		
924														
926														
928														
930														
932														
934														
936														

Detailed Evaporite Mineralogy (North Core)

Depth (cm)	Ankerite $Ca(Fe,Mg)(CO_3)_2$	Benstonite $Ca_7Ba_6(CO_3)_{13}$	Fairchildite $K_2Ca(CO_3)_2$	Gaylussite $Na_2Ca(CO_3)_2 5H_2O$	Arcanite $(K,NH_4)_2SO_4$	Epsomite $MgSO_4 7H_2O$	Eugsterite $Na_2Ca(SO_4)_3 2H_2O$	Gorgeyite $K_2Ca_5(SO_4)_6 2H_2O$	Krausite $KFe(SO_4)_2 H_2O$	Leightonite $K_2Ca_2Cu(SO_4)_4 2H_2O$	Mercallite $KHSO_4$	Polyhalite $K_2Ca_2Mg(SO_4)_4 2H_2O$	Starkeyite $MgSO_4 2H_2O$	Wattevilleite $Na_2Ca(SO_4)_2 4H_2O$
938														
940														
942														
944														
946														
948														
950														
952														
954														
956														
958														
960														
962														
964														
972														
974														
976														
978														
980														
982														
984														
986														
988														
990														
992														
994								X						
996														
998														
1000												X		
1002														
1004														
1006								X						
1008														
1010														
1012														
1014											X			

Detailed Evaporite Mineralogy (North Core)

Depth (cm)	Ankerite $Ca(Fe,Mg)(CO_3)_2$	Benstonite $Ca_7Ba_6(CO_3)_{13}$	Fairchildite $K_2Ca(CO_3)_2$	Gaylussite $Na_2Ca(CO_3)_2 5H_2O$	Arcanite $(K,NH_4)_2SO_4$	Epsomite $MgSO_4 7H_2O$	Eugsterite $Na_2Ca(SO_4)_3 2H_2O$	Gorgeyite $K_2Ca_5(SO_4)_6 2H_2O$	Krausite $KFe(SO_4)_2 H_2O$	Leightonite $K_2Ca_2Cu(SO_4)_4 2H_2O$	Mercallite $KHSO_4$	Polyhalite $K_2Ca_2Mg(SO_4)_4 2H_2O$	Starkeyite $MgSO_4 2H_2O$	Wattevilleite $Na_2Ca(SO_4)_2 4H_2O$
1016					X									
1018														
1020														
1022														
1024												X		
1026														
1028														
1030											X			
1032														
1034											X			
1036														
1038														
1040														
1042														
1044														
1046														
1048				X									X	
1050														
1052														
1054														
1056														
1058														
1060														
1062														
1064														
1066														
1068														
1070												X		
1072			X											
1074													X	
1076														
1078														
1080														
1082														
1084														
1086														

Detailed Evaporite Mineralogy (North Core)

Depth (cm)	Ankerite $Ca(Fe,Mg)(CO_3)_2$	Benstonite $Ca_7Ba_6(CO_3)_{13}$	Fairchildite $K_2Ca(CO_3)_2$	Gaylussite $Na_2Ca(CO_3)_2 5H_2O$	Arcanite $(K,NH_4)_2SO_4$	Epsomite $MgSO_4 7H_2O$	Eugsterite $Na_4Ca(SO_4)_3 2H_2O$	Gorgeyite $K_2Ca_5(SO_4)_6 2H_2O$	Krausite $KFe(SO_4)_2 H_2O$	Leightonite $K_2Ca_2Cu(SO_4)_4 2H_2O$	Mercallite $KHSO_4$	Polyhalite $K_2Ca_2Mg(SO_4)_4 2H_2O$	Starkeyite $MgSO_4 2H_2O$	Wattevilleite $Na_2Ca(SO_4)_2 4H_2O$
1088														
1090														
1092														
1094														
1096														
1098														
1100			X											
1102			X											
1104			X											
1106														
1108														
1110														
1112														
1114														
1116														
1118			X											
1120														
1122														
1124			X											
1126														
1128														
1130														
1132														
1134														
1136														
1138														
1140														
1142			X											
1144														
1148														
1150			X											
1152														
1154			X											
1156														
1158														
1160														

Detailed Evaporite Mineralogy (North Core)

Depth (cm)	Ankerite $Ca(Fe,Mg)(CO_3)_2$	Benstonite $Ca_7Ba_6(CO_3)_{13}$	Fairchildite $K_2Ca(CO_3)_2$	Gaylussite $Na_2Ca(CO_3)_2$ $5H_2O$	Arcanite $(K,NH_4)_2SO_4$	Epsomite $MgSO_4$ $7H_2O$	Eugsterite $Na_2Ca(SO_4)_3$ $2H_2O$	Gorgeyite $K_2Ca_5(SO_4)_6$ $2H_2O$	Krausite $KFe(SO_4)_2$ H_2O	Leightonite $K_2Ca_2Cu(SO_4)_4$ $2H_2O$	Mercallite $KHSO_4$	Polyhalite $K_2Ca_2Mg(SO_4)_4$ $2H_2O$	Starkeyite $MgSO_4$ $2H_2O$	Wattevilleite $Na_2Ca(SO_4)_2$ $4H_2O$
1162														
1164														
1166														
1168														
1170														
1172														
1174														
1176														
1178														
1180														
1182														
1184														
1186														
1188														
1190														
1192														
1194														
1198														
1200														
1202														
1204														
1206														
1208														
1210														
1212														
1214														
1216														
1218														
1220														
1222														
1224														
1326														
1328														
1330														
1332														
1334														

Detailed Evaporite Mineralogy (North Core)

Depth (cm)	Ankerite $Ca(Fe,Mg)(CO_3)_2$	Benstonite $Ca_7Ba_6(CO_3)_{13}$	Fairchildite $K_2Ca(CO_3)_2$	Gaylussite $Na_2Ca(CO_3)_2 5H_2O$	Arcanite $(K,NH_4)_2SO_4$	Epsomite $MgSO_4 7H_2O$	Eugsterite $Na_2Ca(SO_4)_3 2H_2O$	Gorgeyite $K_2Ca_5(SO_4)_6 2H_2O$	Krausite $KFe(SO_4)_2 H_2O$	Leightonite $K_2Ca_2Cu(SO_4)_4 2H_2O$	Mercallite $KHSO_4$	Polyhalite $K_2Ca_2Mg(SO_4)_4 2H_2O$	Starkeyite $MgSO_4 2H_2O$	Wattevilleite $Na_2Ca(SO_4)_2 4H_2O$
1336														
1338														
1340														
1342														
1344														
1346														
1348														
1350														
1352			X											
1354														
1356								X						
1358														
1360														
1362														
1364														
1366														
1368														
1370														
1372			X											
1374														
1376					X									
1380														
1382														
1384														
1386														
1388														
1390							X						X	
1392							X							
1394							X							
1396														
1398														
1400														
1402														
1404														
1406														
1408														

Detailed Evaporite Mineralogy (North Core)

Depth (cm)	Ankerite $Ca(Fe,Mg)(CO_3)_2$	Benstonite $Ca_7Ba_6(CO_3)_{13}$	Fairchildite $K_2Ca(CO_3)_2$	Gaylussite $Na_2Ca(CO_3)_2 5H_2O$	Arcanite $(K,NH_4)_2SO_4$	Epsomite $MgSO_4 7H_2O$	Eugsterite $Na_2Ca(SO_4)_3 2H_2O$	Gorgeyite $K_2Ca_5(SO_4)_6 2H_2O$	Krausite $KFe(SO_4)_2 H_2O$	Leightonite $K_2Ca_2Cu(SO_4)_4 2H_2O$	Mercallite $KHSO_4$	Polyhalite $K_2Ca_2Mg(SO_4)_4 2H_2O$	Starkeyite $MgSO_4 2H_2O$	Wattevilleite $Na_2Ca(SO_4)_2 4H_2O$
1410														
1412														
1414														
1416														
1418														
1420														
1422														
1424														
1426														
1428														
1430														
1432														
1434														
1436														
1438			X											
1440														
1442			X											
1444														
1446								X					X	
1448														
1450														
1452														
1454														
1456														
1458														
1460														
1462														
1464														
1466														
1468			X											
1470														
1472														
1474														
1476														
1478														
1480														

Detailed Evaporite Mineralogy (North Core)

Depth (cm)	Ankerite $Ca(Fe,Mg)(CO_3)_2$	Benstonite $Ca_7Ba_6(CO_3)_{13}$	Fairchildite $K_2Ca(CO_3)_2$	Gaylussite $Na_2Ca(CO_3)_2 \cdot 5H_2O$	Arcanite $(K,NH_4)_2SO_4$	Epsomite $MgSO_4 \cdot 7H_2O$	Eugsterite $Na_4Ca(SO_4)_3 \cdot 2H_2O$	Gorgeyite $K_2Ca_5(SO_4)_6 \cdot 2H_2O$	Krausite $KFe(SO_4)_2 \cdot H_2O$	Leightonite $K_2Ca_2Cu(SO_4)_4 \cdot 2H_2O$	Mercallite $KHSO_4$	Polyhalite $K_2Ca_2Mg(SO_4)_4 \cdot 2H_2O$	Starkeyite $MgSO_4 \cdot 2H_2O$	Wattevilleite $Na_2Ca(SO_4)_2 \cdot 4H_2O$
1482														
1484														
1486														
1488														
1490														
1492														
1494														
1496														
1498														
1500														
1504														
1506														
1508														
1510														
1512			X											
1514														
1516														
1518														
1520														
1522														
1524														
1526														
1528														
1530														
1532														
1534														
1536														
1538														
1540														
1542														
1544														
1546														
1548														
1550														
1552														
1554				X										

Detailed Evaporite Mineralogy (North Core)

Depth (cm)	Ankerite $Ca(Fe,Mg)(CO_3)_2$	Benstonite $Ca_7Ba_6(CO_3)_{13}$	Fairchildite $K_2Ca(CO_3)_2$	Gaylussite $Na_2Ca(CO_3)_2 5H_2O$	Arcanite $(K,NH_4)_2SO_4$	Epsomite $MgSO_4 7H_2O$	Eugsterite $Na_2Ca(SO_4)_3 2H_2O$	Gorgeyite $K_2Ca_5(SO_4)_6 2H_2O$	Krausite $KFe(SO_4)_2 H_2O$	Leightonite $K_2Ca_2Cu(SO_4)_4 2H_2O$	Mercallite $KHSO_4$	Polyhalite $K_2Ca_2Mg(SO_4)_4 2H_2O$	Starkeyite $MgSO_4 2H_2O$	Wattevilleite $Na_2Ca(SO_4)_2 4H_2O$
1556														
1558														
1560														
1562														
1564														
1566														
1568														
1570														
1572														
1574														
1576														
1578														
1580														
1582														
1586														
1588														
1590														
1592														
1594														
1596														
1598														
1600														
1602														
1604														
1606														
1608														
1610														
1612														
1614														
1616														
1618														
1620														
1622														
1624														
1626														
1628														

Detailed Evaporite Mineralogy (North Core)

Depth (cm)	Ankerite $Ca(Fe,Mg)(CO_3)_2$	Benstonite $Ca_7Ba_6(CO_3)_{13}$	Fairchildite $K_2Ca(CO_3)_2$	Gaylussite $Na_2Ca(CO_3)_2 5H_2O$	Arcanite $(K,NH_4)_2SO_4$	Epsomite $MgSO_4 7H_2O$	Eugsterite $Na_2Ca(SO_4)_3 2H_2O$	Gorgeyite $K_2Ca_5(SO_4)_6 2H_2O$	Krausite $KFe(SO_4)_2 H_2O$	Leightonite $K_2Ca_2Cu(SO_4)_4 2H_2O$	Mercallite $KHSO_4$	Polyhalite $K_2Ca_2Mg(SO_4)_4 2H_2O$	Starkeyite $MgSO_4 2H_2O$	Wattevilleite $Na_2Ca(SO_4)_2 4H_2O$
1630														
1632														
1634														
1636														
1638														
1640														
1642														
1644														
1646														
1648														
1650														
1652														
1654														
1656														
1658														
1660														
1662														
1664													X	
1666														
1668														
1670														
1672														
1674														
1676														
1678														
1680														
1730														
1732														
1734														
1736														
1738													X	
1740														
1742														
1744														
1746														
1748														

Detailed Evaporite Mineralogy (North Core)

Depth (cm)	Ankerite $Ca(Fe,Mg)(CO_3)_2$	Benstonite $Ca_7Ba_6(CO_3)_{13}$	Fairchildite $K_2Ca(CO_3)_2$	Gaylussite $Na_2Ca(CO_3)_2$ $5H_2O$	Arcanite $(K,NH_4)_2SO_4$	Epsomite $MgSO_4$ $7H_2O$	Eugsterite $Na_2Ca(SO_4)_3$ $2H_2O$	Gorgeyite $K_2Ca_5(SO_4)_6$ $2H_2O$	Krausite $KFe(SO_4)_2$ H_2O	Leightonite $K_2Ca_2Cu(SO_4)_4$ $2H_2O$	Mercallite $KHSO_4$	Polyhalite $K_2Ca_2Mg(SO_4)_4$ $2H_2O$	Starkeyite $MgSO_4$ $2H_2O$	Wattevilleite $Na_2Ca(SO_4)_2$ $4H_2O$
1750														
1752														
1754								X						
1756														
1758														
1760														
1762														
1764														
1766														
1768														
1770				X										
1772														
1774														
1776														
1778														
1780														
1782														
1786														
1788														
1790														
1792														
1794														
1796														
1798														
1800														
1802														
1804														
1806														
1808														
1810														
1812			X											
1814														
1816														
1818														
1820														
1822														

Detailed Evaporite Mineralogy (North Core)

Depth (cm)	Ankerite $Ca(Fe,Mg)(CO_3)_2$	Benstonite $Ca_7Ba_6(CO_3)_{13}$	Fairchildite $K_2Ca(CO_3)_2$	Gaylussite $Na_2Ca(CO_3)_2$ $5H_2O$	Arcanite $(K,NH_4)_2SO_4$	Epsomite $MgSO_4$ $7H_2O$	Eugsterite $Na_2Ca(SO_4)_3$ $2H_2O$	Gorgeyite $K_2Ca_5(SO_4)_6$ $2H_2O$	Krausite $KFe(SO_4)_2$ H_2O	Leightonite $K_2Ca_2Cu(SO_4)_4$ $2H_2O$	Mercallite $KHSO_4$	Polyhalite $K_2Ca_2Mg(SO_4)_4$ $2H_2O$	Starkeyite $MgSO_4$ $2H_2O$	Wattevilleite $Na_2Ca(SO_4)_2$ $4H_2O$
1824														
1826														
1828														
1830														
1832														
1834														
1836														
1912														
1914														
1916														
1918														
1920			X											
1922														
1924														
1926														
1928														
1930														
1932														
1934														
1936														
1938														
1940														
1942														
1944														
1946														
1948														
1950														
1952														
1954														
1956														
1958														
1960														
1962														
1964														
1966														
1968														

Detailed Evaporite Mineralogy (North Core)

Depth (cm)	Ankerite $Ca(Fe,Mg)(CO_3)_2$	Benstonite $Ca_7Ba_6(CO_3)_{13}$	Fairchildite $K_2Ca(CO_3)_2$	Gaylussite $Na_2Ca(CO_3)_2$ $5H_2O$	Arcanite $(K,NH_4)_2SO_4$	Epsomite $MgSO_4$ $7H_2O$	Eugsterite $Na_2Ca(SO_4)_3$ $2H_2O$	Gorgeyite $K_2Ca_5(SO_4)_6$ $2H_2O$	Krausite $KFe(SO_4)_2$ H_2O	Leightonite $K_2Ca_2Cu(SO_4)_4$ $2H_2O$	Mercallite $KHSO_4$	Polyhalite $K_2Ca_2Mg(SO_4)_4$ $2H_2O$	Starkeyite $MgSO_4$ $2H_2O$	Wattevilleite $Na_2Ca(SO_4)_2$ $4H_2O$
1970														
1974														
1976														
1978														
1980														
1982														
1984														
1986														
1988														
1990														
1992														
1994														
1996														
2000														
2002														
2004														
2006														
2008														
2010														
2012														
2014														
2016														
2018														
2020														
2022														
2024														
2026														
2028														
2030														
2032														
2034														
2036														
2038														
2040														
2042														
2044														

Detailed Evaporite Mineralogy (North Core)

Depth (cm)	Ankerite $Ca(Fe,Mg)(CO_3)_2$	Benstonite $Ca_7Ba_6(CO_3)_{13}$	Fairchildite $K_2Ca(CO_3)_2$	Gaylussite $Na_2Ca(CO_3)_2 5H_2O$	Arcanite $(K,NH_4)_2SO_4$	Epsomite $MgSO_4 7H_2O$	Eugsterite $Na_2Ca(SO_4)_3 2H_2O$	Gorgeyite $K_2Ca_5(SO_4)_6 2H_2O$	Krausite $KFe(SO_4)_2 H_2O$	Leightonite $K_2Ca_2Cu(SO_4)_4 2H_2O$	Mercallite $KHSO_4$	Polyhalite $K_2Ca_2Mg(SO_4)_4 2H_2O$	Starkeyite $MgSO_4 2H_2O$	Wattevilleite $Na_2Ca(SO_4)_2 4H_2O$
2046														
2048														
2052														
2054														
2056														
2058														
2060														
2062														
2064														
2066														
2068														
2070														
2072														
2074														
2076														
2078														
2080														
2082														
2084														
2086														
2088														
2090														
2092														
2094														
2096														
2098														
2100														
2102														
2104														
2108														
2110														
2112														
2114														
2116														
2118														
2120														

Detailed Evaporite Mineralogy (North Core)

Depth (cm)	Ankerite $Ca(Fe,Mg)(CO_3)_2$	Benstonite $Ca_7Ba_6(CO_3)_{13}$	Fairchildite $K_2Ca(CO_3)_2$	Gaylussite $Na_2Ca(CO_3)_2$ $5H_2O$	Arcanite $(K,NH_4)_2SO_4$	Epsomite $MgSO_4$ $7H_2O$	Eugsterite $Na_2Ca(SO_4)_3$ $2H_2O$	Gorgeyite $K_2Ca_5(SO_4)_6$ $2H_2O$	Krausite $KFe(SO_4)_2$ H_2O	Leightonite $K_2Ca_2Cu(SO_4)_4$ $2H_2O$	Mercallite $KHSO_4$	Polyhalite $K_2Ca_2Mg(SO_4)_4$ $2H_2O$	Starkeyite $MgSO_4$ $2H_2O$	Wattevilleite $Na_2Ca(SO_4)_2$ $4H_2O$
2122														
2124														
2126														
2128														
2130														
2132														
2134														
2136														
2138														
2140														
2142														
2144														
2146														
2148														
2150														
2152														
2154														
2156														
2158														
2160														
2162														
2164														
2166														
2168														
2170														
2172														
2174														
2176														
2178														
2180														
2182														
2184														
2186														
2188														
2190														
2192														

Detailed Evaporite Mineralogy (North Core)

Depth (cm)	Ankerite $Ca(Fe,Mg)(CO_3)_2$	Benstonite $Ca_7Ba_6(CO_3)_{13}$	Fairchildite $K_2Ca(CO_3)_2$	Gaylussite $Na_2Ca(CO_3)_2 5H_2O$	Arcanite $(K,NH_4)_2SO_4$	Epsomite $MgSO_4 7H_2O$	Eugsterite $Na_4Ca(SO_4)_3 2H_2O$	Gorgeyite $K_2Ca_5(SO_4)_6 2H_2O$	Krausite $KFe(SO_4)_2 H_2O$	Leightonite $K_2Ca_2Cu(SO_4)_4 2H_2O$	Mercallite $KHSO_4$	Polyhalite $K_2Ca_2Mg(SO_4)_4 2H_2O$	Starkeyite $MgSO_4 2H_2O$	Wattevilleite $Na_2Ca(SO_4)_2 4H_2O$
2194														
2196														
2198														
2200														
2202														
2204														
2206														
2208														
2210														
2212														
2214														
2216														
2218														
2220														
2222														
2224														
2226														
2228														
2230														
2232														
2234														
2236														
2238														
2240														
2242														
2244														
2246														
2250														
2252														
2254														
2256														
2258														
2260														
2262														
2264														
2266														

Detailed Evaporite Mineralogy (North Core)

Depth (cm)	Ankerite $Ca(Fe,Mg)(CO_3)_2$	Benstonite $Ca_7Ba_6(CO_3)_{13}$	Fairchildite $K_2Ca(CO_3)_2$	Gaylussite $Na_2Ca(CO_3)_2 5H_2O$	Arcanite $(K,NH_4)_2SO_4$	Epsomite $MgSO_4 7H_2O$	Eugsterite $Na_2Ca(SO_4)_3 2H_2O$	Gorgeyite $K_2Ca_5(SO_4)_6 2H_2O$	Krausite $KFe(SO_4)_2 H_2O$	Leightonite $K_2Ca_2Cu(SO_4)_4 2H_2O$	Mercallite $KHSO_4$	Polyhalite $K_2Ca_2Mg(SO_4)_4 2H_2O$	Starkeyite $MgSO_4 2H_2O$	Wattevilleite $Na_2Ca(SO_4)_2 4H_2O$
2268														
2270														
2272														
2274														
2276														
2280														
2282														
2284														
2286														
2288														
2290														
2292														
2294														
2296														

Detailed Evaporite Mineralogy (North Core)

Depth (cm)	Bradleyite $Na_3Mg(PO_4)(CO_3)$	Burkeite $Na_4(SO_4)(CO_3,SO_4)$	Hanksite $KNa_{22}(CO_3)_2(SO_4)_9Cl$	Kainite $KMg(SO_4)Cl \cdot 2.75H_2O$	Rapidcreekite $Ca_2(CO_3)SO_4 \cdot 4H_2O$	Tychite $Na_6Mg_2(SO_4)(CO_3)_4$	Bischofite $MgCl_2.6H_2O$	Carnallite $KMgCl_3 \cdot 6H_2O$	Korshunovskite $Mg_2Cl(OH)_3 \cdot 2H_2O$	Niter KNO_3	Nitratine $NaNO_3$	Inderborite $CaMgB_6O_{11} \cdot H_2O$	Sepiolite $Mg_4Si_6O_{15}(OH)_2.6H_2O$
12													
14													
16													
18													
20												X	
22													
24													
26													
28										X			
30									X				
32													
34													
36										X			
38												X	
40												X	
42												X	
44													
46												X	
48												X	
50													
52												X	
54													
56													
58													
60													
62							X						
64													
66												X	
68													
70													
72													
74													
76													
78			X										
80													
82													

Detailed Evaporite Mineralogy (North Core)

Depth (cm)	Bradleyite $Na_3Mg(PO_4)(CO_3)$	Burkeite $Na_4(SO_4)(CO_3,SO_4)$	Hanksite $KNa_{22}(CO_3)_2(SO_4)_9Cl$	Kainite $KMg(SO_4)Cl\ 2.75H_2O$	Rapidcreekite $Ca_2(CO_3)SO_4\ 4H_2O$	Tychite $Na_6Mg_2(SO_4)(CO_3)_4$	Bischofite $MgCl_2.6H_2O$	Carnallite $KMgCl_3\ 6H_2O$	Korshunovskite $Mg_2Cl(OH)_3\ 2H_2O$	Niter KNO_3	Nitratine $NaNO_3$	Inderborite $CaMgB_6O_{11}\ H_2O$	Sepiolite $Mg_4Si_6O_{15}(OH)_2.6H_2O$
84													
86													
88													
90													
92													
94													
96			X										
98													
100													
106			X										
108													
110													
112													
114													
116													
118													
120													
122													
124													
126													
128													
130			X										
132													
134												X	
136													
138													
140													
142													
144													
146													
148													
150													
152													
154													
156													
158													

Detailed Evaporite Mineralogy (North Core)

Depth (cm)	Bradleyite $Na_3Mg(PO_4)(CO_3)$	Burkeite $Na_4(SO_4)(CO_3,SO_4)$	Hanksite $KNa_{22}(CO_3)_2(SO_4)_9Cl$	Kainite $KMg(SO_4)Cl\ 2.75H_2O$	Rapidcreekite $Ca_2(CO_3)SO_4\ 4H_2O$	Tychite $Na_6Mg_2(SO_4)(CO_3)_4$	Bischofite $MgCl_2.6H_2O$	Carnallite $KMgCl_3\ 6H_2O$	Korshunovskite $Mg_2Cl(OH)_3\ 2H_2O$	Niter KNO_3	Nitratine $NaNO_3$	Inderborite $CaMgB_6O_{11}\ H_2O$	Sepiolite $Mg_4Si_6O_{15}(OH)_2.6H_2O$
160												X	
162													
164													
166													
168													
170													
172													
174													
176										X			
178													
180			X										
182													
184													
188													
190													
192												X	
194			X										
196													
198					X								
200													
202													
204													
206			X										
208													
210			X										
212			X										
214													
216													
218			X										
220												X	
222			X										
224													
226												X	
228													
230													
232			X										

Detailed Evaporite Mineralogy (North Core)

Depth (cm)	Bradleyite $Na_3Mg(PO_4)(CO_3)$	Burkeite $Na_4(SO_4)(CO_3,SO_4)$	Hanksite $KNa_{22}(CO_3)_2(SO_4)_9Cl$	Kainite $KMg(SO_4)Cl$ $2.75H_2O$	Rapidcreekite $Ca_2(CO_3)SO_4$ $4H_2O$	Tychite $Na_6Mg_2(SO_4)(CO_3)_4$	Bischofite $MgCl_2.6H_2O$	Carnallite $KMgCl_3$ $6H_2O$	Korshunovskite $Mg_2Cl(OH)_3$ $2H_2O$	Niter KNO_3	Nitratine $NaNO_3$	Inderborite $CaMgB_6O_{11}$ H_2O	Sepiolite $Mg_4Si_6O_{15}(OH)_2.6H_2O$
234													
236													
238													
234			X										
242												X	
244													
246													
248			X										
250			X										
252													
254													
256													
258			X										
260			X										
262													
264			X										
266													
268													
270			X										
272												X	
274			X										
276													
278													
280													
282													
284													
286													
288													
290													
292													
294													
296													
298													
300												X	
302			X										
304			X										

Detailed Evaporite Mineralogy (North Core)

Depth (cm)	Bradleyite $Na_3Mg(PO_4)(CO_3)$	Burkeite $Na_4(SO_4)(CO_3,SO_4)$	Hanksite $KNa_{22}(CO_3)_2(SO_4)_9Cl$	Kainite $KMg(SO_4)Cl\ 2.75H_2O$	Rapidcreekite $Ca_2(CO_3)SO_4\ 4H_2O$	Tychite $Na_6Mg_2(SO_4)(CO_3)_4$	Bischofite $MgCl_2.6H_2O$	Carnallite $KMgCl_3\ 6H_2O$	Korshunovskite $Mg_2Cl(OH)_3\ 2H_2O$	Niter KNO_3	Nitratine $NaNO_3$	Inderborite $CaMgB_6O_{11}\ H_2O$	Sepiolite $Mg_4Si_6O_{15}(OH)_2.6H_2O$
306													
308			X										
310													
312													
314													
316													
318			X										
320													
322													
324													
326													
328			X										
330												X	
332													
334													
336			X										
338													
340			X										
342													
344													
346													
348			X										
350													
352													
354													
356													
358						X							
360													
362			X										
364													
368													
370													
372													
374													
376													
378													

Detailed Evaporite Mineralogy (North Core)

Depth (cm)	Bradleyite $Na_3Mg(PO_4)(CO_3)$	Burkeite $Na_4(SO_4)(CO_3,SO_4)$	Hanksite $KNa_{22}(CO_3)_2(SO_4)_9Cl$	Kainite $KMg(SO_4)Cl\ 2.75H_2O$	Rapidcreekite $Ca_2(CO_3)SO_4\ 4H_2O$	Tychite $Na_6Mg_2(SO_4)(CO_3)_4$	Bischofite $MgCl_2.6H_2O$	Carnallite $KMgCl_3\ 6H_2O$	Korshunovskite $Mg_2Cl(OH)_3\ 2H_2O$	Niter KNO_3	Nitratine $NaNO_3$	Inderborite $CaMgB_6O_{11}\ H_2O$	Sepiolite $Mg_4Si_6O_{15}(OH)_2.6H_2O$
380													
382													
384													
386													
388													
390													
392													
394													
396													
398										X			
400										X			
402													
404													
406													
408													
410													
412													
414										X			
416													
418													
420													
422				X									
424													
426													
428			X							X			
430													
432													
434													
436													
438													
440													
442													
444													
446													
448													
450													

Detailed Evaporite Mineralogy (North Core)

Depth (cm)	Bradleyite $Na_3Mg(PO_4)(CO_3)$	Burkeite $Na_4(SO_4)(CO_3,SO_4)$	Hanksite $KNa_{22}(CO_3)_2(SO_4)_9Cl$	Kainite $KMg(SO_4)Cl \cdot 2.75H_2O$	Rapidcreekite $Ca_2(CO_3)SO_4 \cdot 4H_2O$	Tychite $Na_6Mg_2(SO_4)(CO_3)_4$	Bischofite $MgCl_2.6H_2O$	Carnallite $KMgCl_3 \cdot 6H_2O$	Korshunovskite $Mg_2Cl(OH)_3 \cdot 2H_2O$	Niter KNO_3	Nitratine $NaNO_3$	Inderborite $CaMgB_6O_{11} \cdot H_2O$	Sepiolite $Mg_4Si_6O_{15}(OH)_2.6H_2O$
452													
454													
456											X		
458													
460			X										
462													
464													
466													
468													
470													
472			X										
474													
476													
478													
480													
482													
484			X										
486													
488			X										
490													
492													
494			X									X	
496													
498													
500													
502													
504													
506													
508			X										
510													
512													
514													
516													
518													
520													
522												X	

Detailed Evaporite Mineralogy (North Core)

Depth (cm)	Bradleyite $Na_3Mg(PO_4)(CO_3)$	Burkeite $Na_4(SO_4)(CO_3,SO_4)$	Hanksite $KNa_{22}(CO_3)_2(SO_4)_9Cl$	Kainite $KMg(SO_4)Cl$ $2.75H_2O$	Rapidcreekite $Ca_2(CO_3)SO_4$ $4H_2O$	Tychite $Na_6Mg_2(SO_4)(CO_3)_4$	Bischofite $MgCl_2.6H_2O$	Carnallite $KMgCl_3$ $6H_2O$	Korshunovskite $Mg_2Cl(OH)_3$ $2H_2O$	Niter KNO_3	Nitratine $NaNO_3$	Inderborite $CaMgB_6O_{11}$ H_2O	Sepiolite $Mg_4Si_6O_{15}(OH)_2.6H_2O$
526												X	
528													
532													
534			X									X	
536												X	
538													
540												X	
542												X	
544													
546													
548													
550			X										
552													
554													
556												X	
558													
560												X	
564			X										
566			X										
568													
570													
572													
574													
576													
578													
580													
582													
584													
586													
588													
590					X								
592													X
594													
596													
598													X
600													

Detailed Evaporite Mineralogy (North Core)

Depth (cm)	Bradleyite $Na_3Mg(PO_4)(CO_3)$	Burkeite $Na_4(SO_4)(CO_3,SO_4)$	Hanksite $KNa_{22}(CO_3)_2(SO_4)_9Cl$	Kainite $KMg(SO_4)Cl\ 2.75H_2O$	Rapidcreekite $Ca_2(CO_3)SO_4\ 4H_2O$	Tychite $Na_6Mg_2(SO_4)(CO_3)_4$	Bischofite $MgCl_2.6H_2O$	Carnallite $KMgCl_3\ 6H_2O$	Korshunovskite $Mg_2Cl(OH)_3\ 2H_2O$	Niter KNO_3	Nitratine $NaNO_3$	Inderborite $CaMgB_6O_{11}\ H_2O$	Sepiolite $Mg_4Si_6O_{15}(OH)_2.6H_2O$
602													
604			X										
606													
608													
616													
618												X	
620													
622													
624													
626													
628													
630			X										
634			X										
636													
638													
640			X										
642			X										
644													
646			X										
648													
650												X	
652			X										
654													
656													
658													
660			X										
662			X										
664													X
666													
668													
670													
672													
674													
676													
678													
680													

Detailed Evaporite Mineralogy (North Core)

Depth (cm)	Bradleyite $Na_3Mg(PO_4)(CO_3)$	Burkeite $Na_4(SO_4)(CO_3,SO_4)$	Hanksite $KNa_{22}(CO_3)_2(SO_4)_9Cl$	Kainite $KMg(SO_4)Cl\ 2.75H_2O$	Rapidcreekite $Ca_2(CO_3)SO_4\ 4H_2O$	Tychite $Na_6Mg_2(SO_4)(CO_3)_4$	Bischofite $MgCl_2.6H_2O$	Carnallite $KMgCl_3\ 6H_2O$	Korshunovskite $Mg_2Cl(OH)_3\ 2H_2O$	Niter KNO_3	Nitratine $NaNO_3$	Inderborite $CaMgB_6O_{11}\ H_2O$	Sepiolite $Mg_4Si_6O_{15}(OH)_2.6H_2O$
682			X										
684													
686													
688													
690													
692													
694													
696													
698													
700													
702			X										
704													
706													
708			X										
710													
714													
716													
718													
720													
722													
724													
728												X	
730		X											
732			X										
734													
736													
738			X										
740													
746													
748													
750			X										
752			X										
754													
756													
758			X										
760													

Detailed Evaporite Mineralogy (North Core)

Depth (cm)	Bradleyite $Na_3Mg(PO_4)(CO_3)$	Burkeite $Na_4(SO_4)(CO_3,SO_4)$	Hanksite $KNa_{22}(CO_3)_2(SO_4)_9Cl$	Kainite $KMg(SO_4)Cl\ 2.75H_2O$	Rapidcreekite $Ca_2(CO_3)SO_4\ 4H_2O$	Tychite $Na_6Mg_2(SO_4)(CO_3)_4$	Bischofite $MgCl_2.6H_2O$	Carnallite $KMgCl_3\ 6H_2O$	Korshunovskite $Mg_2Cl(OH)_3\ 2H_2O$	Niter KNO_3	Nitratine $NaNO_3$	Inderborite $CaMgB_6O_{11}\ H_2O$	Sepiolite $Mg_4Si_6O_{15}(OH)_2.6H_2O$
762													
764													
792			X										
794													X
796			X										
798													
800			X										
802			X										
804													
806													
808													
810													
812			X										
814													
816													
818			X										
820			X									X	
822													
824			X									X	
826													
828												X	
830			X										
832												X	
834													
836													
838													
840			X										
842			X										
844													
846													
848			X										
850			X									X	
852													
856			X										
860			X										
862													

Detailed Evaporite Mineralogy (North Core)

Depth (cm)	Bradleyite $Na_3Mg(PO_4)(CO_3)$	Burkeite $Na_4(SO_4)(CO_3,SO_4)$	Hanksite $KNa_{22}(CO_3)_2(SO_4)_9Cl$	Kainite $KMg(SO_4)Cl \cdot 2.75H_2O$	Rapidcreekite $Ca_2(CO_3)SO_4 \cdot 4H_2O$	Tychite $Na_6Mg_2(SO_4)(CO_3)_4$	Bischofite $MgCl_2.6H_2O$	Carnallite $KMgCl_3 \cdot 6H_2O$	Korshunovskite $Mg_2Cl(OH)_3 \cdot 2H_2O$	Niter KNO_3	Nitratine $NaNO_3$	Inderborite $CaMgB_6O_{11} \cdot H_2O$	Sepiolite $Mg_4Si_6O_{15}(OH)_2.6H_2O$
864			X										
866		X	X										
868												X	
870													
872													
874			X										
876			X										
878			X										
880													
882			X										
884												X	
886													
888			X										
890													
892													
894			X										
896			X										
898			X					X					
900			X										
902			X										
904			X										
906			X										
908			X										
910													
912													
914			X										
916													
918	X												
920													
924	X		X										
926			X										
928													
930			X										
932													
934			X									X	
936													

Detailed Evaporite Mineralogy (North Core)

Depth (cm)	Bradleyite $Na_3Mg(PO_4)(CO_3)$	Burkeite $Na_4(SO_4)(CO_3,SO_4)$	Hanksite $KNa_{22}(CO_3)_2(SO_4)_9Cl$	Kainite $KMg(SO_4)Cl\ 2.75H_2O$	Rapidcreekite $Ca_2(CO_3)SO_4\ 4H_2O$	Tychite $Na_6Mg_2(SO_4)(CO_3)_4$	Bischofite $MgCl_2.6H_2O$	Carnallite $KMgCl_3\ 6H_2O$	Korshunovskite $Mg_2Cl(OH)_3\ 2H_2O$	Niter KNO_3	Nitratine $NaNO_3$	Inderborite $CaMgB_6O_{11}\ H_2O$	Sepiolite $Mg_4Si_6O_{15}(OH)_2.6H_2O$
938		X											
940													X
942													
944													
946													
948	X												
950													
952													
954													
956			X										
958													
960													
962													
964													
972			X										
974													
976			X										
978			X										
980			X										
982													
984													
986			X										
988													
990			X										
992													
994			X										
996			X										
998													
1000													
1002													
1004													
1006													
1008													
1010					X							X	
1012													
1014													

Detailed Evaporite Mineralogy (North Core)

Depth (cm)	Bradleyite $Na_3Mg(PO_4)(CO_3)$	Burkeite $Na_4(SO_4)(CO_3,SO_4)$	Hanksite $KNa_{22}(CO_3)_2(SO_4)_9Cl$	Kainite $KMg(SO_4)Cl\ 2.75H_2O$	Rapidcreekite $Ca_2(CO_3)SO_4\ 4H_2O$	Tychite $Na_6Mg_2(SO_4)(CO_3)_4$	Bischofite $MgCl_2.6H_2O$	Carnallite $KMgCl_3\ 6H_2O$	Korshunovskite $Mg_2Cl(OH)_3\ 2H_2O$	Niter KNO_3	Nitratine $NaNO_3$	Inderborite $CaMgB_6O_{11}\ H_2O$	Sepiolite $Mg_4Si_6O_{15}(OH)_2.6H_2O$
1016			X										
1018													
1020													
1022			X										
1024			X										
1026													
1028													
1030									X				
1032													
1034													
1036													
1038			X										
1040													
1042													
1044													
1046													
1048													
1050													
1052													
1054			X										
1056													
1058			X										
1060													
1062			X										
1064													
1066													
1068													
1070			X										
1072													
1074													
1076													
1078													
1080													
1082													
1084			X										
1086			X										

Detailed Evaporite Mineralogy (North Core)

Depth (cm)	Bradleyite $Na_3Mg(PO_4)(CO_3)$	Burkeite $Na_4(SO_4)(CO_3,SO_4)$	Hanksite $KNa_{22}(CO_3)_2(SO_4)_9Cl$	Kainite $KMg(SO_4)Cl\ 2.75H_2O$	Rapidcreekite $Ca_2(CO_3)SO_4\ 4H_2O$	Tychite $Na_6Mg_2(SO_4)(CO_3)_4$	Bischofite $MgCl_2.6H_2O$	Carnallite $KMgCl_3\ 6H_2O$	Korshunovskite $Mg_2Cl(OH)_3\ 2H_2O$	Niter KNO_3	Nitratine $NaNO_3$	Inderborite $CaMgB_6O_{11}\ H_2O$	Sepiolite $Mg_4Si_6O_{15}(OH)_2.6H_2O$
1088			X										
1090													
1092													
1094													
1096											X		
1098													
1100												X	
1102													
1104													
1106													
1108													
1110													
1112			X		X								
1114													
1116													
1118			X									X	
1120													X
1122													
1124											X		
1126													
1128													
1130													
1132													
1134													
1136													
1138													
1140													
1142													
1144					X								
1148													
1150													
1152													
1154													
1156					X								
1158	X												
1160													

Detailed Evaporite Mineralogy (North Core)

Depth (cm)	Bradleyite $Na_3Mg(PO_4)(CO_3)$	Burkeite $Na_4(SO_4)(CO_3,SO_4)$	Hanksite $KNa_{22}(CO_3)_2(SO_4)_9Cl$	Kainite $KMg(SO_4)Cl$ $2.75H_2O$	Rapidcreekite $Ca_2(CO_3)SO_4$ $4H_2O$	Tychite $Na_6Mg_2(SO_4)(CO_3)_4$	Bischofite $MgCl_2.6H_2O$	Carnallite $KMgCl_3$ $6H_2O$	Korshunovskite $Mg_2Cl(OH)_3$ $2H_2O$	Niter KNO_3	Nitratine $NaNO_3$	Inderborite $CaMgB_6O_{11}$ H_2O	Sepiolite $Mg_4Si_6O_{15}(OH)_2.6H_2O$
1162													
1164			X									X	
1166											X		
1168			X										
1170			X										
1172											X		
1174			X										
1176													
1178													
1180			X		X								
1182											X		
1184													
1186													
1188													
1190													
1192													
1194													
1198													
1200													
1202													
1204											X		
1206											X		
1208													
1210											X		
1212													
1214													
1216											X		
1218													
1220													
1222													
1224											X		
1326													
1328			X										
1330													
1332											X		
1334													

Detailed Evaporite Mineralogy (North Core)

Depth (cm)	Bradleyite $Na_3Mg(PO_4)(CO_3)$	Burkeite $Na_4(SO_4)(CO_3,SO_4)$	Hanksite $KNa_{22}(CO_3)_2(SO_4)_9Cl$	Kainite $KMg(SO_4)Cl\ 2.75H_2O$	Rapidcreekite $Ca_2(CO_3)SO_4\ 4H_2O$	Tychite $Na_6Mg_2(SO_4)(CO_3)_4$	Bischofite $MgCl_2.6H_2O$	Carnallite $KMgCl_3\ 6H_2O$	Korshunovskite $Mg_2Cl(OH)_3\ 2H_2O$	Niter KNO_3	Nitratine $NaNO_3$	Inderborite $CaMgB_6O_{11}\ H_2O$	Sepiolite $Mg_4Si_6O_{15}(OH)_2.6H_2O$
1336													
1338			X										
1340			X									X	
1342			X										
1344													
1346													
1348											X		
1350												X	
1352												X	
1354												X	
1356													
1358												X	
1360												X	
1362												X	
1364													
1366													
1368			X										
1370												X	
1372													
1374													
1376													
1380	X												
1382													
1384													
1386			X										
1388													
1390													
1392													
1394													
1396			X		X								
1398													
1400													
1402			X										
1404			X										
1406													
1408													

Detailed Evaporite Mineralogy (North Core)

Depth (cm)	Bradleyite $Na_3Mg(PO_4)(CO_3)$	Burkeite $Na_4(SO_4)(CO_3,SO_4)$	Hanksite $KNa_{22}(CO_3)_2(SO_4)_9Cl$	Kainite $KMg(SO_4)Cl$ $2.75H_2O$	Rapidcreekite $Ca_2(CO_3)SO_4$ $4H_2O$	Tychite $Na_6Mg_2(SO_4)(CO_3)_4$	Bischofite $MgCl_2.6H_2O$	Carnallite $KMgCl_3$ $6H_2O$	Korshunovskite $Mg_2Cl(OH)_3$ $2H_2O$	Niter KNO_3	Nitratine $NaNO_3$	Inderborite $CaMgB_6O_{11}$ H_2O	Sepiolite $Mg_4Si_6O_{15}(OH)_2.6H_2O$
1410			X										
1412			X										
1414													
1416													
1418													
1420													
1422											X		
1424													
1426													
1428													
1430													
1432													
1434													
1436													
1438													
1440													
1442			X								X		
1444													
1446													
1448			X										
1450													
1452			X										
1454			X										
1456			X										
1458													
1460													
1462											X		
1464													
1466											X		
1468													
1470													
1472												X	
1474			X										
1476													
1478													
1480											X		

Detailed Evaporite Mineralogy (North Core)

Depth (cm)	Bradleyite $Na_3Mg(PO_4)(CO_3)$	Burkeite $Na_4(SO_4)(CO_3,SO_4)$	Hanksite $KNa_{22}(CO_3)_2(SO_4)_9Cl$	Kainite $KMg(SO_4)Cl\ 2.75H_2O$	Rapidcreekite $Ca_2(CO_3)SO_4\ 4H_2O$	Tychite $Na_6Mg_2(SO_4)(CO_3)_4$	Bischofite $MgCl_2.6H_2O$	Carnallite $KMgCl_3\ 6H_2O$	Korshunovskite $Mg_2Cl(OH)_3\ 2H_2O$	Niter KNO_3	Nitratine $NaNO_3$	Inderborite $CaMgB_6O_{11}\ H_2O$	Sepiolite $Mg_4Si_6O_{15}(OH)_2.6H_2O$
1482													
1484													
1486													
1488											X		
1490											X		
1492			X										
1494													
1496													
1498													
1500													
1504			X										
1506													
1508													
1510													
1512													
1514			X										
1516			X										
1518			X										
1520													
1522													
1524											X		
1526													
1528			X										
1530													
1532													
1534			X										
1536													
1538			X										
1540											X		
1542											X		
1544											X		
1546													
1548			X										
1550													
1552											X		
1554													

Detailed Evaporite Mineralogy (North Core)

Depth (cm)	Bradleyite $Na_3Mg(PO_4)(CO_3)$	Burkeite $Na_4(SO_4)(CO_3,SO_4)$	Hanksite $KNa_{22}(CO_3)_2(SO_4)_9Cl$	Kainite $KMg(SO_4)Cl$ $2.75H_2O$	Rapidcreekite $Ca_2(CO_3)SO_4$ $4H_2O$	Tychite $Na_6Mg_2(SO_4)(CO_3)_4$	Bischofite $MgCl_2.6H_2O$	Carnallite $KMgCl_3$ $6H_2O$	Korshunovskite $Mg_2Cl(OH)_3$ $2H_2O$	Niter KNO_3	Nitratine $NaNO_3$	Inderborite $CaMgB_6O_{11}$ H_2O	Sepiolite $Mg_4Si_6O_{15}(OH)_2.6H_2O$
1556													
1558													
1560			X										
1562			X										
1564			X										
1566													
1568													
1570			X										
1572											X		
1574													
1576			X								X		
1578													
1580													
1582													
1586													
1588													
1590											X		
1592			X										
1594													
1596													
1598													
1600											X		
1602											X		
1604													
1606													
1608													
1610											X		
1612													
1614											X		
1616	X		X								X		
1618													
1620			X										
1622													
1624			X										
1626			X										
1628													

Detailed Evaporite Mineralogy (North Core)

Depth (cm)	Bradleyite $Na_3Mg(PO_4)(CO_3)$	Burkeite $Na_4(SO_4)(CO_3,SO_4)$	Hanksite $KNa_{22}(CO_3)_2(SO_4)_9Cl$	Kainite $KMg(SO_4)Cl\ 2.75H_2O$	Rapidcreekite $Ca_2(CO_3)SO_4\ 4H_2O$	Tychite $Na_6Mg_2(SO_4)(CO_3)_4$	Bischofite $MgCl_2.6H_2O$	Carnallite $KMgCl_3\ 6H_2O$	Korshunovskite $Mg_2Cl(OH)_3\ 2H_2O$	Niter KNO_3	Nitratine $NaNO_3$	Inderborite $CaMgB_6O_{11}\ H_2O$	Sepiolite $Mg_4Si_6O_{15}(OH)_2.6H_2O$
1630			X										
1632													
1634													
1636													
1638													
1640											X		
1642													
1644			X								X		
1646													
1648			X										
1650													
1652											X		
1654													
1656													
1658													
1660													
1662													
1664													
1666			X										
1668			X										
1670													
1672													
1674													
1676													
1678													
1680													
1730			X										
1732			X										
1734											X		
1736													
1738			X		X								
1740											X		
1742			X										
1744													
1746													
1748													

Detailed Evaporite Mineralogy (North Core)

Depth (cm)	Bradleyite $Na_3Mg(PO_4)(CO_3)$	Burkeite $Na_4(SO_4)(CO_3,SO_4)$	Hanksite $KNa_{22}(CO_3)_2(SO_4)_9Cl$	Kainite $KMg(SO_4)Cl\ 2.75H_2O$	Rapidcreekite $Ca_2(CO_3)SO_4\ 4H_2O$	Tychite $Na_6Mg_2(SO_4)(CO_3)_4$	Bischofite $MgCl_2.6H_2O$	Carnallite $KMgCl_3\ 6H_2O$	Korshunovskite $Mg_2Cl(OH)_3\ 2H_2O$	Niter KNO_3	Nitratine $NaNO_3$	Inderborite $CaMgB_6O_{11}\ H_2O$	Sepiolite $Mg_4Si_6O_{15}(OH)_2.6H_2O$
1750													
1752													
1754			X										
1756													
1758													
1760											X		
1762											X		
1764			X										
1766													
1768													
1770			X										
1772											X		
1774													
1776											X		
1778													
1780													
1782													
1786			X										
1788			X										
1790													
1792													
1794													
1796			X										
1798											X		
1800											X		
1802											X		
1804											X		
1806											X		
1808											X		
1810			X										
1812											X		
1814											X		
1816													
1818													
1820													
1822													

Detailed Evaporite Mineralogy (North Core)

Depth (cm)	Bradleyite $Na_3Mg(PO_4)(CO_3)$	Burkeite $Na_4(SO_4)(CO_3,SO_4)$	Hanksite $KNa_{22}(CO_3)_2(SO_4)_9Cl$	Kainite $KMg(SO_4)Cl\ 2.75H_2O$	Rapidcreekite $Ca_2(CO_3)SO_4\ 4H_2O$	Tychite $Na_6Mg_2(SO_4)(CO_3)_4$	Bischofite $MgCl_2.6H_2O$	Carnallite $KMgCl_3\ 6H_2O$	Korshunovskite $Mg_2Cl(OH)_3\ 2H_2O$	Niter KNO_3	Nitratine $NaNO_3$	Inderborite $CaMgB_6O_{11}\ H_2O$	Sepiolite $Mg_4Si_6O_{15}(OH)_2.6H_2O$
1824													
1826											X		
1828													
1830													
1832													
1834													
1836													
1912											X		
1914													
1916													
1918													
1920													
1922													
1924													
1926			X										
1928											X		
1930											X		
1932													
1934													
1936													
1938													
1940											X		
1942											X		
1944													
1946											X		
1948													
1950													
1952											X		
1954											X		
1956											X		
1958											X		
1960											X		
1962											X		
1964											X		
1966													
1968													

Detailed Evaporite Mineralogy (North Core)

Depth (cm)	Bradleyite $Na_3Mg(PO_4)(CO_3)$	Burkeite $Na_4(SO_4)(CO_3,SO_4)$	Hanksite $KNa_{22}(CO_3)_2(SO_4)_9Cl$	Kainite $KMg(SO_4)Cl \cdot 2.75H_2O$	Rapidcreekite $Ca_2(CO_3)SO_4 \cdot 4H_2O$	Tychite $Na_6Mg_2(SO_4)(CO_3)_4$	Bischofite $MgCl_2.6H_2O$	Carnallite $KMgCl_3 \cdot 6H_2O$	Korshunovskite $Mg_2Cl(OH)_3 \cdot 2H_2O$	Niter KNO_3	Nitratine $NaNO_3$	Inderborite $CaMgB_6O_{11} \cdot H_2O$	Sepiolite $Mg_4Si_6O_{15}(OH)_2.6H_2O$
1970											X		
1974											X		
1976											X		
1978													
1980											X		
1982											X		
1984											X		
1986													
1988											X		
1990											X		
1992											X		
1994													
1996											X		
2000											X		
2002													
2004											X		
2006													
2008											X		
2010													
2012													
2014											X		
2016											X		
2018											X		
2020											X		
2022											X		
2024													
2026													
2028			X										
2030													
2032											X		
2034											X		
2036													
2038													
2040											X		
2042											X		
2044											X		

Detailed Evaporite Mineralogy (North Core)

Depth (cm)	Bradleyite $Na_3Mg(PO_4)(CO_3)$	Burkeite $Na_4(SO_4)(CO_3,SO_4)$	Hanksite $KNa_{22}(CO_3)_2(SO_4)_9Cl$	Kainite $KMg(SO_4)Cl\ 2.75H_2O$	Rapidcreekite $Ca_2(CO_3)SO_4\ 4H_2O$	Tychite $Na_6Mg_2(SO_4)(CO_3)_4$	Bischofite $MgCl_2.6H_2O$	Carnallite $KMgCl_3\ 6H_2O$	Korshunovskite $Mg_2Cl(OH)_3\ 2H_2O$	Niter KNO_3	Nitratine $NaNO_3$	Inderborite $CaMgB_6O_{11}\ H_2O$	Sepiolite $Mg_4Si_6O_{15}(OH)_2.6H_2O$
2046													
2048													
2052											X		
2054											X		
2056											X		
2058											X		
2060													
2062													
2064													
2066											X		
2068													
2070											X		
2072													
2074													
2076													
2078													
2080													
2082											X		
2084											X		
2086													
2088											X		
2090													
2092													
2094											X		
2096											X		
2098													
2100											X		
2102													
2104											X		
2108													
2110													
2112											X		
2114											X		
2116											X		
2118											X		
2120													

Detailed Evaporite Mineralogy (North Core)

Depth (cm)	Bradleyite $Na_3Mg(PO_4)(CO_3)$	Burkeite $Na_4(SO_4)(CO_3,SO_4)$	Hanksite $KNa_{22}(CO_3)_2(SO_4)_9Cl$	Kainite $KMg(SO_4)Cl\ 2.75H_2O$	Rapidcreekite $Ca_2(CO_3)SO_4\ 4H_2O$	Tychite $Na_6Mg_2(SO_4)(CO_3)_4$	Bischofite $MgCl_2.6H_2O$	Carnallite $KMgCl_3\ 6H_2O$	Korshunovskite $Mg_2Cl(OH)_3\ 2H_2O$	Niter KNO_3	Nitratine $NaNO_3$	Inderborite $CaMgB_6O_{11}\ H_2O$	Sepiolite $Mg_4Si_6O_{15}(OH)_2.6H_2O$
2122											X		
2124											X		
2126													
2128											X		
2130											X		
2132											X		
2134											X		
2136													
2138											X		
2140													
2142											X		
2144											X		
2146											X		
2148											X		
2150													
2152											X		
2154											X		
2156											X		
2158											X		
2160											X		
2162													
2164													
2166											X		
2168											X		
2170											X		
2172													
2174													
2176													
2178													
2180													
2182											X		
2184											X		
2186													
2188													
2190													
2192											X		

Detailed Evaporite Mineralogy (North Core)

Depth (cm)	Bradleyite $Na_3Mg(PO_4)(CO_3)$	Burkeite $Na_4(SO_4)(CO_3,SO_4)$	Hanksite $KNa_{22}(CO_3)_2(SO_4)_9Cl$	Kainite $KMg(SO_4)Cl\ 2.75H_2O$	Rapidcreekite $Ca_2(CO_3)SO_4\ 4H_2O$	Tychite $Na_6Mg_2(SO_4)(CO_3)_4$	Bischofite $MgCl_2.6H_2O$	Carnallite $KMgCl_3\ 6H_2O$	Korshunovskite $Mg_2Cl(OH)_3\ 2H_2O$	Niter KNO_3	Nitratine $NaNO_3$	Inderborite $CaMgB_6O_{11}\ H_2O$	Sepiolite $Mg_4Si_6O_{15}(OH)_2.6H_2O$
2194													
2196											X		
2198													
2200											X		
2202													
2204			X										
2206													
2208													
2210											X		
2212													
2214													
2216													
2218											X		
2220											X		
2222													
2224													
2226													
2228											X		
2230											X		
2232											X		
2234													
2236													
2238											X		
2240													
2242											X		
2244													
2246													
2250											X		
2252													
2254											X		
2256													
2258													
2260											X		
2262											X		
2264											X		
2266			X										

Detailed Evaporite Mineralogy (North Core)

Depth (cm)	Bradleyite $Na_3Mg(PO_4)(CO_3)$	Burkeite $Na_4(SO_4)(CO_3,SO_4)$	Hanksite $KNa_{22}(CO_3)_2(SO_4)_9Cl$	Kainite $KMg(SO_4)Cl\ 2.75H_2O$	Rapidcreekite $Ca_2(CO_3)SO_4\ 4H_2O$	Tychite $Na_6Mg_2(SO_4)(CO_3)_4$	Bischofite $MgCl_2.6H_2O$	Carnallite $KMgCl_3\ 6H_2O$	Korshunovskite $Mg_2Cl(OH)_3\ 2H_2O$	Niter KNO_3	Nitratine $NaNO_3$	Inderborite $CaMgB_6O_{11}\ H_2O$	Sepiolite $Mg_4Si_6O_{15}(OH)_2.6H_2O$
2268													
2270											X		
2272											X		
2274											X		
2276											X		
2280													
2282													
2284											X		
2286											X		
2288													
2290													
2292											X		
2294													
2296													

Detailed Evaporite Mineralogy (South Core)

Depth (cm)	Ankerite $Ca(Fe,Mg)(CO_3)_2$	Artinite $Mg_2CO_3(OH)_2 3H_2O$	Fairchildite $K_2Ca(CO_3)_2$	Gaylussite $Na_2Ca(CO_3)_2$ $5H_2O$	Kutnohorite $Ca(Mn,Mg)(CO_3)_2$	Minrecordite $CaZn(CO_3)_2$	Zemkorite $Na_2Ca(CO_3)_2$	Arcanite $(K,NH_4)2SO_4$	Epsomite $MgSO_4$ $7H_2O$	Eugsterite $Na_2Ca(SO_4)_3$ $2H_2O$	Gorgeyite $K_2Ca_5(SO_4)_6$ $2H_2O$	Mercallite $KHSO_4$	Polyhalite $K_2Ca_2Mg(SO_4)_4$ $2H_2O$	Starkeyite $MgSO_4$ $4H_2O$
10														
12						X								
14						X								
16						X								
18						X								
20						X								
22						X								
24						X								
26						X								
28						X								
30	X					X								
32	X					X								
34	X					X								
36						X								
38						X								
40						X								
42						X								
44	X													
46						X								
48														
50														
52														
54														
56														
58														
60														
62														
64														
66														
68														
70														
72														
74							X							
76														
78														
80														
82														
84														

Detailed Evaporite Mineralogy (South Core)

Depth (cm)	Ankerite $Ca(Fe,Mg)(CO_3)_2$	Artinite $Mg_2CO_3(OH)_2 3H_2O$	Fairchildite $K_2Ca(CO_3)_2$	Gaylussite $Na_2Ca(CO_3)_2 5H_2O$	Kutnohorite $Ca(Mn,Mg)(CO_3)_2$	Minrecordite $CaZn(CO_3)_2$	Zemkorite $Na_2Ca(CO_3)_2$	Arcanite $(K,NH_4)2SO_4$	Epsomite $MgSO_4 7H_2O$	Eugsterite $Na_2Ca(SO_4)_3 2H_2O$	Gorgeyite $K_2Ca_5(SO_4)_6 2H_2O$	Mercallite $KHSO_4$	Polyhalite $K_2Ca_2Mg(SO_4)_4 2H_2O$	Starkeyite $MgSO_4 4H_2O$
86														
88														
90														
92			X											
94														
96														
98														
100														
102														
104														
106														
108														
110														
112														
114														
116														
118														
120														
122														
124														
126														
128														
130														
132														
134														
136														
138			X											
140														
142														
144														
146														
148														
150			X											
152			X											
154														
156														
158														
160														

Detailed Evaporite Mineralogy (South Core)

Depth (cm)	Ankerite $Ca(Fe,Mg)(CO_3)_2$	Artinite $Mg_2CO_3(OH)_2 3H_2O$	Fairchildite $K_2Ca(CO_3)_2$	Gaylussite $Na_2Ca(CO_3)_2 5H_2O$	Kutnohorite $Ca(Mn,Mg)(CO_3)_2$	Minrecordite $CaZn(CO_3)_2$	Zemkorite $Na_2Ca(CO_3)_2$	Arcanite $(K,NH_4)2SO_4$	Epsomite $MgSO_4 7H_2O$	Eugsterite $Na_2Ca(SO_4)_3 2H_2O$	Gorgeyite $K_2Ca_5(SO_4)_6 2H_2O$	Mercallite $KHSO_4$	Polyhalite $K_2Ca_2Mg(SO_4)_4 2H_2O$	Starkeyite $MgSO_4 4H_2O$
162														
164														
166														
168														
170														
172														
174														
176														
178														
180														
182														
184														
186														
188														
190														
192														
194														
196														
198			X											
200														
202			X											
204														
206														
208														
210														
212														
214														
216														
218														
220														
222														
224														
226					X									
228														
230														
232														
234														
236														

Detailed Evaporite Mineralogy (South Core)

Depth (cm)	Ankerite $Ca(Fe,Mg)(CO_3)_2$	Artinite $Mg_2CO_3(OH)_2 3H_2O$	Fairchildite $K_2Ca(CO_3)_2$	Gaylussite $Na_2Ca(CO_3)_2 5H_2O$	Kutnohorite $Ca(Mn,Mg)(CO_3)_2$	Minrecordite $CaZn(CO_3)_2$	Zemkorite $Na_2Ca(CO_3)_2$	Arcanite $(K,NH_4)2SO_4$	Epsomite $MgSO_4 7H_2O$	Eugsterite $Na_2Ca(SO_4)_3 2H_2O$	Gorgeyite $K_2Ca_5(SO_4)_6 2H_2O$	Mercallite $KHSO_4$	Polyhalite $K_2Ca_2Mg(SO_4)_4 2H_2O$	Starkeyite $MgSO_4 4H_2O$
238			X											
240			X											
242														
244														
246														
248														
250														
252														
254			X											
256			X											
258														
260														
262														
264														
266														
268														
270														
272														
274														
276														
278														
280														
282														
284														
286														
288														
290														
292														
294														
296														
298														
300														
302														
304														
306														
308														
310														
312														

Detailed Evaporite Mineralogy (South Core)

Depth (cm)	Ankerite $Ca(Fe,Mg)(CO_3)_2$	Artinite $Mg_2CO_3(OH)_2 3H_2O$	Fairchildite $K_2Ca(CO_3)_2$	Gaylussite $Na_2Ca(CO_3)_2 5H_2O$	Kutnohorite $Ca(Mn,Mg)(CO_3)_2$	Minrecordite $CaZn(CO_3)_2$	Zemkorite $Na_2Ca(CO_3)_2$	Arcanite $(K,NH_4)2SO_4$	Epsomite $MgSO_4 7H_2O$	Eugsterite $Na_2Ca(SO_4)_3 2H_2O$	Gorgeyite $K_2Ca_5(SO_4)_6 2H_2O$	Mercallite $KHSO_4$	Polyhalite $K_2Ca_2Mg(SO_4)_4 2H_2O$	Starkeyite $MgSO_4 4H_2O$
314														
316														
318														
320														
322														
324														
326														
328														
330														
332														
334														
336														
338														
340														
342														
344														
346														
348														
350														
352														
354														
356														
358														
360														
362														
364														
366														
368														
370														
372														
374														
376														
378														
380														
382														
384														
386														
388														

Detailed Evaporite Mineralogy (South Core)

Depth (cm)	Ankerite $Ca(Fe,Mg)(CO_3)_2$	Artinite $Mg_2CO_3(OH)_2 3H_2O$	Fairchildite $K_2Ca(CO_3)_2$	Gaylussite $Na_2Ca(CO_3)_2 5H_2O$	Kutnohorite $Ca(Mn,Mg)(CO_3)_2$	Minrecordite $CaZn(CO_3)_2$	Zemkorite $Na_2Ca(CO_3)_2$	Arcanite $(K,NH_4)2SO_4$	Epsomite $MgSO_4 7H_2O$	Eugsterite $Na_2Ca(SO_4)_3 2H_2O$	Gorgeyite $K_2Ca_5(SO_4)_6 2H_2O$	Mercallite $KHSO_4$	Polyhalite $K_2Ca_2Mg(SO_4)_4 2H_2O$	Starkeyite $MgSO_4 4H_2O$
390														
392														
394														
396								X						
398														
400														
402						X								
404														
406														
408														
410														
412														
414														
416														
500														
502														
504														
508														
510														
512								X						
514														
516														
518								X						
520			X											
522														
524														
526								X						
528								X						
530														
532														
534														
536														
538														
540														
542														
544														
546														
548								X						

Detailed Evaporite Mineralogy (South Core)

Depth (cm)	Ankerite $Ca(Fe,Mg)(CO_3)_2$	Artinite $Mg_2CO_3(OH)_2 3H_2O$	Fairchildite $K_2Ca(CO_3)_2$	Gaylussite $Na_2Ca(CO_3)_2 5H_2O$	Kutnohorite $Ca(Mn,Mg)(CO_3)_2$	Minrecordite $CaZn(CO_3)_2$	Zemkorite $Na_2Ca(CO_3)_2$	Arcanite $(K,NH_4)2SO_4$	Epsomite $MgSO_4 7H_2O$	Eugsterite $Na_2Ca(SO_4)_3 2H_2O$	Gorgeyite $K_2Ca_5(SO_4)_6 2H_2O$	Mercallite $KHSO_4$	Polyhalite $K_2Ca_2Mg(SO_4)_4 2H_2O$	Starkeyite $MgSO_4 4H_2O$
550														
552														
554														
556														
558														
560														
562														
564														
566														
568														X
570														
572														
574														
576														
578														
580														
582														
584														
586														
588								X						
590														
592														
594														
596														
598														
600			X											
602														
604														
606														
608														
610														
612														
614														
616												X		
618														
620														
622														
624														

Detailed Evaporite Mineralogy (South Core)

Depth (cm)	Ankerite $Ca(Fe,Mg)(CO_3)_2$	Artinite $Mg_2CO_3(OH)_2 3H_2O$	Fairchildite $K_2Ca(CO_3)_2$	Gaylussite $Na_2Ca(CO_3)_2 5H_2O$	Kutnohorite $Ca(Mn,Mg)(CO_3)_2$	Minrecordite $CaZn(CO_3)_2$	Zemkorite $Na_2Ca(CO_3)_2$	Arcanite $(K,NH_4)2SO_4$	Epsomite $MgSO_4 7H_2O$	Eugsterite $Na_2Ca(SO_4)_3 2H_2O$	Gorgeyite $K_2Ca_5(SO_4)_6 2H_2O$	Mercallite $KHSO_4$	Polyhalite $K_2Ca_2Mg(SO_4)_4 2H_2O$	Starkeyite $MgSO_4 4H_2O$
626														
628														
630														
632														
634														
636														
638														
640														
642														
644														
646														
648														
650														
652														
654														
656			X											
658														
660														
662														
664														
666														
668														
670														
672														
674														
676														
678														
680								X						
682														
684														
686														
824														
826														
828														
830														
832														
834														
836														

Detailed Evaporite Mineralogy (South Core)

Depth (cm)	Ankerite $Ca(Fe,Mg)(CO_3)_2$	Artinite $Mg_2CO_3(OH)_2 3H_2O$	Fairchildite $K_2Ca(CO_3)_2$	Gaylussite $Na_2Ca(CO_3)_2 5H_2O$	Kutnohorite $Ca(Mn,Mg)(CO_3)_2$	Minrecordite $CaZn(CO_3)_2$	Zemkorite $Na_2Ca(CO_3)_2$	Arcanite $(K,NH_4)2SO_4$	Epsomite $MgSO_4 7H_2O$	Eugsterite $Na_2Ca(SO_4)_3 2H_2O$	Gorgeyite $K_2Ca_5(SO_4)_6 2H_2O$	Mercallite $KHSO_4$	Polyhalite $K_2Ca_2Mg(SO_4)_4 2H_2O$	Starkeyite $MgSO_4 4H_2O$
838														
840														
842														
844														
846														
848														
850														
852														
854								X						X
856														
858														
860														
862														
864														
866														
868														
870														
872								X						
874														
876														
878														
880														
882														
884														
886								X						
888								X						
890														
892														
894														
896														

Detailed Evaporite Mineralogy (South Core)

Depth (cm)	Wattevilleite $Na_2Ca(SO_4)_2$ $4H_2O$	Burkeite $Na_4(SO_4)$ $(CO_3.SO_4)$	Hanksite $KNa_{22}(CO_3)_2$ $(SO_4)_9Cl$	Kainite $KMg(SO_4)$ $Cl.2.75H_2O$	Rapidcreekite $Ca_2(CO_3)$ $SO_4.4H_2O$	Tychite $Na_6Mg_2(SO_4)$ $(CO_3)_4$	Bischofite $MgCl_2.6H_2O$	Carnallite $KMgCl_3$ $6H_2O$	Niter KNO_3	Nitratine $NaNO_3$	Inderborite $CaMgB_6O_{11}$ H_2O	Sepiolite $Mg_4Si_6O_{15}$ $(OH)_2.6H_2O$
10												
12											X	
14												
16												
18												
20												
22											X	
24												
26												
28												
30												
32												
34												
36												
38												
40												
42												
44												
46												
48												
50												
52											X	
54											X	
56												
58												
60												
62												
64												
66												
68												
70											X	
72												
74												
76												
78												
80											X	X
82												
84												

Detailed Evaporite Mineralogy (South Core)

Depth (cm)	Wattevilleite $Na_2Ca(SO_4)_2$ $4H_2O$	Burkeite $Na_4(SO_4)$ $(CO_3.SO_4)$	Hanksite $KNa_{22}(CO_3)_2$ $(SO_4)_9Cl$	Kainite $KMg(SO_4)$ $Cl.2.75H_2O$	Rapidcreekite $Ca_2(CO_3)$ $SO_4.4H_2O$	Tychite $Na_6Mg_2(SO_4)$ $(CO_3)_4$	Bischofite $MgCl_2.6H_2O$	Carnallite $KMgCl_3$ $6H_2O$	Niter KNO_3	Nitratine $NaNO_3$	Inderborite $CaMgB_6O_{11}$ H_2O	Sepiolite $Mg_4Si_6O_{15}$ $(OH)_2.6H_2O$
86												
88												
90												
92											X	X
94												
96												
98												
100												
102											X	
104												
106												
108												
110												
112												
114												
116												
118												
120										X		
122										X		
124										X		
126										X		
128										X		
130										X		
132			X									
134												
136												
138												
140												
142										X		
144												
146										X		
148										X		
150												
152												
154										X		
156												
158												
160												

Detailed Evaporite Mineralogy (South Core)

Depth (cm)	Wattevilleite $Na_2Ca(SO_4)_2$ $4H_2O$	Burkeite $Na_4(SO_4)$ $(CO_3.SO_4)$	Hanksite $KNa_{22}(CO_3)_2$ $(SO_4)_9Cl$	Kainite $KMg(SO_4)$ $Cl.2.75H_2O$	Rapidcreekite $Ca_2(CO_3)$ $SO_4.4H_2O$	Tychite $Na_6Mg_2(SO_4)$ $(CO_3)_4$	Bischofite $MgCl_2.6H_2O$	Carnallite $KMgCl_3$ $6H_2O$	Niter KNO_3	Nitratine $NaNO_3$	Inderborite $CaMgB_6O_{11}$ H_2O	Sepiolite $Mg_4Si_6O_{15}$ $(OH)_2.6H_2O$
162												
164												
166										X		
168												
170										X		
172										X		
174										X		
176												
178										X		
180										X		
182										X		
184											X	
186										X		
188												
190			X									
192										X		
194										X		
196										X		
198												
200												
202												
204										X		
206										X		
208										X		
210												
212												
214												
216												
218												
220												
222										X		
224										X		
226												
228										X		
230												
232										X		
234												
236										X		

Detailed Evaporite Mineralogy (South Core)

Depth (cm)	Wattevilleite $Na_2Ca(SO_4)_2$ $4H_2O$	Burkeite $Na_4(SO_4)$ $(CO_3.SO_4)$	Hanksite $KNa_{22}(CO_3)_2$ $(SO_4)_9Cl$	Kainite $KMg(SO_4)$ $Cl.2.75H_2O$	Rapidcreekite $Ca_2(CO_3)$ $SO_4.4H_2O$	Tychite $Na_6Mg_2(SO_4)$ $(CO_3)_4$	Bischofite $MgCl_2.6H_2O$	Carnallite $KMgCl_3$ $6H_2O$	Niter KNO_3	Nitratine $NaNO_3$	Inderborite $CaMgB_6O_{11}$ H_2O	Sepiolite $Mg_4Si_6O_{15}$ $(OH)_2.6H_2O$
238												
240												
242												
244												
246												
248										X	X	
250												
252												
254												
256										X		
258										X		
260											X	
262												
264												
266			X							X		
268												
270												
272										X		
274												
276												
278			X								X	
280												
282			X									
284										X	X	
286			X									
288												
290			X									
292			X									
294												
296										X	X	
298											X	
300												
302												
304												
306			X								X	
308												
310											X	
312												

Detailed Evaporite Mineralogy (South Core)

Depth (cm)	Wattevilleite $Na_2Ca(SO_4)_2$ $4H_2O$	Burkeite $Na_4(SO_4)$ (CO_3,SO_4)	Hanksite $KNa_{22}(CO_3)_2$ $(SO_4)_9Cl$	Kainite $KMg(SO_4)$ $Cl.2.75H_2O$	Rapidcreekite $Ca_2(CO_3)$ $SO_4.4H_2O$	Tychite $Na_6Mg_2(SO_4)$ $(CO_3)_4$	Bischofite $MgCl_2.6H_2O$	Carnallite $KMgCl_3$ $6H_2O$	Niter KNO_3	Nitratine $NaNO_3$	Inderborite $CaMgB_6O_{11}$ H_2O	Sepiolite $Mg_4Si_6O_{15}$ $(OH)_2.6H_2O$
314												
316												
318											X	
320			X									
322			X									
324			X								X	
326												
328												
330												
332								X		X		
334			X									
336												
338			X									
340			X								X	
342			X									
344												
346			X					X				
348			X									
350										X		
352												
354			X									
356										X		
358										X		
360										X		
362												
364												
366												
368												
370												
372											X	
374											X	
376										X		
378												
380												
382												
384												
386												
388										X		

Detailed Evaporite Mineralogy (South Core)

Depth (cm)	Wattevilleite $Na_2Ca(SO_4)_2 \cdot 4H_2O$	Burkeite $Na_4(SO_4)(CO_3.SO_4)$	Hanksite $KNa_{22}(CO_3)_2(SO_4)_9Cl$	Kainite $KMg(SO_4)Cl.2.75H_2O$	Rapidcreekite $Ca_2(CO_3)SO_4.4H_2O$	Tychite $Na_6Mg_2(SO_4)(CO_3)_4$	Bischofite $MgCl_2.6H_2O$	Carnallite $KMgCl_3 \cdot 6H_2O$	Niter KNO_3	Nitratine $NaNO_3$	Inderborite $CaMgB_6O_{11} \cdot H_2O$	Sepiolite $Mg_4Si_6O_{15}(OH)_2.6H_2O$
390										X		
392						X				X	X	
394												
396					X							
398										X		
400			X		X							
402											X	
404										X		
406												
408												
410										X		
412										X		
414												
416												
500												
502										X		
504											X	
508												
510			X					X				
512					X							
514			X									
516												
518											X	
520					X							
522			X							X		
524												
526												
528			X									
530			X									
532												
534			X								X	
536												
538												
540			X									
542												
544					X					X		
546												
548												

Detailed Evaporite Mineralogy (South Core)

Depth (cm)	Wattevilleite $Na_2Ca(SO_4)_2$ $4H_2O$	Burkeite $Na_4(SO_4)$ $(CO_3.SO_4)$	Hanksite $KNa_{22}(CO_3)_2$ $(SO_4)_9Cl$	Kainite $KMg(SO_4)$ $Cl.2.75H_2O$	Rapidcreekite $Ca_2(CO_3)$ $SO_4.4H_2O$	Tychite $Na_6Mg_2(SO_4)$ $(CO_3)_4$	Bischofite $MgCl_2.6H_2O$	Carnallite $KMgCl_3$ $6H_2O$	Niter KNO_3	Nitratine $NaNO_3$	Inderborite $CaMgB_6O_{11}$ H_2O	Sepiolite $Mg_4Si_6O_{15}$ $(OH)_2.6H_2O$
550										X		
552												
554			X								X	
556												
558												
560			X									
562												
564										X		
566												
568												
570												
572					X						X	
574			X									
576			X									
578												
580			X					X		X		
582			X								X	
584												
586												
588												
590					X							
592												
594										X		
596												
598										X		
600												
602												
604					X							
606												
608			X									
610												
612			X									
614												
616												
618												
620												
622												
624												

Detailed Evaporite Mineralogy (South Core)

Depth (cm)	Wattevilleite $Na_2Ca(SO_4)_2$ $4H_2O$	Burkeite $Na_4(SO_4)$ $(CO_3.SO_4)$	Hanksite $KNa_{22}(CO_3)_2$ $(SO_4)_9Cl$	Kainite $KMg(SO_4)$ $Cl.2.75H_2O$	Rapidcreekite $Ca_2(CO_3)$ $SO_4.4H_2O$	Tychite $Na_6Mg_2(SO_4)$ $(CO_3)_4$	Bischofite $MgCl_2.6H_2O$	Camallite $KMgCl_3$ $6H_2O$	Niter KNO_3	Nitratine $NaNO_3$	Inderborite $CaMgB_6O_{11}$ H_2O	Sepiolite $Mg_4Si_6O_{15}$ $(OH)_2.6H_2O$
626								X			X	
628			X									
630											X	
632												
634												
636												
638			X									
640												
642												
644											X	
646										X		
648												
650			X									
652												
654												
656												
658										X		
660												
662												
664											X	
666												
668												
670			X								X	
672												
674										X		
676												
678												
680			X									
682			X									
684			X									
686												
824												
826												
828												
830												
832												
834												
836												

Detailed Evaporite Mineralogy (South Core)

Depth (cm)	Wattevilleite $Na_2Ca(SO_4)_2$ $4H_2O$	Burkeite $Na_4(SO_4)$ $(CO_3.SO_4)$	Hanksite $KNa_{22}(CO_3)_2$ $(SO_4)_9Cl$	Kainite $KMg(SO_4)$ $Cl.2.75H_2O$	Rapidcreekite $Ca_2(CO_3)$ $SO_4.4H_2O$	Tychite $Na_6Mg_2(SO_4)$ $(CO_3)_4$	Bischofite $MgCl_2.6H_2O$	Carnallite $KMgCl_3$ $6H_2O$	Niter KNO_3	Nitratine $NaNO_3$	Inderborite $CaMgB_6O_{11}$ H_2O	Sepiolite $Mg_4Si_6O_{15}$ $(OH)_2.6H_2O$
838												
840												
842											X	
844												
846												
848												
850										X		
852												
854												
856			X								X	
858												
860												
862			X									
864											X	
866												
868												
870												
872			X									
874												
876												
878												
880											X	
882												
884												
886												
888												
890												
892												
894												
896												

Appendix D Major Ion Ratios of Different Stratigraphic Units

Stratigraphic Variation in Major Ion Ratios of North Core at North Ingebright Lake

Depth (cm)	Ca/Na	Mg/Na	SO_4/Na	CO_3/Na	CO_3/SO_4
12	1.50	1.50	1.00	3.00	3.00
16	0.00	0.00	1.00	0.28	0.28
18	0.34	0.66	0.68	0.44	0.65
20	2.57	2.57	1.00	5.43	5.43
22	4.12	2.41	2.72	4.81	1.77
24	1.92	1.92	1.00	3.85	3.85
26	0.13	0.42	0.72	0.04	0.06
28	0.38	0.81	0.57	0.77	1.34
30	3.22	3.22	1.00	6.44	6.44
32	0.73	0.00	1.73	0.00	0.00
36	2.82	1.68	2.14	3.36	1.57
38	0.71	0.71	1.00	1.42	1.42
40	0.37	0.72	0.65	0.73	1.13
42	0.48	0.54	0.94	0.22	0.24
44	0.95	0.95	1.00	1.90	1.90
46	0.19	0.19	1.00	0.41	0.41
48	0.54	0.54	1.00	1.08	1.08
50	0.08	0.08	1.00	0.15	0.15
52	0.11	0.11	1.00	0.22	0.22
54	0.03	0.03	1.00	0.05	0.05
56	0.03	0.03	1.00	0.07	0.07
58	0.04	0.04	1.00	0.08	0.08
60	0.04	0.04	1.00	0.08	0.08
62	0.05	0.05	1.00	0.10	0.10
64	0.11	0.00	1.11	0.00	0.00
66	0.04	0.04	1.00	0.09	0.09
68	0.05	0.05	1.00	0.10	0.10
70	0.03	0.03	1.00	0.06	0.06
72	0.03	0.03	1.00	0.06	0.06
74	0.03	0.03	1.00	0.06	0.06
76	0.03	0.03	1.00	0.07	0.07
78	0.03	0.03	1.00	0.06	0.06
80	0.03	0.03	1.00	0.08	0.08
82	0.03	0.03	1.00	0.05	0.05
84	0.03	0.03	1.00	0.05	0.05
86	0.02	0.02	1.00	0.04	0.04
88	0.00	0.00	1.00	0.00	0.00
90	0.02	0.02	1.00	0.04	0.04
92	0.00	0.00	1.00	0.00	0.00
94	0.00	0.00	1.00	0.00	0.00
96	0.03	0.03	1.00	0.05	0.05
98	0.02	0.02	1.00	0.04	0.04
100	0.02	0.02	1.00	0.04	0.04
106	0.00	0.00	1.00	0.00	0.00
108	0.00	0.00	1.00	0.00	0.00
110	0.00	0.00	1.00	0.00	0.00
112	0.00	0.00	1.00	0.00	0.00
114	0.00	0.08	0.92	0.00	0.00
116	0.01	0.01	1.00	0.03	0.03
118	0.00	0.00	1.00	0.00	0.00
120	0.00	0.00	1.00	0.00	0.00
122	0.00	0.00	1.00	0.00	0.00
126	0.00	0.00	1.00	0.00	0.00
128	0.00	0.00	1.00	0.00	0.00
130	0.01	0.01	1.00	0.02	0.02
132	0.11	0.00	1.11	0.00	0.00

Stratigraphic Variation in Major Ion Ratios of North Core at North Ingebright Lake

Depth (cm)	Ca/Na	Mg/Na	SO_4/Na	CO_3/Na	CO_3/SO_4
134	0.02	0.02	1.00	0.04	. 0.04
136	0.10	0.00	1.10	0.00	0.00
138	0.02	0.02	1.00	0.04	0.04
140	0.03	0.03	1.00	0.06	0.06
142	0.03	0.03	1.00	0.05	0.05
144	0.00	0.00	1.00	0.00	0.00
146	0.09	0.09	1.00	0.18	0.18
148	0.09	0.09	1.00	0.17	0.17
150	0.12	0.12	1.00	0.25	0.25
152	0.11	0.11	1.00	0.24	0.24
154	0.02	0.02	1.00	0.04	0.04
156	0.00	0.00	1.00	0.00	0.00
158	0.00	0.00	1.00	0.00	0.00
160	0.00	0.00	1.00	0.00	0.00
162	0.00	0.00	1.00	0.00	0.00
164	0.00	0.00	1.00	0.00	0.00
166	0.07	0.00	1.07	0.00	0.00
168	0.00	0.00	1.00	0.00	0.00
170	0.01	0.07	0.94	0.02	0.02
172	0.00	0.00	1.00	0.00	0.00
174	0.00	0.00	1.00	0.00	0.00
176	0.00	0.00	1.00	0.02	0.02
178	0.07	0.01	1.06	0.03	0.02
180	0.01	0.01	1.00	0.03	0.03
182	0.01	0.09	0.92	0.02	0.02
184	0.07	0.00	1.07	0.00	0.00
188	0.08	0.02	1.07	0.04	0.03
190	0.21	0.00	1.21	0.00	0.00
192	0.11	0.02	1.09	0.05	0.04
194	0.01	0.01	1.00	0.02	0.02
196	0.11	0.00	1.11	0.00	0.00
198	0.14	0.02	1.12	0.05	0.04
200	0.13	0.00	1.13	0.00	0.00
202	0.13	0.02	1.12	0.04	0.03
204	0.13	0.02	1.12	0.04	0.03
206	0.27	0.02	1.25	0.04	0.03
208	0.22	0.04	1.18	0.08	0.07
210	0.16	0.00	1.16	0.04	0.04
212	0.33	0.02	1.31	0.04	0.03
214	0.21	0.03	1.18	0.05	0.05
216	0.10	0.02	1.08	0.04	0.04
218	0.14	0.03	1.11	0.06	0.05
220	0.16	0.02	1.14	0.04	0.03
222	0.27	0.12	1.24	0.15	0.12
224	0.25	0.13	1.21	0.18	0.15
226	0.03	0.03	1.00	0.06	0.06
228	0.42	0.03	1.39	0.06	0.04
230	0.14	0.01	1.00	0.14	0.14
232	0.13	0.02	1.11	0.04	0.03
234	0.18	0.03	1.14	0.07	0.06
236	0.13	0.00	1.13	0.00	0.00
238	0.33	0.00	1.33	0.00	0.00
240	0.22	0.03	1.20	0.05	0.04
242	0.19	0.02	1.13	0.12	0.11
244	0.17	0.00	1.17	0.03	0.03
246	0.22	0.00	1.22	0.00	0.00
248	0.13	0.04	1.09	0.13	0.12

Stratigraphic Variation in Major Ion Ratios of North Core at North Ingebright Lake

Depth (cm)	Ca/Na	Mg/Na	SO_4/Na	CO_3/Na	CO_3/SO_4
250	0.35	0.03	1.32	0.10	0.07
252	0.35	0.03	1.32	0.10	0.07
254	0.02	0.02	1.00	0.10	0.10
256	0.36	0.04	1.32	0.11	0.08
258	0.17	0.03	1.14	0.09	0.08
260	0.11	0.04	1.08	0.11	0.10
262	0.32	0.04	1.28	0.12	0.09
264	0.28	0.06	1.22	0.15	0.12
266	0.22	0.03	1.19	0.06	0.05
268	0.17	0.03	1.14	0.06	0.05
270	0.13	0.04	1.09	0.09	0.08
272	0.47	0.04	1.43	0.12	0.09
274	0.28	0.04	1.24	0.12	0.10
276	0.15	0.04	1.12	0.07	0.06
278	0.00	0.00	1.00	0.04	0.04
280	0.31	0.03	1.28	0.10	0.08
282	0.04	0.04	1.00	0.15	0.15
284	0.15	0.02	1.13	0.06	0.05
286	0.08	0.00	1.08	0.04	0.03
290	0.07	0.00	1.07	0.00	0.00
292	0.01	0.01	1.00	0.05	0.05
294	0.00	0.00	1.00	0.00	0.00
296	0.05	0.05	1.00	0.14	0.14
298	0.03	0.00	1.03	0.02	0.02
300	0.02	0.02	1.00	0.07	0.07
302	0.23	0.02	1.22	0.07	0.06
304	0.22	0.02	1.20	0.03	0.03
306	0.15	0.00	1.15	0.02	0.01
308	0.07	0.00	1.07	0.00	0.00
310	0.08	0.00	1.08	0.02	0.02
312	0.02	0.02	1.00	0.03	0.03
314	0.00	0.00	1.00	0.00	0.00
316	0.00	0.00	1.00	0.00	0.00
318	0.00	0.00	1.00	0.00	0.00
320	0.00	0.00	1.00	0.00	0.00
322	0.01	0.01	1.00	0.03	0.03
324	0.00	0.00	1.00	0.00	0.00
326	0.00	0.00	1.00	0.00	0.00
328	0.01	0.01	1.00	0.03	0.03
330	0.00	0.00	1.00	0.00	0.00
332	0.01	0.01	1.00	0.02	0.02
334	0.28	0.01	1.27	0.02	0.01
336	0.01	0.01	1.00	0.02	0.02
338	0.01	0.01	1.00	0.02	0.02
340	0.01	0.01	1.00	0.03	0.03
342	0.00	0.00	1.00	0.00	0.00
344	0.00	0.00	1.00	0.00	0.00
346	0.01	0.01	1.00	0.02	0.02
348	0.00	0.00	1.00	0.00	0.00
350	0.00	0.00	1.00	0.00	0.00
352	0.00	0.00	1.00	0.00	0.00
354	0.00	0.00	1.00	0.00	0.00
356	0.02	0.02	1.00	0.03	0.03
358	0.00	0.00	1.00	0.00	0.00
360	0.00	0.00	1.00	0.00	0.00
362	0.01	0.01	1.00	0.03	0.03
364	0.01	0.01	1.00	0.02	0.02

Stratigraphic Variation in Major Ion Ratios of North Core at North Ingebright Lake

Depth (cm)	Ca/Na	Mg/Na	SO_4/Na	CO_3/Na	CO_3/SO_4
368	0.00	0.00	1.00	0.00	0.00
370	0.01	0.01	1.00	0.02	0.02
372	0.18	0.01	1.15	0.04	0.04
374	0.07	0.00	1.07	0.00	0.00
376	0.00	0.00	1.00	0.00	0.00
378	0.00	0.00	1.00	0.00	0.00
380	0.01	0.01	1.00	0.02	0.02
382	0.00	0.00	1.00	0.00	0.00
384	0.01	0.01	1.00	0.03	0.03
386	0.00	0.00	1.00	0.00	0.00
388	0.00	0.00	1.00	0.00	0.00
390	0.00	0.00	1.00	0.00	0.00
392	0.00	0.00	1.00	0.00	0.00
394	0.00	0.00	1.00	0.00	0.00
396	0.05	0.00	1.05	0.00	0.00
398	0.00	0.00	1.00	0.00	0.00
400	0.00	0.00	1.00	0.00	0.00
402	0.01	0.01	1.00	0.02	0.02
404	0.00	0.00	1.00	0.00	0.00
406	0.00	0.00	1.00	0.00	0.00
408	0.00	0.00	1.00	0.00	0.00
410	0.00	0.00	1.00	0.00	0.00
412	0.00	0.00	1.00	0.00	0.00
414	0.00	0.00	1.00	0.00	0.00
416	0.00	0.00	1.00	0.00	0.00
418	0.00	0.00	1.00	0.00	0.00
420	0.00	0.00	1.00	0.00	0.00
422	0.04	0.00	1.04	0.00	0.00
424	0.00	0.00	1.00	0.00	0.00
426	0.00	0.00	1.00	0.00	0.00
428	0.00	0.00	1.00	0.00	0.00
430	0.00	0.00	1.00	0.00	0.00
432	0.00	0.00	1.00	0.00	0.00
434	0.00	0.00	1.00	0.00	0.00
436	0.00	0.00	1.00	0.00	0.00
438	0.00	0.00	1.00	0.00	0.00
440	0.00	0.00	1.00	0.00	0.00
442	0.00	0.00	1.00	0.00	0.00
444	0.00	0.00	1.00	0.00	0.00
446	0.01	0.01	1.00	0.02	0.02
448	0.00	0.00	1.00	0.00	0.00
450	0.00	0.00	1.00	0.00	0.00
452	0.00	0.00	1.00	0.00	0.00
454	0.07	0.00	1.07	0.00	0.00
456	0.00	0.00	1.00	0.00	0.00
458	0.07	0.00	1.07	0.00	0.00
460	0.02	0.02	1.00	0.05	0.05
462	0.10	0.00	1.10	0.03	0.03
464	0.08	0.01	1.07	0.02	0.02
466	0.12	0.00	1.12	0.00	0.00
468	0.00	0.00	1.00	0.00	0.00
470	0.00	0.00	1.00	0.00	0.00
472	0.10	0.02	1.08	0.04	0.03
474	0.02	0.02	1.00	0.03	0.03
476	0.62	0.02	1.61	0.04	0.02
478	0.10	0.10	1.08	0.13	0.12
480	0.00	0.05	1.00	0.05	0.05

Stratigraphic Variation in Major Ion Ratios of North Core at North Ingebright Lake

Depth (cm)	Ca/Na	Mg/Na	SO_4/Na	CO_3/Na	CO_3/SO_4
482	0.11	0.00	1.11	0.00	0.00
484	0.14	0.03	1.11	0.05	0.05
486	0.02	0.02	1.00	0.04	0.04
488	0.46	0.02	1.44	0.04	0.03
490	0.08	0.00	1.08	0.00	0.00
492	0.00	0.00	1.00	0.00	0.00
494	0.09	0.01	1.07	0.02	0.02
496	0.05	0.00	1.05	0.00	0.00
498	0.21	0.00	1.21	0.00	0.00
500	0.00	0.00	1.00	0.03	0.03
502	0.40	0.00	1.40	0.00	0.00
504	0.00	0.00	1.00	0.00	0.00
506	0.02	0.02	1.00	0.03	0.03
508	0.27	0.02	1.26	0.03	0.03
510	0.15	0.02	1.13	0.04	0.04
512	0.18	0.04	1.14	0.07	0.06
514	0.21	0.04	1.17	0.08	0.07
516	0.18	0.04	1.14	0.07	0.06
518	0.21	0.04	1.17	0.08	0.06
520	0.20	0.03	1.17	0.07	0.06
522	0.19	0.02	1.17	0.05	0.04
526	0.08	0.00	1.08	0.00	0.00
528	0.00	0.00	1.00	0.00	0.00
532	0.00	0.00	1.00	0.00	0.00
534	0.00	0.00	1.00	0.00	0.00
536	0.03	0.03	1.00	0.05	0.05
538	0.02	0.00	1.00	0.02	0.02
540	0.00	0.00	1.00	0.00	0.00
542	0.02	0.02	1.00	0.04	0.04
544	0.05	0.02	1.00	0.07	0.07
546	0.06	0.00	1.06	0.00	0.00
548	0.06	0.00	1.06	0.00	0.00
550	0.07	0.03	1.00	0.10	0.10
552	0.09	0.02	1.08	0.03	0.03
554	0.07	0.08	1.07	0.08	0.07
556	0.03	0.03	1.00	0.07	0.07
558	0.00	0.00	1.00	0.00	0.00
560	0.04	0.04	1.00	0.07	0.07
564	0.03	0.13	1.00	0.15	0.15
566	0.01	0.01	1.00	0.02	0.02
568	0.26	0.02	1.24	0.04	0.03
570	0.06	0.00	1.06	0.00	0.00
572	0.10	0.02	1.08	0.05	0.04
574	0.16	0.03	1.13	0.06	0.06
576	0.05	0.00	1.05	0.00	0.00
578	0.07	0.01	1.06	0.03	0.03
580	0.01	0.01	1.00	0.02	0.02
582	0.02	0.02	1.00	0.03	0.03
584	0.02	0.02	1.00	0.04	0.04
586	0.00	0.00	1.00	0.00	0.00
588	0.02	0.02	1.00	0.04	0.04
590	0.00	0.00	1.00	0.00	0.00
592	0.00	0.00	1.00	0.00	0.00
594	0.16	0.00	1.16	0.00	0.00
596	0.00	0.00	1.00	0.00	0.00
598	0.22	0.28	1.15	0.35	0.30
600	0.16	0.12	1.13	0.14	0.13

Stratigraphic Variation in Major Ion Ratios of North Core at North Ingebright Lake

Depth (cm)	Ca/Na	Mg/Na	SO_4/Na	CO_3/Na	CO_3/SO_4
602	0.16	0.04	1.12	0.07	0.07
604	0.07	0.35	1.00	0.42	0.42
606	0.14	0.14	1.13	0.16	0.14
608	0.09	0.15	1.07	0.18	0.17
616	0.08	0.00	1.08	0.00	0.00
618	0.00	0.00	1.00	0.00	0.00
620	0.01	0.01	1.00	0.02	0.02
622	0.11	0.00	1.11	0.00	0.00
624	0.10	0.02	1.08	0.03	0.03
626	0.00	0.00	1.00	0.00	0.00
628	0.12	0.03	1.09	0.06	0.05
630	0.15	0.03	1.12	0.06	0.05
634	0.23	0.06	1.17	0.12	0.11
636	0.03	0.03	1.00	0.06	0.06
638	0.01	0.01	1.00	0.03	0.03
640	0.00	0.00	1.00	0.00	0.00
642	0.02	0.02	1.00	0.04	0.04
644	0.00	0.00	1.00	0.00	0.00
646	0.29	0.03	1.26	0.05	0.04
648	0.13	0.02	1.11	0.05	0.04
650	0.00	0.00	1.00	0.00	0.00
652	0.13	0.02	1.11	0.05	0.04
654	0.16	0.02	1.14	0.03	0.03
656	0.00	0.00	1.00	0.00	0.00
658	0.01	0.01	1.00	0.03	0.03
660	0.02	0.02	1.00	0.04	0.04
662	0.34	0.02	1.07	0.28	0.26
664	0.00	0.00	1.00	0.00	0.00
666	0.09	0.00	1.09	0.00	0.00
668	0.09	0.00	1.09	0.00	0.00
670	0.08	0.02	1.06	0.03	0.03
672	0.01	0.01	1.00	0.02	0.02
674	0.04	0.00	1.00	0.04	0.04
676	0.09	0.03	1.06	0.06	0.05
678	0.09	0.01	1.08	0.03	0.02
680	0.14	0.02	1.12	0.03	0.03
682	0.01	0.01	1.00	0.02	0.02
684	0.00	0.00	1.00	0.00	0.00
686	0.03	0.00	1.00	0.03	0.03
688	2.28	0.00	3.28	0.00	0.00
690	0.00	0.00	1.00	0.00	0.00
692	0.07	0.00	1.07	0.00	0.00
694	0.12	0.01	1.11	0.03	0.03
696	0.03	0.00	1.00	0.03	0.03
698	0.01	0.01	1.00	0.02	0.02
700	0.00	0.00	1.00	0.00	0.00
704	0.02	0.02	1.00	0.04	0.04
706	0.00	0.00	1.00	0.00	0.00
708	0.15	0.01	1.12	0.04	0.04
710	0.00	0.00	1.00	0.00	0.00
714	0.14	0.00	1.14	0.00	0.00
716	0.00	0.00	1.00	0.00	0.00
718	0.18	0.01	1.17	0.02	0.02
720	0.00	0.00	1.00	0.00	0.00
722	0.05	0.00	1.05	0.00	0.00
724	0.02	0.02	1.00	0.03	0.03
728	0.00	0.00	1.00	0.00	0.00

Stratigraphic Variation in Major Ion Ratios of North Core at North Ingebright Lake

Depth (cm)	Ca/Na	Mg/Na	SO_4/Na	CO_3/Na	CO_3/SO_4
730	0.18	0.03	1.16	0.05	0.04
732	0.13	0.03	1.10	0.06	0.05
734	0.01	0.01	1.00	0.03	0.03
736	0.07	0.00	1.07	0.00	0.00
738	0.26	0.11	1.23	0.14	0.11
740	0.00	0.00	1.00	0.00	0.00
746	0.15	0.02	1.11	0.06	0.06
748	0.01	0.01	1.00	0.02	0.02
750	0.10	0.02	1.08	0.04	0.04
752	0.12	0.09	1.10	0.12	0.11
754	0.22	0.03	1.19	0.05	0.05
756	0.02	0.10	1.00	0.12	0.12
758	0.08	0.02	1.06	0.03	0.03
760	0.02	0.13	1.00	0.15	0.15
762	0.14	0.01	1.11	0.05	0.04
764	0.08	0.00	1.06	0.02	0.02
792	0.07	0.02	1.06	0.03	0.03
794	0.00	0.00	1.00	0.00	0.00
796	0.09	0.02	1.07	0.04	0.04
798	0.00	0.04	1.00	0.04	0.04
800	0.15	0.02	1.10	0.07	0.06
802	0.09	0.01	1.08	0.02	0.02
804	0.08	0.00	1.08	0.00	0.00
806	0.12	0.00	1.12	0.00	0.00
808	0.14	0.11	1.08	0.17	0.16
810	0.10	0.02	1.09	0.03	0.03
812	0.02	0.02	1.00	0.04	0.04
814	0.13	0.00	1.13	0.00	0.00
816	0.03	0.00	1.00	0.03	0.03
818	0.10	0.09	1.07	0.11	0.10
820	0.13	0.02	1.11	0.04	0.03
822	0.49	0.19	1.46	0.23	0.16
824	0.36	0.02	1.29	0.09	0.07
826	0.16	0.09	1.14	0.11	0.10
828	0.19	0.18	1.15	0.21	0.18
830	0.21	0.18	1.17	0.22	0.18
832	0.18	0.03	1.12	0.09	0.08
834	0.19	0.12	1.11	0.20	0.18
836	0.26	0.19	1.21	0.24	0.20
838	0.33	0.26	1.18	0.40	0.34
840	0.14	0.03	1.11	0.05	0.05
842	0.17	0.03	1.14	0.06	0.05
844	0.24	0.15	1.20	0.19	0.16
846	0.31	0.14	1.29	0.16	0.13
848	0.16	0.03	1.13	0.06	0.06
850	0.31	0.03	1.28	0.05	0.04
852	0.15	0.03	1.13	0.05	0.05
856	0.28	0.03	1.25	0.05	0.04
860	0.27	0.02	1.24	0.05	0.04
862	0.22	0.02	1.20	0.04	0.03
864	0.51	0.13	1.48	0.16	0.11
866	0.75	0.03	1.72	0.06	0.03
868	0.32	0.16	1.29	0.19	0.15
870	0.25	0.15	1.09	0.03	0.03
872	0.56	0.03	1.54	0.06	0.04
874	0.19	0.01	1.18	0.03	0.02
876	0.37	0.03	1.34	0.06	0.04

Stratigraphic Variation in Major Ion Ratios of North Core at North Ingebright Lake

Depth (cm)	Ca/Na	Mg/Na	SO_4/Na	CO_3/Na	CO_3/SO_4
878	0.27	0.02	1.25	0.05	0.04
880	0.42	0.02	1.40	0.04	0.03
882	0.20	0.01	1.19	0.02	0.02
884	0.25	0.02	1.23	0.05	0.04
886	0.18	0.02	1.16	0.04	0.03
888	0.32	0.03	1.29	0.05	0.04
890	3.13	0.03	4.10	0.05	0.01
892	0.28	0.01	1.26	0.03	0.02
894	0.10	0.02	1.09	0.04	0.03
896	0.22	0.06	1.22	0.06	0.05
898	1.42	0.11	2.40	0.13	0.06
900	0.14	0.08	1.12	0.09	0.08
902	0.28	0.02	1.26	0.04	0.03
904	0.30	0.01	1.29	0.03	0.02
906	0.31	0.02	1.29	0.03	0.03
908	0.25	0.10	1.23	0.12	0.10
910	0.24	0.02	1.23	0.03	0.03
912	0.23	0.02	1.21	0.03	0.03
914	0.05	0.25	1.00	0.30	0.30
916	0.45	0.26	1.40	0.31	0.22
918	0.04	0.04	1.00	0.07	0.07
920	0.02	0.00	1.00	0.02	0.02
924	0.73	0.18	1.70	0.22	0.13
926	0.31	0.03	1.24	0.09	0.07
928	0.23	0.02	1.21	0.04	0.03
930	0.26	0.11	1.23	0.14	0.11
932	0.24	0.02	1.22	0.05	0.04
934	0.23	0.02	1.21	0.05	0.04
936	0.21	0.12	1.18	0.14	0.12
938	0.37	0.03	1.34	0.05	0.04
940	0.14	0.10	1.12	0.12	0.11
942	0.03	0.03	1.00	0.06	0.06
944	0.03	0.02	1.01	0.04	0.04
946	0.08	0.02	1.06	0.04	0.04
948	0.14	0.03	1.10	0.07	0.06
950	0.02	0.00	1.00	0.02	0.02
952	0.02	0.02	1.00	0.04	0.04
954	0.08	0.02	1.06	0.04	0.03
956	0.11	0.01	1.10	0.03	0.03
958	0.01	0.01	1.00	0.03	0.03
960	0.12	0.02	1.11	0.03	0.03
962	0.28	0.00	1.28	0.00	0.00
964	0.38	0.00	1.38	0.00	0.00
972	0.32	0.02	1.31	0.04	0.03
974	0.92	0.00	1.92	0.00	0.00
976	0.16	0.09	1.14	0.11	0.09
978	0.37	0.02	1.32	0.07	0.06
980	0.14	0.01	1.13	0.02	0.02
982	0.17	0.02	1.16	0.03	0.03
984	0.15	0.00	1.15	0.00	0.00
986	0.18	0.11	1.15	0.13	0.11
988	0.11	0.02	1.10	0.03	0.03
990	0.11	0.12	1.08	0.15	0.14
992	0.47	0.02	1.45	0.04	0.03
994	0.45	0.13	1.41	0.19	0.14
996	1.42	0.22	2.37	0.27	0.11
998	1.08	0.17	2.05	0.20	0.10

Stratigraphic Variation in Major Ion Ratios of North Core at North Ingebright Lake

Depth (cm)	Ca/Na	Mg/Na	SO_4/Na	CO_3/Na	CO_3/SO_4
1000	0.31	0.22	1.25	0.29	0.23
1002	0.13	0.02	1.11	0.03	0.03
1004	0.20	0.02	1.17	0.04	0.04
1006	0.09	0.00	1.09	0.04	0.04
1008	0.21	0.07	1.21	0.07	0.06
1010	0.02	0.02	1.00	0.04	0.04
1012	0.09	0.06	0.99	0.06	0.06
1014	0.26	0.15	1.22	0.19	0.15
1016	0.15	0.16	1.03	0.19	0.18
1018	0.03	0.14	1.00	0.16	0.16
1020	0.26	0.10	1.24	0.12	0.10
1022	0.09	0.02	1.08	0.04	0.03
1024	0.25	0.11	1.23	0.13	0.11
1026	0.14	0.09	1.12	0.11	0.10
1028	0.26	0.02	1.21	0.07	0.05
1030	0.34	0.13	1.28	0.20	0.15
1032	0.62	0.00	1.62	0.00	0.00
1034	0.14	0.11	1.12	0.13	0.11
1036	0.12	0.01	1.11	0.02	0.02
1038	0.19	0.00	1.19	0.00	0.00
1040	0.07	0.00	1.07	0.00	0.00
1042	0.19	0.00	1.19	0.00	0.00
1044	0.05	0.04	1.05	0.04	0.03
1046	0.13	0.03	1.13	0.03	0.03
1048	0.18	0.11	1.11	0.18	0.16
1050	0.09	0.13	1.07	0.15	0.14
1052	0.12	0.00	1.12	0.00	0.00
1054	0.19	0.11	1.17	0.13	0.11
1056	0.21	0.12	1.18	0.14	0.12
1058	0.17	0.01	1.15	0.03	0.03
1060	0.18	0.01	1.17	0.03	0.02
1062	0.14	0.02	1.10	0.06	0.06
1064	0.28	0.00	1.28	0.00	0.00
1066	3.53	0.02	4.51	0.04	0.01
1068	0.18	0.03	1.12	0.09	0.08
1070	0.37	0.02	1.30	0.09	0.07
1072	0.22	0.02	1.20	0.05	0.04
1074	0.27	0.02	1.21	0.09	0.07
1076	0.29	0.02	1.24	0.06	0.05
1078	0.15	0.01	1.11	0.05	0.04
1080	0.11	0.02	1.09	0.04	0.04
1082	0.25	0.00	1.25	0.00	0.00
1084	0.05	0.02	1.00	0.07	0.07
1086	0.12	0.14	1.09	0.17	0.15
1088	0.59	0.02	1.56	0.04	0.03
1090	0.15	0.13	1.12	0.16	0.14
1092	0.13	0.00	1.13	0.00	0.00
1094	5.25	2.16	5.83	2.58	0.44
1096	0.12	0.00	1.09	0.02	0.02
1098	0.15	0.00	1.15	0.00	0.00
1100	0.00	0.00	1.00	0.01	0.01
1102	0.10	0.01	1.09	0.01	0.01
1104	0.00	0.00	1.00	0.00	0.00
1106	0.12	0.02	1.10	0.04	0.03
1108	0.14	0.00	1.05	0.00	0.00
1110	0.00	0.00	1.00	0.00	0.00
1112	0.19	0.01	1.18	0.03	0.02

Stratigraphic Variation in Major Ion Ratios of North Core at North Ingebright Lake

Depth (cm)	Ca/Na	Mg/Na	SO_4/Na	CO_3/Na	CO_3/SO_4
1114	0.38	0.00	1.38	0.00	0.00
1116	0.75	0.00	1.75	0.00	0.00
1118	0.18	0.01	1.16	0.03	0.02
1120	0.11	0.01	1.10	0.02	0.02
1122	0.49	0.00	1.49	0.00	0.00
1124	0.41	0.00	1.41	0.00	0.00
1126	0.17	0.00	1.17	0.00	0.00
1128	1.11	0.00	2.11	0.00	0.00
1130	0.23	0.08	1.23	0.08	0.06
1132	0.22	0.00	1.22	0.00	0.00
1134	1.49	0.00	2.49	0.00	0.00
1136	0.23	0.00	1.23	0.00	0.00
1138	0.11	0.00	1.11	0.00	0.00
1140	0.67	0.00	1.67	0.00	0.00
1142	0.16	0.00	1.16	0.00	0.00
1144	0.02	0.02	1.00	0.04	0.04
1148	0.15	0.00	1.14	0.02	0.01
1150	0.11	0.00	1.11	0.00	0.00
1152	0.34	0.00	1.34	0.00	0.00
1154	0.63	0.01	1.59	0.05	0.03
1156	0.23	0.02	1.21	0.03	0.03
1158	0.12	0.00	1.12	0.00	0.00
1160	0.25	0.01	1.24	0.03	0.02
1162	0.22	0.01	1.20	0.03	0.02
1164	0.43	0.02	1.36	0.09	0.06
1166	0.13	0.02	1.11	0.06	0.05
1168	0.13	0.01	1.11	0.03	0.02
1170	0.46	0.01	1.44	0.03	0.02
1172	0.09	0.00	1.09	0.00	0.00
1174	0.20	0.12	1.17	0.14	0.12
1176	0.37	0.02	1.35	0.03	0.03
1178	0.18	0.00	1.18	0.00	0.00
1180	0.28	0.02	1.27	0.03	0.03
1182	0.36	0.00	1.34	0.03	0.02
1184	0.16	0.02	1.10	0.08	0.08
1186	0.08	0.01	1.06	0.03	0.02
1188	0.00	0.00	1.00	0.00	0.00
1190	0.07	0.00	1.07	0.00	0.00
1192	0.22	0.00	1.22	0.00	0.00
1194	0.00	0.00	1.00	0.00	0.00
1198	0.00	0.00	1.00	0.00	0.00
1200	0.00	0.00	1.00	0.00	0.00
1202	0.01	0.01	1.00	0.02	0.02
1204	0.00	0.00	1.00	0.00	0.00
1206	0.06	0.00	1.06	0.00	0.00
1208	0.08	0.00	1.08	0.00	0.00
1210	0.00	0.03	1.00	0.03	0.03
1212	0.00	0.00	1.00	0.00	0.00
1214	0.00	0.00	1.00	0.00	0.00
1216	0.00	0.00	1.00	0.00	0.00
1218	0.00	0.00	1.00	0.00	0.00
1220	0.06	0.00	1.06	0.00	0.00
1222	0.00	0.00	1.00	0.00	0.00
1224	0.00	0.00	1.00	0.00	0.00
1326	0.02	0.02	1.00	0.04	0.04
1328	0.01	0.01	1.00	0.02	0.02
1330	0.11	0.01	1.10	0.02	0.02

Stratigraphic Variation in Major Ion Ratios of North Core at North Ingebright Lake

Depth (cm)	Ca/Na	Mg/Na	SO_4/Na	CO_3/Na	CO_3/SO_4
1332	0.01	0.01	1.00	0.02	0.02
1334	0.00	0.00	1.00	0.00	0.00
1336	0.06	0.00	1.06	0.00	0.00
1338	0.00	0.04	1.00	0.04	0.04
1340	0.16	0.02	1.14	0.05	0.05
1342	0.02	0.02	1.00	0.03	0.03
1344	0.20	0.00	1.20	0.00	0.00
1346	0.50	0.00	1.50	0.03	0.02
1348	0.11	0.00	1.09	0.03	0.02
1350	0.07	0.07	1.00	0.15	0.15
1352	0.14	0.14	1.00	0.27	0.27
1354	0.17	0.04	1.13	0.09	0.08
1356	0.09	0.08	1.09	0.14	0.13
1358	0.26	0.18	1.08	0.07	0.06
1360	0.29	0.14	1.14	0.04	0.04
1362	0.32	0.03	1.19	0.06	0.05
1364	0.31	0.15	1.14	0.02	0.02
1366	0.09	0.00	1.09	0.00	0.00
1368	0.28	0.09	1.26	0.12	0.09
1370	0.09	0.17	0.92	0.00	0.00
1372	0.16	0.03	0.99	0.05	0.06
1374	0.15	0.02	1.13	0.04	0.03
1376	0.17	0.20	1.13	0.24	0.21
1380	0.14	0.16	1.11	0.19	0.18
1382	0.25	0.18	1.17	0.31	0.26
1384	0.18	0.14	1.08	0.24	0.22
1386	0.22	0.21	1.10	0.33	0.30
1388	0.18	0.26	1.13	0.32	0.28
1390	0.19	0.15	1.17	0.18	0.16
1392	0.29	0.33	1.20	0.42	0.35
1394	0.19	0.32	1.11	0.43	0.39
1396	0.11	0.10	1.09	0.11	0.10
1398	0.02	0.09	1.00	0.11	0.11
1400	0.21	0.11	1.19	0.14	0.12
1402	0.09	0.02	1.07	0.04	0.04
1404	0.10	0.11	1.07	0.14	0.13
1406	0.26	0.23	1.21	0.28	0.23
1408	0.00	0.00	1.00	0.00	0.00
1410	0.04	0.01	1.04	0.02	0.01
1412	0.03	0.14	1.00	0.18	0.18
1414	0.02	0.00	1.00	0.02	0.02
1416	0.00	0.00	1.00	0.00	0.00
1418	0.00	0.00	1.00	0.00	0.00
1420	0.00	0.00	1.00	0.00	0.00
1422	0.00	0.00	1.00	0.00	0.00
1424	0.00	0.00	1.00	0.00	0.00
1426	0.01	0.01	1.00	0.02	0.02
1428	0.03	0.16	1.00	0.19	0.19
1430	0.03	0.03	1.00	0.06	0.06
1432	0.01	0.01	1.00	0.02	0.02
1434	0.02	0.02	1.00	0.03	0.03
1436	0.06	0.12	1.00	0.18	0.18
1438	0.07	0.03	1.00	0.09	0.09
1440	0.00	0.00	1.00	0.00	0.00
1442	0.04	0.02	1.00	0.06	0.06
1444	0.03	0.03	1.00	0.06	0.06
1446	0.03	0.11	1.00	0.15	0.15

Stratigraphic Variation in Major Ion Ratios of North Core at North Ingebright Lake

Depth (cm)	Ca/Na	Mg/Na	SO_4/Na	CO_3/Na	CO_3/SO_4
1448	0.04	0.02	1.00	0.06	0.06
1450	0.04	0.04	1.00	0.07	0.07
1452	0.02	0.09	1.00	0.11	0.11
1454	0.02	0.02	1.00	0.05	0.05
1456	0.02	0.02	1.00	0.04	0.04
1458	0.06	0.01	1.05	0.02	0.02
1460	0.02	0.02	1.00	0.04	0.04
1462	0.04	0.01	1.00	0.05	0.05
1464	0.00	0.00	1.00	0.00	0.00
1466	0.00	0.00	1.00	0.00	0.00
1468	0.02	0.14	1.00	0.16	0.16
1470	0.00	0.00	1.00	0.00	0.00
1472	0.00	0.00	1.00	0.00	0.00
1474	0.00	0.00	1.00	0.00	0.00
1476	0.00	0.00	1.00	0.00	0.00
1478	0.00	0.03	1.00	0.03	0.03
1480	0.00	0.00	1.00	0.00	0.00
1482	0.02	0.13	1.00	0.16	0.16
1484	0.02	0.08	1.00	0.09	0.09
1486	0.05	0.09	1.00	0.14	0.14
1488	0.08	0.01	1.04	0.06	0.06
1490	0.00	0.00	1.00	0.00	0.00
1492	0.04	0.01	1.00	0.06	0.06
1494	0.00	0.00	1.00	0.00	0.00
1496	0.01	0.01	1.00	0.02	0.02
1498	0.02	0.02	1.00	0.04	0.04
1500	0.05	0.18	1.00	0.22	0.22
1504	0.02	0.02	1.00	0.06	0.06
1506	0.07	0.02	1.05	0.04	0.04
1508	0.01	0.01	1.00	0.02	0.02
1510	0.01	0.01	1.00	0.02	0.02
1512	0.07	0.13	1.00	0.20	0.20
1514	0.01	0.01	1.00	0.03	0.03
1516	0.03	0.02	1.00	0.05	0.05
1518	0.03	0.06	1.00	0.10	0.10
1520	0.02	0.00	1.00	0.02	0.02
1522	0.27	0.00	1.27	0.00	0.00
1524	0.00	0.00	1.00	0.00	0.00
1526	0.00	0.00	1.00	0.00	0.00
1528	0.07	0.02	1.05	0.04	0.04
1530	0.00	0.00	1.00	0.00	0.00
1532	0.00	0.00	1.00	0.00	0.00
1534	0.08	0.12	1.06	0.15	0.14
1536	0.01	0.01	1.00	0.02	0.02
1538	0.02	0.00	1.00	0.02	0.02
1540	0.02	0.00	1.00	0.02	0.02
1542	0.01	0.01	1.00	0.01	0.01
1544	0.05	0.00	1.05	0.00	0.00
1546	0.00	0.00	1.00	0.00	0.00
1548	0.03	0.01	1.00	0.05	0.05
1550	0.01	0.01	1.00	0.02	0.02
1552	0.00	0.00	1.00	0.00	0.00
1554	0.07	0.14	1.00	0.21	0.21
1556	0.08	0.13	1.00	0.21	0.21
1558	0.04	0.08	1.00	0.12	0.12
1560	0.00	0.00	1.00	0.00	0.00
1562	0.04	0.07	1.00	0.11	0.11

Stratigraphic Variation in Major Ion Ratios of North Core at North Ingebright Lake

Depth (cm)	Ca/Na	Mg/Na	SO_4/Na	CO_3/Na	CO_3/SO_4
1564	0.04	0.01	1.00	0.05	0.05
1566	0.02	0.07	1.00	0.09	0.09
1568	0.07	0.11	1.00	0.17	0.17
1570	0.02	0.02	1.00	0.04	0.04
1572	0.03	0.13	1.00	0.16	0.16
1574	0.05	0.00	1.05	0.00	0.00
1576	0.02	0.08	1.00	0.10	0.10
1578	0.06	0.10	1.00	0.16	0.16
1580	0.00	0.00	1.00	0.00	0.00
1582	0.00	0.00	1.00	0.00	0.00
1586	0.02	0.12	1.00	0.14	0.14
1588	0.07	0.31	1.00	0.38	0.38
1590	0.02	0.02	1.00	0.04	0.04
1592	0.06	0.02	1.00	0.08	0.08
1594	0.02	0.10	1.00	0.12	0.12
1596	0.07	0.15	1.00	0.22	0.22
1598	0.01	0.01	1.00	0.03	0.03
1600	0.00	0.00	1.00	0.00	0.00
1602	0.00	0.00	1.00	0.00	0.00
1604	0.01	0.01	1.00	0.02	0.02
1606	0.01	0.00	1.00	0.01	0.01
1608	0.00	0.03	1.00	0.03	0.03
1610	0.00	0.00	1.00	0.00	0.00
1612	0.00	0.00	1.00	0.00	0.00
1614	0.00	0.00	1.00	0.00	0.00
1616	0.01	0.01	1.00	0.02	0.02
1618	0.01	0.01	1.00	0.03	0.03
1620	0.03	0.01	1.00	0.05	0.05
1622	0.03	0.02	1.00	0.05	0.05
1624	0.02	0.11	1.00	0.13	0.13
1626	0.02	0.09	1.00	0.11	0.11
1628	0.06	0.02	1.00	0.08	0.08
1630	0.03	0.01	1.00	0.04	0.04
1632	0.01	0.01	1.00	0.02	0.02
1634	0.00	0.00	1.00	0.00	0.00
1636	0.00	0.00	1.00	0.00	0.00
1638	0.00	0.00	1.00	0.00	0.00
1640	0.02	0.00	1.00	0.02	0.02
1642	0.00	0.00	1.00	0.00	0.00
1644	0.01	0.01	1.00	0.02	0.02
1646	0.09	0.01	1.08	0.03	0.02
1648	0.01	0.01	1.00	0.02	0.02
1650	0.00	0.00	1.00	0.00	0.00
1652	0.06	0.00	1.06	0.00	0.00
1654	0.00	0.00	1.00	0.00	0.00
1656	0.00	0.00	1.00	0.00	0.00
1658	0.02	0.00	1.00	0.02	0.02
1660	0.13	0.08	1.07	0.14	0.13
1662	0.08	0.12	1.05	0.15	0.14
1664	0.03	0.13	1.00	0.16	0.16
1666	0.05	0.02	1.00	0.07	0.07
1668	0.01	0.01	1.00	0.03	0.03
1670	0.00	0.00	1.00	0.00	0.00
1672	0.00	0.00	1.00	0.00	0.00
1674	0.00	0.00	1.00	0.02	0.02
1676	0.00	0.00	1.00	0.00	0.00
1678	0.01	0.01	1.00	0.02	0.02

Stratigraphic Variation in Major Ion Ratios of North Core at North Ingebright Lake

Depth (cm)	Ca/Na	Mg/Na	SO_4/Na	CO_3/Na	CO_3/SO_4
1680	0.00	0.00	1.00	0.00	0.00
1730	0.14	0.10	1.12	0.12	0.11
1732	0.23	0.08	1.18	0.13	0.11
1734	0.10	0.00	1.10	0.00	0.00
1736	0.16	0.08	1.12	0.12	0.11
1738	0.15	0.07	1.14	0.09	0.08
1740	0.00	0.00	1.00	0.00	0.00
1742	0.00	0.00	1.00	0.00	0.00
1744	0.00	0.00	1.00	0.00	0.00
1746	0.00	0.00	1.00	0.00	0.00
1748	0.00	0.00	1.00	0.00	0.00
1750	0.00	0.00	1.00	0.00	0.00
1752	0.00	0.00	1.00	0.00	0.00
1754	0.02	0.02	1.00	0.05	0.05
1756	0.00	0.00	1.00	0.00	0.00
1758	0.00	0.00	1.00	0.00	0.00
1760	0.00	0.00	1.00	0.00	0.00
1762	0.00	0.00	1.00	0.00	0.00
1764	0.00	0.00	1.00	0.00	0.00
1766	0.00	0.00	0.96	0.00	0.00
1768	0.00	0.00	1.00	0.00	0.00
1770	0.02	0.12	1.00	0.15	0.15
1772	0.00	0.00	1.00	0.00	0.00
1774	0.00	0.00	1.00	0.00	0.00
1776	0.00	0.00	1.00	0.00	0.00
1778	0.06	0.00	1.06	0.00	0.00
1780	0.02	0.00	1.00	0.02	0.02
1782	0.00	0.00	1.00	0.00	0.00
1786	0.01	0.01	1.00	0.03	0.03
1788	0.00	0.00	1.00	0.00	0.00
1790	0.00	0.00	1.00	0.00	0.00
1792	0.01	0.01	1.00	0.02	0.02
1794	0.00	0.00	1.00	0.00	0.00
1796	0.21	0.02	1.19	0.04	0.03
1798	0.08	0.00	1.08	0.00	0.00
1800	0.00	0.00	1.00	0.00	0.00
1802	0.00	0.00	1.00	0.00	0.00
1804	0.00	0.00	1.00	0.00	0.00
1806	0.00	0.00	1.00	0.00	0.00
1808	0.00	0.00	1.00	0.00	0.00
1810	0.00	0.00	1.00	0.00	0.00
1812	0.00	0.00	1.00	0.00	0.00
1814	0.05	0.00	1.05	0.00	0.00
1816	0.00	0.00	1.00	0.00	0.00
1818	0.00	0.00	1.00	0.00	0.00
1820	0.00	0.00	1.00	0.00	0.00
1822	0.00	0.09	0.91	0.00	0.00
1824	0.00	0.00	1.00	0.00	0.00
1826	0.00	0.00	1.00	0.00	0.00
1828	0.09	0.00	1.09	0.00	0.00
1830	0.00	0.00	1.00	0.00	0.00
1832	0.00	0.00	1.00	0.00	0.00
1834	0.00	0.00	1.00	0.00	0.00
1836	0.00	0.00	1.00	0.00	0.00
1912	0.00	0.00	1.00	0.00	0.00
1914	0.00	0.00	1.00	0.00	0.00
1916	0.00	0.00	1.00	0.00	0.00

Stratigraphic Variation in Major Ion Ratios of North Core at North Ingebright Lake

Depth (cm)	Ca/Na	Mg/Na	SO_4/Na	CO_3/Na	CO_3/SO_4
1918	0.00	0.00	1.00	0.00	0.00
1920	0.00	0.00	1.00	0.00	0.00
1922	0.00	0.00	1.00	0.00	0.00
1924	0.00	0.00	1.00	0.00	0.00
1926	0.07	0.02	1.05	0.03	0.03
1928	0.00	0.00	1.00	0.00	0.00
1930	0.00	0.00	1.00	0.00	0.00
1932	0.00	0.00	1.00	0.00	0.00
1934	0.00	0.00	1.00	0.00	0.00
1936	0.00	0.00	1.00	0.00	0.00
1938	0.00	0.00	1.00	0.00	0.00
1940	0.00	0.00	1.00	0.00	0.00
1942	0.00	0.00	1.00	0.00	0.00
1944	0.00	0.00	1.00	0.00	0.00
1946	0.00	0.00	1.00	0.00	0.00
1948	0.00	0.00	1.00	0.00	0.00
1950	0.00	0.00	1.00	0.00	0.00
1952	0.00	0.00	1.00	0.00	0.00
1954	0.01	0.01	1.00	0.02	0.02
1956	0.00	0.00	1.00	0.00	0.00
1958	0.00	0.00	1.00	0.00	0.00
1960	0.00	0.00	1.00	0.00	0.00
1962	0.00	0.00	1.00	0.00	0.00
1964	0.00	0.00	1.00	0.00	0.00
1966	0.00	0.00	1.00	0.00	0.00
1968	0.00	0.00	1.00	0.00	0.00
1970	0.00	0.00	1.00	0.00	0.00
1974	0.00	0.00	1.00	0.00	0.00
1976	0.00	0.00	1.00	0.00	0.00
1978	0.00	0.00	1.00	0.00	0.00
1980	0.00	0.00	1.00	0.00	0.00
1982	0.00	0.00	1.00	0.00	0.00
1984	0.00	0.00	1.00	0.00	0.00
1986	0.00	0.00	1.00	0.00	0.00
1988	0.00	0.00	1.00	0.00	0.00
1990	0.00	0.00	1.00	0.00	0.00
1992	0.00	0.00	1.00	0.00	0.00
1994	0.00	0.00	1.00	0.00	0.00
1996	0.00	0.00	1.00	0.00	0.00
2000	0.00	0.00	1.00	0.00	0.00
2002	0.00	0.00	1.00	0.00	0.00
2004	0.00	0.00	1.00	0.00	0.00
2006	0.00	0.00	1.00	0.00	0.00
2008	0.00	0.00	1.00	0.00	0.00
2010	0.00	0.00	1.00	0.00	0.00
2012	0.00	0.00	1.00	0.00	0.00
2014	0.00	0.00	1.00	0.00	0.00
2016	0.00	0.00	1.00	0.00	0.00
2018	0.00	0.00	1.00	0.00	0.00
2020	0.00	0.00	1.00	0.00	0.00
2022	0.00	0.00	1.00	0.00	0.00
2024	0.00	0.00	1.00	0.00	0.00
2026	0.00	0.00	1.00	0.00	0.00
2028	0.00	0.00	1.00	0.00	0.00
2030	0.00	0.00	1.00	0.00	0.00
2032	0.00	0.00	1.00	0.00	0.00
2034	0.00	0.00	1.00	0.00	0.00

Stratigraphic Variation in Major Ion Ratios of North Core at North Ingebright Lake

Depth (cm)	Ca/Na	Mg/Na	SO_4/Na	CO_3/Na	CO_3/SO_4
2036	0.00	0.00	1.00	0.00	0.00
2038	0.00	0.00	0.96	0.00	0.00
2040	0.00	0.00	1.00	0.00	0.00
2042	0.00	0.00	1.00	0.00	0.00
2044	0.00	0.00	1.00	0.00	0.00
2046	0.00	0.00	1.00	0.00	0.00
2048	0.05	0.00	1.05	0.00	0.00
2052	0.00	0.00	1.00	0.00	0.00
2054	0.00	0.00	1.00	0.00	0.00
2056	0.00	0.00	1.00	0.00	0.00
2058	0.00	0.00	1.00	0.00	0.00
2060	0.00	0.00	1.00	0.00	0.00
2062	0.00	0.00	1.00	0.00	0.00
2064	0.00	0.00	1.00	0.00	0.00
2066	0.01	0.01	1.00	0.01	0.01
2068	0.00	0.00	1.00	0.00	0.00
2070	0.00	0.00	1.00	0.00	0.00
2072	0.00	0.00	1.00	0.00	0.00
2074	0.01	0.01	1.00	0.02	0.02
2076	0.00	0.00	1.00	0.00	0.00
2078	0.02	0.08	0.92	0.02	0.02
2080	0.00	0.00	1.00	0.00	0.00
2082	0.00	0.00	1.00	0.00	0.00
2084	0.00	0.00	1.00	0.00	0.00
2086	0.00	0.00	1.00	0.00	0.00
2088	0.00	0.00	1.00	0.00	0.00
2090	0.00	0.00	1.00	0.00	0.00
2092	0.00	0.00	1.00	0.00	0.00
2094	0.00	0.00	1.00	0.00	0.00
2096	0.00	0.00	1.00	0.00	0.00
2098	0.00	0.00	1.00	0.00	0.00
2100	0.00	0.00	1.00	0.00	0.00
2102	0.00	0.00	1.00	0.00	0.00
2104	0.02	0.02	1.00	0.03	0.03
2108	0.00	0.00	1.00	0.00	0.00
2110	0.00	0.00	1.00	0.00	0.00
2112	0.00	0.00	1.00	0.00	0.00
2114	0.00	0.00	1.00	0.00	0.00
2116	0.00	0.00	1.00	0.00	0.00
2118	0.00	0.00	1.00	0.00	0.00
2120	0.00	0.00	1.00	0.00	0.00
2122	0.00	0.00	1.00	0.00	0.00
2124	0.00	0.00	1.00	0.00	0.00
2126	0.00	0.00	1.00	0.00	0.00
2128	0.00	0.00	1.00	0.00	0.00
2130	0.00	0.00	1.00	0.00	0.00
2132	0.00	0.00	1.00	0.00	0.00
2134	0.00	0.00	1.00	0.00	0.00
2136	0.00	0.00	1.00	0.00	0.00
2138	0.00	0.00	1.00	0.00	0.00
2140	0.00	0.00	1.00	0.00	0.00
2142	0.00	0.00	1.00	0.00	0.00
2144	0.00	0.00	1.00	0.00	0.00
2146	0.00	0.00	1.00	0.00	0.00
2148	0.00	0.00	1.00	0.00	0.00
2150	0.00	0.00	1.00	0.00	0.00
2152	0.00	0.00	1.00	0.00	0.00

Stratigraphic Variation in Major Ion Ratios of North Core at North Ingebright Lake

Depth (cm)	Ca/Na	Mg/Na	SO_4/Na	CO_3/Na	CO_3/SO_4
2154	0.00	0.00	1.00	0.00	. 0.00
2156	0.00	0.00	1.00	0.00	0.00
2158	0.00	0.00	1.00	0.00	0.00
2160	0.00	0.00	1.00	0.00	0.00
2162	0.00	0.00	1.00	0.00	0.00
2164	0.00	0.00	1.00	0.00	0.00
2166	0.00	0.00	1.00	0.00	0.00
2168	0.00	0.00	1.00	0.00	0.00
2170	0.00	0.00	1.00	0.00	0.00
2172	0.00	0.00	1.00	0.00	0.00
2174	0.00	0.00	1.00	0.00	0.00
2176	0.00	0.00	1.00	0.00	0.00
2178	0.00	0.00	1.00	0.00	0.00
2180	0.00	0.00	1.00	0.00	0.00
2182	0.00	0.00	1.00	0.00	0.00
2184	0.00	0.00	1.00	0.00	0.00
2186	0.00	0.00	1.00	0.00	0.00
2188	0.00	0.00	1.00	0.00	0.00
2190	0.00	0.00	1.00	0.00	0.00
2192	0.00	0.00	1.00	0.00	0.00
2194	0.00	0.00	1.00	0.00	0.00
2196	0.00	0.00	1.00	0.00	0.00
2198	0.00	0.00	1.00	0.00	0.00
2200	0.05	0.00	1.05	0.00	0.00
2202	0.00	0.00	1.00	0.00	0.00
2204	0.00	0.00	1.00	0.00	0.00
2206	0.00	0.00	1.00	0.00	0.00
2208	0.00	0.00	1.00	0.00	0.00
2210	0.00	0.00	1.00	0.00	0.00
2212	0.00	0.00	1.00	0.00	0.00
2214	0.00	0.00	1.00	0.00	0.00
2216	0.00	0.00	1.00	0.00	0.00
2218	0.00	0.00	1.00	0.00	0.00
2220	0.05	0.00	1.05	0.00	0.00
2222	0.00	0.00	1.00	0.00	0.00
2224	0.00	0.00	1.00	0.00	0.00
2226	0.00	0.00	1.00	0.00	0.00
2228	0.00	0.00	1.00	0.00	0.00
2230	0.00	0.00	1.00	0.00	0.00
2232	0.00	0.00	1.00	0.00	0.00
2234	0.00	0.00	1.00	0.00	0.00
2236	0.00	0.00	1.00	0.00	0.00
2238	0.00	0.00	1.00	0.00	0.00
2240	0.00	0.00	1.00	0.00	0.00
2242	0.00	0.00	1.00	0.00	0.00
2244	0.00	0.00	1.00	0.00	0.00
2246	0.00	0.00	1.00	0.00	0.00
2250	0.00	0.00	1.00	0.00	0.00
2252	0.00	0.00	1.00	0.00	0.00
2254	0.00	0.00	1.00	0.00	0.00
2256	0.00	0.00	1.00	0.00	0.00
2258	0.00	0.00	1.00	0.00	0.00
2260	0.00	0.00	1.00	0.00	0.00
2262	0.00	0.00	1.00	0.00	0.00
2264	0.00	0.00	1.00	0.00	0.00
2266	0.00	0.00	1.00	0.00	0.00
2268	0.00	0.00	1.00	0.00	0.00

Stratigraphic Variation in Major Ion Ratios of North Core at North Ingebright Lake

Depth (cm)	Ca/Na	Mg/Na	SO_4/Na	CO_3/Na	CO_3/SO_4
2270	0.00	0.00	1.00	0.00	0.00
2272	0.00	0.00	1.00	0.00	0.00
2274	0.00	0.00	1.00	0.00	0.00
2276	0.00	0.00	1.00	0.00	0.00
2280	0.00	0.00	1.00	0.00	0.00
2282	0.00	0.00	1.00	0.00	0.00
2284	0.00	0.00	1.00	0.00	0.00
2286	0.00	0.00	1.00	0.00	0.00
2288	0.00	0.00	1.00	0.00	0.00
2290	0.00	0.00	1.00	0.00	0.00
2292	0.00	0.00	1.00	0.00	0.00
2294	0.00	0.00	1.00	0.00	0.00
2296	0.00	0.00	1.00	0.00	0.00

Stratigraphic Variation in Major Ion Ratios of South Core at North Ingebright Lake

Depth (cm)	Ca/Na	Mg/Na	SO_4/Na	CO_3/Na	CO_3/SO_4
10	0.00	0.00	1.00	0.00	0.00
12	0.26	0.50	0.76	0.30	0.40
14	0.00	0.00	1.00	0.00	0.00
16	0.00	0.00	1.00	0.00	0.00
18	0.00	0.00	1.00	0.05	0.05
20	0.00	0.00	1.00	0.00	0.00
22	1.38	1.38	1.00	3.00	1.00
24	0.00	0.00	1.00	0.00	0.00
26	0.00	0.00	1.00	0.13	0.13
28	0.83	0.83	1.00	1.65	1.65
30	1.00	1.00	1.00	1.00	1.20
32	1.22	1.22	1.00	2.44	2.44
34	0.00	0.00	1.00	0.00	0.00
36	0.00	0.00	1.00	0.00	0.00
38	2.50	2.50	0.00	5.00	1.00
40	1.00	1.00	1.00	1.00	1.00
42	0.00	0.00	1.00	0.00	0.00
44	0.00	0.00	1.00	0.00	0.00
46	0.00	0.00	1.00	0.14	0.14
48	0.00	0.00	1.00	0.22	0.22
50	0.73	0.00	1.00	0.73	0.73
52	0.00	0.00	1.00	0.00	0.00
54	0.00	0.00	1.00	0.67	0.67
56	0.01	0.01	1.00	0.03	0.03
58	0.00	0.00	1.00	0.01	0.01
60	0.00	0.00	1.00	0.00	0.00
62	0.00	0.00	1.00	0.00	0.00
64	0.00	0.00	0.00	0.00	1.00
66	0.00	0.00	1.00	0.00	0.00
68	0.00	0.00	1.00	0.00	0.00
70	0.00	0.00	1.00	0.00	0.00
72	0.00	0.00	1.00	0.00	0.00
74	0.00	0.00	1.00	0.00	0.00
76	0.00	0.00	1.00	0.00	0.00
78	0.00	0.00	1.00	0.00	0.00
80	0.00	0.00	1.00	0.00	0.00
82	0.00	0.00	1.00	0.00	0.00
84	0.00	0.00	1.00	0.00	0.00
86	0.00	0.00	1.00	0.00	0.00
88	0.00	0.00	1.00	0.00	0.00
90	0.00	0.00	1.00	0.00	0.00
92	0.00	0.00	1.00	0.00	0.00
94	0.00	0.00	1.00	0.00	0.00
96	0.00	0.00	1.00	0.00	0.00
98	0.00	0.00	1.00	0.00	0.00
100	0.00	0.00	1.00	0.00	0.00
102	0.00	0.00	1.00	0.00	0.00
104	0.00	0.00	1.00	0.00	0.00
106	0.00	0.00	1.00	0.00	0.00
108	0.00	0.00	1.00	0.00	0.00
110	0.00	0.00	1.00	0.00	0.00
112	0.00	0.00	1.00	0.00	0.00
114	0.00	0.00	1.00	0.00	0.00
116	0.00	0.00	1.00	0.00	0.00
118	0.00	0.00	1.00	0.00	0.00
120	0.00	0.00	1.00	0.00	0.00
122	0.00	0.00	1.00	0.00	0.00
124	0.00	0.00	1.00	0.00	0.00

Stratigraphic Variation in Major Ion Ratios of South Core at North Ingebright Lake

Depth (cm)	Ca/Na	Mg/Na	SO_4/Na	CO_3/Na	CO_3/SO_4
126	0.00	0.00	1.00	0.00	0.00
128	0.00	0.00	1.00	0.00	0.00
130	0.05	0.00	1.05	0.00	0.00
132	0.00	0.00	1.00	0.00	0.00
134	0.03	0.00	1.00	0.03	0.03
136	0.00	0.00	1.00	0.00	0.00
138	0.00	0.00	1.00	0.00	0.00
140	0.00	0.00	1.00	0.00	0.00
142	0.00	0.00	1.00	0.00	0.00
144	0.00	0.00	1.00	0.00	0.00
146	0.00	0.00	1.00	0.00	0.00
148	0.00	0.00	1.00	0.00	0.00
150	0.00	0.00	1.00	0.00	0.00
152	0.00	0.00	1.00	0.00	0.00
154	0.00	0.00	1.00	0.00	0.00
156	0.04	0.00	1.04	0.00	0.00
158	0.00	0.00	1.00	0.00	0.00
160	0.00	0.00	1.00	0.00	0.00
162	0.00	0.00	1.00	0.00	0.00
164	0.00	0.00	1.00	0.00	0.00
166	0.00	0.00	1.00	0.00	0.00
168	0.00	0.00	1.00	0.00	0.00
170	0.00	0.00	1.00	0.00	0.00
172	0.00	0.00	1.00	0.00	0.00
174	0.00	0.00	1.00	0.00	0.00
176	0.00	0.00	1.00	0.00	0.00
178	0.00	0.00	1.00	0.00	0.00
180	0.04	0.00	1.04	0.00	0.00
182	0.01	0.01	1.00	0.03	0.03
184	0.00	0.00	1.00	0.00	0.00
186	0.00	0.00	1.00	0.00	0.00
188	0.00	0.00	1.00	0.00	0.00
190	0.03	0.00	1.00	0.03	0.03
192	0.00	0.00	1.00	0.00	0.00
194	0.00	0.00	1.00	0.00	0.00
196	0.00	0.00	1.00	0.00	0.00
198	0.00	0.00	1.00	0.00	0.00
200	0.14	0.00	1.14	0.02	0.01
202	0.00	0.00	1.00	0.00	0.00
204	0.00	0.00	1.00	0.00	0.00
226	0.00	0.00	1.00	0.00	0.00
228	0.00	0.00	1.00	0.00	0.00
230	0.00	0.00	1.00	0.00	0.00
232	0.00	0.00	1.00	0.00	0.00
234	0.00	0.00	1.00	0.00	0.00
236	0.08	0.00	1.08	0.00	0.00
238	0.00	0.00	1.00	0.00	0.00
240	0.00	0.00	1.00	0.00	0.00
242	0.00	0.00	1.00	0.00	0.00
244	0.11	0.00	1.11	0.00	0.00
246	0.12	0.00	1.12	0.00	0.00
248	0.08	0.00	1.08	0.00	0.00
250	0.01	0.01	1.00	0.03	0.03
252	0.10	0.00	1.10	0.00	0.00
254	0.00	0.00	1.00	0.00	0.00
256	0.00	0.00	1.00	0.00	0.00
258	0.06	0.00	1.06	0.00	0.00
260	0.08	0.00	1.08	0.00	0.00
262	0.18	0.00	1.18	0.00	0.00

Stratigraphic Variation in Major Ion Ratios of South Core at North Ingebright Lake

Depth (cm)	Ca/Na	Mg/Na	SO_4/Na	CO_3/Na	CO_3/SO_4
264	0.11	0.00	1.11	0.00	0.00
266	0.11	0.00	1.10	0.02	0.01
268	0.14	0.00	1.14	0.00	0.00
270	0.00	0.00	1.00	0.00	0.00
272	0.02	0.00	1.00	0.02	0.02
274	0.00	0.00	1.00	0.00	0.00
276	0.00	55.26	1.00	55.26	55.26
278	0.06	0.02	1.00	0.08	0.08
280	0.13	0.00	1.13	0.00	0.00
282	0.27	0.10	1.25	0.13	0.10
284	0.18	0.00	1.18	0.00	0.00
286	0.01	0.01	1.00	0.03	0.03
288	0.08	0.00	1.08	0.00	0.00
290	0.14	0.11	1.11	0.14	0.12
292	0.13	0.03	1.10	0.05	0.05
294	0.02	0.02	1.00	0.10	0.10
296	0.12	0.00	1.12	0.00	0.00
298	0.08	0.06	1.08	0.06	0.06
300	0.00	0.00	1.00	0.00	0.00
302	0.10	0.02	1.08	0.04	0.04
304	0.02	0.02	1.00	0.04	0.04
306	0.01	0.01	1.00	0.03	0.03
308	0.08	0.00	1.08	0.00	0.00
310	0.06	0.00	1.06	0.00	0.00
312	0.00	0.00	1.00	0.00	0.00
314	0.08	0.02	1.06	0.03	0.03
316	0.12	0.02	1.10	0.03	0.03
318	0.02	0.02	1.00	0.03	0.03
320	0.02	0.02	1.00	0.06	0.06
322	0.08	0.02	1.06	0.04	0.04
324	0.02	0.02	1.00	0.04	0.04
326	0.06	0.06	1.00	0.11	0.11
328	0.02	0.02	1.00	0.07	0.07
330	0.02	0.11	1.00	0.13	0.13
332	0.00	0.09	0.91	0.00	0.00
334	0.07	0.02	1.05	0.03	0.03
336	0.02	0.02	1.00	0.03	0.03
338	0.02	0.02	1.00	0.04	0.04
340	0.10	0.02	1.08	0.03	0.03
342	0.02	0.02	1.00	0.03	0.03
344	0.02	0.08	1.00	0.10	0.10
346	0.02	0.11	1.00	0.16	0.16
348	0.09	0.02	1.06	0.04	0.04
350	0.00	0.00	1.00	0.00	0.00
352	0.00	0.00	1.00	0.00	0.00
354	0.08	0.02	1.07	0.03	0.03
356	0.00	0.00	1.00	0.00	0.00
358	0.00	1.00	0.00	0.00	0.00
360	0.02	0.02	1.00	0.03	0.03
362	0.00	0.00	1.00	0.00	0.00
364	0.01	0.01	1.00	0.03	0.03
366	0.00	0.00	1.00	0.00	0.00
368	0.05	0.00	1.05	0.00	0.00
370	0.00	0.06	0.94	0.00	0.00
372	0.01	0.01	1.00	0.03	0.03
374	0.06	0.02	1.05	0.03	0.03
376	0.00	0.00	1.00	0.00	0.00
378	0.00	0.00	1.00	0.00	0.00
380	0.03	0.03	1.00	0.06	0.06

Stratigraphic Variation in Major Ion Ratios of South Core at North Ingebright Lake

Depth (cm)	Ca/Na	Mg/Na	SO_4/Na	CO_3/Na	CO_3/SO_4
382	0.06	0.00	1.06	0.00	0.00
384	0.08	0.00	1.08	0.00	0.00
386	0.00	0.00	1.00	0.00	0.00
388	0.00	0.00	1.00	0.00	0.00
390	0.00	0.00	1.00	0.00	0.00
392	0.02	0.02	1.00	0.04	0.04
394	0.00	0.00	1.00	0.00	0.00
396	0.13	0.11	1.11	0.13	0.12
398	0.10	0.02	1.08	0.03	0.03
400	0.19	0.08	1.17	0.09	0.08
404	0.10	0.00	1.10	0.00	0.00
406	0.01	0.01	1.00	0.03	0.03
408	0.11	0.02	1.07	0.07	0.06
410	0.00	0.06	1.00	0.06	0.06
412	0.12	0.07	1.10	0.10	0.09
414	0.15	0.09	1.09	0.18	0.17
416	0.02	0.02	1.00	0.04	0.04
500	0.03	0.14	1.00	0.16	0.16
502	0.08	0.00	1.08	0.00	0.00
504	0.00	0.13	0.88	0.03	0.04
508	0.12	0.05	1.07	0.10	0.09
510	0.05	0.05	1.00	0.11	0.11
512	0.45	0.05	1.41	0.09	0.06
514	0.16	0.03	1.13	0.05	0.05
516	0.41	0.05	1.36	0.09	0.07
518	0.43	0.24	1.38	0.29	0.21
520	0.18	0.03	1.15	0.05	0.04
522	0.15	0.13	1.13	0.15	0.13
524	0.13	0.15	1.10	0.18	0.16
526	0.30	0.30	1.22	0.37	0.30
528	0.03	0.03	1.00	0.05	0.05
530	0.02	0.02	1.00	0.05	0.05
532	0.10	0.10	1.10	0.10	0.09
534	0.13	0.02	1.11	0.04	0.04
536	0.28	0.03	1.25	0.06	0.04
538	0.25	0.14	1.22	0.17	0.14
540	0.64	0.24	1.60	0.28	0.18
542	0.27	0.18	1.24	0.21	0.17
544	0.47	0.20	1.43	0.23	0.16
546	0.50	0.33	1.42	0.42	0.29
550	0.23	0.26	1.16	0.32	0.28
552	0.16	0.16	1.14	0.19	0.17
554	0.18	0.02	1.16	0.04	0.03
556	0.47	0.03	1.43	0.07	0.05
558	0.33	0.18	1.30	0.21	0.16
560	0.15	0.02	1.12	0.05	0.04
562	0.26	0.06	1.21	0.12	0.10
564	0.23	0.03	1.20	0.05	0.04
566	0.19	0.14	1.16	0.16	0.14
568	0.43	0.11	1.40	0.14	0.10
570	0.27	0.07	1.24	0.10	0.08
572	0.02	0.02	1.00	0.04	0.04
574	0.17	0.11	1.15	0.13	0.11
576	0.22	0.12	1.20	0.15	0.12
578	0.15	0.13	1.13	0.15	0.14
580	0.32	0.03	1.29	0.05	0.04
582	0.30	0.03	1.28	0.05	0.04
584	0.25	0.10	1.24	0.12	0.10
586	0.40	0.00	1.40	0.02	0.02

Stratigraphic Variation in Major Ion Ratios of South Core at North Ingebright Lake

Depth (cm)	Ca/Na	Mg/Na	SO_4/Na	CO_3/Na	CO_3/SO_4
588	0.40	0.14	1.37	0.17	0.13
590	0.24	0.02	1.21	0.05	0.04
592	0.29	0.02	1.27	0.05	0.04
594	0.14	0.02	1.12	0.06	0.05
596	0.29	0.02	1.26	0.05	0.04
598	0.43	0.14	1.37	0.09	0.06
600	0.20	0.03	1.18	0.05	0.04
602	0.19	0.14	1.16	0.16	0.14
604	0.15	0.03	1.13	0.05	0.04
606	0.24	0.12	1.22	0.15	0.12
608	0.27	0.02	1.24	0.05	0.04
610	0.18	0.09	1.16	0.11	0.10
612	0.17	0.02	1.16	0.03	0.03
614	0.02	0.02	1.00	0.03	0.03
616	0.42	0.00	1.36	0.08	0.06
618	0.37	0.00	1.33	0.04	0.03
620	0.32	0.00	1.23	0.13	0.10
622	0.35	0.00	1.25	0.10	0.08
624	0.22	0.00	1.22	0.00	0.00
626	0.79	0.03	1.69	0.17	0.10
628	0.35	0.00	1.20	0.14	0.12
630	0.17	0.15	0.96	0.07	0.07
632	0.25	0.00	1.21	0.08	0.06
634	0.19	0.11	1.04	0.06	0.05
636	0.05	0.00	1.03	0.02	0.01
638	0.05	0.02	1.00	0.06	0.06
640	0.17	0.02	1.10	0.08	0.08
642	0.05	0.00	1.00	0.10	0.10
644	0.05	0.24	0.90	0.21	0.23
646	0.36	0.02	1.33	0.05	0.04
648	0.15	0.02	1.10	0.07	0.06
650	0.11	0.02	1.09	0.07	0.06
652	0.14	0.00	1.10	0.03	0.03
654	0.10	0.00	1.10	0.00	0.00
656	0.10	0.00	1.10	0.00	0.00
658	0.06	0.00	1.06	0.00	0.00
660	0.00	0.00	1.00	0.00	0.00
662	1.38	0.00	2.38	0.00	0.00
664	0.26	0.00	1.26	0.00	0.00
666	0.97	0.03	1.94	0.06	0.03
668	0.41	0.00	1.41	0.00	0.00
670	0.60	0.03	1.58	0.05	0.03
672	2.28	0.11	3.22	0.17	0.05
674	0.54	0.00	1.54	0.00	0.00
676	0.55	0.02	1.52	0.05	0.03
678	1.12	0.04	2.04	0.12	0.06
680	0.29	0.02	1.27	0.05	0.04
682	1.95	0.05	2.90	0.10	0.03
684	0.56	0.03	1.53	0.06	0.04
686	0.24	0.02	1.22	0.04	0.04
824	0.17	0.00	1.17	0.00	0.00
826	0.29	0.00	1.29	0.00	0.00
828	0.35	0.00	1.35	0.00	0.00
830	0.12	0.00	1.12	0.00	0.00
832	0.67	0.00	1.67	0.00	0.00
834	0.10	0.00	1.10	0.00	0.00
836	0.18	0.03	1.15	0.05	0.04
838	0.00	0.00	1.00	0.00	0.00
840	0.02	0.02	1.00	0.05	0.05

Stratigraphic Variation in Major Ion Ratios of South Core at North Ingebright Lake

Depth (cm)	Ca/Na	Mg/Na	SO_4/Na	CO_3/Na	CO_3/SO_4
842	0.00	0.03	1.00	0.03	0.03
844	0.36	0.25	1.29	0.32	0.25
846	0.73	0.36	1.64	0.45	0.28
848	0.06	0.00	1.06	0.00	0.00
850	0.10	0.02	1.07	0.07	0.07
852	0.05	0.02	1.00	0.06	0.06
854	3.80	0.30	4.70	0.40	0.09
856	0.11	0.02	1.09	0.04	0.04
858	0.02	0.02	1.00	0.04	0.04
860	0.35	0.02	1.33	0.04	0.03
862	0.10	0.02	1.08	0.03	0.03
864	0.28	0.13	1.26	0.15	0.12
866	0.34	0.19	1.31	0.22	0.17
868	1.20	0.30	2.10	0.40	0.19
870	15.00	0.00	16.00	0.33	0.02
872	21.50	2.50	22.00	3.00	0.14
874	10.00	0.00	11.00	0.00	0.00
876	13.00	0.00	13.67	0.33	0.02
878	25.00	0.00	26.00	0.50	0.02
880	47.00	0.00	48.00	0.00	0.00
882	13.00	0.33	13.33	1.00	0.08
884	4.50	0.00	5.50	0.00	0.00
886	13.00	0.00	13.75	0.25	0.02
888	16.00	0.33	16.33	1.00	0.06
890	53.00	0.00	54.00	0.00	0.00
892	23.50	0.00	24.00	0.50	0.02
894	55.00	0.00	55.00	1.00	0.02
896	15.67	0.00	16.33	0.33	0.02

Appendix E Core Descriptions

Core Descriptions (North Core, North Ingebright Lake)

Depth (cm)			Description
0	-	12	missing core
12	-	37	mud
37	-	55	muddy salt
55	-	75	muddy salt, small crystal aggregate and mud materials occurs between salt crystals
75	-	153	muddy salt, salt crystal size: 2-5 mm.
153	-	228	muddy salt, crystal size becomes bigger , 3-6 mm.
228	-	306	mud and salt, mud materials: 30-40%, intrasedimentary crystals are common
306	-	381	massive salt, mud material decreases, salt crystal size: 0.5-2 cm.
381	-	459	massive salt
459	-	534	massive salt, colourless, large salt crystal size: 1-2 cm,
534	-	612	massive salt
612	-	687	massive salt
687	-	765	clear salt crystals containing about 10% mud or organic debris inclusions
765	-	790	missing core
790	-	840	massive salt
840	-	918	massive salt
918	-	993	muddy salt
993	-	1071	massive salt
1071	-	1146	massive salt
1146	-	1224	very clear salt, crystal size: 2-5 cm
1224	-	1324	missing core
1324	-	1374	dirty salt
1374	-	1449	massive salt
1449	-	1527	massive salt
1527	-	1602	massive salt
1602	-	1680	clear salt, compacted, recrystallized
1680	-	1730	missing core
1730	-	1805	massive salt
1805	-	1837	massive salt
1837	-	1912	missing core
1912	-	1990	colourless, structureless, very-well consolidated salt
1990	-	2065	clear salt

2065	-	2143	clear salt
2143	-	2218	clear salt
2218	-	2296	clear salt, odour smell (H_2S), redox environment

Core Descriptions (South Core, North Ingebright Lake)

Depth (cm)			Description
0	-	10	missing core
10	-	46	black green mud (fine-grained sands, silts and clays), intrasedimentary crystals of mirabilite, thenardite, and gypsum are abundant, grain size: 0.1 - 0.5 cm, no lamination
46	-	75	muddy salt, grey colour, massive structure, mud materials: 40 - 50%
75	-	150	smoky colour, compacted, well-consolidated salt, long axis of black needle-like sediments or organic debris is vertical.
150	-	226	broken salt
226	-	302	dirty salt, massive crystalline aggregates.
302	-	377	smoke colour, compacted, muddy salt, mud materials: 5 - 10%.
377	-	417	muddy salt
417	-	499	missing core
499	-	575	massive muddy salt
575	-	610	muddy salt
610	-	686	salt, crystal grain size: 0.5-1 cm, mud materials commonly fill space between salt crystal grains
686	-	822	missing core
822	-	896	massive salt, bottom 30 cm core consists of black green mud containing abundant intrasedimentary salt crystals. Crystals appear in the form of rounded accretionary grains or tabular crystals, grain size: 1-5 cm.
896	-	916	highly reducing, fine-grained sand, silt and clay

Appendix F Statistical Analyses

Appendix F Statistical Analyses

The sediment of North Ingebright Lake offer unusual opportunities for selected geochemical and mineralogical studies. It contains a complete and well-preserved Holocene sediment record. Twenty one major and minor minerals are reported, together with chemical properties of sediments for 1310 subsamples from two cores. These data constitute an excellent data matrix for statistical analysis. When the set of data is large and the underlying causal structure is obscure, multivariate statistical techniques can be an important aid in revealing simple patterns in complex information. In the following section multivariate techniques, sequentially employing correlation, Q-mode and R-mode analyses, were applied to the mineralogical and geochemical data in order to examine possible interrelationships between various variables, and to define statistically recognizable controlling factors.

Correlation Analysis

Pearson's product-moment coefficient of linear correlation was used to assess the linear relationship between variables. The correlation coefficient γ is given by

$$\gamma = \sum(x-\bar{x})(y-\bar{y})/\langle\sum(x-\bar{x})^2 \sum(y-\bar{y})^2\rangle^{1/2}$$

where $\bar{x}$ and $\bar{y}$ are the mean values of variable x and y. This formula is the ratio of how much x and y vary together about their means to total variation of x and y.

Values of γ can vary between +1 and -1. γ = +1 represents a perfect linear relationship between x and y. γ = -1 expresses a perfect negative correlation between x and y. γ = 0 means that x and y are uncorrelated variables (Klovan, 1975).

Simple linear correlation coefficients of mineralogical and geochemical data were calculated for all possible variable pairs. Table G-1 is a matrix of the correlation coefficients that were obtained using SAS computer program. As expected, detrital components are all positively correlated with organic matter content, whereas they are strongly inversely proportional to endogenic components. Significantly high coefficients were obtained for quartz to organic matter, 0.552; quartz to high Mg calcite, 0.553; organic matter to protodolomite, 0.477; and thenardite to depth, 0.439. Strongly negative coefficients were found for organic matter to thenardite, -0.632; total clay minerals to thenardite, -0.596; and gypsum to thenardite, -0.525.

Among the detrital components, quartz, k-feldspar, clay minerals, calcite and dolomite all show positive correlation with each other. Only plagioclase is negatively correlated with quartz, k-feldspar, and total clay minerals. Endogenic mineralogical components determined in this study show striking correlation with one another. Thenardite shows moderate to strong negative association with all endogenic minerals: high Mg calcite, protodolomite, aragonite, magnesite, gypsum, anhydrite, bloedite and halite. High Mg calcite, protodolomite, aragonite and magnesite are inversely related to bloedite, gypsum and anhydrite, while halite varies positively with carbonate and sulphate minerals. These relationships can be well explained by evaporative evolution of natural waters.

Cluster Analysis

The objective of cluster analysis is to find new, hypothetical "sample" whose compositions are linear combinations of those of the original samples (Imbrie and Purdy, 1962). In this study, cluster analysis was employed to help define groups (units) of samples by considering simultaneously all the variables that have been measured. After the unit classifications, factor analysis was carried out for each of individual units because factor analysis requires a homogeneous population to be meaningful.

A vast number of clustering methods have been developed in past decades, such as correlation coefficient, coefficient of proportional similarity, and distance coefficient methods (Klovan, 1975). The simulation study indicates that the clustering method with the best overall performance has been either average linkage or Ward's minimum variance method (SAS User's Guide, 1990). Therefore, average linkage method was chosen to group samples from North Ingebright Lake.

The similarities between all possible pairs of samples were calculated and shown both in table and histogram. The table and histogram contain all the information concerning the interrelations between the samples. However, the table and histogram are too large to be attached in this document. At the 0.2 distance coefficient level seven clusters of samples are readily identified. Each of these clusters approximately correspond to one lithostratigraphic unit.

Factor Analysis

Factor analysis is designed to represent complex relationships between a large number of variables by simple relationships amongst fewer hypothetical variables. These new variables are linearly related to the original ones by rotation in space and should contain the same amount of information (Jöreskog et al., 1976). Various mathematical procedures have been proposed to perform factor analysis. Although factor analysis was initially used by psychologists, its significance in earth science was soon realized by geologists. Imbries and Purdy (1962) successfully used factor analysis to classify the modern carbonate sediments of the Great Bahama Bank. Klovan (1966) employed factor analysis to define sedimentary environments from grain size data. Hitchon et al. (1971) and Reed, Hitchon, and Levinson (1972) used factor analysis to reveal the controls on water chemistry. More recently Last (1992) applied factor analysis to classify salt lakes in western Canada and discover the controls on water chemistry of salt lakes. Thirteen major water chemistry types were clearly identified. Groundwater composition, climate, and the elevation of the lake within the drainage system were revealed as major factors in controlling brine chemistry and salinity in salt lakes.

There are three major methods available for factor analysis: principle factor method, varimax method, and promax method. In the principle factor method, the total variation in the data set is represented by a small number of geological factors, each manifested in a degree of correlation (elongation) in the data scatter. Each successive factor accounts for a lesser amount of the variance of variable than the preceding one. Factors accounting for small quantities of variance therefore can be identified and neglected without losing useful information. In the varimax method, orthogonal rotation of the axis system is attempted to account for as much of the variance as possible. The promax method allows the axes to rotate out of perpendicular, in which the reference vectors of the scheme are taken as unit vectors passed through the positions of the m real sample vectors occupying extreme positions in the configuration (Imbrie and Van Andel, 1964; Sas User's Guide, 1990).

Initially the data set from North Ingebright Lake was processed using all these three methods. However, factors extracted by the varimax and promax method are usually mathematically abstractions difficult to interpret geologically. They are over-simply focused on the individual variable. In most cases each variable only has high loadings on one factor. This violates with the natural process: any geological product is a result of multi-factor interplays. Therefore, in this research, only factors extracted by the principle method are used for the further geological interpretation.

The results of the R-mode factor analysis of the Units 2, 3, 4, 5, 6, 7 and 8 samples are shown in Tables G-2, 3, 4, 5, 6, 7 and 8. Eight to eleven factors were extracted from the different units. They account for over 91-98 per cent of the sample variance. Factor interpretations for each units are similar. Therefore, only interpretation for unit 2 is given below.

Ten factors explain over 95% of the total variance of the data set of the unit 2. Factor 1 accounts for 25.16% of the total data variability, with high positive loadings on quartz, plagioclase, total clay minerals and dolomite. This factor is interpreted as representing the detrital products, which were brought to lake basin by sheetflow or eolian activities. Factors 2 and 3, which consists of bloedite, thenardite, aragonite, and magnesite, account for 25.08% of the total data variability. These two factors essentially represent endogenic chemical sedimentation components. Factors 4 and 5, accounting for 17.34% of the total data variability, are dominated by high positive loading on organic matter and total carbonate contents. This factor is interpreted as a lake production factor. Factors 6, 7, 8, 9 and 10 are minor and their eigen values are less than 0.5. They may be picking up just random effects.

Table F-1 Pearson Correlation Coefficient Matrix of Mineralogical and Geochemical Variables from North Ingebright lake

	Depth	Organic Matter	Carbonate Content	Quartz	K-feldspar	Plagioclase	Calcite
Depth	1.0000	-0.4120	-0.1089	-0.3685	-0.1683	-0.1758	-0.0326
Organic Matter	-0.4120	1.0000	0.1340	0.5521	0.2930	0.0260	0.0087
Carbonate Content	-0.1089	0.1340	1.0000	0.1111	0.0526	0.1254	0.0060
Quartz	-0.3685	0.5521	0.1111	1.0000	0.3950	-0.0155	0.0082
K-feldspar	-0.1683	0.2930	0.0526	0.3950	1.0000	-0.0047	-0.0009
Plagioclase	-0.1758	0.0260	0.1254	-0.0155	-0.0047	1.0000	0.1105
Calcite	-0.0326	0.0087	0.0060	0.0082	-0.0009	0.1105	1.0000
High Mg Calcite	-0.1148	0.1138	0.0170	0.5533	0.0565	-0.0289	0.0045
Protodolomite	-0.2387	0.4772	0.0857	0.4440	0.3083	-0.0185	-0.0049
Dolomite	-0.1462	0.1597	0.0564	0.1672	0.0048	0.0308	0.0092
Bloedite	-0.0952	0.2663	0.0621	0.1144	0.1409	-0.0240	0.0186
Clay Mineral	-0.1691	0.3613	0.0108	0.0636	0.0159	-0.0780	-0.0267
Magnesite	0.0302	0.1440	-0.0169	-0.0109	-0.0135	-0.0493	-0.0168
Thenardite	0.4394	-0.6319	-0.1294	-0.4613	-0.2766	-0.3169	-0.0501
Aragonite	0.0330	0.0218	-0.0362	-0.0187	-0.0232	-0.0685	-0.0127
Anhydrite	-0.1104	0.2518	0.0360	0.2073	0.0622	-0.0100	-0.0037
Gypsum	-0.1995	0.2084	0.0131	0.0116	0.0140	-0.0621	0.0033
Halite	0.0227	0.0156	-0.0084	0.0098	0.0358	-0.0256	-0.0040
Mg in High Mg Calcite	-0.2103	0.2186	0.0394	0.2420	0.0506	-0.0562	0.0265
Ca in Protodolomite	-0.3406	0.4020	0.0473	0.1580	0.0623	0.0325	0.0274
Ca in Dolomite	-0.2423	0.2441	0.0474	0.1439	0.0148	0.0049	0.0887

Table F-1 Pearson Correlation Coefficient Matrix of Mineralogical and Geochemical Variables from North Ingebright lake

	High Mg Calcite	Protodolomite	Dolomite	Bloedite	Clay Mineral	Magnesite	Thenardite
Depth	-0.1148	-0.2387	-0.1462	-0.0952	-0.1691	0.0302	0.4394
Organic Matter	0.1138	0.4772	0.1597	0.2663	0.3613	0.1440	-0.6319
Carbonate Content	0.0170	0.0857	0.0564	0.0621	0.0108	-0.0169	-0.1294
Quartz	0.5533	0.4440	0.1672	0.1144	0.0636	-0.0109	-0.4613
K-feldspar	0.0565	0.3083	0.0048	0.1409	0.0159	-0.0135	-0.2766
Plagioclase	-0.0289	-0.0185	0.0308	-0.0240	-0.0780	-0.0493	-0.3169
Calcite	0.0045	-0.0049	0.0092	0.0186	-0.0267	-0.0168	-0.0501
High Mg Calcite	1.0000	0.0592	0.0565	-0.0006	0.0138	-0.0146	-0.1966
Protodolomite	0.0592	1.0000	-0.0157	0.1247	0.0843	0.0579	-0.4186
Dolomite	0.0565	-0.0157	1.0000	0.0310	0.0578	0.0160	-0.2676
Bloedite	-0.0006	0.1247	0.0310	1.0000	0.0330	-0.0400	-0.2585
Clay Mineral	0.0138	0.0843	0.0578	0.0330	1.0000	0.3719	-0.5963
Magnesite	-0.0146	0.0579	0.0160	-0.0400	0.3719	1.0000	-0.2972
Thenardite	-0.1966	-0.4186	-0.2676	-0.2585	-0.5963	-0.2972	1.0000
Aragonite	-0.0212	0.0021	-0.0202	-0.0182	0.1131	0.1647	-0.0487
Anhydrite	-0.0037	0.1936	0.0153	0.1671	0.0577	-0.0018	-0.1705
Gypsum	0.0164	-0.0120	0.0365	0.0147	0.1467	0.1414	-0.5247
Halite	-0.0092	-0.0081	0.0011	-0.0094	0.0180	0.0395	-0.0340
Mg in High Mg Calcite	0.4391	0.0601	0.1451	0.0699	0.1219	-0.0218	-0.1909
Ca in Protodolomite	0.0014	0.2911	0.0155	0.0259	0.4813	0.3364	-0.5006
Ca in Dolomite	0.1446	-0.0151	0.3107	0.0305	0.3530	0.1643	-0.4030

Table F-1 Pearson Correlation Coefficient Matrix of Mineralogical and Geochemical Variables from North Ingebright lake

	Aragonite	Anhydrite	Gypsum	Halite	Ma in High Mg Calcite	Ca in Protodolomite	Ca in Dolomite
Depth	0.0330	-0.1104	-0.1995	0.0227	-0.2103	-0.3406	-0.2423
Organic Matter	0.0218	0.2518	0.2084	0.0156	0.2186	0.4020	0.2441
Carbonate Content	-0.0362	0.0360	0.0131	-0.0084	0.0394	0.0473	0.0474
Quartz	-0.0187	0.2073	0.0116	0.0098	0.2420	0.1580	0.1439
K-feldspar	-0.0232	0.0622	0.0140	0.0358	0.0506	0.0623	0.0148
Plagioclase	-0.0685	-0.0100	-0.0621	-0.0256	-0.0562	0.0325	0.0049
Calcite	-0.0127	-0.0037	0.0033	-0.0040	0.0265	0.0274	0.0887
High Mg Calcite	-0.0212	-0.0037	0.0164	-0.0092	0.4391	0.0014	0.1446
Protodolomite	0.0021	0.1936	-0.0120	-0.0081	0.0601	0.2911	-0.0151
Dolomite	-0.0202	0.0153	0.0365	0.0011	0.1451	0.0155	0.3107
Bloedite	-0.0182	0.1671	0.0147	-0.0094	0.0699	0.0259	0.0305
Clay Mineral	0.1131	0.0577	0.1467	0.0180	0.1219	0.4813	0.3530
Magnesite	0.1647	-0.0018	0.1414	0.0395	-0.0218	0.3364	0.1643
Thenardite	-0.0487	-0.1705	-0.5247	-0.0340	-0.1909	-0.5006	-0.4030
Aragonite	1.0000	-0.0205	-0.0004	-0.0217	-0.0206	0.1448	0.0248
Anhydrite	-0.0205	1.0000	-0.0367	-0.0064	0.0205	0.0219	0.0075
Gypsum	-0.0004	-0.0367	1.0000	0.0472	0.0591	0.2501	0.2727
Halite	-0.0217	-0.0064	0.0472	1.0000	-0.0185	-0.0059	0.0359
Mg in High Mg Calcite	-0.0206	0.0205	0.0591	-0.0185	1.0000	0.0854	0.2433
Ca in Protodolomite	0.1448	0.0219	0.2501	-0.0059	0.0854	1.0000	0.2434
Ca in Dolomite	0.0248	0.0075	0.2727	0.0359	0.2433	0.2434	1.0000

Table F-2 Principle Factor Matrix of Sediment Data of Unit 2

	Factor 1	Factor 2	Factor 3	Factor 4	Factor 5	Factor 6	Factor 7	Factor 8	Factor 9	Factor 10	Communality
Organic Matter	0.15	0.06	-0.03	0.48	0.40	0.17	0.74	-0.10	-0.02	-0.05	1.00
Carbonate Content	0.17	0.13	0.09	0.44	0.64	0.11	-0.50	0.23	0.15	0.02	1.00
Quartz	0.47	-0.06	-0.55	0.27	-0.34	-0.04	0.06	0.17	0.44	0.02	0.94
K-feldspar	0.00	0.00	0.00	0.00	0.00	0.00	0.00	0.00	0.00	0.00	0.00
Plagioclase	0.24	0.44	-0.25	-0.69	0.40	0.02	0.11	-0.01	0.13	0.01	0.98
Calcite	0.00	0.00	0.00	0.00	0.00	0.00	0.00	0.00	0.00	0.00	0.00
High Mg Calcite	0.00	0.00	0.00	0.00	0.00	0.00	0.00	0.00	0.00	0.00	0.00
Protodolomite	0.73	-0.22	-0.13	0.17	0.01	0.01	-0.21	-0.27	-0.30	-0.19	0.87
Dolomite	0.54	-0.35	0.32	-0.14	-0.01	-0.02	0.19	0.58	-0.22	0.18	0.99
Bloedite	0.17	0.71	0.34	0.17	-0.27	-0.04	0.01	0.20	-0.07	-0.44	1.00
Clay Mineral	0.81	-0.24	0.34	-0.01	0.03	0.01	-0.07	-0.24	0.00	0.13	0.91
Magnesite	0.71	-0.37	0.28	-0.09	-0.08	-0.01	0.05	-0.07	0.31	-0.17	0.87
Thenardite	-0.85	-0.42	0.10	0.27	-0.08	-0.02	-0.01	0.01	0.04	0.04	0.99
Aragonite	0.22	0.65	0.41	0.22	-0.22	-0.03	-0.01	-0.16	0.06	0.44	0.97
Anhydrite	0.00	0.00	0.00	0.00	0.00	0.00	0.00	0.00	0.00	0.00	0.00
Gypsum	0.40	0.19	-0.74	0.17	-0.11	-0.01	-0.06	0.08	-0.27	0.15	0.89
Halite	-0.02	0.00	0.01	-0.10	-0.19	0.98	-0.06	0.02	0.00	0.01	1.00
Percent of variance explained by factor	25.16	13.22	11.86	9.41	7.93	7.68	6.97	4.89	4.24	4.09	

Table F-3 Principle Factor Matrix of Sediment Data of Unit 3

	Factor 1	Factor 2	Factor 3	Factor 4	Factor 5	Factor 6	Factor 7	Factor 8	Factor 9	Factor 10	Factor 11	Communality
Organic Matter	0.74	-0.11	0.09	0.07	0.10	-0.22	0.22	-0.11	0.02	-0.07	-0.09	0.71
Carbonate Content	0.08	0.12	0.29	0.28	-0.04	0.83	0.29	0.13	-0.15	0.02	-0.06	0.99
Quartz	0.76	0.07	0.18	0.02	0.29	-0.12	0.21	0.02	0.00	0.16	-0.17	0.81
K-feldspar	0.63	0.46	0.02	-0.41	-0.04	0.12	-0.07	0.02	0.17	0.07	0.06	0.84
Plagioclase	-0.18	0.26	0.28	0.19	-0.58	-0.30	0.35	0.41	0.24	0.09	0.01	1.00
Calcite	0.30	0.54	-0.55	0.05	0.03	0.09	0.12	0.00	-0.01	0.29	0.33	0.89
High Mg Calcite	0.22	-0.02	0.25	0.61	0.38	0.03	-0.34	0.00	0.48	0.14	0.04	0.99
Protodolomite	0.52	-0.50	0.04	-0.13	0.21	-0.07	0.49	-0.15	-0.02	0.10	-0.04	0.86
Dolomite	0.53	0.11	0.14	0.22	-0.24	-0.15	-0.33	-0.05	-0.46	0.45	-0.10	0.97
Bloedite	0.40	0.54	-0.51	0.10	0.02	0.04	0.09	-0.07	0.17	-0.13	-0.27	0.86
Clay Mineral	0.54	-0.47	-0.15	-0.10	-0.43	0.24	-0.29	-0.14	0.14	-0.07	-0.16	0.95
Magnesite	0.49	-0.60	-0.11	0.09	-0.12	0.04	0.06	0.03	0.04	0.02	0.48	0.88
Thenardite	-0.87	0.10	0.06	-0.09	0.36	-0.02	0.08	-0.12	-0.07	0.20	0.05	0.98
Aragonite	0.10	-0.40	-0.33	-0.16	0.30	0.03	-0.13	0.74	-0.06	0.10	-0.14	0.99
Anhydrite	0.00	0.00	0.00	0.00	0.00	0.00	0.00	0.00	0.00	0.00	0.00	0.00
Gypsum	0.56	0.35	0.14	0.23	0.18	-0.13	-0.10	0.17	-0.32	-0.50	0.18	0.98
Halite	0.34	0.26	0.51	-0.63	0.09	0.09	-0.17	0.08	0.12	0.04	0.11	0.91
Percent of variance explained by factor	25.93	13.18	7.91	7.67	7.13	6.12	5.81	5.31	4.56	4.24	3.53	

Table F-4 Principle Factor Matrix of Sediment Data of Unit 4

	Factor 1	Factor 2	Factor 3	Factor 4	Factor 5	Factor 6	Factor 7	Factor 8	Factor 9	Factor 10	Factor 11	Communality
Organic Matter	0.52	0.15	0.18	-0.09	-0.13	0.02	-0.08	0.08	-0.50	0.11	0.26	0.98
Carbonate Content	0.11	0.08	0.82	-0.12	0.05	0.09	0.07	0.17	0.13	-0.07	0.23	0.94
Quartz	0.68	0.27	0.31	0.11	0.10	-0.06	0.03	0.03	0.16	0.02	0.14	0.74
K-feldspar	0.06	0.04	-0.14	-0.03	0.29	0.77	-0.36	0.00	0.33	0.10	0.17	1.00
Plagioclase	-0.31	-0.29	0.57	0.04	0.05	0.06	-0.13	-0.11	0.01	0.31	-0.52	0.98
Calcite	0.00	0.00	0.00	0.00	0.00	0.00	0.00	0.00	0.00	0.00	0.00	0.00
High Mg Calcite	-0.09	0.14	-0.09	0.52	-0.34	-0.14	-0.32	0.49	0.24	-0.03	0.08	1.00
Protodolomite	0.70	0.20	0.01	-0.31	0.02	-0.12	0.03	0.11	0.15	-0.33	-0.18	0.83
Dolomite	0.51	-0.01	0.04	0.36	-0.28	-0.10	0.03	0.00	0.27	0.36	-0.12	0.94
Bloedite	0.02	-0.12	0.00	0.15	-0.38	0.43	0.73	-0.01	0.16	-0.15	-0.04	1.00
Clay Mineral	0.71	0.00	-0.18	0.04	-0.11	0.22	-0.03	-0.04	-0.36	0.24	-0.11	1.00
Magnesite	0.64	-0.12	-0.14	0.02	0.37	-0.08	-0.03	0.09	0.21	-0.23	-0.35	0.85
Thenardite	-0.63	0.73	0.06	0.02	0.04	-0.03	0.00	-0.01	0.02	-0.13	-0.08	0.99
Aragonite	0.05	0.28	-0.17	-0.55	-0.15	-0.22	0.11	-0.15	0.43	0.44	0.12	1.00
Anhydrite	0.20	0.06	0.09	0.40	0.00	-0.12	-0.12	-0.79	0.11	-0.18	0.18	0.99
Gypsum	-0.04	-0.89	0.01	-0.11	0.03	-0.20	-0.04	0.07	0.17	-0.06	0.30	1.00
Halite	-0.05	0.10	-0.08	0.36	0.70	-0.15	0.43	0.15	-0.04	0.29	0.14	0.98
Percent of variance explained by factor	18.52	10.61	7.78	7.26	6.91	6.38	6.32	6.15	6.08	5.22	4.93	

Table F-5 Principle Factor Matrix of Sediment Data of Unit 5

	Factor 1	Factor 2	Factor 3	Factor 4	Factor 5	Factor 6	Factor 7	Factor 8	Factor 9	Factor 10	Factor 11	Communality
Organic Matter	0.25	0.57	0.15	-0.15	-0.24	0.18	-0.10	-0.11	-0.04	0.27	-0.29	1.00
Carbonate Content	0.05	-0.02	0.70	0.26	0.14	0.10	0.00	-0.04	0.31	0.37	-0.15	1.00
Quartz	-0.50	0.47	0.20	0.08	-0.12	-0.01	-0.08	0.14	0.13	0.23	0.22	1.00
K-feldspar	0.04	-0.05	-0.18	-0.29	0.38	0.25	0.65	0.39	0.16	0.21	-0.13	1.00
Plagioclase	0.74	-0.39	0.06	0.25	-0.28	0.10	0.09	-0.06	0.20	0.02	0.22	1.00
Calcite	0.14	-0.18	0.05	0.09	-0.25	0.16	-0.32	0.77	-0.36	0.08	-0.10	1.00
High Mg Calcite	-0.23	0.08	0.24	-0.02	-0.34	-0.52	0.26	0.35	0.39	-0.33	-0.04	1.00
Protodolomite	0.31	0.12	-0.10	-0.11	0.45	-0.69	-0.27	0.11	-0.05	0.31	0.03	1.00
Dolomite	0.00	0.10	0.51	0.27	0.53	0.12	0.02	0.10	-0.27	-0.42	0.13	1.00
Bloedite	0.00	0.00	0.00	0.00	0.00	0.00	0.00	0.00	0.00	0.00	0.00	0.00
Clay Mineral	0.24	0.69	-0.21	0.23	0.03	0.04	0.02	0.00	0.03	-0.32	-0.40	1.00
Magnesite	0.10	0.44	0.05	0.13	-0.22	-0.14	0.50	-0.05	-0.50	0.17	0.34	1.00
Thenardite	-0.91	-0.25	-0.03	0.05	-0.05	0.03	0.00	-0.11	-0.17	0.10	-0.14	1.00
Aragonite	-0.17	0.35	-0.43	0.37	0.15	0.24	-0.20	0.18	0.37	0.06	0.36	1.00
Anhydrite	0.00	0.00	0.00	0.00	0.00	0.00	0.00	0.00	0.00	0.00	0.00	0.00
Gypsum	0.06	0.25	0.23	-0.79	-0.01	0.21	-0.20	0.02	0.08	-0.18	0.28	1.00
Halite	0.00	0.00	0.00	0.00	0.00	0.00	0.00	0.00	0.00	0.00	0.00	0.00
Percent of variance explained by factor	14.09	11.97	8.57	8.37	7.57	7.38	7.18	6.99	6.79	6.23	5.32	

Table F-6 Principle Factor Matrix of Sediment Data of Unit 6

	Factor 1	Factor 2	Factor 3	Factor 4	Factor 5	Factor 6	Factor 7	Factor 8	Communality
Organic Matter	0.21	-0.06	0.79	0.10	-0.03	0.34	0.22	-0.39	1.00
Carbonate Content	0.05	0.01	0.39	-0.54	0.63	0.21	-0.01	0.33	1.00
Quartz	0.17	-0.28	0.40	0.58	0.23	-0.23	-0.54	0.03	1.00
K-feldspar	0.00	0.00	0.00	0.00	0.00	0.00	0.00	0.00	0.00
Plagioclase	0.29	-0.56	-0.50	0.31	0.34	0.26	0.26	-0.04	1.00
Calcite	0.00	0.00	0.00	0.00	0.00	0.00	0.00	0.00	0.00
High Mg Calcite	0.00	0.00	0.00	0.00	0.00	0.00	0.00	0.00	0.00
Protodolomite	0.19	0.46	0.26	0.46	0.13	-0.43	0.48	0.20	1.00
Dolomite	0.21	-0.58	0.29	0.07	-0.56	0.21	0.09	0.41	1.00
Bloedite	0.00	0.00	0.00	0.00	0.00	0.00	0.00	0.00	0.00
Clay Mineral	0.45	-0.32	0.12	-0.60	-0.15	-0.52	0.03	-0.11	1.00
Magnesite	0.00	0.00	0.00	0.00	0.00	0.00	0.00	0.00	0.00
Thenardite	-0.86	0.44	0.15	-0.03	-0.16	0.14	-0.05	0.05	1.00
Aragonite	0.70	0.58	-0.11	0.10	-0.17	0.21	-0.15	0.12	0.96
Anhydrite	0.00	0.00	0.00	0.00	0.00	0.00	0.00	0.00	0.00
Gypsum	0.84	0.44	-0.08	-0.13	-0.03	0.16	-0.10	-0.06	0.96
Halite	0.00	0.00	0.00	0.00	0.00	0.00	0.00	0.00	0.00
Percent of variance explained by factor	23.77	17.75	13.93	13.49	9.79	8.57	6.81	5.04	

Table F-7 Principle Factor Matrix of Sediment Data of Unit 7

	Factor 1	Factor 2	Factor 3	Factor 4	Factor 5	Factor 6	Factor 7	Factor 8	Factor 9	Factor 10	Factor 11	Communality
Organic Matter	0.80	0.15	-0.32	-0.27	0.05	0.08	0.06	0.02	0.13	-0.09	0.12	0.89
Carbonate Content	0.50	0.29	-0.30	0.56	-0.02	0.09	-0.08	0.00	-0.05	0.02	-0.05	0.76
Quartz	0.52	-0.80	-0.05	0.23	-0.02	0.00	0.01	0.03	-0.02	0.10	0.00	0.98
K-feldspar	0.33	0.32	-0.26	0.34	0.09	-0.30	-0.04	-0.26	0.24	0.44	-0.36	0.94
Plagioclase	0.45	0.33	0.66	0.28	0.02	0.04	0.02	0.05	-0.02	0.11	0.03	0.84
Calcite	0.07	-0.07	0.05	0.00	0.78	0.18	0.04	0.49	0.16	-0.09	-0.25	1.00
High Mg Calcite	0.38	-0.89	0.02	0.18	-0.04	-0.03	-0.03	-0.02	-0.06	0.06	0.01	0.98
Protodolomite	0.44	0.31	-0.40	0.38	0.02	0.08	0.04	0.27	-0.16	-0.09	0.45	0.92
Dolomite	0.28	0.18	0.84	0.16	0.10	0.05	-0.03	-0.19	-0.01	-0.07	0.12	0.90
Bloedite	-0.13	-0.02	0.11	0.14	-0.19	-0.58	0.46	0.33	0.48	-0.13	0.11	0.99
Clay Mineral	0.63	0.19	-0.09	-0.32	-0.31	0.02	-0.02	0.03	-0.01	-0.44	-0.39	0.99
Magnesite	0.22	0.11	0.16	-0.34	-0.35	0.15	0.09	0.55	-0.20	0.52	-0.08	0.99
Thenardite	-0.92	0.13	-0.26	0.17	0.04	0.07	0.00	0.07	-0.11	0.10	0.00	0.98
Aragonite	-0.05	-0.04	-0.05	0.04	-0.10	0.67	0.57	-0.25	0.37	0.09	0.01	1.00
Anhydrite	-0.13	-0.04	0.04	0.06	-0.23	0.24	-0.67	0.19	0.61	0.01	0.10	1.00
Gypsum	0.39	0.07	-0.11	-0.65	0.31	-0.18	-0.06	-0.22	0.16	0.26	0.30	0.95
Halite	0.00	0.00	0.00	0.00	0.00	0.00	0.00	0.00	0.00	0.00	0.00	0.00
Percent of variance explained by factor	21.13	12.21	10.56	9.54	6.61	6.54	6.36	6.17	5.90	5.15	4.34	

Table F-8 Principle Factor Matrix of Sediment Data of Unit 8

	Factor 1	Factor 2	Factor 3	Factor 4	Factor 5	Factor 6	Factor 7	Factor 8	Communality
Organic Matter	0.95	-0.10	0.09	0.06	0.04	-0.03	-0.19	0.07	0.97
Carbonate Content	0.81	-0.09	0.02	0.02	-0.17	-0.14	0.44	-0.06	0.91
Quartz	0.79	0.16	-0.35	0.08	0.06	-0.01	-0.21	-0.36	0.96
K-feldspar	0.73	0.03	-0.39	-0.40	-0.08	0.00	-0.07	-0.28	0.93
Plagioclase	0.63	0.21	-0.14	0.59	-0.16	0.04	0.01	0.34	0.95
Calcite	0.00	0.00	0.00	0.00	0.00	0.00	0.00	0.00	0.00
High Mg Calcite	0.41	0.53	0.14	-0.40	0.39	0.06	0.43	0.05	0.97
Protodolomite	0.76	-0.18	-0.44	-0.11	0.00	0.04	0.03	0.40	0.98
Dolomite	0.28	0.61	0.38	0.56	0.04	-0.13	0.01	-0.19	0.97
Bloedite	0.35	-0.34	0.58	-0.15	-0.59	0.08	0.12	-0.09	0.97
Clay Mineral	0.35	-0.48	0.45	-0.05	0.45	-0.47	-0.12	0.07	0.99
Magnesite	0.00	0.00	0.00	0.00	0.00	0.00	0.00	0.00	0.00
Thenardite	-0.98	0.09	-0.14	0.00	0.02	0.04	0.07	0.03	0.99
Aragonite	0.00	0.00	0.00	0.00	0.00	0.00	0.00	0.00	0.00
Anhydrite	0.29	-0.51	0.14	0.33	0.38	0.59	0.10	-0.15	1.00
Gypsum	0.36	0.44	0.49	-0.41	-0.01	0.31	-0.33	0.18	0.97
Halite	0.00	0.00	0.00	0.00	0.00	0.00	0.00	0.00	0.00
Percent of variance explained by factor	41.07	12.20	11.43	10.13	6.98	5.53	4.71	4.55	